Mechanical Engineering
Design

Lecturer

Mazin Yaseen Abbood (Teacher) – Ph.D. Applied Mechanics

University of Anbar
Mechanical Department

Main reference

Shigley's Mechanical Engineering Design, Eighth Edition

Syllabus

1. Load and Stress Analysis
2. Failures Resulting from Static Loading
3. Fatigue Failure Resulting from Variable Loading
4. Shafts and Shaft Components
5. Screws, Fasteners, and the Design of Nonpermanent Joints
6. Welding, Bonding, and the Design of Permanent Joints
7. Mechanical Springs
8. Rolling−Contact Bearings
9. Lubrication and Journal Bearings
10. Gears

Introduction

Mechanical design is a complex undertaking, requiring many skills. Extensive relationships need to be subdivided into a series of simple tasks. The complexity of the subject requires a sequence in which ideas are introduced and iterated. To design is either to formulate a plan for the satisfaction of a specified need or to solve a problem. If the plan results in the creation of something having a physical reality, then the product must be functional, safe, reliable, competitive, usable, manufacturable, and marketable.

The complete design process, from start to finish, is often outlined as in Fig.(1).The process begins with an identification of a need and a decision to do something about it. After many iterations, the process ends with the presentation of the plans for satisfying the need. Depending on the nature of the design task, several design phases may be repeated throughout the life of the product, from inception to termination.
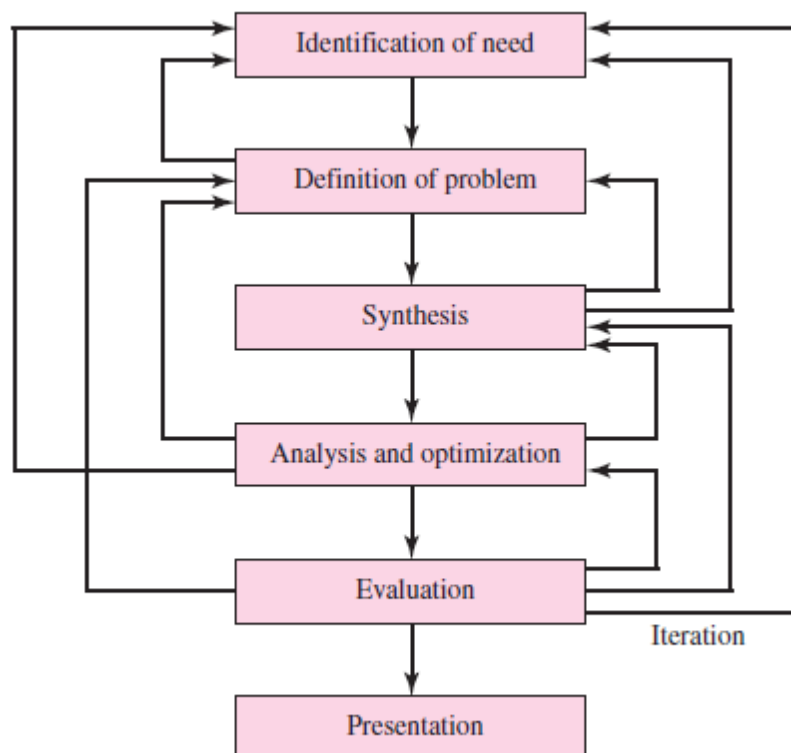

Figure (1)
The phases in design, acknowledging the many feedbacks and iterations

1. Load and Stress Analysis

The ability to quantify the stress condition at a critical location in a machine element is an important skill of the engineer. Why? Whether the member fails or not is assessed by comparing the (damaging) stress at a critical location with the corresponding material strength at this location.
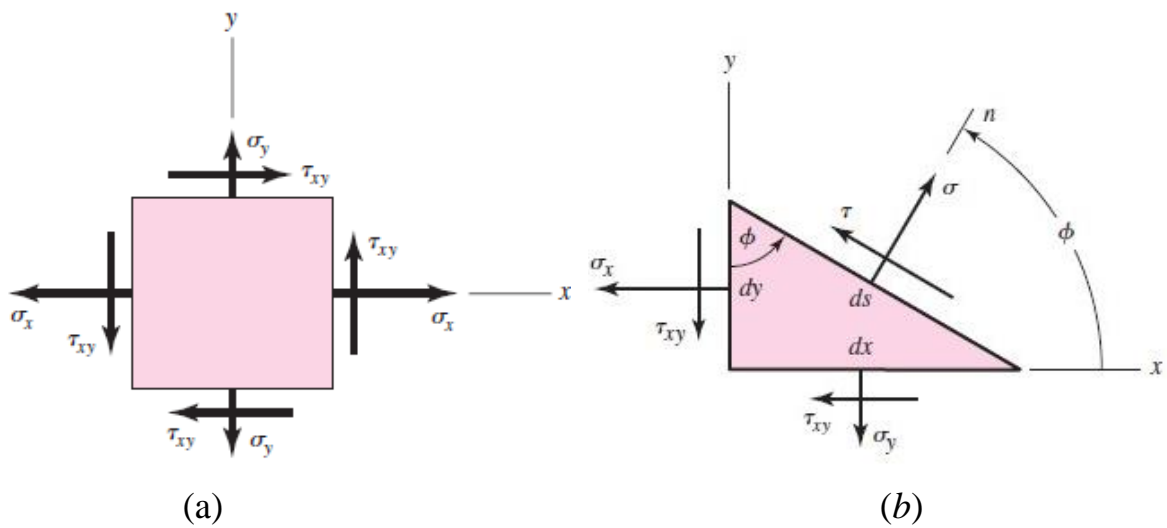
1-1. Mohr's Circle for Plane Stress

(a)   (b)

Figure (1-1)

Suppose the *dx dy dz* element of Fig. (1–1a) is cut by an oblique plane with a normal *n* at an arbitrary angle ϕ counterclockwise from the *x* axis as shown in Fig. (1–1b). This section is concerned with the stresses σ and τ that act upon this oblique plane. By summing the forces caused by all the stress components to zero, the stresses σ and τ are found to be

$$\sigma = \frac{\sigma_x + \sigma_y}{2} + \frac{\sigma_x - \sigma_y}{2} \cos 2\phi + \tau_{xy} \sin 2\phi \qquad\qquad 1\text{-}1$$

$$\tau = -\frac{\sigma_x - \sigma_y}{2} \sin 2\phi + \tau_{xy} \cos 2\phi \qquad\qquad 1\text{-}2$$

Equations (1–1) and (1–2) are called the *plane-stress transformation equations*. Differentiating Eq. (1–1) with respect to ϕ and setting the result equal to zero gives

$$\tan 2\phi_p = \frac{2\tau_{xy}}{\sigma_x - \sigma_y} \qquad \text{1-3}$$

Equation (1–3) defines two particular values for the angle $2\phi_p$, one of which defines the maximum normal stress σ_1 and the other, the minimum normal stress σ_2. These two stresses are called the *principal stresses,* and their corresponding directions, the *principal directions.* The angle between the principal directions is 90°. It is important to note that Eq. (1–3) can be written in the form

$$\frac{\sigma_x - \sigma_y}{2} \sin 2\phi_p - \tau_{xy} \cos 2\phi_p = 0 \qquad \text{a}$$

Comparing this with Eq. (1–2), we see that $\tau = 0$, meaning that the *surfaces containing principal stresses have zero shear stresses*. In a similar manner, we differentiate Eq. (1–2), set the result equal to zero, and obtain

$$\tan 2\phi_s = -\frac{\sigma_x - \sigma_y}{2\tau_{xy}} \qquad \text{1-4}$$

Equation (1–4) defines the two values of $2\phi_s$ at which the shear stress τ reaches an extreme value. The angle between the surfaces containing the maximum shear stresses is 90°. Equation (1–4) can also be written as

$$\frac{\sigma_x - \sigma_y}{2} \cos 2\phi_p + \tau_{xy} \sin 2\phi_p = 0 \qquad \text{b}$$

Substituting this into Eq. (1–1) yields

$$\sigma = \frac{\sigma_x + \sigma_y}{2} \qquad \text{1-5}$$

Equation (1–5) tells us that the two surfaces containing the maximum shear stresses also contain equal normal stresses of

$(\sigma_x + \sigma_y)/2$. Comparing Eqs. (1–3) and (1–4), we see that $\tan 2\phi_s$ is the negative reciprocal of $\tan 2\phi_p$. This means that $2\phi_s$ and $2\phi_p$ are angles 90° apart, and thus the angles between the surfaces containing the maximum shear stresses and the surfaces containing the principal stresses are ±45°. Formulas for the two principal stresses can be obtained by substituting the angle $2\phi_p$ from Eq. (1–3) in Eq. (1–1). The result is

$$\sigma_1, \sigma_2 = \frac{\sigma_x + \sigma_y}{2} \pm \sqrt{\left(\frac{\sigma_x - \sigma_y}{2}\right)^2 + \tau_{xy}^2} \qquad \text{1-6}$$

In a similar manner the two extreme-value shear stresses are found to be

$$\tau_1, \tau_2 = \pm\sqrt{\left(\frac{\sigma_x - \sigma_y}{2}\right)^2 + \tau_{xy}^2} \qquad \text{1-7}$$

Your particular attention is called to the fact that an extreme value of the shear stress *may not be the same as the actual maximum value.*

It is important to note that the equations given to this point are quite sufficient for performing any plane stress transformation. However, extreme care must be exercised when applying them. For example, say you are attempting to determine the principal state of stress for a problem where σ_x = 14 MPa, σ_y = −10 MPa, and τ_{xy} = −16 MPa. Equation (1–3) yields ϕ_p = −26.57° and 63.43° to locate the principal stress surfaces, whereas, Eq. (1–6) gives σ_1 = 22 MPa and σ_2 = −18 MPa for the principal stresses. If all we wanted was the principal stresses, we would be finished. However, what if we wanted to draw the element containing the principal stresses properly oriented relative to the *x, y* axes? Well, we have two values of ϕ_p and two values for the principal stresses. How do we know which value of ϕ_p corresponds to which value of the principal stress? To clear this up we would need to substitute one of the values of ϕ_p into Eq. (1–1) to determine the normal stress corresponding to that angle. A graphical method for expressing the relations developed in this section, called *Mohr's circle diagram,* is a very effective means of visualizing the stress state at a point and

keeping track of the directions of the various components associated with plane stress. Equations (1–1) and (1–2) can be shown to be a set of parametric equations for σ and τ, where the parameter is 2ϕ. The relationship between σ and τ is that of a circle plotted in the σ, τ plane, where the center of the circle is located at $C = (\sigma, \tau) = [(\sigma_x + \sigma_y)/2, 0]$ and has a radius of

$$R = \sqrt{\left(\frac{\sigma_x - \sigma_y}{2}\right)^2 + \left(\tau_{xy}\right)^2}.$$

A problem arises in the sign of the shear stress. The transformation equations are based on a positive ϕ being counterclockwise, as shown in Fig. (1–2). If a positive τ were plotted above the σ axis, points would rotate clockwise on the circle 2ϕ in the opposite direction of rotation on the element. It would be convenient if the rotations were in the same direction. One could solve the problem easily by plotting positive τ below the axis. However, the classical approach to Mohr's circle uses a different convention for the shear stress.

1-2. Mohr's Circle Shear Convention

This convention is followed in drawing Mohr's circle:
• Shear stresses tending to rotate the element clockwise (cw) are plotted *above* the σ axis.
• Shear stresses tending to rotate the element counterclockwise (ccw) are plotted *below* the σ axis.
For example, consider the right face of the element in Fig. (1–1*a*). By Mohr's circle convention the shear stress shown is plotted *below* the σ axis because it tends to rotate the element counterclockwise. The shear stress on the top face of the element is plotted *above* the σ axis because it tends to rotate the element clockwise. In Fig. (1–2) we create a coordinate system with normal stresses plotted along the abscissa and shear stresses plotted as the ordinates. On the abscissa, tensile (positive) normal stresses are plotted to the right of the origin *O* and compressive (negative) normal stresses to the left. On the ordinate, clockwise (cw) shear stresses are plotted up; counterclockwise (ccw) shear stresses are plotted down.

Using the stress state of Fig. (1–1*a*), we plot Mohr's circle, Fig. (1–2), by first looking at the right surface of the element containing σ_x to establish the sign of σ_x and the cw or ccw direction of the shear stress. The right face is called the *x face* where $\phi = 0°$. If

σ_x is positive and the shear stress τ_{xy} is ccw as shown in Fig. (1–1a), we can establish point A with coordinates $(\sigma_x, \tau_{xy}^{ccw})$ in Fig. (1–2).
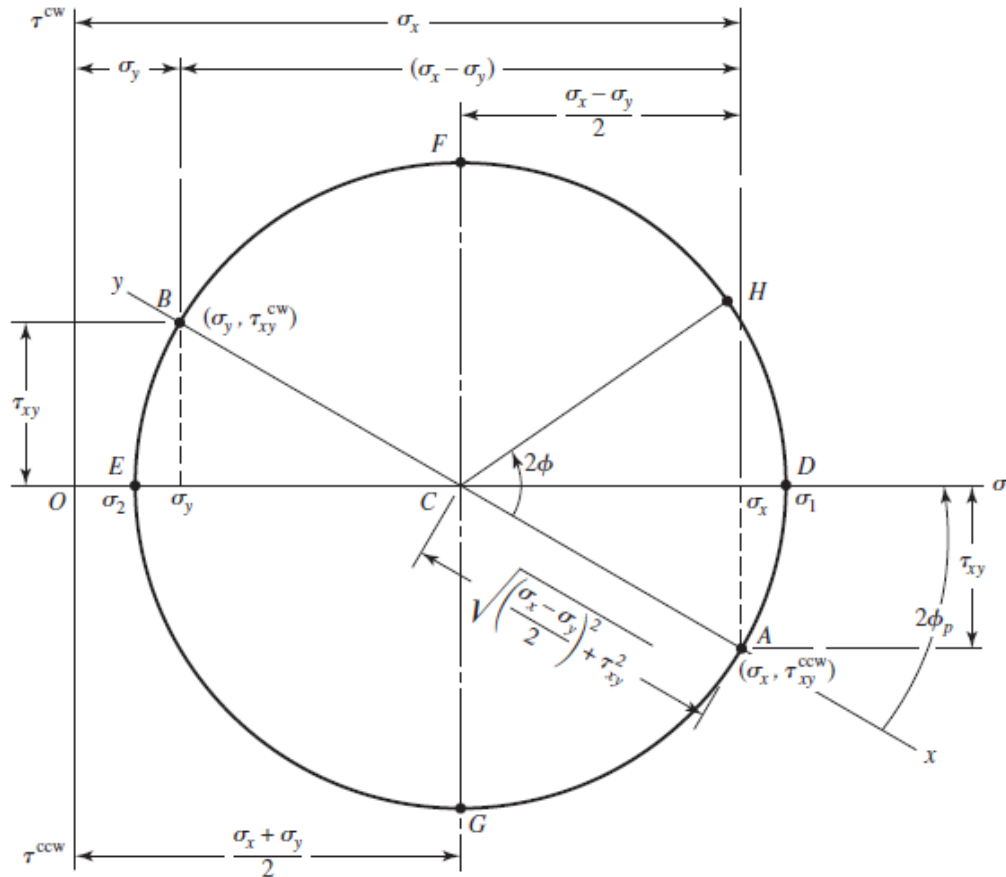

Figure (1-2)
Mohr's circle diagram.

Next, we look at the top y *face,* where $\phi = 90\circ$, which contains σ_y, and repeat the process to obtain point B with coordinates $(\sigma_y, \quad \tau_{xy}^{ccw})$ as shown in Fig. (1–2). The two states of stress for the element are $\Delta\phi = 90\degree$ from each other on the element so they will be $2\Delta\phi = 180\degree$ from each other on Mohr's circle. Points A and B are the same vertical distance from the σ axis. Thus, AB must be on the diameter of the circle, and the center of the circle C is where AB intersects the σ axis. With points A and B on the circle, and center C, the complete circle can then be drawn. Note that the extended ends of line AB are labeled x and y as references to the normal to the surfaces for which points A and B represent the stresses. The entire Mohr's circle

represents the state of stress at a *single* point in a structure. Each point on the circle represents the stress state for a *specific* surface intersecting the point in the structure. Each pair of points on the circle $180°$ apart represent the state of stress on an element whose surfaces are $90°$ apart. Once the circle is drawn, the states of stress can be visualized for various surfaces intersecting the point being analyzed. For example, the principal stresses σ_1 and σ_2 are points D and E, respectively, and their values obviously agree with Eq. (1–6). We also see that the shear stresses are zero on the surfaces containing σ_1 and σ_2. The two extreme-value shear stresses, one clockwise and one counterclockwise, occur at F and G with magnitudes equal to the radius of the circle. The surfaces at F and G each also contain normal stresses of $(\sigma_x + \sigma_y)/2$ as noted earlier in Eq. (1–5). Finally, the state of stress on an arbitrary surface located at an angle ϕ counterclockwise from the x face is point H.

At one time, Mohr's circle was used graphically where it was drawn to scale very accurately and values were measured by using a scale and protractor. Here, we are strictly using Mohr's circle as a visualization aid and will use a semi-graphical approach, calculating values from the properties of the circle. This is illustrated by the following example.

EXAMPLE 1–1

A stress element has $\sigma_x = 80$ MPa and $\tau_{xy} = 50$ MPa cw, as shown in Fig. (1–3*a*).

(a) Using Mohr's circle, find the principal stresses and directions, and show these on a stress element correctly aligned with respect to the xy coordinates. Draw another stress element to show τ_1 and τ_2, find the corresponding normal stresses, and label the drawing completely.

(b) Repeat part *a* using the transformation equations only.

Solution

(a) In the semi-graphical approach used here, we first make an approximate freehand sketch of Mohr's circle and then use the geometry of the figure to obtain the desired information.

Draw the σ and τ axes first (Fig. 1–3*b*) and from the x face locate $\sigma_x = 80$ MPa along the σ axis. On the x face of the element, we see that the shear stress is 50 MPa in the cw direction. Thus, for

the x face, this establishes point A (80, 50cw) MPa. Corresponding to the y face, the stress is $\sigma = 0$ and $\tau = 50$ MPa in the ccw direction. This locates point B (0, 50ccw) MPa. The line AB forms the diameter of the required circle, which can now be drawn. The intersection of the circle with the σ axis defines σ_1 and σ_2 as shown. Now, noting the triangle ACD, indicate on the sketch the length of the legs AD and CD as 50 and 40 MPa, respectively. The length of the hypotenuse AC is

$$\tau_1 = \sqrt{(50)^2 + (40)^2} = 64.0 \text{ MPa} \qquad Ans.$$

and this should be labeled on the sketch too. Since intersection C is 40 MPa from the origin, the principal stresses are now found to be

$\sigma_1 = 40 + 64 = 104$ MPa and $\sigma_2 = 40 - 64 = -24$ MPa $\qquad Ans.$

The angle 2ϕ from the x axis cw to σ_1 is

$$2\phi_p = \tan^{-1}\tfrac{50}{40} = 51.3° \qquad Ans.$$

To draw the principal stress element (Fig. 1–3c), sketch the x and y axes parallel to the original axes. The angle ϕ_p on the stress element must be measured in the *same* direction as is the angle $2\phi_p$ on the Mohr circle. Thus, from x measure 25.7° (half of 51.3°) clockwise to locate the σ_1 axis. The σ_2 axis is 90° from the σ_1 axis and the stress element can now be completed and labeled as shown. Note that there are *no* shear stresses on this element. The two maximum shear stresses occur at points E and F in Fig. (1–3b). The two normal stresses corresponding to these shear stresses are each 40 MPa, as indicated. Point E is 38.7° ccw from point A on Mohr's circle. Therefore, in Fig. (1–3d), draw a stress element oriented 19.3° (half of 38.7°) ccw from x. The element should then be labeled with magnitudes and directions as shown. In constructing these stress elements it is important to indicate the x and y directions of the original reference system. This completes the link between the original machine element and the orientation of its principal stresses.
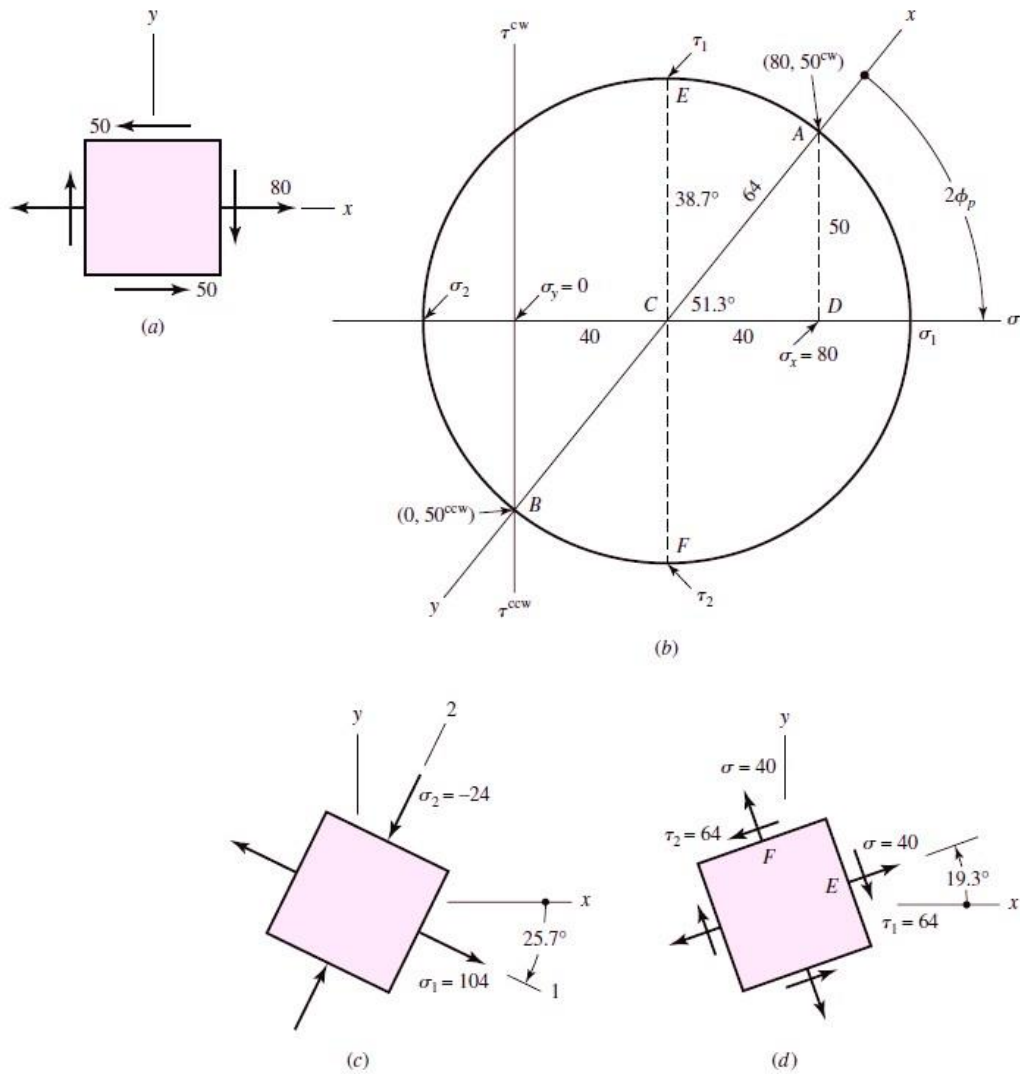
(a)

(b)

(c)

(d)

Figure (1-3)
All stresses in MPa.

(b) The transformation equations are programmable. From Eq. (1–3),

$$\phi_p = \frac{1}{2} \tan^{-1} \left(\frac{2\tau_{xy}}{\sigma_x - \sigma_y} \right) = \frac{1}{2} \tan^{-1} \left(\frac{2(-50)}{80} \right) = -25.7°, 64.3°$$

From Eq. (1–2), for the first angle $\phi_p = -25.7°$,

$$\sigma = \frac{80 + 0}{2} + \frac{80 - 0}{2} \cos[2(-25.7)] + (-50) \sin[2(-25.7)] = 104.03 \text{ MPa}$$

9

which confirms that 104.03 MPa is a principal stress. From Eq. (1–1), for $\phi_p = 64.3°$,

$$\sigma = \frac{80+0}{2} + \frac{80-0}{2}\cos[2(64.3)] + (-50)\sin[2(64.3)] = -24.03 \text{ MPa}$$

Substituting $\phi_p = 64.3°$ into Eq. (3–9) again yields $\tau = 0$, indicating that −24.03 MPa is also a principal stress. Once the principal stresses are calculated they can be ordered such that $\sigma_1 \geq \sigma_2$. Thus, $\sigma_1 = 104.03$ MPa and $\sigma_2 = -24.03$ MPa.   *Ans.*

Since for $\sigma_1 = 104.03$ MPa, $\phi_p = -25.7°$, and since ϕ is defined positive ccw in the transformation equations, we rotate *clockwise* 25.7° for the surface containing σ_1. We see in Fig. (1–3c) that this totally agrees with the semigraphical method.
To determine τ_1 and τ_2, we first use Eq. (1–4) to calculate ϕ_s :

$$\phi_s = \frac{1}{2}\tan^{-1}\left(-\frac{\sigma_x - \sigma_y}{2\tau_{xy}}\right) = \frac{1}{2}\tan^{-1}\left(-\frac{80}{2(-50)}\right) = 19.3°, 109.3°$$

For $\phi_s = 19.3°$, Eqs. (1–1) and (1–2) yield

$$\sigma = \frac{80+0}{2} + \frac{80-0}{2}\cos[2(19.3)] + (-50)\sin[2(19.3)] = 40.0 \text{ MPa}$$

$$\tau = -\frac{80-0}{2}\sin[2(19.3)] + (-50)\cos[2(19.3)] = -64.0 \text{ MPa}$$

         Ans.

Remember that Eqs. (1–1) and (1–2) are *coordinate* transformation equations. Imagine that we are rotating the *x*, *y* axes 19.3° counterclockwise and *y* will now point up and to the left. So a negative shear stress on the rotated *x* face will point down and to the right as shown in Fig. (1–3d). Thus again, results agree with the semigraphical method. For $\phi_s = 109.3°$, Eqs. (1–1) and (1–2) give $\sigma = 40.0$ MPa and $\tau = +64.0$ MPa.
Using the same logic for the coordinate transformation we find that results again agree with Fig. (1–3d).

Homework

For each of the plane stress states listed below, draw a Mohr's circle diagram properly labeled, find the principal normal and shear stresses, and determine the angle from the x axis to σ_1. Draw stress elements as in Fig. (1–3c and d) and label all details.

(1) $\sigma_x = 12$, $\sigma_y = 6$, $\tau_{xy} = 4$ cw
(2) $\sigma_x = 16$, $\sigma_y = 9$, $\tau_{xy} = 5$ ccw
(3) $\sigma_x = 10$, $\sigma_y = 24$, $\tau_{xy} = 6$ ccw
(4) $\sigma_x = 9$, $\sigma_y = 19$, $\tau_{xy} = 8$ cw
(5) $\sigma_x = -4$, $\sigma_y = 12$, $\tau_{xy} = 7$ ccw
(6) $\sigma_x = 6$, $\sigma_y = -5$, $\tau_{xy} = 8$ ccw
(7) $\sigma_x = -8$, $\sigma_y = 7$, $\tau_{xy} = 6$ cw
(8) $\sigma_x = 9$, $\sigma_y = -6$, $\tau_{xy} = 3$ cw
(9) $\sigma_x = 20$, $\sigma_y = -10$, $\tau_{xy} = 8$ cw
(10) $\sigma_x = 30$, $\sigma_y = -10$, $\tau_{xy} = 10$ ccw
(11) $\sigma_x = -10$, $\sigma_y = 18$, $\tau_{xy} = 9$ cw
(12) $\sigma_x = -12$, $\sigma_y = 22$, $\tau_{xy} = 12$ cw

1-3. General Three-Dimensional Stress

As in the case of plane stress, a particular orientation of a stress element occurs in space for which all shear-stress components are zero. When an element has this particular orientation, the normals to the faces are mutually orthogonal and correspond to the principal directions, and the normal stresses associated with these faces are the principal stresses. Since there are three faces, there are three principal directions and three principal stresses σ_1, σ_2, and σ_3. For plane stress, the stress-free surface contains the third principal stress which is zero. The process in finding the three principal stresses from the six stress components σ_x , σ_y , σ_z , τ_{xy} , τ_{yz}, and τ_{zx} , involves finding the roots of the cubic equation

$$\sigma^3 - (\sigma_x + \sigma_y + \sigma_z)\sigma^2 + \left(\sigma_x\sigma_y + \sigma_x\sigma_z + \sigma_y\sigma_z - \tau_{xy}^2 - \tau_{yz}^2 - \tau_{zx}^2\right)\sigma$$
$$- \left(\sigma_x\sigma_y\sigma_z + 2\tau_{xy}\tau_{yz}\tau_{zx} - \sigma_x\tau_{yz}^2 - \sigma_y\tau_{zx}^2 - \sigma_z\tau_{xy}^2\right) = 0 \qquad 1\text{-}8$$
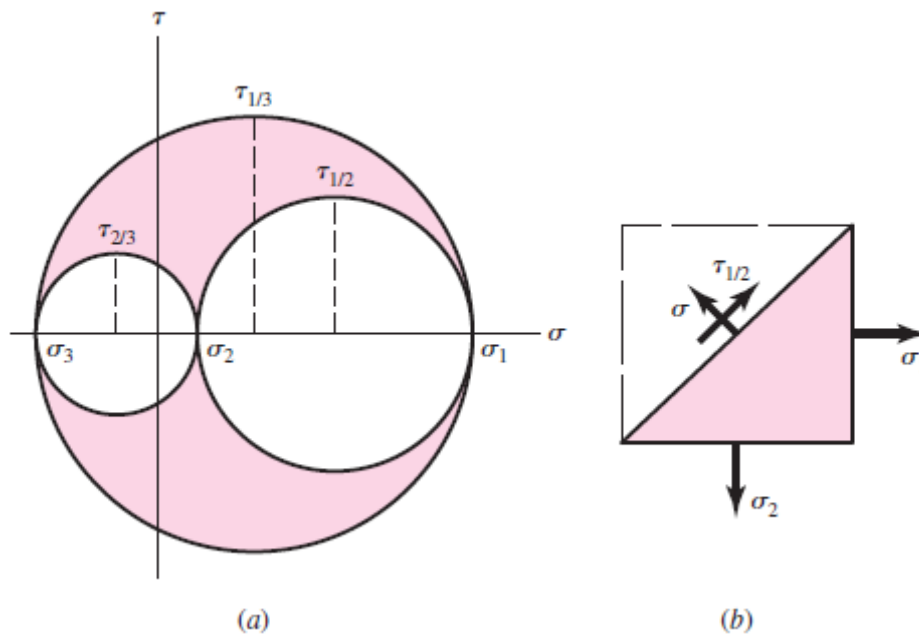
Figure (1-4)
Mohr's circles for three-dimensional stress

In plotting Mohr's circles for three-dimensional stress, the principal normal stresses are ordered so that $\sigma_1 \geq \sigma_2 \geq \sigma_3$. Then the result appears as in Fig. (1–4a). The stress coordinates σ, τ for any arbitrarily located plane will always lie on the boundaries or within the shaded area. Figure (1–4a) also shows the three *principal shear stresses* $\tau_{1/2}$, $\tau_{2/3}$, and $\tau_{1/3}$. Each of these occurs on the two planes, one of which is shown in Fig. (3–12b). The figure shows that the principal shear stresses are given by the equations

$$\tau_{1/2} = \frac{\sigma_1 - \sigma_2}{2} \qquad \tau_{2/3} = \frac{\sigma_2 - \sigma_3}{2} \qquad \tau_{1/3} = \frac{\sigma_1 - \sigma_3}{2} \qquad \text{1-9}$$

Of course, $\tau_{\max} = \tau_{1/3}$ when the normal principal stresses are ordered $(\sigma_1 > \sigma_2 > \sigma_3)$, so always order your principal stresses. Do this in any computer code you generate and you'll always generate $\tau_{\max}$.

1-4. Elastic Strain

Normal strain ε is given by the equation $\epsilon = \delta/l$, where δ is the total elongation of the bar within the length l. Hooke's law for the tensile specimen is given by the equation

$$\sigma = E\epsilon \qquad\qquad 1\text{-}10$$

where the constant E is called *Young's modulus* or the *modulus of elasticity*.

When a material is placed in tension, there exists not only an axial strain, but also negative strain (contraction) perpendicular to the axial strain. Assuming a linear, homogeneous, isotropic material, this lateral strain is proportional to the axial strain. If the axial direction is x, then the lateral strains are $\epsilon_y = \epsilon_z = -\nu\epsilon_x$. The constant of proportionality ν is called *Poisson's ratio*, which is about 0.3 for most structural metals.

If the axial stress is in the x direction, then from Eq. (1–10)

$$\epsilon_x = \frac{\sigma_x}{E} \qquad \epsilon_y = \epsilon_z = -\nu\frac{\sigma_x}{E} \qquad\qquad 1\text{-}11$$

For a stress element undergoing σ_x , σ_y , and σ_z simultaneously, the normal strains are given by

$$\epsilon_x = \frac{1}{E}\left[\sigma_x - \nu(\sigma_y + \sigma_z)\right]$$
$$\epsilon_y = \frac{1}{E}\left[\sigma_y - \nu(\sigma_x + \sigma_z)\right] \qquad\qquad 1\text{-}12$$
$$\epsilon_z = \frac{1}{E}\left[\sigma_z - \nu(\sigma_x + \sigma_y)\right]$$

Shear strain γ is the change in a right angle of a stress element when subjected to pure shear stress, and Hooke's law for shear is given by

$$\tau = G\gamma \qquad\qquad 1\text{-}13$$

where the constant G is the *shear modulus of elasticity* or *modulus of rigidity*.

It can be shown for a linear, isotropic, homogeneous material; the three elastic constants are related to each other by

$$E = 2G(1 + v) \qquad\qquad \text{1-14}$$

1-5. Uniformly Distributed Stresses

The assumption of a uniform distribution of stress is frequently made in design. The result is then often called *pure tension, pure compression,* or *pure shear,* depending upon how the external load is applied to the body under study. The word *simple* is sometimes used instead of *pure* to indicate that there are no other complicating effects.

For *pure tension* and *pure compression*

$$\sigma = \frac{F}{A} \qquad\qquad \text{1-15}$$

and for *pure shear*

$$\tau = \frac{F}{A} \qquad\qquad \text{1-16}$$

1-6. Normal Stresses for Beams in Bending
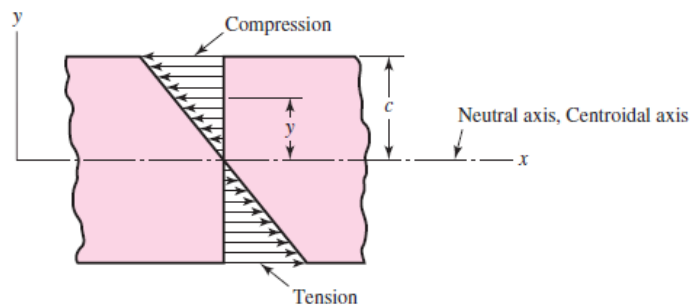
Figure (1-5)
Bending stresses according to Eq. (1–17)

The bending stress varies linearly with the distance from the neutral axis, y, and is given by

1-17
$$\sigma_x = -\frac{My}{I}$$

where I is the second *moment of area* about the z axis. That is

$$I = \int y^2 dA \qquad\qquad \text{1-18}$$

So, the maximum *magnitude* of the bending stress is

$$\sigma_{max} = \frac{Mc}{I} \qquad \text{or} \qquad \sigma_{max} = \frac{M}{Z} \qquad \text{1-19}$$
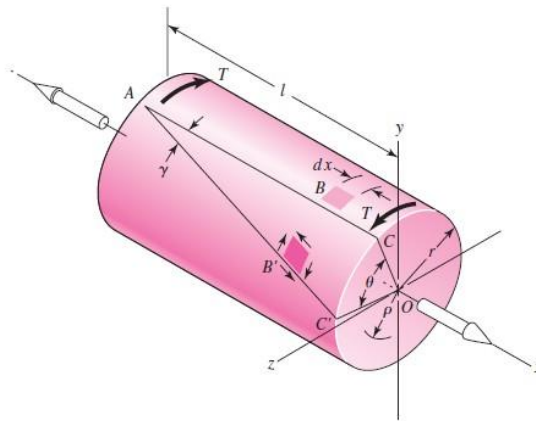
where $Z = I/c$ is called the *section modulus.*

1-7. Torsion

Figure (1-5)

The angle of twist, in radians, for a solid round bar is

$$\theta = \frac{Tl}{GJ} \qquad\qquad \text{1-20}$$

where T = torque, l = length, G = modulus of rigidity, *and* J = polar second moment of area.

Shear stresses develop throughout the cross section. For a round bar in torsion, these stresses are proportional to the radius ρ and are given by

$$\tau = \frac{T\rho}{J} \qquad\qquad \text{1-21}$$

Designating r as the radius to the outer surface, we have

$$\tau_{max} = \frac{Tr}{J} \qquad\qquad \text{1-22}$$

Equation (1–22) applies *only* to circular sections. For a solid round section,

$$J = \frac{\pi d^4}{32} \qquad \text{1-23}$$

where *d* is the diameter of the bar. For a hollow round section,

$$J = \frac{\pi}{32}\left(d_o^4 - d_i^4\right) \qquad \text{1-24}$$

where the subscripts *o* and *i* refer to the outside and inside diameters, respectively.

In using Eq. (1–22) it is often necessary to obtain the torque *T* from a consideration of the power and speed of a rotating shaft. For convenience when U. S. Customary units are used, three forms of this relation are

$$H = \frac{FV}{33\,000} = \frac{2\pi Tn}{33\,000(12)} = \frac{Tn}{63\,025} \qquad \text{1-25}$$

where H = power, hp, T = torque, lbf · in, n = shaft speed, rev/min, F = force, lbf, and V = velocity, ft/min.

When SI units are used, the equation is

$$H = T\omega \qquad \text{1-26}$$

where H =power, W, T =torque, N.m, and ω=angular velocity, rad/s

The torque *T* corresponding to the power in watts is given approximately by

$$T = 9.55\frac{H}{n} \qquad \text{1-27}$$

where *n* is in revolutions per minute.

There are some applications in machinery for noncircular-cross-section members and shafts where a regular polygonal cross section is useful in transmitting torque to a gear or pulley that can have an axial change in position. Because no key or keyway is needed, the possibility of a lost key is avoided. Saint Venant (1855)

showed that the maximum shearing stress in a rectangular $b \times c$ section bar occurs in the middle of the *longest* side b and is of the magnitude

$$\tau_{\max} = \frac{T}{\alpha bc^2} \doteq \frac{T}{bc^2}\left(3 + \frac{1.8}{b/c}\right) \qquad \text{1-28}$$

where b is the longer side, c the shorter side, and α a factor that is a function of the ratio b/c as shown in the following table. The angle of twist is given by

$$\theta = \frac{Tl}{\beta bc^3 G} \qquad \text{1-29}$$

where β is a function of b/c, as shown in the table.

b/c	1.00	1.50	1.75	2.00	2.50	3.00	4.00	6.00	8.00	10	∞
α	0.208	0.231	0.239	0.246	0.258	0.267	0.282	0.299	0.307	0.313	0.333
β	0.141	0.196	0.214	0.228	0.249	0.263	0.281	0.299	0.307	0.313	0.333

In Eqs. (1–28) and (1–29) b and c are the width (long side) and thickness (short side) of the bar, respectively. They cannot be interchanged. Equation (1–28) is also approximately valid for equal-sided angles; these can be considered as two rectangles, each of which is capable of carrying half the torque.

EXAMPLE 1-2

Figure (1–6) shows a crank loaded by a force $F = 300$ lbf that causes twisting and bending of a 3/4-in-diameter shaft fixed to a support at the origin of the reference system. In actuality, the support may be an inertia that we wish to rotate, but for the purposes of a stress analysis we can consider this a statics problem.
(a) Draw separate free-body diagrams of the shaft AB and the arm BC, and compute the values of all forces, moments, and torques that act. Label the directions of the coordinate axes on these diagrams.
(b) Compute the maxima of the torsional stress and the bending stress in the arm BC and indicate where these act.
(c) Locate a stress element on the top surface of the shaft at A, and calculate all the stress components that act upon this element.
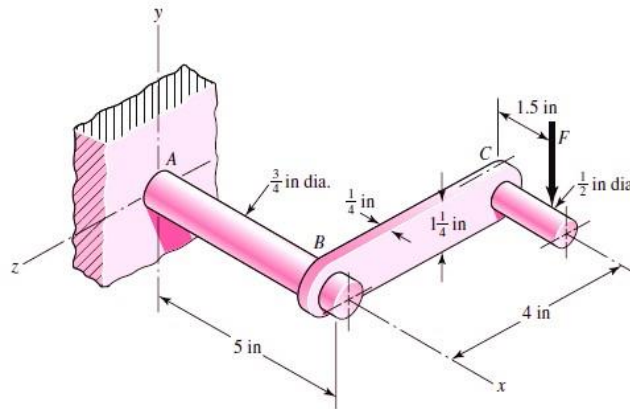(d) Determine the maximum normal and shear stresses at A.

Figure (1-6)

Solution

(a) The two free-body diagrams are shown in Fig. (1–7). The results are

At end *C* of arm *BC*: $\mathbf{F} = -300\mathbf{j}$ lbf, $\mathbf{T}_C = -450\mathbf{k}$ lbf · in

At end *B* of arm *BC*: $\mathbf{F} = 300\mathbf{j}$ lbf, $\mathbf{M}_1 = 1200\mathbf{i}$ lbf · in, $\mathbf{T}_1 = 450\mathbf{k}$ lbf · in
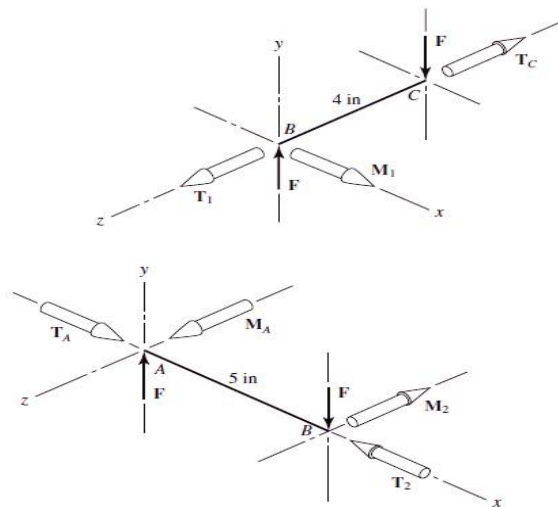
At end *B* of shaft *AB*: $\mathbf{F} = -300\mathbf{j}$ lbf, $\mathbf{T}_2 = -1200\mathbf{i}$ lbf · in, $\mathbf{M}_2 = -450\mathbf{k}$ lbf · in

At end *A* of shaft *AB*: $\mathbf{F} = 300\mathbf{j}$ lbf, $\mathbf{M}_A = 1950\mathbf{k}$ lbf · in, $\mathbf{T}_A = 1200\mathbf{i}$ lbf · in

Figure (1-7)

(b) For arm *BC*, the bending moment will reach a maximum near the shaft at *B*. If we assume this is 1200 lbf · in, then the bending stress for a rectangular section will be

Ans.
$$\sigma = \frac{M}{I/c} = \frac{6M}{bh^2} = \frac{6(1200)}{0.25(1.25)^2} = 18\ 400 \text{ psi}$$

Of course, this is not exactly correct, because at B the moment is actually being transferred into the shaft, probably through a weldment.

For the torsional stress, use Eq. (1–28). Thus

$$\tau_{max} = \frac{T}{bc^2}\left(3 + \frac{1.8}{b/c}\right) = \frac{450}{1.25(0.25^2)}\left(3 + \frac{1.8}{1.25/0.25}\right) = 19\,400 \text{ psi}$$

Ans.

This stress occurs at the middle of the $1\frac{1}{4}$-in side.

(c) For a stress element at A, the bending stress is tensile and is

$$\sigma_x = \frac{M}{I/c} = \frac{32M}{\pi d^3} = \frac{32(1950)}{\pi(0.75)^3} = 47\,100 \text{ psi} \qquad Ans.$$

The torsional stress is

$$\tau_{xz} = \frac{-T}{J/c} = \frac{-16T}{\pi d^3} = \frac{-16(1200)}{\pi(0.75)^3} = -14\,500 \text{ psi } Ans.$$

where the reader should verify that the negative sign accounts for the direction of τ_{xz}.

(d) Point A is in a state of plane stress where the stresses are in the xz plane. Thus the principal stresses are given by Eq. (1–6) with subscripts corresponding to the x, z axes.

The maximum normal stress is then given by

$$\sigma_1 = \frac{\sigma_x + \sigma_z}{2} + \sqrt{\left(\frac{\sigma_x - \sigma_z}{2}\right)^2 + \tau_{xz}^2}$$

$$= \frac{47.1 + 0}{2} + \sqrt{\left(\frac{47.1 - 0}{2}\right)^2 + (-14.5)^2} = 51.2 \text{ kpsi}$$

Ans.

19

The maximum shear stress at *A* occurs on surfaces different than the surfaces containing the principal stresses or the surfaces containing the bending and torsional shear stresses. The maximum shear stress is given by Eq. (1–7), again with modified subscripts, and is given by

$$\tau_1 = \sqrt{\left(\frac{\sigma_x - \sigma_z}{2}\right)^2 + \tau_{xz}^2} = \sqrt{\left(\frac{47.1 - 0}{2}\right)^2 + (-14.5)^2} = 27.7 \text{ kpsi}$$

Ans.

1-8. Stress Concentration

In the development of the basic stress equations for tension, compression, bending, and torsion, it was assumed that no geometric irregularities occurred in the member under consideration. But it is quite difficult to design a machine without permitting some changes in the cross sections of the members. Rotating shafts must have shoulders designed on them so that the bearings can be properly seated and so that they will take thrust loads; and the shafts must have key slots machined into them for securing pulleys and gears. A bolt has a head on one end and screw threads on the other end, both of which account for abrupt changes in the cross section. Other parts require holes, oil grooves, and notches of various kinds. Any discontinuity in a machine part alters the stress distribution in the neighborhood of the discontinuity so that the elementary stress equations no longer describe the state of stress in the part at these locations. Such discontinuities are called *stress raisers,* and the regions in which they occur are called areas of *stress concentration*.

The distribution of elastic stress across a section of a member may be uniform as in a bar in tension, linear as a beam in bending, or even rapid and curvaceous as in a sharply curved beam. Stress concentrations can arise from some irregularity not inherent in the member, such as tool marks, holes, notches, grooves, or threads. The *nominal stress* is said to exist if the member is free of the stress raiser. This definition is not always honored, so check the definition on the stress-concentration chart or table you are using.

A *theoretical,* or *geometric, stress-concentration factor* K_t or K_{ts} is used to relate the actual maximum stress at the discontinuity to the nominal stress. The factors are defined by the equations

$$K_t = \frac{\sigma_{max}}{\sigma_0} \qquad K_{ts} = \frac{\tau_{max}}{\tau_0} \qquad \text{1-30}$$

where K_t is used for normal stresses and K_{ts} for shear stresses. The nominal stress σ_0 or τ_0 is more difficult to define. Generally, it is the stress calculated by using the elementary stress equations and the net area, or net cross section. But sometimes the gross cross section is used instead, and so it is always wise to double check your source of K_t or K_{ts} before calculating the maximum stress.

The subscript t in K_t means that this stress-concentration factor depends for its value only on the *geometry* of the part. That is, the particular material used has no effect on the value of K_t. This is why it is called a *theoretical* stress-concentration factor.

The analysis of geometric shapes to determine stress-concentration factors is a difficult problem, and not many solutions can be found. Most stress-concentration factors are found by using experimental techniques. Though the finite-element method has been used, the fact that the elements are indeed finite prevents finding the true maximum stress. Experimental approaches generally used include photoelasticity, grid methods, brittle-coating methods, and electrical strain-gauge methods. Of course, the grid and strain-gauge methods both suffer from the same drawback as the finite-element method.

Stress-concentration factors for a variety of geometries may be found in the following charts.
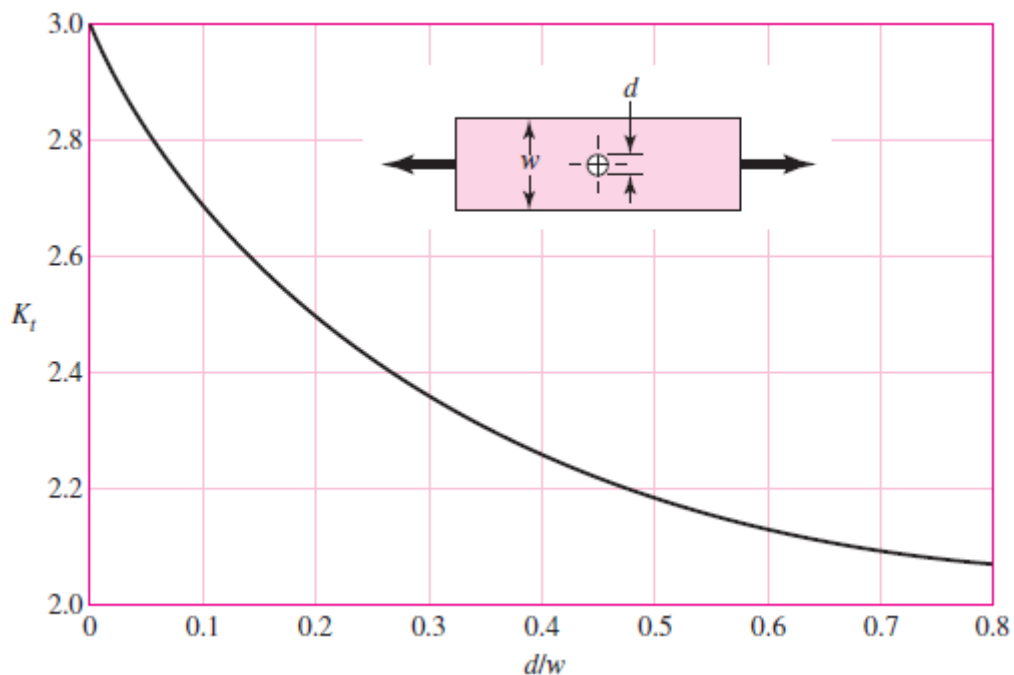

Figure (1-8)
Bar in tension or simple compression with a transverse hole.
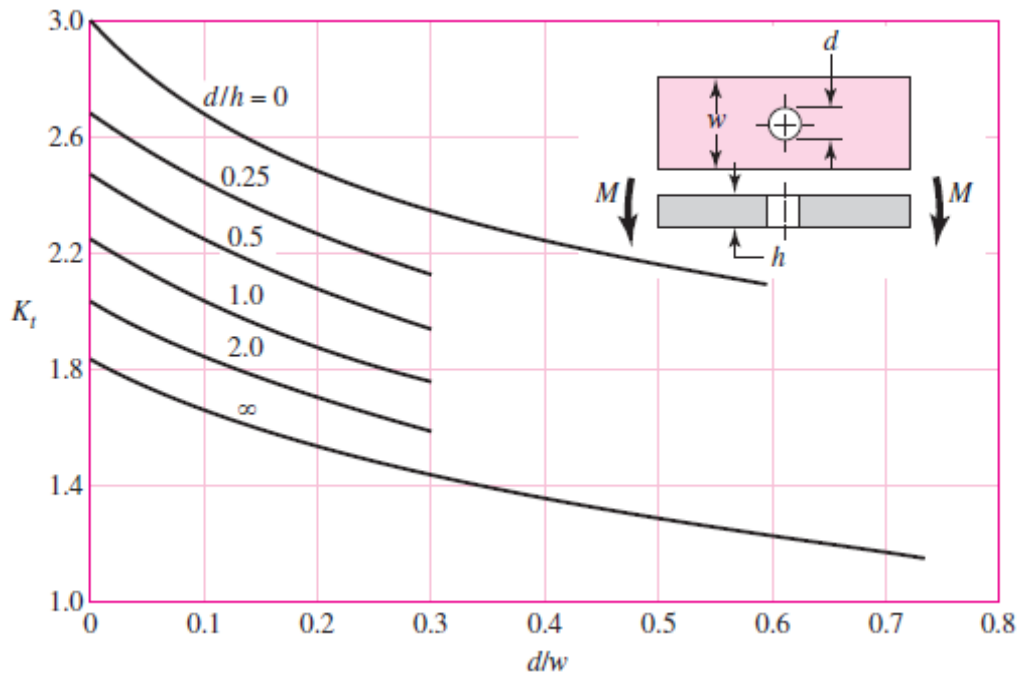$\sigma_0 = F/A$, where $A = (w - d)t$ and t is the thickness.

Figure (1-9)
Rectangular bar with a transverse hole in bending.
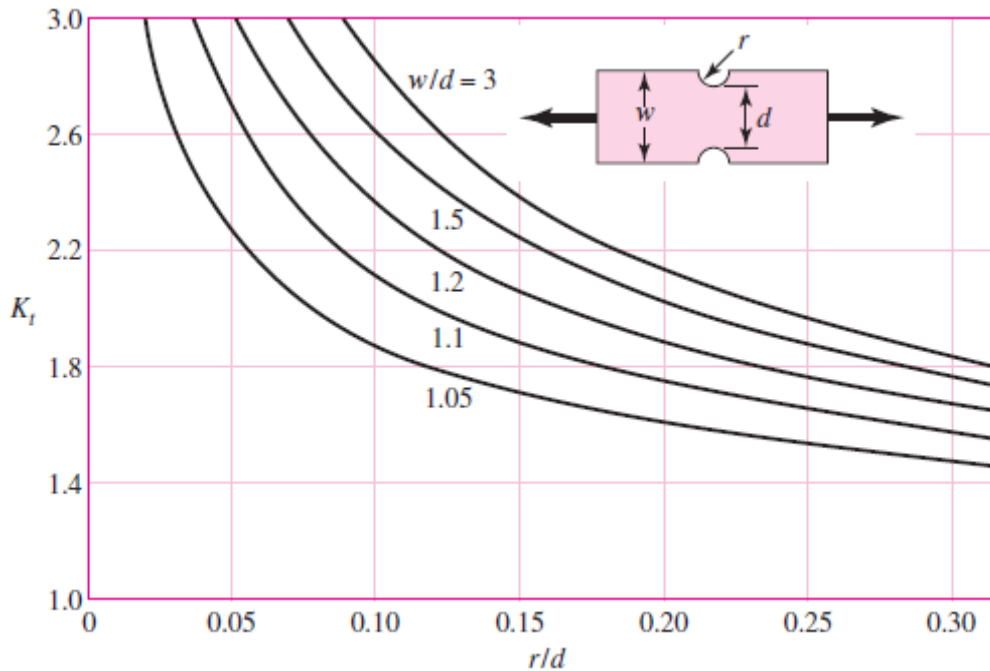$\sigma_0 = Mc/I$, where $I = (w - d)h^3/12$.

Figure (1-10)
Notched rectangular bar intension or simple compression.
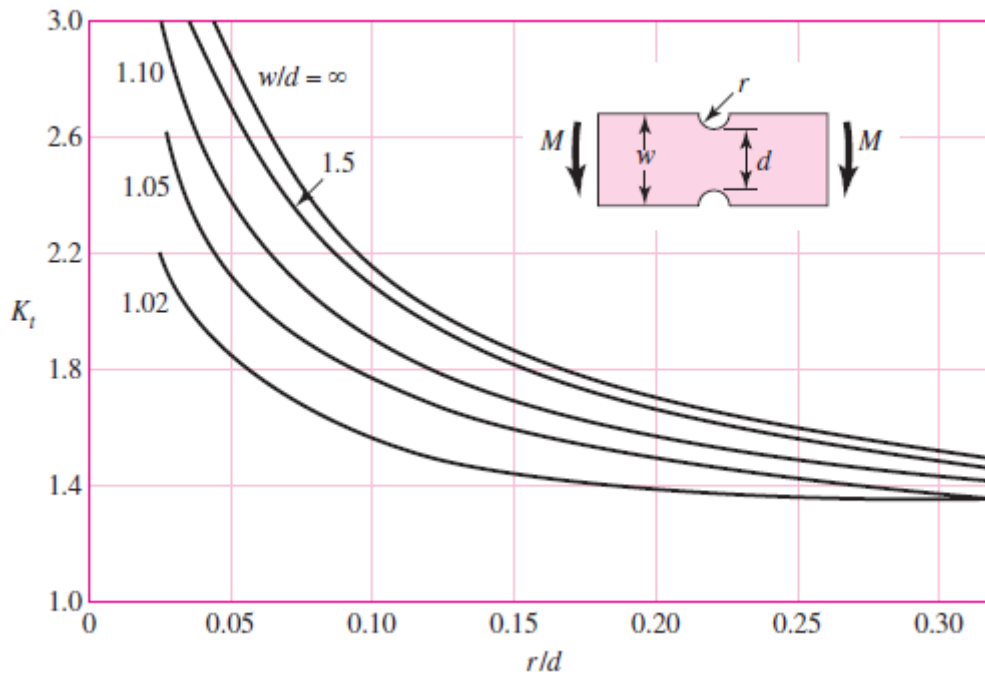$\sigma_0 = F/A$, where $A = dt$ and t is the thickness.

Figure (1-11)
Notched rectangular bar in bending. $\sigma_0 = Mc/I$, where
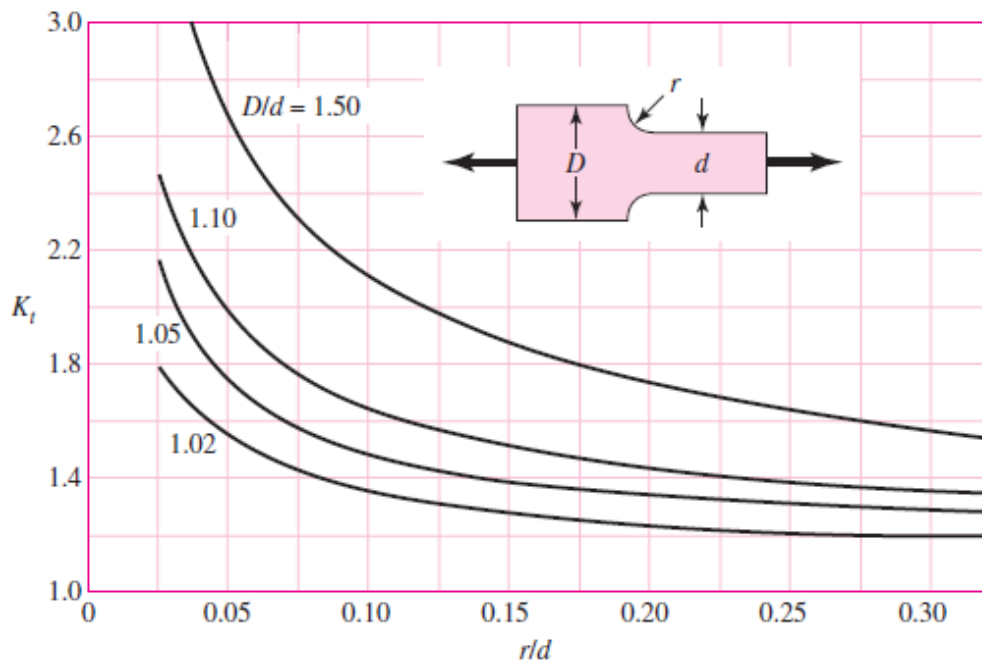$c = d/2$, $I = td^3/12$, and t is the thickness.

Figure (1-12)
Rectangular filleted bar in tension or simple compression.
$\sigma_0 = F/A$, where $A = dt$ and t is the thickness.
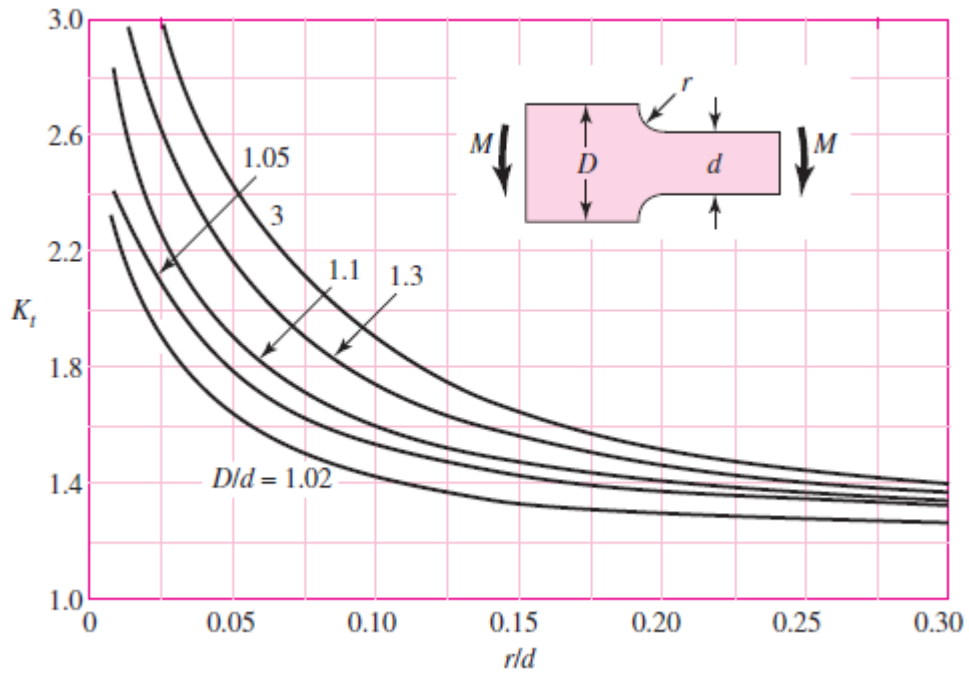
Figure (1-13)
Rectangular filleted bar in bending. $\sigma_0 = Mc/I$, where
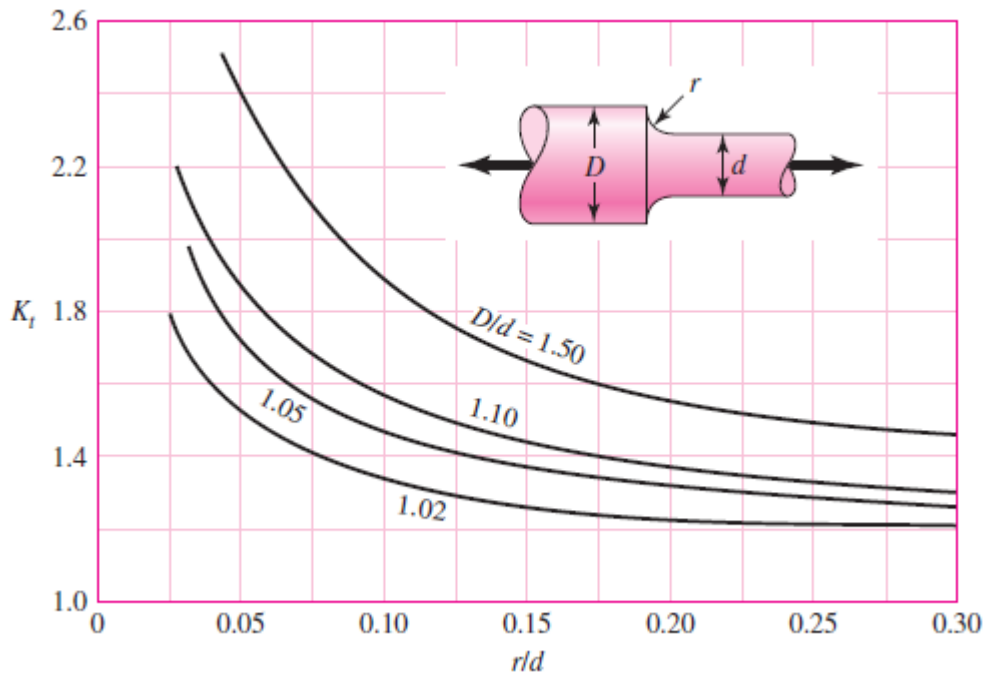$c = d/2$, $I = td^3/12$, t is the thickness.

Figure (1-14)
Round shaft with shoulder fillet in tension. $\sigma_0 = F/A$, where
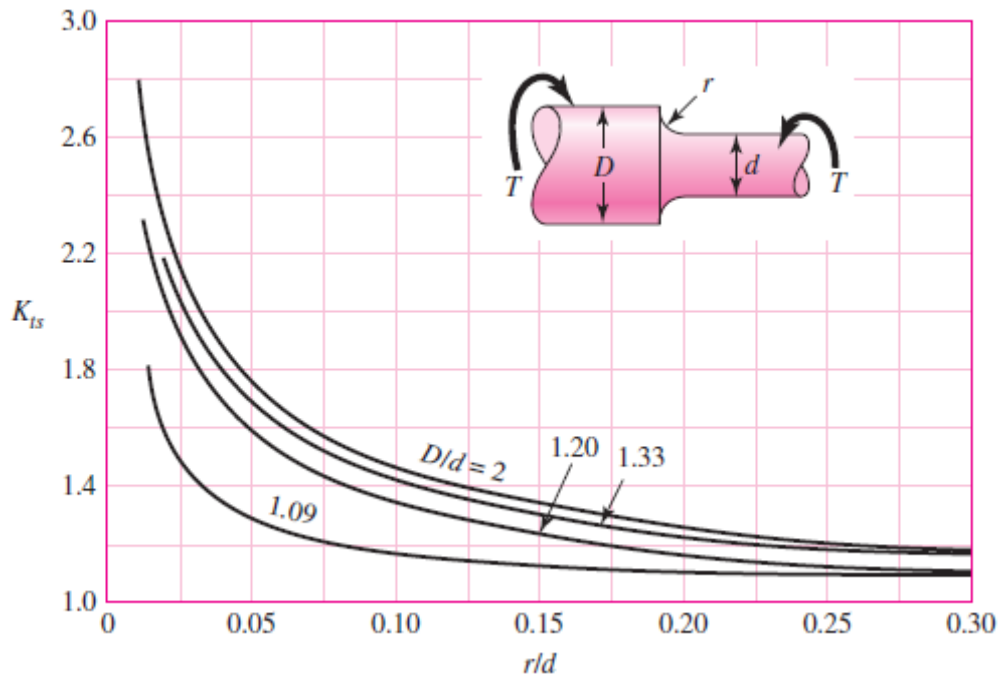$A = \pi d^2/4$.

Figure (1-15)
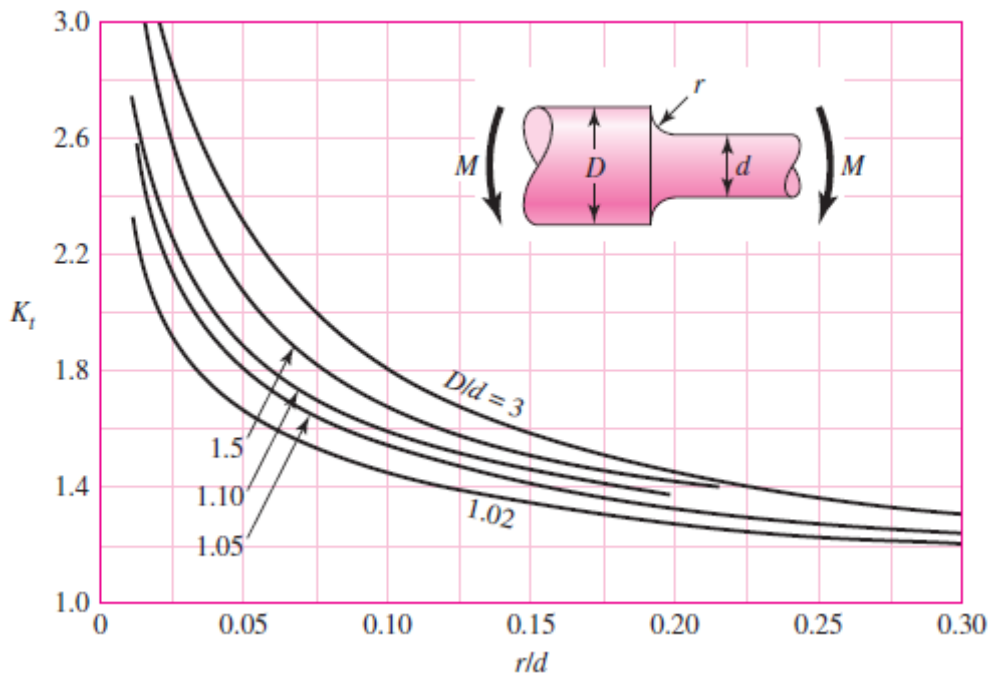Round shaft with shoulder fillet in torsion. $\tau_0 = Tc/J$, where $c = d/2$ and $J = \pi d^4/32$.

Figure (1-16)
Round shaft with shoulder fillet in bending. $\sigma_0 = Mc/I$, where $c = d/2$ and $I = \pi d^4/64$.
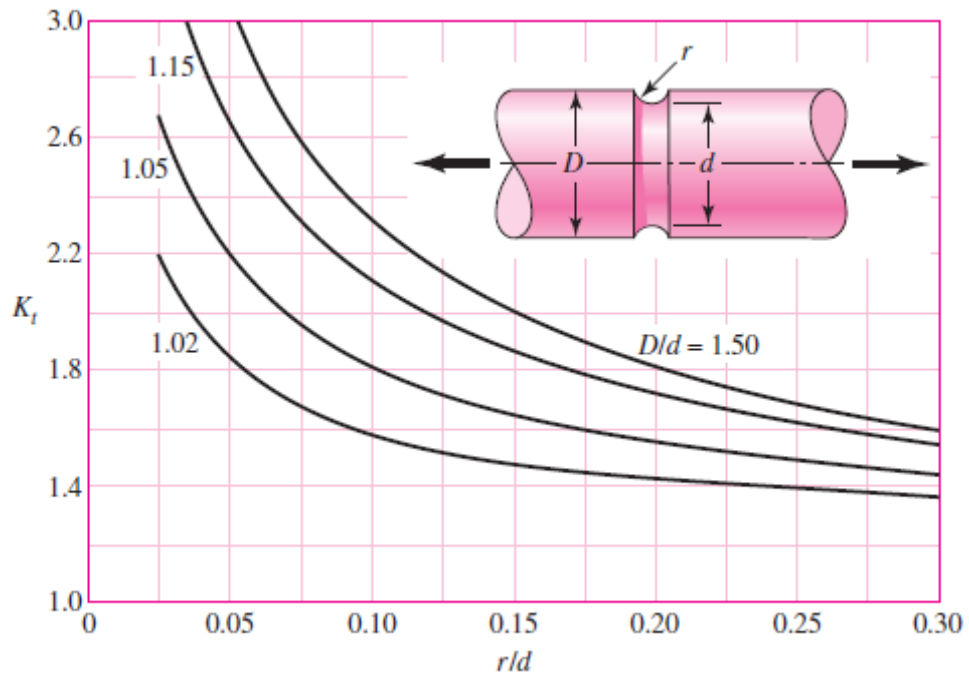
Figure (1-17)
Grooved round bar in tension. $\sigma_0 = F/A$, where
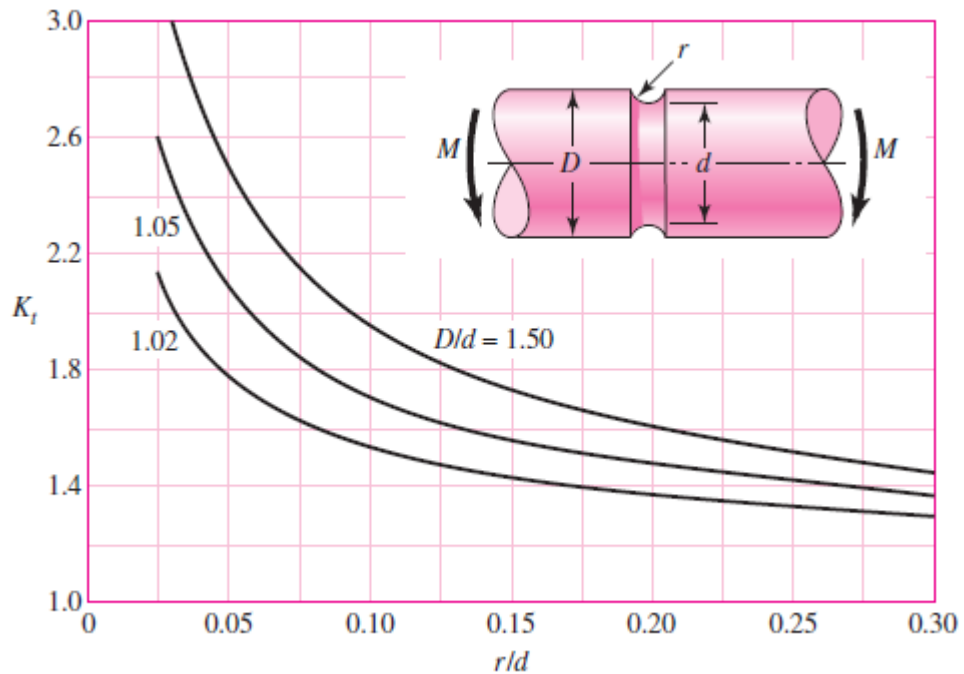$A = \pi d^2/4$.

Figure (1-18)
Grooved round bar in bending. $\sigma_0 = Mc/l$, where
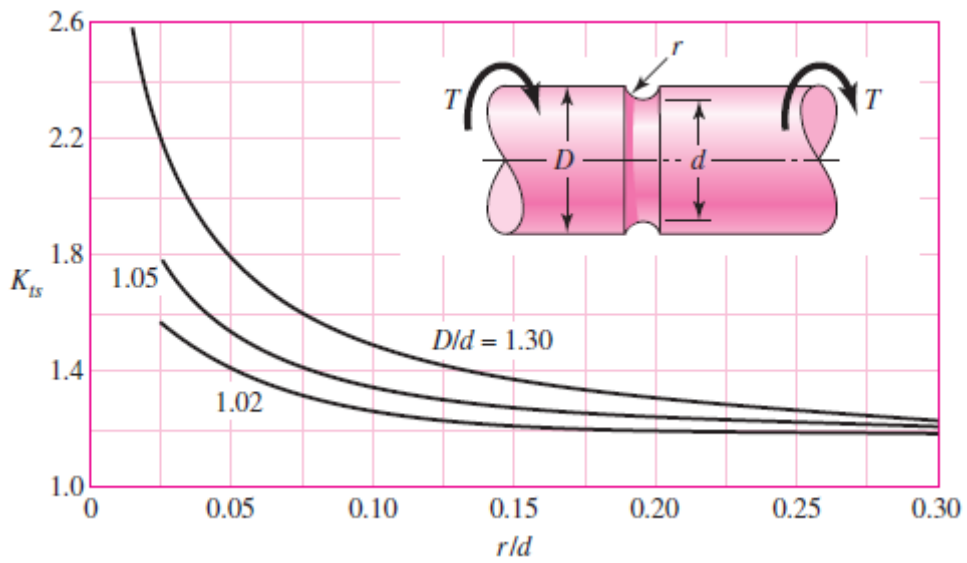$c = d/2$ and $I = \pi d^4/64$.

Figure (1-19)
Grooved round bar in torsion. $\tau_0 = Tc/J$, where
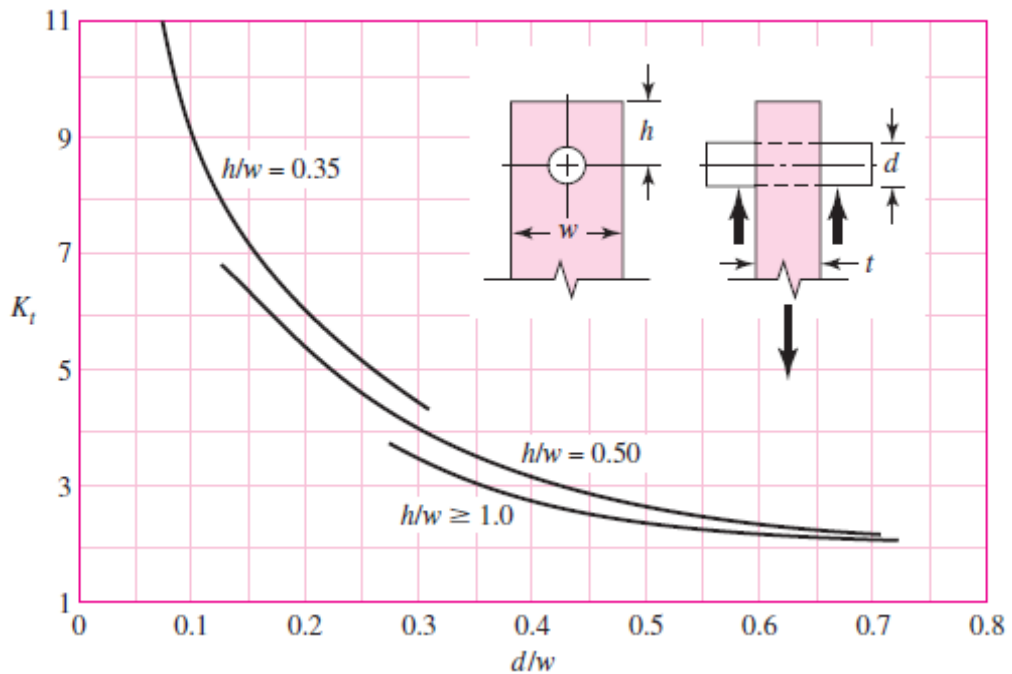$c = d/2$ and $J = \pi d^4/32$.

Figure (1-20)
Plate loaded in tension by a pin through a hole. $\sigma_0 = F/A$,
where $A = (w - d)t$.

EXAMPLE 1-3

Considering the stress concentration at point A shown in Fig. (1–21), determine the maximum normal and shear stresses at A if $F = 200$ lbf.

Solution

$$D/d = \frac{1.5}{1} = 1.5$$

$$r/d = \frac{1/8}{1} = 0.125$$

From Fig. (1–15):

$$K_{ts} \doteq 1.39$$

From Fig. (1–16):

$$K_t \doteq 1.60$$

Figure (1-21)

$$\sigma_A = K_t \frac{Mc}{I} = \frac{32 K_t M}{\pi d^3} = \frac{32(1.6)(200)(14)}{\pi(1^3)} = 45\,630 \text{ psi}$$

$$\tau_A = K_{ts} \frac{Tc}{J} = \frac{16 K_{ts} T}{\pi d^3} = \frac{16(1.39)(200)(15)}{\pi(1^3)} = 21\,240 \text{ psi}$$

$$\sigma_{max} = \frac{\sigma_A}{2} + \sqrt{\left(\frac{\sigma_A}{2}\right)^2 + \tau_A^2} = \frac{45.63}{2} + \sqrt{\left(\frac{45.63}{2}\right)^2 + 21.24^2}$$

$$= 54.0 \text{ kpsi} \quad Ans.$$

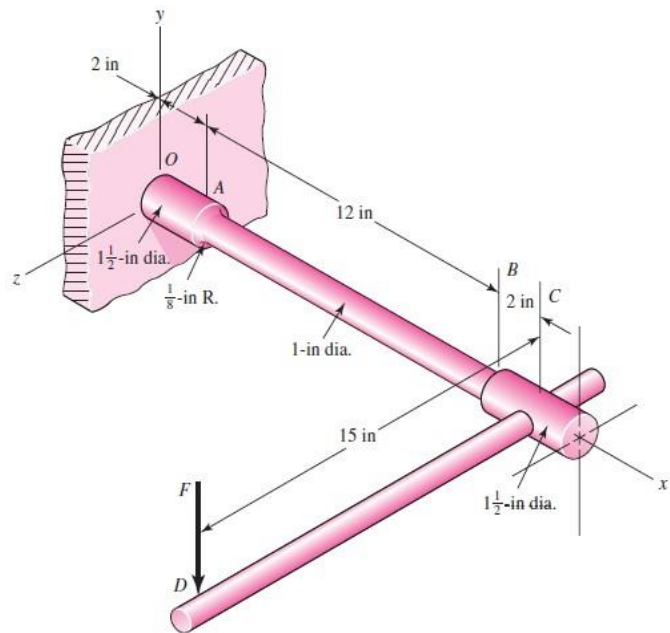$$\tau_{max} = \sqrt{\left(\frac{45.63}{2}\right)^2 + 21.24^2} = 31.2 \text{ kpsi} \qquad Ans.$$

2. Failures Resulting from Static Loading

A *static load* is a stationary force or couple applied to a member. To be stationary, the force or couple must be unchanging in magnitude, point or points of application, and direction. A static load can produce axial tension or compression, a shear load, a bending load, a torsional load, or any combination of these. To be considered static, the load cannot change in any manner.

In this part we consider the relations between strength and static loading in order to make the decisions concerning material and its treatment, fabrication, and geometry for satisfying the requirements of functionality, safety, reliability, competitiveness, usability, manufacturability, and marketability. How far we go down this list is related to the scope of the examples.

Stress Concentration

Stress concentration (see Sec. 1–8) is a highly localized effect. In some instances it may be due to a surface scratch. If the material is ductile and the load static, the design load may cause yielding in the critical location in the notch. This yielding can involve strain strengthening of the material and an increase in yield strength at the small critical notch location. Since the loads are static and the material is ductile, that part can carry the loads satisfactorily with no general yielding. In these cases the designer sets the geometric (theoretical) stress concentration factor K_t to unity.

When using this rule for ductile materials with static loads, be careful to assure yourself that the material is not susceptible to brittle fracture in the environment of use.

Brittle materials do not exhibit a plastic range. A brittle material "feels" the stress concentration factor K_t or K_{ts}.

An exception to this rule is a brittle material that inherently contains microdiscontinuity stress concentration, worse than the macrodiscontinuity that the designer has in mind. Sand molding introduces sand particles, air, and water vapor bubbles. The grain structure of cast iron contains graphite flakes (with little strength), which are literally cracks introduced during the solidification process. When a tensile test on a cast iron is performed, the strength reported in the literature *includes* this stress concentration. In such cases K_t or K_{ts} need not be applied.

2-1. Failure Theories

Unfortunately, there is no universal theory of failure for the general case of material properties and stress state. Instead, over the years several hypotheses have been formulated and tested, leading to today's accepted practices. Being accepted, we will characterize these "practices" as *theories* as most designers do.

Structural metal behavior is typically classified as being ductile or brittle, although under special situations, a material normally considered ductile can fail in a brittle manner. Ductile materials are normally classified such that $\varepsilon_f \geq 0.05$ and have an identifiable yield strength that is often the same in compression as in tension ($S_{yt} = S_{yc} = S_y$). Brittle materials, $\varepsilon_f < 0.05$, do not exhibit an identifiable yield strength, and are typically classified by ultimate tensile and compressive strengths, S_{ut} and S_{uc}, respectively (where S_{uc} is given as a positive quantity). The generally accepted theories are:

> **Ductile materials** (yield criteria)
> • Maximum shear stress (MSS)
> • Distortion energy (DE)
> • Ductile Coulomb-Mohr (DCM)
>
> **Brittle materials** (fracture criteria)
> • Maximum normal stress (MNS)
> • Brittle Coulomb-Mohr (BCM)
> • Modified Mohr (MM)

2-2. Maximum-Shear-Stress Theory for Ductile Materials (MSS)

The *maximum-shear-stress theory* predicts that *yielding begins whenever the maximum shear stress in any element equals or exceeds the maximum shear stress in a tension-test specimen of the same material when that specimen begins to yield*.

The maximum-shear-stress theory predicts yielding when

$$\tau_{max} = \frac{\sigma_1 - \sigma_2}{2} = \frac{S_y}{2n}$$

Where S_y is the yielding stress, and n is the factor of safety. Note that this implies that the yield strength in shear is given by

$$S_{sy} = 0.5S_y$$

The MSS theory is also referred to as the *Tresca* or *Guest theory*. It is an acceptable theory but conservative predictor of failure; and since engineers are conservative by nature, it is quite often used.

2-3. Distortion-Energy Theory for Ductile Materials (DE)

The distortion-energy theory predicts that yielding occurs when the distortion strain energy per unit volume reaches or exceeds the distortion strain energy per unit volume for yield in simple tension or compression of the same material.

The distortion-energy theory is also called:
• The von Mises or von Mises–Hencky theory
• The shear-energy theory
• The octahedral-shear-stress theory

The distortion-energy theory predicts yielding when

$$\sigma' = \frac{S_y}{n}$$

where σ' is usually called the *von Mises stress,* named after Dr. R. von Mises, who contributed to the theory; and

$$\sigma' = \left(\sigma_x^2 - \sigma_x\sigma_y + \sigma_y^2 + 3\tau_{xy}^2\right)^{1/2}$$

The shear yield strength predicted by the distortion-energy theory is

$$S_{sy} = 0.577S_y$$

EXAMPLE 2-1

A hot-rolled steel has a yield strength of $S_{yt} = S_{yc} = 100$ kpsi and a true strain at fracture of $\varepsilon_f = 0.55$. Estimate the factor of safety for the following principal stress states:

(*a*) 70, 70, 0 Mpa
(*b*) 30, 70, 0 Mpa.
(*c*) 0, 70, −30 Mpa.
(*d*) 0, −30, −70 Mpa.
(*e*) 30, 30, 30 Mpa.

Solution

2-4. Coulomb-Mohr Theory for Ductile Materials (DCM)

A variation of Mohr's theory, called the *Coulomb-Mohr theory* or the *internal-friction theory*.
Not all materials have compressive strengths equal to their corresponding tensile values. For example, the yield strength of magnesium alloys in compression may be as little as 50 percent of their yield strength in tension. The ultimate strength of gray cast irons in compression varies from 3 to 4 times greater than the ultimate tensile strength. So, this theory can be used to predict failure for materials whose strengths in tension and compression are not equal; this is can be expressed as a design equation with a factor of safety, *n*, as

$$\frac{\sigma_1}{S_t} - \frac{\sigma_3}{S_c} = 1$$

where either yield strength or ultimate strength can be used.
The torsional yield strength occurs when $\tau_{max} = S_{sy}$; then

$$S_{sy} = \frac{S_{yt} S_{yc}}{S_{yt} + S_{yc}}$$

EXAMPLE 2-2

A 25-mm-diameter shaft is statically torqued to 230 N·m. It is made of cast 195-T6 aluminum, with a yield strength in tension of 160 MPa and a yield strength in compression of 170 MPa. It is machined to final diameter. Estimate the factor of safety of the shaft.

Solution
The maximum shear stress is given by

$$\tau = \frac{16T}{\pi d^3} = \frac{16(230)}{\pi \left[25\left(10^{-3}\right)\right]^3} = 75\left(10^6\right) \text{N/m}^2 = 75\,\text{MPa}$$

The two nonzero principal stresses are 75 and −75 MPa, making the ordered principal stresses $\sigma_1 = 75$, $\sigma_2 = 0$, and $\sigma_3 = -75$ MPa. From Eq. (2–6), for yield,

$$n = \frac{1}{\sigma_1/S_{yt} - \sigma_3/S_{yc}} = \frac{1}{75/160 - (-75)/170} = 1.10$$

Alternatively, from Eq. (2–7),

$$S_{sy} = \frac{S_{yt}\,S_{yc}}{S_{yt} + S_{yc}} = \frac{160(170)}{160 + 170} = 82.4\,\text{MPa}$$

and $\tau_{\max} = 75$ MPa. Thus,

$$n = \frac{S_{sy}}{\tau_{\max}} = \frac{82.4}{75} = 1.10$$

2-5. Maximum-Normal-Stress Theory for Brittle Materials (MNS)

The maximum-normal-stress (MNS) theory states that *failure occurs whenever one of the three principal stresses equals or exceeds the strength*. Again we arrange the principal stresses for a general stress state in the ordered form $\sigma_1 \geq \sigma_2 \geq \sigma_3$. This theory then predicts that failure occurs whenever

$$\sigma_1 \geq S_{ut} \qquad \text{or} \qquad \sigma_3 \leq -S_{uc}$$

where S_{ut} and S_{uc} are the ultimate tensile and compressive strengths, respectively, given as positive quantities.

2-6. Modifications of the Mohr Theory for Brittle Materials

We will discuss two modifications of the Mohr theory for brittle materials: the Brittle- Coulomb-Mohr (BCM) theory and the modified Mohr (MM) theory. The equations provided for the theories will be restricted to plane stress and be of the design type incorporating the factor of safety.

Brittle-Coulomb-Mohr (BCM)

$$\sigma_A = \frac{S_{ut}}{n} \qquad \sigma_A \geq \sigma_B \geq 0$$

$$\frac{\sigma_A}{S_{ut}} - \frac{\sigma_B}{S_{uc}} = \frac{1}{n} \qquad \sigma_A \geq 0 \geq \sigma_B$$

$$\sigma_B = -\frac{S_{uc}}{n} \qquad 0 \geq \sigma_A \geq \sigma_B$$

Modified Mohr (MM)

$$\sigma_A = \frac{S_{ut}}{n} \qquad \sigma_A \geq \sigma_B \geq 0$$

$$\sigma_A \geq 0 \geq \sigma_B \quad \text{and} \quad \left|\frac{\sigma_B}{\sigma_A}\right| \leq 1$$

$$\frac{(S_{uc} - S_{ut})\sigma_A}{S_{uc}S_{ut}} - \frac{\sigma_B}{S_{uc}} = \frac{1}{n} \qquad \sigma_A \geq 0 \geq \sigma_B \quad \text{and} \quad \left|\frac{\sigma_B}{\sigma_A}\right| > 1$$

$$\sigma_B = -\frac{S_{uc}}{n} \qquad 0 \geq \sigma_A \geq \sigma_B$$

EXAMPLE 2-4

Consider the wrench in Ex. (2–3), Fig. (2–1), as made of cast iron, machined to dimension. The force *F* required to fracture this part can be regarded as the strength of the component part. If the material is cast iron, the tensile ultimate strength is 31 kpsi and the compressive ultimate strength is 109 kpsi, find the force *F* with
(a) Coulomb-Mohr failure model   (*b*) Modified Mohr failure model.

2-7. Selection of Failure Criteria

For ductile behavior the preferred criterion is the distortion-energy theory, although some designers also apply the maximum-shear-stress theory because of its simplicity and conservative nature. In the rare case when $S_{yt} \neq S_{yc}$, the ductile Coulomb-Mohr method is employed.

For brittle behavior, the original Mohr hypothesis, constructed with tensile, compression, and torsion tests, with a curved failure locus is the best hypothesis we have. However, the difficulty of applying it without a computer leads engineers to choose modifications, namely, Coulomb Mohr, or modified Mohr. Figure (2–2) provides a summary flowchart for the selection of an effective procedure for analyzing or predicting failures from static loading for brittle or ductile behavior.
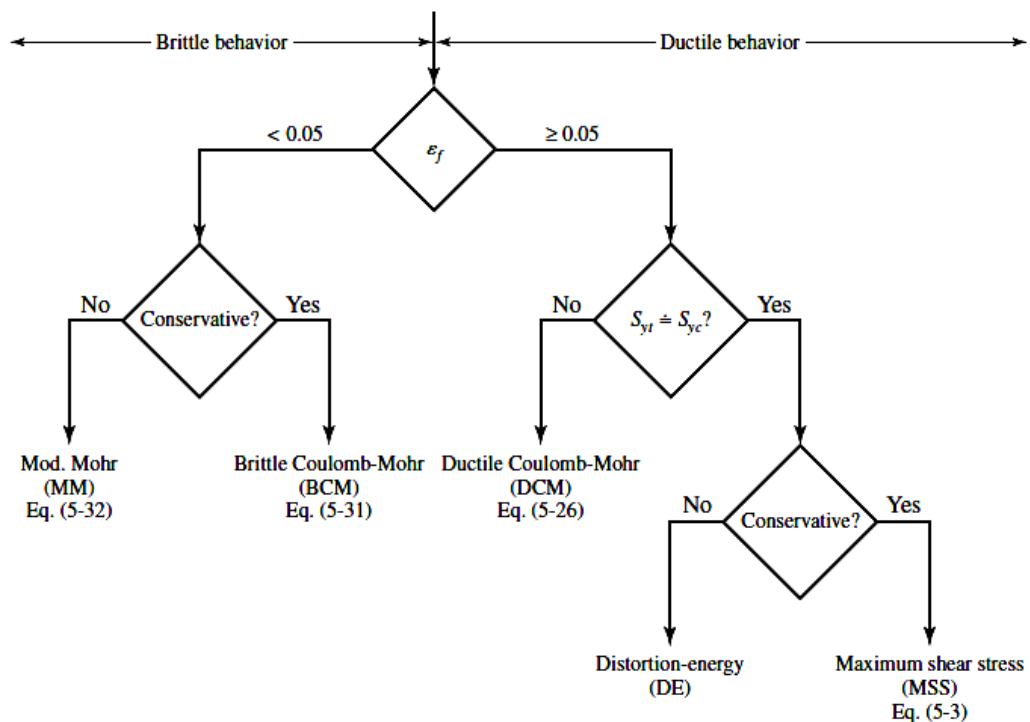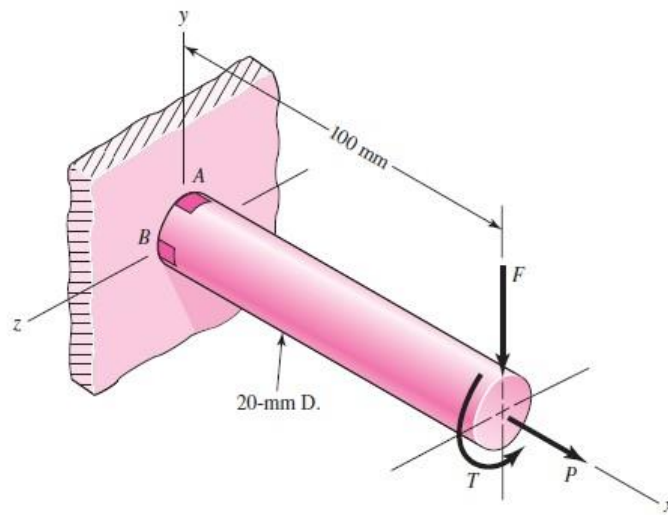

Figure (2-2)

Failure theory selection flowchart.

35

Homework

(1)   The cantilevered bar shown in the figure is made of AISI 1006 cold-drawn steel with (S_y = 280 MPa) and is loaded by the forces F = 0.55 kN, P = 8 kN, and T = 30 N·m. Compute the factor of safety, based upon the distortion-energy theory, for stress elements at A. (*Ans./ n* = 2.77)

3. Fatigue Failure Resulting from Variable Loading

In most testing of those properties of materials that relate to the stress-strain diagram, the load is applied gradually, to give sufficient time for the strain to fully develop. Furthermore, the specimen is tested to destruction, and so the stresses are applied only once. Testing of this kind is applicable, to what are known as *static conditions;* such conditions closely approximate the actual conditions to which many structural and machine members are subjected.

The condition frequently arises, however, in which the stresses vary with time or they fluctuate between different levels. For example, a particular fiber on the surface of a rotating shaft subjected to the action of bending loads undergoes both tension and compression for each revolution of the shaft. If the shaft is part of an electric motor rotating at 1725 rev/min, the fiber is stressed in tension and compression 1725 times each minute. If, in addition, the shaft is also axially loaded (as it would be, for example, by a helical or worm gear), an axial component of stress is superposed upon the bending component. In this case, some stress is always present in any one fiber, but now the *level* of stress is fluctuating. These and other kinds of loading occurring in machine members produce stresses that are called *variable, repeated, alternating,* or *fluctuating* stresses.

Often, machine members are found to have failed under the action of repeated or fluctuating stresses; yet the most careful analysis reveals that the actual maximum stresses were well below the ultimate strength of the material, and quite frequently even below the yield strength. The most distinguishing characteristic of these failures is that the stresses have been repeated a very large number of times. Hence the failure is called a *fatigue failure*.

When machine parts fail statically, they usually develop a very large deflection, because the stress has exceeded the yield strength, and the part is replaced before fracture actually occurs. Thus many static failures give visible warning in advance. But a fatigue failure gives no warning! It is sudden and total, and hence dangerous. It is relatively simple to design against a static failure, because our knowledge is comprehensive. Fatigue is a much more complicated phenomenon, only partially understood, and the engineer seeking competence must acquire as much knowledge of the subject as possible.

Fatigue failure is due to crack formation and propagation. A fatigue crack will typically initiate at a discontinuity in the material where the cyclic stress is a maximum. Discontinuities can arise because of:

• Design of rapid changes in cross section, keyways, holes, etc. where stress concentrations occur
• Elements that roll and/or slide against each other (bearings, gears, cams, etc.) under high contact pressure, developing concentrated subsurface contact stresses that can cause surface pitting or spalling after many cycles of the load
• Carelessness in locations of stamp marks, tool marks, scratches, and burrs; poor joint design; improper assembly; and other fabrication faults
• Composition of the material itself as processed by rolling, forging, casting, extrusion, drawing, heat treatment, etc. Microscopic and submicroscopic surface and subsurface discontinuities arise, such as inclusions of foreign material, alloy segregation, voids, hard precipitated particles, and crystal discontinuities

Various conditions that can accelerate crack initiation include residual tensile stresses, elevated temperatures, temperature cycling, a corrosive environment, and high-frequency cycling.

Approach to Fatigue Failure in Analysis and Design

As noted in the previous section, there are a great many factors to be considered, even for very simple load cases. The methods of fatigue failure analysis represent a combination of engineering and science. Often science fails to provide the complete answers that are needed. But the airplane must still be made to fly—safely. And the automobile must be manufactured with a reliability that will ensure a long and trouble free life and at the same time produce profits for the stockholders of the industry. Thus, while science has not yet completely explained the complete mechanism of fatigue, the engineer must still design things that will not fail. In a sense this is a classic example of the true meaning of engineering as contrasted with science. Engineers use science to solve their problems if the science is available. But available or not, the problem must be solved, and whatever form the solution takes under these conditions is called *engineering*.

3.1 The Stress-Life Method

To determine the strength of materials under the action of fatigue loads, specimens are subjected to repeated or varying forces of specified magnitudes while the cycles or stress reversals are counted to destruction.

To establish the fatigue strength of a material, quite a number of tests are necessary because of the statistical nature of fatigue. The results are plotted as an *S-N* diagram (Fig. 3–1). This chart may be plotted on semilog paper or on log-log paper. In the case of ferrous metals and alloys, the graph becomes horizontal after the material has been stressed for a certain number of cycles.
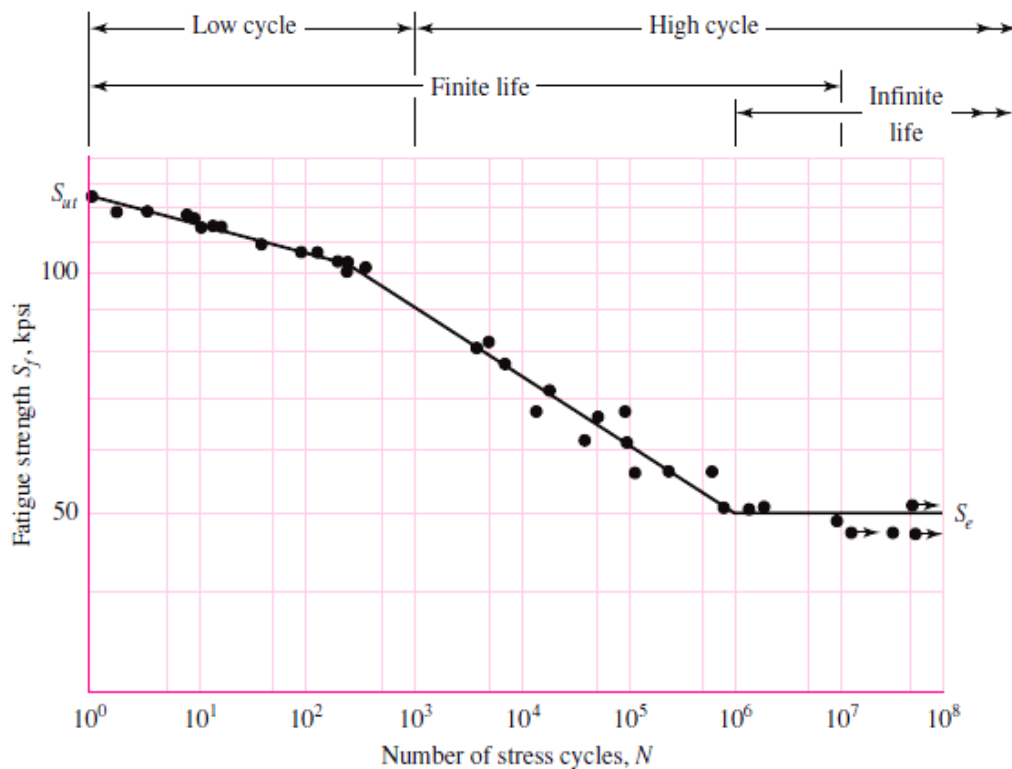

Figure (3-1)
An *S-N* diagram plotted from the results of completely reversed axial fatigue tests. Material: UNS G41300 steel, normalized; S_{ut}=116 kpsi.

The ordinate of the *S-N* diagram is called the *fatigue strength S_f* ; a statement of this strength value must always be accompanied by a statement of the number of cycles *N* to which it corresponds.

39

In the case of the steels, a knee occurs in the graph, and beyond this knee failure will not occur, no matter how great the number of cycles. The strength corresponding to the knee is called the *endurance limit* (S_e), or the fatigue limit. The graph of Fig. (3–1) never does become horizontal for nonferrous metals and alloys, and hence these materials do not have an endurance limit.

The body of knowledge available on fatigue failure from $N = 1$ to $N = 1000$ cycles is generally classified as *low-cycle fatigue,* as indicated in Fig. (3–1). *High-cycle fatigue,* then, is concerned with failure corresponding to stress cycles greater than 10^3 cycles.

Also a *finite-life region* and an *infinite-life region* are distinguished. The boundary between these regions cannot be clearly defined except for a specific material; but it lies somewhere between 10^6 and 10^7 cycles for steels, as shown in the figure.
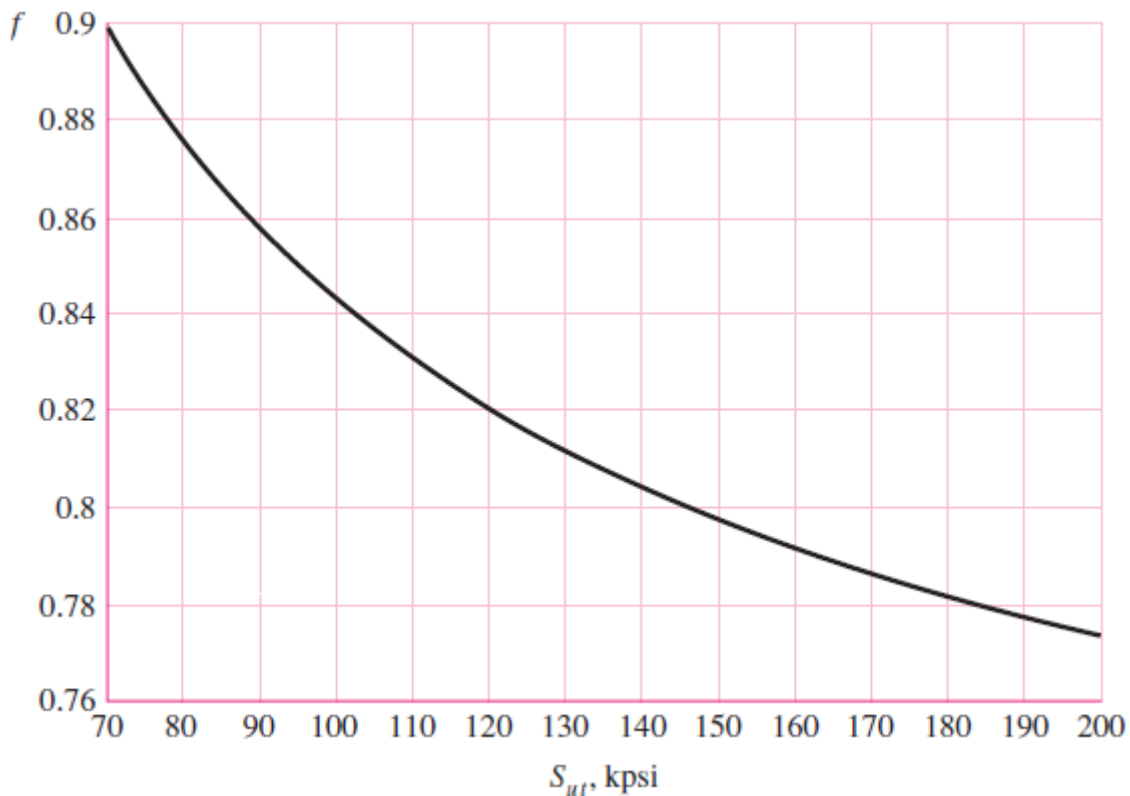
Fatigue strength fraction, f, of S_{ut} at 103 cycles for $S_e = S'_e = 0.5S_{ut}$.

$$a = \frac{(f\,S_{ut})^2}{S_e} \qquad\qquad b = -\frac{1}{3} \log\left(\frac{f\,S_{ut}}{S_e}\right)$$

If a completely reversed stress σ_a is given, the number of cycles-to-failure can be expressed as

$$N = \left(\frac{\sigma_a}{a}\right)^{1/b}$$

3.2 The endurance Limit

The determination of endurance limits by fatigue testing is now routine, though a lengthy procedure. Generally, stress testing is preferred to strain testing for endurance limits.

There are great quantities of data in the literature on the results of rotating-beam tests and simple tension tests of specimens taken from the same bar or ingot. The endurance limit ranges from about 40 to 60 percent of the tensile strength for steels up to about 210 kpsi (1450 MPa). For steels, the endurance limit may be estimated as

$$S_e' = \begin{cases} 0.5S_{ut} & S_{ut} \le 200 \text{ kpsi (1400 MPa)} \\ 100 \text{ kpsi} & S_{ut} > 200 \text{ kpsi} \\ 700 \text{ MPa} & S_{ut} > 1400 \text{ MPa} \end{cases} \qquad 3\text{-}1$$

where S_{ut} is the *minimum* tensile strength. The prime mark on S_e' in this equation refers to the *rotating-beam specimen*.

When designs include detailed heat-treating specifications to obtain specific microstructures, it is possible to use an estimate of the endurance limit based on test data for the particular microstructure; such estimates are much more reliable and indeed should be used.

3.3 Endurance Limit Modifying Factors

Joseph Marin identified factors that quantified the effects of surface condition, size, loading, temperature, and miscellaneous items. A Marin equation is written as

$$S_e = k_a k_b k_c k_d k_e k_f \ S'_e \qquad\qquad 3\text{-}2$$

Where

k_a = surface condition modification factor
k_b = size modification factor
k_c = load modification factor
k_d = temperature modification factor
k_e = reliability factor
k_f = miscellaneous-effects modification factor
S'_e = rotary-beam test specimen endurance limit
S_e = endurance limit at the critical location of a machine part
 in the geometry and condition of use

When endurance tests of parts are not available, estimations are made by applying Marin factors to the endurance limit.

➢ *Surface Factor k_a*

$$k_a = a S_{ut}^b \qquad\qquad 3\text{-}3$$

where S_{ut} is the minimum tensile strength and *a* and *b* are to be found in the following table.

Table (3–1)
Parameters for Marin surface modification factor, Eq. (3–3)

Surface finish	Factor *a*		Exponent *b*
	S_{ut}, kpsi	S_{ut}, MPa	
Ground	1.34	1.58	−0.085
Machined or cold-drawn	2.7	4.51	−0.265
Hot-rolled	14.4	57.7	−0.718
As-forged	39.9	272	−0.995

EXAMPLE 3–1

A steel has a minimum ultimate strength of 520 MPa and a machined surface. Estimate k_a.

Solution

From Table (3–1), $a = 4.51$ and $b = -0.265$. Then, from Eq. (3–3)

$$k_a = 4.51(520)^{-0.265} = 0.860 \qquad\qquad Ans.$$

Again, it is important to note that this is an approximation as the data is typically quite scattered. Furthermore, this is not a correction to take lightly. For example, if in the previous example the steel was forged, the correction factor would be 0.540, a significant reduction of strength.

➢ **Size Factor k_b**

For round shafts in bending and torsion when rotating, k_b　　　may be expressed as

$$k_b = \begin{cases} (d/0.3)^{-0.107} = 0.879d^{-0.107} & 0.11 \leq d \leq 2 \text{ in} \\ 0.91d^{-0.157} & 2 < d \leq 10 \text{ in} \\ (d/7.62)^{-0.107} = 1.24d^{-0.107} & 2.79 \leq d \leq 51 \text{ mm} \\ 1.51d^{-0.157} & 51 < d \leq 254 \text{ mm} \end{cases} \qquad 3\text{-}4$$

The effective size of a round corresponding to a non-rotating solid or hollow round,

$$d_e = 0.37d \qquad\qquad 3\text{-}5$$

For a rectangular section of dimensions $h \times b$

$$d_e = 0.808(hb)^{1/2} \qquad\qquad 3\text{-}6$$

For axial loading there is no size effect, so

$$k_b = 1 \qquad\qquad 3\text{-}7$$

EXAMPLE 3–2

A steel shaft loaded in bending is 32 mm in diameter, abutting a filleted shoulder 38 mm in diameter. The shaft material has a mean ultimate tensile strength of 690 MPa. Estimate the Marin size factor k_b if the shaft is used in
(a) A rotating mode.
(b) A non-rotating mode.

Solution

(a) From Eq. (3–4)
$k_b = (d/7.62)^{-0.107} = (32/7.62)^{-0.107} = 0.858$ *Ans.*

(b) From Eq. (3–5),
$d_e = 0.37d = 0.37(32) = 11.84$ mm

Then, from Eq. (3–4)
$k_b = (d/7.62)^{-0.107} = (11.84/7.62)^{-0.107} = 0.954$ *Ans.*

➤ *Loading Factor k_c*

When fatigue tests are carried out with rotating bending, axial (push-pull), and torsional loading, the endurance limits differ with S_{ut}. The average values of the load factor are specified as

$$k_c = \begin{cases} 1 & \text{bending} \\ 0.85 & \text{axial} \\ 0.59 & \text{torsion}^* \end{cases} \qquad \text{3-8}$$

*The latter is used only for pure torsional fatigue loading. When torsion is combined with other stresses, such as bending, $k_c = 1$.

➤ *Temperature Factor k_d*

When operating temperatures are below room temperature, brittle fracture is a strong possibility and should be investigated first. When the operating temperatures are higher than room temperature, yielding should be investigated first because the yield strength drops

off so rapidly with temperature; see Fig. (3–2). Any stress will induce creep in a material operating at high temperatures; so this factor must be considered too.

Finally, it may be true that there is no fatigue limit for materials operating at high temperatures. Because of the reduced fatigue resistance, the failure process is, to some extent, dependent on time.
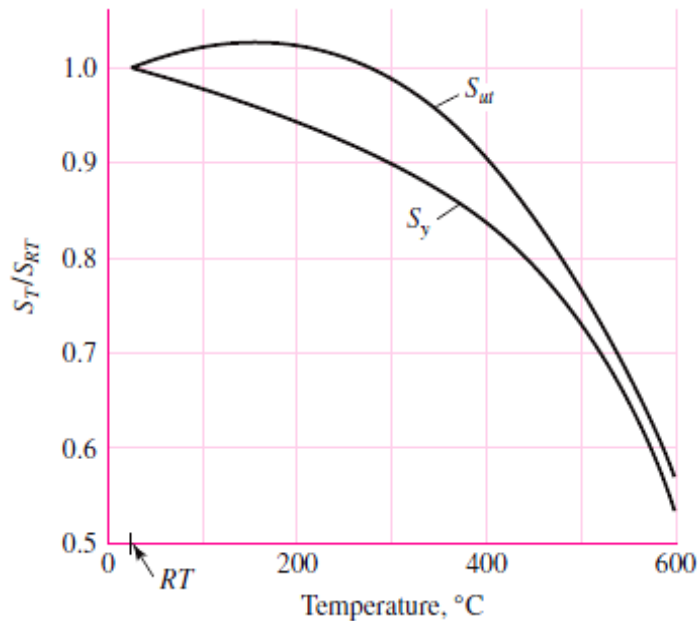

Figure (3–2)
A plot of the results of 145 tests of 21 carbon and alloy steels showing the effect of operating temperature on the yield strength S_y and the ultimate strength S_{ut} . The ordinate is the ratio of the strength at the operating temperature (S_T) to the strength at room temperature (S_{RT}).

Table (3–2) has been obtained from Fig. (3–2) by using only the tensile-strength data. Note that the table represents 145 tests of 21 different carbon and alloy steels. A fourth-order polynomial curve fit to the data underlying Fig. (3–2) gives

$$k_d = 0.975 + 0.432(10^{-3})T_F - 0.115(10^{-5})T_F^2$$
$$+ 0.104(10^{-8})T_F^3 - 0.595(10^{-12})T_F^4 \qquad \text{3-9}$$

where $70 \leq T_F \leq 1000$ F.

Table (3–2)
Effect of operating temperature on the tensile strength of
steel. (S_T = tensile strength at operating temperature;
S_{RT} = tensile strength at room temperature)

Temperature °C	S_T/S_{RT}	Temperature °F	S_T/S_{RT}
20	1.000	70	1.000
50	1.010	100	1.008
100	1.020	200	1.020
150	1.025	300	1.024
200	1.020	400	1.018
250	1.000	500	0.995
300	0.975	600	0.963
350	0.943	700	0.927
400	0.900	800	0.872
450	0.843	900	0.797
500	0.768	1000	0.698
550	0.672	1100	0.567
600	0.549	*Data sourc : Fig. (3–2)*	

Two types of problems arise when temperature is a consideration. If
the rotating beam endurance limit is known at room temperature,
then use

$$k_d = S_T/S_{RT} \qquad\qquad \text{3-10}$$

from Table (3–2) or Eq. (3–9) and proceed as usual. If the rotating-beam endurance limit is not given, then compute it using Eq. (3–1) and the temperature-corrected tensile strength obtained by using the factor from Table (3–2). Then use $k_d = 1$.

EXAMPLE 3–3

A 1035 steel has a tensile strength of 70 kpsi and is to be used for a part that sees 450°F in service. Estimate the Marin temperature modification factor and $(S_e)_{450°}$ if

(a) The room-temperature endurance limit by test is $(S'_e)_{70°}=$ 39 kpsi

(b) Only the tensile strength at room temperature is known

Solution

(a) First, from Eq. (3–9),

$$k_d = 0.975 + 0.432(10^{-3})(450) - 0.115(10^{-5})(450^2)$$
$$+ 0.104(10^{-8})(450^3) - 0.595(10^{-12})(450^4) = 1.007$$

Thus,

$$(S_e)_{450°} = k_d(S'_e)_{70°} = 1.007(39) = 39.3 \text{ kpsi} \hspace{2cm} Ans.$$

(b) Interpolating from Table (3–2) gives

$$(S_T/S_{RT})_{450°} = 1.018 + (0.995 - 1.018)\frac{450 - 400}{500 - 400} = 1.007$$

Thus, the tensile strength at 450°F is estimated as

$$(S_{ut})_{450°} = (S_T/S_{RT})_{450°}(S_{ut})_{70°} = 1.007(70) = 70.5 \text{ kpsi}$$

From Eq. (3–1) then,

$$(S_e)_{450°} = 0.5(S_{ut})_{450°} = 0.5(70.5) = 35.2 \text{ kpsi}$$

Part *a* gives the better estimate due to actual testing of the particular material.

➤ *Reliability Factor k_e*

The reliability modification factor can be determined from the following table.

Table (3–3)
Reliability factors k_e corresponding to 8 percent standard deviation of the endurance limit

Reliability,%	Reliability factors k_e
50	1.000
90	0.897
95	0.868
99	0.814
99.9	0.753
99.99	0.702
99.999	0.659
99.9999	0.620
99.99999	0.584

➢ *Miscellaneous-Effects Factor k_f*

Though the factor k_f is intended to account for the reduction in endurance limit due to all other effects, it is really intended as a reminder that these must be accounted for, because actual values of k_f are not always available.

    Residual stresses may either improve the endurance limit or affect it adversely. Generally, if the residual stress in the surface of the part is compression, the endurance limit is improved. Fatigue failures appear to be tensile failures, or at least to be caused by tensile stress, and so anything that reduces tensile stress will also reduce the possibility of a fatigue failure. Operations such as shot peening, hammering, and cold rolling build compressive stresses into the surface of the part and improve the endurance limit significantly. Of course, the material must not be worked to exhaustion. The endurance limits of parts that are made from rolled or drawn sheets or bars, as well as parts that are forged, may be affected by the so-called *directional characteristics* of the operation. Rolled or drawn parts, for example, have an endurance limit in the transverse direction that may be 10 to 20 percent less than the endurance limit in the longitudinal direction.

    Corrosion, electrolytic plating, metal spraying, cyclic frequency and frottage corrosion may also have an effect on the endurance limit.

3.4 Stress Concentration and Notch Sensitivity

It turns out that some materials are not fully sensitive to the presence of notches and hence, for these, a reduced value of K_t can be used. For these materials, the maximum stress is, in fact,

$$\sigma_{max} = K_f \sigma_o \qquad \text{or} \qquad \tau_{max} = K_{fs} \tau_o \qquad\qquad \text{3-11}$$

where K_f is a reduced value of K_t and σ_o is the nominal stress. The factor K_f is commonly called a *fatigue stress-concentration factor,* and hence the subscript f. So it is convenient to think of K_f as a stress-concentration factor reduced from K_t because of lessened sensitivity to notches. The resulting factor is defined by the equation

$$K_f = \frac{\text{maximum stress in notched specimen}}{\text{stress in notch-free specimen}}$$

Notch sensitivity q is defined by the equation

$$q = \frac{K_f - 1}{K_t - 1} \qquad \text{or} \qquad q_{shear} = \frac{K_{fs} - 1}{K_{ts} - 1}$$

where q is usually between zero and unity. Equation (2–12) shows that if $q = 0$, then $K_f = 1$, and the material has no sensitivity to notches at all. On the other hand, if $q = 1$, then $K_f = K_t$, and the material has full notch sensitivity. In analysis or design work, find K_t first, from the geometry of the part. Then specify the material, find q, and solve for K_f from the equation

$$K_f = 1 + q(K_t - 1) \qquad \text{or} \qquad K_{fs} = 1 + q_{shear}(K_{ts} - 1) \qquad \text{3-13}$$

For steels and 2024 aluminum alloys, use Fig. (3–3) to find q for bending and axial loading. For shear loading, use Fig. (3–4).

The notch sensitivity of the cast irons is very low, varying from 0 to about 0.2, depending upon the tensile strength. To be on the conservative side,

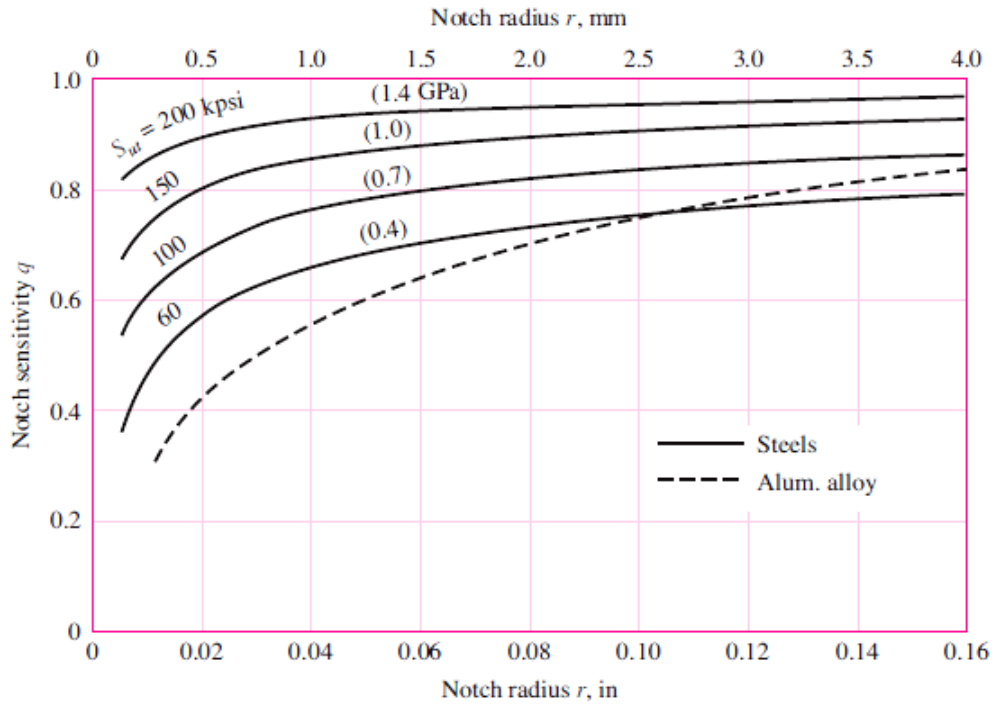$$q = 0.2 \qquad\qquad \textit{for all grades of cast iron}$$

Figure (3–3)

Notch-sensitivity charts for steels and UNS A92024-T wrought aluminum alloys subjected to reversed bending or reversed axial loads. For larger notch radii, use the values of q corresponding to the $r = 0.16$-in (4-mm)
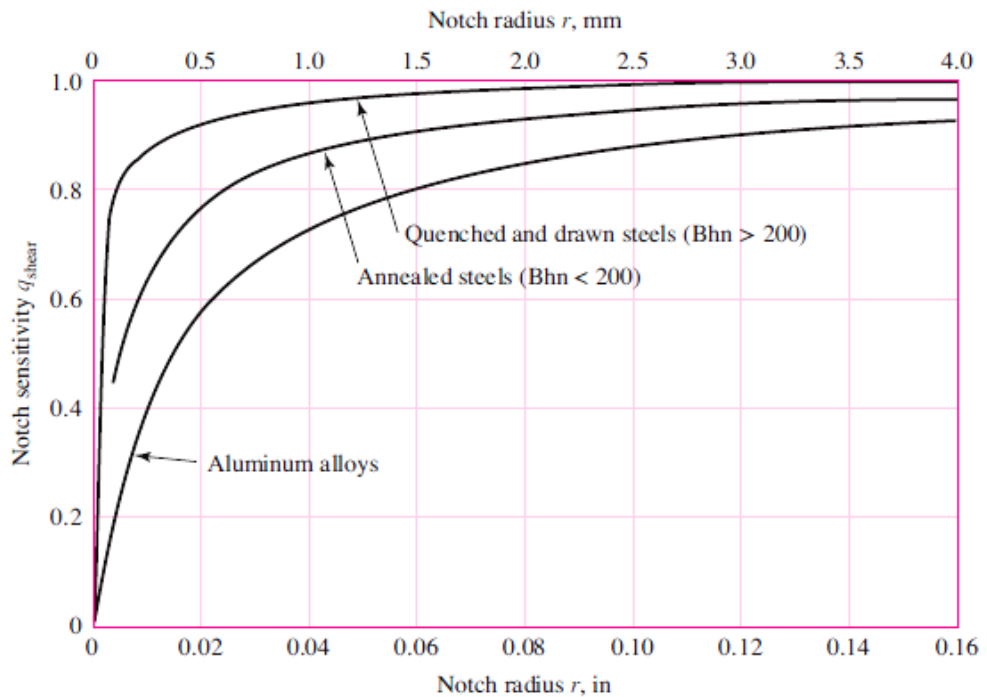

Figure (3–4)

Notch-sensitivity curves for materials in reversed torsion. For larger notch radii, use the values of q_{shear} corresponding to $r = 0.16$-in (4-mm)

EXAMPLE 3–4

A steel shaft in bending has an ultimate strength of 690 MPa and a shoulder with a fillet radius of 3 mm connecting a 32-mm diameter with a 38-mm diameter. Estimate K_f.

Solution

From Fig. (1–16), using $D/d = 38/32 = 1.1875$, $r/d = 3/32 = 0.09375$, we read the graph to find ($K_t = 1.65$)

From Fig. (3–3), for $S_{ut} = 690$ MPa and $r = 3$ mm, ($q = 0.84$). Thus, from Eq. (3–13)

$$K_f = 1 + q(K_t - 1) = 1 + 0.84(1.65 - 1) = 1.55 \qquad\qquad Ans.$$

EXAMPLE 3–5

A 1015 hot-rolled steel bar has been machined to a diameter of 1 in. It is to be placed in reversed axial loading for 70 000 cycles to failure in an operating environment of 550°F. Using ASTM minimum properties, and a reliability of 99 percent, estimate the endurance limit.

Solution

From Table (3–4), $S_{ut} = 50$ kpsi at 70°F. Since the rotating-beam specimen endurance limit is not known at room temperature, we determine the ultimate strength at the elevated temperature first, using Table (3–2):

$$(S_T/S_{RT})_{550°} = (0.995 + 0.963)/2 = 0.979$$

The ultimate strength at 550°F is then

$$(S_{ut})_{550°} = (S_T/S_{RT})_{550°} (S_{ut})_{70°} = 0.979(50) = 49 \text{ kpsi}$$

The rotating-beam specimen endurance limit at 550°F is then estimated from Eq. (3–1) as

$S'_e = 0.5(49) = 24.5$ kpsi

Next, we determine the Marin factors. For the machined surface, Eq. (3–3) with Table (3–1) gives

$$k_a = aS_{ut}^b = 2.70(49)^{-0.265} = 0.963$$

For axial loading, from Eq. (3–7), the size factor $k_b = 1$, and from Eq. (3–8) the loading factor is $k_c = 0.85$. The temperature factor $k_d = 1$, since we accounted for the temperature in modifying the ultimate strength and consequently the endurance limit. For 99 percent reliability, from Table (3–3), $k_e = 0.814$. Finally, since no other conditions were given, the miscellaneous factor is $k_f = 1$. The endurance limit for the part is estimated by Eq. (3–2) as

$$S_e = k_a\, k_b\, k_c\, k_d\, k_e\, k_f \quad S'_e = 0.963(1)(0.85)(1)(0.814)(1)24.5$$
$$= 16.3 \text{ kpsi} \qquad\qquad Ans.$$

Table (3–4)

Deterministic ASTM minimum tensile and yield strengths for some hot-rolled (HR) and cold-drawn (CD) steels. [The strengths listed are estimated ASTM minimum values in the size range 18 to 32 mm (34 to 114 in). These strengths are suitable for use with the design factor, provided the materials conform to ASTM A6 or A568 requirements or are required in the purchase specifications]

| UNS No.	SAE and/or AISI No.	Proces-sing	Tensile Strength, MPa (kpsi)	Yield Strength, MPa (kpsi)	Elongation in 2 in, %	Reduction in Area, %	Brinell Hardness
G10060	1006	HR	300 (43)	170 (24)	30	55	86
		CD	330 (48)	280 (41)	20	45	95
G10100	1010	HR	320 (47)	180 (26)	28	50	95
		CD	370 (53)	300 (44)	20	40	105
G10150	1015	HR	340 (50)	190 (27.5)	28	50	101
		CD	390 (56)	320 (47)	18	40	111
G10180	1018	HR	400 (58)	220 (32)	25	50	116
		CD	440 (64)	370 (54)	15	40	126
G10200	1020	HR	380 (55)	210 (30)	25	50	111
		CD	470 (68)	390 (57)	15	40	131
G10300	1030	HR	470 (68)	260 (37.5)	20	42	137
		CD	520 (76)	440 (64)	12	35	149
G10350	1035	HR	500 (72)	270 (39.5)	18	40	143
		CD	550 (80)	460 (67)	12	35	163
G10400	1040	HR	520 (76)	290 (42)	18	40	149
		CD	590 (85)	490 (71)	12	35	170
G10450	1045	HR	570 (82)	310 (45)	16	40	163
		CD	630 (91)	530 (77)	12	35	179
G10500	1050	HR	620 (90)	340 (49.5)	15	35	179
		CD	690 (100)	580 (84)	10	30	197
G10600	1060	HR	680 (98)	370 (54)	12	30	201
G10800	1080	HR	770 (112)	420 (61.5)	10	25	229
G10950	1095	HR	830 (120)	460 (66)	10	25	248

EXAMPLE 3–6

Figure (3–5*a*) shows a rotating shaft simply supported in ball bearings at *A* and *D* and loaded by a non-rotating force *F* of 6.8 kN. Using ASTM "minimum" strengths, estimate the endurance limit and the reversing bending stress.

Solution

From Fig. (3–5*b*) we learn that failure will probably occur at *B* rather than at *C* or at the point of maximum moment. Point *B* has a smaller cross section, a higher bending moment, and a higher stress-concentration factor than *C*, and the location of maximum moment has a larger size and no stress-concentration factor.
    We shall solve the problem by first estimating the strength at point *B*, since the strength will be different elsewhere, and comparing this strength with the stress at the same point.

(*a*)

(*b*)
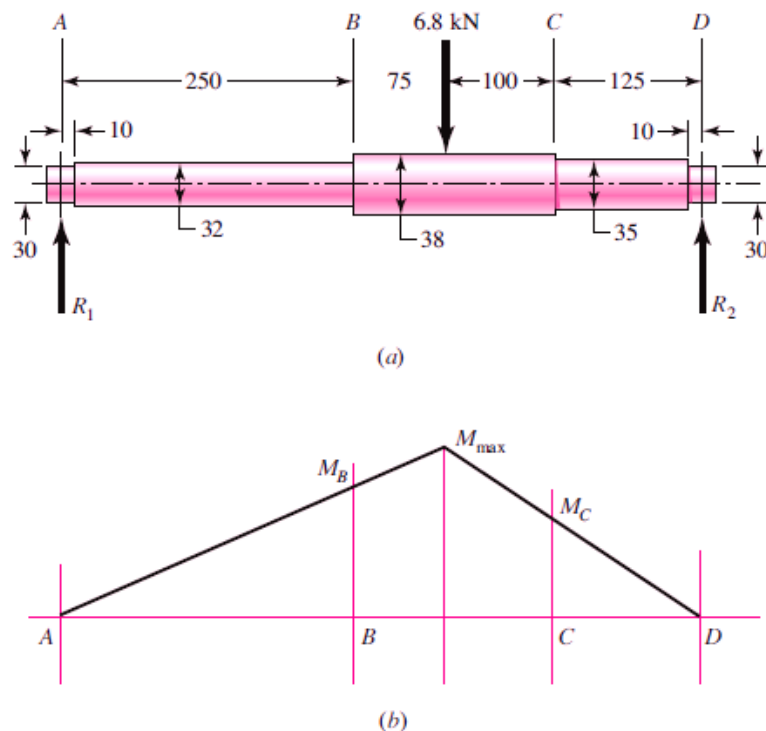
Figure (3–5)
(a) Shaft drawing showing all dimensions in millimeters; all fillets 3-mm radius. The shaft rotates and the load is stationary; material is machined from AISI 1050 cold-drawn steel.
(b) Bending-moment diagram.

From Table (3–4) we find $S_{ut} = 690$ MPa and $S_y = 580$ MPa.

$S'_e = 0.5(690) = 345$ MPa
$k_a = 4.51(690)^{-0.265} = 0.798$
$k_b = (32/7.62)^{-0.107} = 0.858$
$k_c = k_d = k_e = k_f = 1$

Then, $S_e = 0.798(0.858)345 = 236$ MPa   *Ans.*

Same as Example (3–4), $K_f = 1.55$

The next step is to estimate the bending stress at point B. The bending moment is $M_B = 695.5$ N·m

Then, the reversing bending stress is,

$$\frac{M_B c}{I} = 335.1 \text{ MPa}$$ *Ans.*

This stress is greater than S_e and less than S_y. This means we have both finite life and no yielding on the first cycle
For finite life, The ultimate strength, $S_{ut} = 690$ MPa $= 100$ kpsi. From Fig. 6–18, $f = 0.844$.

$$a = \frac{(f\ S_{ut})^2}{S_e} = \frac{[0.844(690)]^2}{236} = 1437 \text{ MPa}$$

$$b = -\frac{1}{3}\log\left(\frac{f\ S_{ut}}{S_e}\right) = -\frac{1}{3}\log\left[\frac{0.844(690)}{236}\right] = -0.1308$$

$$N = \left(\frac{\sigma_a}{a}\right)^{1/b} = \left(\frac{335.1}{1437}\right)^{-1/0.1308} = 68(10^3) \text{ cycles}$$

3.5 Characterizing Fluctuating Stresses

Fluctuating stresses in machinery often take the form of a sinusoidal pattern because of the nature of some rotating machinery. However, other patterns, some quite irregular, do occur. It has been found that in periodic patterns exhibiting a single maximum and a single minimum of force, the shape of the wave is not important, but the peaks on both the high side (maximum) and the low side (minimum) are important. Thus F_{max} and F_{min} in a cycle of force can be used to

characterize the force pattern. It is also true that ranging above and below some baseline can be equally effective in characterizing the force pattern. If the largest force is F_{max} and the smallest force is F_{min}, then a steady component and an alternating component can be constructed as follows:

$$F_m = \frac{F_{max} + F_{min}}{2} \qquad\qquad F_a =$$

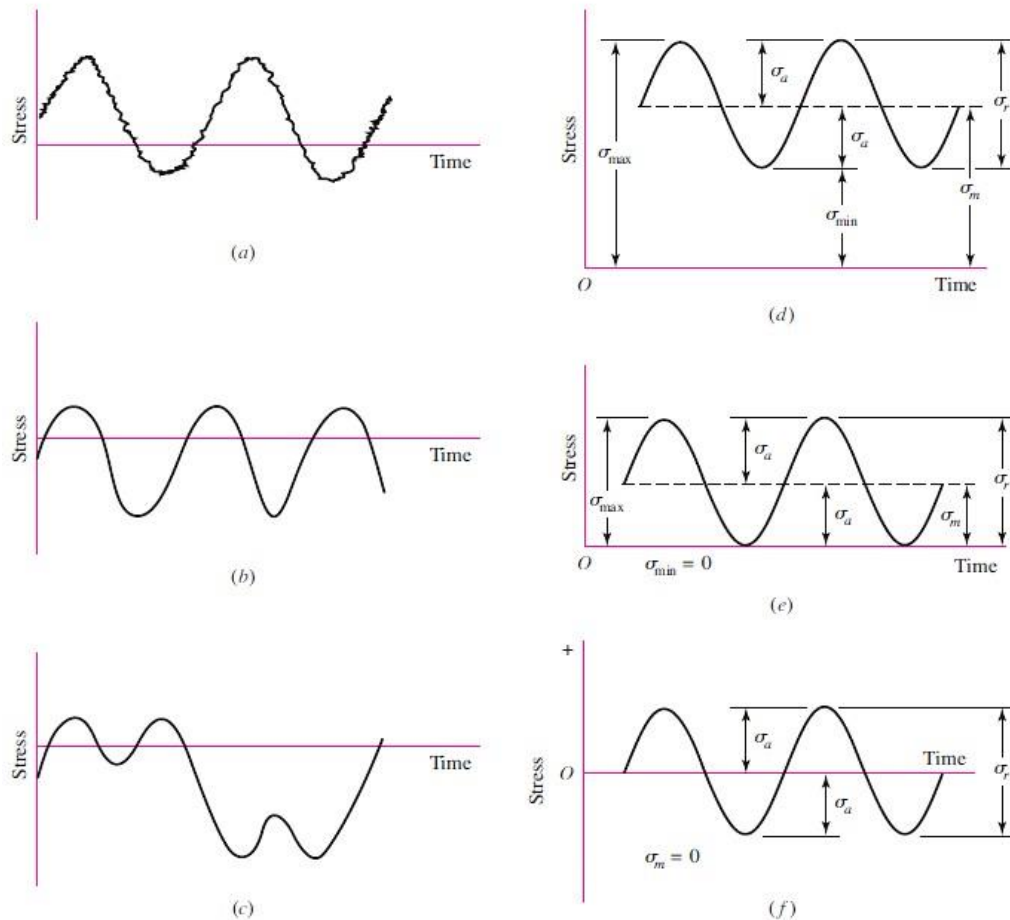where F_m is the midrange steady component of force, and F_a is the amplitude of the alternating component of force.

Figure (3–6)
Some stress-time relations: (*a*) fluctuating stress with high- frequency ripple;
(*b* and *c*) non-sinusoidal fluctuating stress; (*d*) sinusoidal fluctuating stress; (*e*)
repeated stress; (*f*) completely reversed sinusoidal stress.

Figure (3–6) illustrates some of the various stress-time traces that occur. The components of stress, some of which are shown in Fig. (3–6*d*), are

σ_{min} = minimum stress σ_m = midrange component
σ_{max} = maximum stress σ_r = range of stress
σ_a = amplitude component σ_s = static or steady stress

The steady, or static, stress is *not* the same as the midrange stress; in fact, it may have any value between σ_{min} and σ_{max}. The steady stress exists because of a fixed load or preload applied to the part, and it is usually independent of the varying portion of the load. A helical

compression spring, for example, is always loaded into a space shorter than the free length of the spring. The stress created by this initial compression is called the steady, or static, component of the stress. It is not the same as the midrange stress. We shall have occasion to apply the subscripts of these components to shear stresses as well as normal stresses.

The following relations are evident from Fig. (3–6):

$$\sigma_m = \frac{\sigma_{max} + \sigma_{min}}{2} \qquad \sigma_a = \left| \frac{\sigma_{max} - \sigma_{min}}{2} \right| \qquad \text{3- 14}$$

In addition to Eq. (3–14), the *stress ratio*

$$R = \frac{\sigma_{min}}{\sigma_{max}} \qquad \text{3-15}$$

and the *amplitude ratio* $\qquad A = \frac{\sigma_a}{\sigma_m} \qquad \text{3-16}$

are also defined and used in connection with fluctuating stresses.

Equations (3–14) utilize symbols σ_a and σ_m as the stress components at the location under scrutiny. This means, in the absence of a notch, σ_a and σ_m are equal to the nominal stresses σ_{ao} and σ_{mo} induced by loads F_a and F_m, respectively; in the presence of a notch they are $(K_f \sigma_{ao})$ and $(K_f \sigma_{mo})$, respectively, as long as the material remains without plastic strain. In other words, the fatigue stress concentration factor K_f is applied to *both* components.

3.6 Fatigue Failure Criteria for Fluctuating Stress

Five criteria of failure are diagrammed in Fig. (3–7): the *Soderberg*, the *modified Goodman*, the *Gerber*, the *ASME-elliptic*, and *yielding*. The diagram shows that only the Soderberg criterion guards against any yielding, but is biased low.
Considering the modified Goodman line as a criterion, point *A* represents a limiting point with an alternating strength S_a and midrange strength S_m. The slope of the load line shown is defined as $r = S_a/S_m$.
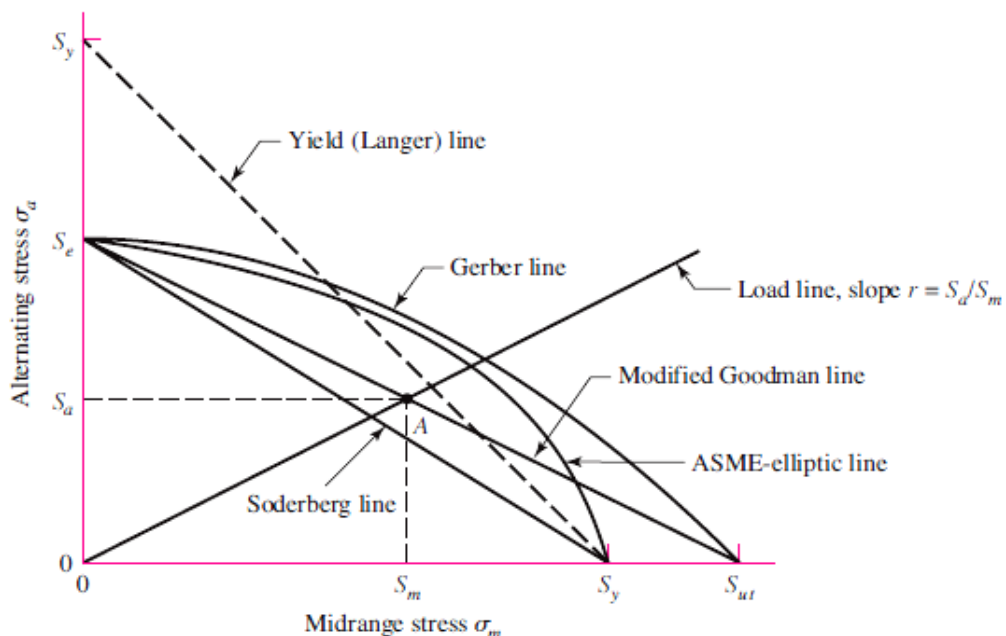
Figure (3–7)
Fatigue diagram showing various criteria of failure. For each criterion, points on or "above" the respective line indicate failure. Some point *A* on the Goodman line, for example, gives the strength S_m as the limiting value of σ_m corresponding to the strength S_a, which, paired with σ_m, is the limiting value of σ_a.

The line equations for every criterion are :

Soderberg line is: $\dfrac{S_a}{S_e} + \dfrac{S_m}{S_y} = 1$ 3-17

modified Goodman : $\dfrac{S_a}{S_e} + \dfrac{S_m}{S_{ut}} = 1$ 3-18

The Gerber failure criterion is: $\dfrac{S_a}{S_e} + \left(\dfrac{S_m}{S_{ut}}\right)^2 = 1$ 3-19

ASME-elliptic is : $\left(\dfrac{S_a}{S_e}\right)^2 + \left(\dfrac{S_m}{S_y}\right)^2 = 1$ 3-20

The Langer first-cycle-yielding criterion is used in connection with the fatigue curve:

$$S_a + S_m = S_y$$

3-21

The stresses $n\sigma_a$ and $n\sigma_m$ can replace S_a and S_m, where n is the design factor or factor of safety. Then, the last Eqs. become

Soderberg: $\quad \dfrac{S_a}{S_e} + \dfrac{S_m}{S_y} = 1$ $\qquad\qquad\qquad\qquad$ 3-22

mod-Goodman : $\quad \dfrac{\sigma_a}{S_e} + \dfrac{\sigma_m}{S_{ut}} = \dfrac{1}{n}$ $\qquad\qquad\qquad$ 3-23

Gerber : $\quad \dfrac{n\sigma_a}{S_e} + \left(\dfrac{n\sigma_m}{S_{ut}}\right)^2 = 1$ $\qquad\qquad\qquad$ 3-24

ASME-elliptic: $\quad \left(\dfrac{n\sigma_a}{S_e}\right)^2 + \left(\dfrac{n\sigma_m}{S_y}\right)^2 = 1$ $\qquad\qquad$ 3-25

Langer static yield: $\quad \sigma_a + \sigma_m = \dfrac{S_y}{n}$ $\qquad\qquad\qquad$ 3-26

The Gerber and ASME-elliptic are emphasized for fatigue failure criterion and the Langer for first-cycle yielding. Conservative designers often use the modified Goodman criterion.

The failure criteria are used in conjunction with a load line, $\quad r = S_a/S_m = \sigma_a/\sigma_m$. Principal intersections are tabulated in Tables (3–5 to 3–7). Formal expressions for fatigue factor of safety are given in the lower panel of Tables (3–5 to 3–7). The first row of each table corresponds to the fatigue criterion, the second row is the static Langer criterion, and the third row corresponds to the intersection of the static and fatigue criteria. The first column gives the intersecting equations and the second column the intersection coordinates.

There are two ways to proceed with a typical analysis. One method is to assume that fatigue occurs first and use one of Eqs. (3–22) to (3–25) to determine n or size, depending on the task. Most often fatigue is the governing failure mode. Then follow with a static check. If static failure governs then the analysis is repeated using Eq. (3–6). Alternatively, one could use the tables. Determine the load line and establish which criterion the load line intersects first and use the corresponding equations in the tables. Some examples will help solidify the ideas just discussed.

Table (3–5)

Amplitude and steady coordinates of strength and important intersections in first quadrant for *modified Goodman* and *Langer* failure criteria

Intersecting Equations	Intersection Coordinates
$\dfrac{S_a}{S_e} + \dfrac{S_m}{S_{ut}} = 1$	$S_a = \dfrac{r\,S_e\,S_{ut}}{r\,S_{ut} + S_e}$
Load line $r = \dfrac{S_a}{S_m}$	$S_m = \dfrac{S_a}{r}$
$\dfrac{S_a}{S_y} + \dfrac{S_m}{S_y} = 1$	$S_a = \dfrac{r\,S_y}{1+r}$
Load line $r = \dfrac{S_a}{S_m}$	$S_m = \dfrac{S_y}{1+r}$
$\dfrac{S_a}{S_e} + \dfrac{S_m}{S_{ut}} = 1$	$S_m = \dfrac{(S_y - S_e)\,S_{ut}}{S_{ut} - S_e}$
$\dfrac{S_a}{S_y} + \dfrac{S_m}{S_y} = 1$	$S_a = S_y - S_m,\ r_{crit} = S_a/S_m$

Fatigue factor of safety

$$n_f = \dfrac{1}{\dfrac{\sigma_a}{S_e} + \dfrac{\sigma_m}{S_{ut}}}$$

Table (3–6)

Amplitude and steady coordinates of strength and important intersections in first quadrant for *Gerber* and *Langer* failure criteria

Intersecting Equations	Intersection Coordinates
$\dfrac{S_a}{S_e} + \left(\dfrac{S_m}{S_{ut}}\right)^2 = 1$	$S_a = \dfrac{r^2 S_{ut}^2}{2 S_e}\left[-1 + \sqrt{1 + \left(\dfrac{2 S_e}{r\,S_{ut}}\right)^2}\right]$
Load line $r = \dfrac{S_a}{S_m}$	$S_m = \dfrac{S_a}{r}$
$\dfrac{S_a}{S_y} + \dfrac{S_m}{S_y} = 1$	$S_a = \dfrac{r\,S_y}{1+r}$
Load line $r = \dfrac{S_a}{S_m}$	$S_m = \dfrac{S_y}{1+r}$
$\dfrac{S_a}{S_e} + \left(\dfrac{S_m}{S_{ut}}\right)^2 = 1$	$S_m = \dfrac{S_{ut}^2}{2 S_e}\left[1 - \sqrt{1 + \left(\dfrac{2 S_e}{S_{ut}}\right)^2\left(1 - \dfrac{S_y}{S_e}\right)}\right]$
$\dfrac{S_a}{S_y} + \dfrac{S_m}{S_y} = 1$	$S_a = S_y - S_m,\ r_{crit} = S_a/S_m$

Fatigue factor of safety

$$n_f = \dfrac{1}{2}\left(\dfrac{S_{ut}}{\sigma_m}\right)^2 \dfrac{\sigma_a}{S_e}\left[-1 + \sqrt{1 + \left(\dfrac{2\sigma_m S_e}{S_{ut}\sigma_a}\right)^2}\right] \qquad \sigma_m > 0$$

Table (3–7)

Amplitude and steady coordinates of strength and important intersections in first quadrant for ***ASME-elliptic*** and ***Langer*** failure criteria

Intersecting Equations	Intersection Coordinates
$\left(\dfrac{S_a}{S_e}\right)^2 + \left(\dfrac{S_m}{S_y}\right)^2 = 1$ Load line $r = S_a/S_m$	$S_a = \sqrt{\dfrac{r^2 S_e^2 S_y^2}{S_e^2 + r^2 S_y^2}}$ $S_m = \dfrac{S_a}{r}$
$\dfrac{S_a}{S_y} + \dfrac{S_m}{S_y} = 1$ Load line $r = S_a/S_m$	$S_a = \dfrac{r S_y}{1+r}$ $S_m = \dfrac{S_y}{1+r}$
$\left(\dfrac{S_a}{S_e}\right)^2 + \left(\dfrac{S_m}{S_y}\right)^2 = 1$ $\dfrac{S_a}{S_y} + \dfrac{S_m}{S_y} = 1$	$S_a = 0, \quad \dfrac{2 S_y S_e^2}{S_e^2 + S_y^2}$ $S_m = S_y - S_a, \ r_{crit} = S_a/S_m$

Fatigue factor of safety

$$n_f = \sqrt{\dfrac{1}{(\sigma_a/S_e)^2 + (\sigma_m/S_y)^2}}$$

EXAMPLE 3–7

A 1.5-in-diameter bar has been machined from an AISI 1050 cold-drawn bar. This part is to withstand a fluctuating tensile load varying from 0 to 16 kip. Because of the ends, and the fillet radius, a fatigue stress-concentration factor K_f is 1.85 for 10^6 or larger life. Find S_a and S_m and the factor of safety guarding against fatigue and first-cycle yielding, using (*a*) the Gerber fatigue line and (*b*) the ASME-elliptic fatigue line.

Solution

From Table (3–4), $S_{ut} = 100$ kpsi and $S_y = 84$ kpsi.

$F_a = F_m = 8$ kip.

$k_a = 2.7(100)^{-0.265} = 0.797$

$k_b = 1$ (axial loading)

$k_c = 0.85$

$k_d = k_e = k_f = 1$

$S_e = 0.797(1)0.85(1)(1)(1)0.5(100) = 33.9$ kpsi

The nominal axial stress components σ_{ao} and σ_{mo} are

$$\sigma_{ao} = \frac{4F_a}{\pi d^2} = \frac{4(8)}{\pi\, 1.5^2} = 4.53 \text{ kpsi} \qquad \sigma_{mo} = \frac{4F_m}{\pi d^2} = \frac{4(8)}{\pi\, 1.5^2} = 4.53 \text{ kpsi}$$

Applying K_f to both components σ_{ao} and σ_{mo} constitutes a prescription of no notch yielding:

$$\sigma_a = K_f\, \sigma_{ao} = 1.85(4.53) = 8.38 \text{ kpsi} = \sigma_m$$

(a) Let us calculate the factors of safety first. From the bottom panel from Table (3–6) the factor of safety for fatigue is

$$n_f = \frac{1}{2}\left(\frac{100}{8.38}\right)^2 \left(\frac{8.38}{33.9}\right) \left\{ -1 + \sqrt{1 + \left[\frac{2(8.38)33.9}{100(8.38)}\right]^2} \right\} = 3.66$$

From Eq. (3–26) the factor of safety guarding against first-cycle yield is

$$n_y = \frac{S_y}{\sigma_a + \sigma_m} = \frac{84}{8.38 + 8.38} = 5.01$$

Thus, we see that fatigue will occur first and the factor of safety is (3.68). This can be seen in Fig. (3–8) where the load line intersects the Gerber fatigue curve first at point *B*. If the plots are created to true scale it would be seen that $n_f = OB/OA$.

From the first panel of Table (3–6), $r = \sigma_a/\sigma_m = 1$,

$$S_a = \frac{(1)^2 100^2}{2(33.9)} \left\{ -1 + \sqrt{1 + \left[\frac{2(33.9)}{(1)100}\right]^{-2}} \right\} = 30.7 \text{ kpsi}$$

$$S_m = \frac{S_a}{r} = \frac{30.7}{1} = 30.7 \text{ kpsi}$$

As a check on the previous result,

$n_f = OB/OA = S_a/\sigma_a = S_m/\sigma_m = 30.7/8.38 = 3.66$ and we see total agreement.
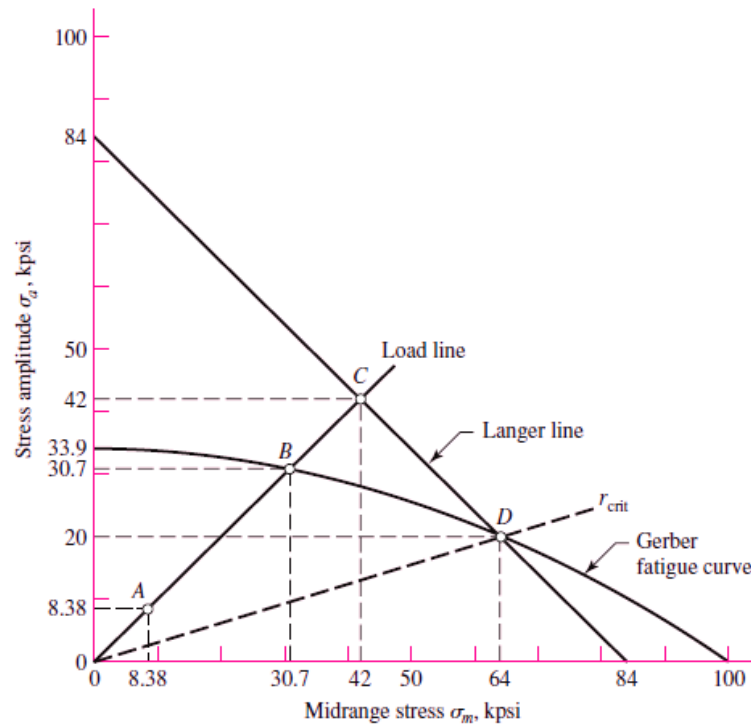
Figure (3–8)
Principal points *A*, *B*, *C*, and *D* on the designer's diagram drawn for
Gerber, *Langer*, and *load line*

We could have detected that fatigue failure would occur first without drawing Fig. (3–8) by calculating r_{crit} . From the third row third column panel of Table (3–6), the intersection point between fatigue and first-cycle yield is

$$S_m = \frac{100^2}{2(33.9)} \left[1 - \sqrt{1 + \left(\frac{2(33.9)}{100} \right)^2 \left(1 - \frac{84}{33.9} \right)} \right] = 64.0 \text{ kpsi}$$

$$S_a = S_y - S_m = 84 - 64 = 20 \text{ kpsi}$$

The critical slope is thus

$$r_{crit} = \frac{S_a}{S_m} = \frac{20}{64} = 0.312$$

which is less than the actual load line of $r = 1$. This indicates that fatigue occurs before first-cycle-yield.

(b) Repeating the same procedure for the ASME-elliptic line, for fatigue

$$n_f = \sqrt{\frac{1}{(8.38/33.9)^2 + (8.38/84)^2}} = 3.75$$

64
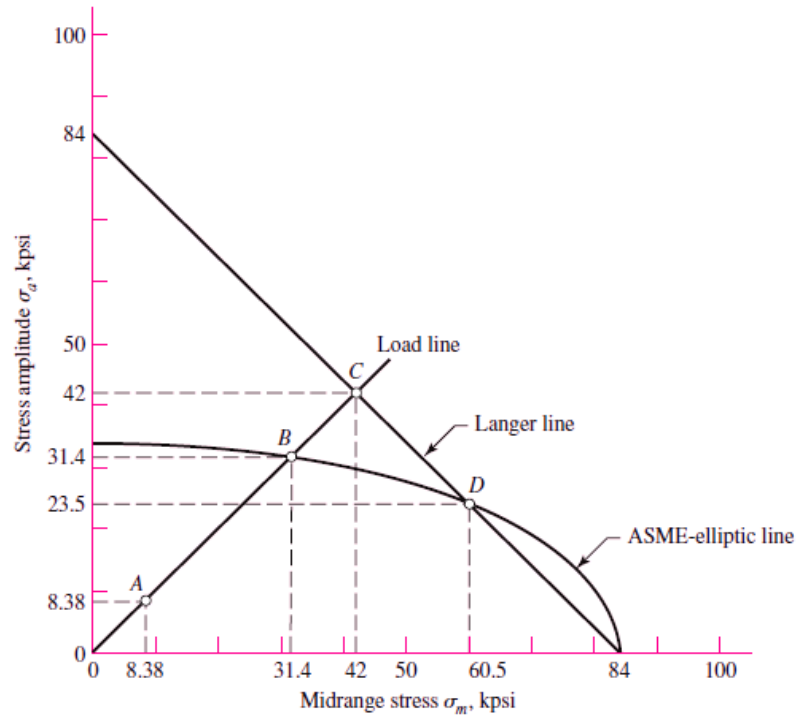
Figure (3–9)

Principal points *A*, *B*, *C*, and *D* on the designer's diagram drawn for
***ASME-elliptic*, *Langer*,** and *load line*

Again, this is less than $n_y = 5.01$ and fatigue is predicted to occur
first. From the first row second column panel of Table (3–7), with
$r = 1$, we obtain the coordinates S_a and S_m of point *B* in Fig. (3–9) as

$$S_a = \sqrt{\frac{(1)^2 33.9^2 (84)^2}{33.9^2 + (1)^2 84^2}} = 31.4 \text{ kpsi}, \quad S_m = \frac{S_a}{r} = \frac{31.4}{1} = 31.4 \text{ kpsi}$$

The fatigue factor of safety, $n_f = S_a/\sigma_a = 31.4/8.38 = 3.75$

As before, r_{crit}. From the third row second column panel of
Table (3–7),

$$S_a = \frac{2(84)33.9^2}{33.9^2 + 84^2} = 23.5 \text{ kpsi}, \quad S_m = S_y - S_a = 84 - 23.5 = 60.5 \text{ kpsi}$$

$$r_{crit} = \frac{S_a}{S_m} = \frac{23.5}{60.5} = 0.388$$

which again is less than $r = 1$, verifying that fatigue occurs first with
$n_f = 3.75$.

The Gerber and the ASME-elliptic fatigue failure criteria are very close to each other and are used interchangeably. The ANSI/ASME Standard B106.1M–1985 uses ASME-elliptic for shafting.

For many *brittle* materials, the first quadrant fatigue failure criteria follows a concave upward Smith-Dolan locus represented by

$$\frac{S_a}{S_e} = \frac{1 - S_m/S_{ut}}{1 + S_m/S_{ut}} \qquad \text{3-27}$$

or as a design equation,

$$\frac{n\sigma_a}{S_e} = \frac{1 - n\sigma_m/S_{ut}}{1 + n\sigma_m/S_{ut}} \qquad \text{3-28}$$

For a radial load line of slope r, we substitute S_a/r for S_m in Eq. (3–27) and solve for S_a , obtaining

$$S_a = \frac{r\,S_{ut} + S_e}{2}\left[-1 + \sqrt{1 + \frac{4r\,S_{ut}\,S_e}{(r\,S_{ut} + S_e)^2}}\right] \qquad \text{3-29}$$

The most likely domain of designer use is in the range from $-S_{ut} \le \sigma_m \le S_{ut}$. The locus in the first quadrant is Goodman, Smith-Dolan, or something in between. The portion of the second quadrant that is used is represented by a straight line between the points $-S_{ut}$, S_{ut} and 0, S_e, which has the equation

$$S_a = S_e + \left(\frac{S_e}{S_{ut}} - 1\right) S_m \qquad -S_{ut} \le S_m \le 0 \quad \text{(for cast iron)} \qquad \text{3-30}$$

EXAMPLE 3–8

A grade 30 gray cast iron (S_{ut} = 31 kpsi, S_{uc} = 109 kpsi, $k_a k_b\, S_e'$ = 14 kpsi, and k_c for axial loading is 0.9) is subjected to a load F applied to a 1 by 3/8 -in cross-section link with a 1/4 -in-diameter hole drilled in the center as depicted in Fig. (3–10*a*). The surfaces are machined. In the neighborhood of the hole, what is the factor of safety guarding against failure under the following conditions:

(a) The load $F = 1000$ lbf tensile, steady.
(b) The load is 1000 lbf repeatedly applied.
(c) The load fluctuates between (-1000 lbf and 300 lbf) without column action.
Use the Smith-Dolan fatigue locus.

Solution

$$S_e = (k_a k_b S'_e)k_c = 14(0.9) = 12.6 \text{ kpsi.}$$
$$K_t = 2.45 \text{ (HW)}$$
The notch sensitivity (q) for cast iron is 0.2
$$K_f = 1 + q(K_t - 1) = 1 + 0.2(2.45 - 1) = 1.29$$

(a) $\sigma_a = \dfrac{K_f F_a}{A} = \dfrac{1.29(0)}{0.281} = 0 \qquad \sigma_m = \dfrac{K_f F_m}{A} = \dfrac{1.29(1000)}{0.281}(10^{-3}) = 4.59 \text{ kpsi}$

then, the factor of safety guarding against failure

$$n = \frac{S_{ut}}{\sigma_m} = \frac{31.0}{4.59} = 6.75$$

(b) $F_a = F_m = \dfrac{F}{2} = \dfrac{1000}{2} = 500 \text{ lbf}$

$$\sigma_a = \sigma_m = \frac{K_f F_a}{A} = \frac{1.29(500)}{0.281}(10^{-3}) = 2.30 \text{ kpsi}$$

$$r = \frac{\sigma_a}{\sigma_m} = 1$$

From Eq. (3-29)

$$S_a = \frac{(1)31 + 12.6}{2}\left[-1 + \sqrt{1 + \frac{4(1)31(12.6)}{[(1)31 + 12.6]^2}}\right] = 7.63 \text{ kpsi}$$

$$n = \frac{S_a}{\sigma_a} = \frac{7.63}{2.30} = 3.32$$

(c) $F_a = \dfrac{1}{2}|300 - (-1000)| = 650 \text{ lbf} \qquad \sigma_a = \dfrac{1.29(650)}{0.281}(10^{-3}) = 2.98 \text{ kpsi}$

$F_m = \dfrac{1}{2}[300 + (-1000)] = -350 \text{ lbf} \qquad \sigma_m = \dfrac{1.29(-350)}{0.281}(10^{-3}) = -1.61 \text{ kpsi}$

$$r = \frac{\sigma_a}{\sigma_m} = \frac{3.0}{-1.61} = -1.86$$

From Eq. (3-30), $S_a = S_e + (S_e/S_{ut} - 1)S_m$ and $S_m = S_a/r$. It follows that

$$S_a = \frac{S_e}{1 - \dfrac{1}{r}\left(\dfrac{S_e}{S_{ut}} - 1\right)} = \frac{12.6}{1 - \dfrac{1}{-1.86}\left(\dfrac{12.6}{31} - 1\right)} = 18.5 \text{ kpsi}$$

$$n = \frac{S_a}{\sigma_a} = \frac{18.5}{2.98} = 6.20$$

Figure (3–10*b*) shows the portion of the designer's fatigue diagram that was constructed.
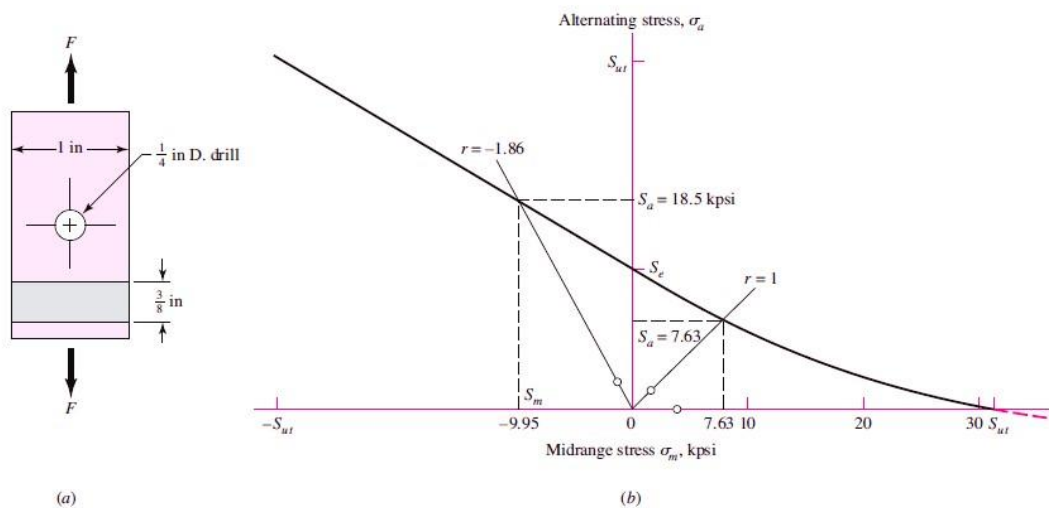
Figure (3–10)
The grade 30 cast-iron part in axial fatigue with (*a*) its geometry displayed and
(*b*) its designer's fatigue diagram

3.7 Torsional Fatigue Strength under Fluctuating Stresses

Use the same equations as apply for $\sigma_m \geq 0$, except replace σ_m and σ_a with τ_m and τ_a, use $k_c = 0.59$ for S_e, replace S_{ut} with $S_{su} = 0.67S_{ut}$, and replace S_y with $S_{sy} = 0.577S_y$.

3.8 Combinations of Loading Modes

It may be helpful to think of fatigue problems as being in three categories:

• Completely reversing simple loads
• Fluctuating simple loads
• *Combinations of loading modes*

For the last one, calculate von Mises stresses for alternating and midrange stress states, σ'_a and σ'_m. When determining S_e, do not use k_c nor divide by K_f or K_{fs}. Apply K_f and/or K_{fs} directly to each specific alternating and midrange stress. If axial stress is present divide the alternating axial stress by $k_c = 0.85$. For the special case of combined bending, torsional shear, and axial stresses

$$\sigma'_a = \left\{ \left[(K_f)_{bending}(\sigma_a)_{bending} + (K_f)_{axial}\frac{(\sigma_a)_{axial}}{0.85} \right]^2 + 3\left[(K_{fs})_{torsion}(\tau_a)_{torsion} \right]^2 \right\}^{1/2}$$

$$\sigma'_m = \left\{ \left[(K_f)_{bending}(\sigma_m)_{bending} + (K_f)_{axial}(\sigma_m)_{axial} \right]^2 + 3\left[(K_{fs})_{torsion}(\tau_m)_{torsion} \right]^2 \right\}^{1/2}$$

Then apply stresses to fatigue criterion.

EXAMPLE 3–9

A rotating shaft is made of (42×4 mm) AISI 1018 cold-drawn steel tubing and has a 6-mm-diameter hole drilled transversely through it. Estimate the factor of safety guarding against fatigue and static failures using the Gerber and Langer failure criteria for the following loading conditions:
(a) The shaft is subjected to a completely reversed torque of 120 N·m in phase with a completely reversed bending moment of 150 N·m.
(b) The shaft is subjected to a pulsating torque fluctuating from 20 to 160 N·m and a steady bending moment of 150 N·m.

Solution

Here we follow the procedure of estimating the strengths and then the stresses, followed by relating the two.

From Table (3–4): S_{ut} = 440 MPa and S_y = 370 MPa.

$$S_e' = 0.5(440) = 220 \text{ MPa.}$$
$$k_a = 4.51(440)^{-0.265} = 0.899$$
$$k_b = \left(\frac{d}{7.62}\right)^{-0.107} = \left(\frac{42}{7.62}\right)^{-0.107} = 0.833$$

The remaining Marin factors are all unity, so the modified endurance strength S_e is
$$S_e = 0.899(0.833)220 = 165 \text{ MPa}$$

(*a*)

K_t = 2.366 for bending; and K_{ts} = 1.75 for torsion (HW)

Thus, for bending,

$$Z_{net} = \frac{\pi A}{32D}(D^4 - d^4) = \frac{\pi(0.798)}{32(42)}[(42)^4 - (34)^4] = 3.31\ (10^3)\text{mm}^3$$

and for torsion

$$J_{net} = \frac{\pi A}{32}(D^4 - d^4) = \frac{\pi(0.89)}{32}[(42)^4 - (34)^4] = 155\ (10^3)\text{mm}^4$$

q = 0.78 for bending and q = 0.96 for torsion (HW)

$K_f = 1 + q(K_t - 1) = 1 + 0.78(2.366 - 1) = 2.07$
$K_{fs} = 1 + 0.96(1.75 - 1) = 1.72$

The alternating bending stress is now found to be

$$\sigma_{xa} = K_f \frac{M}{Z_{net}} = 2.07\frac{150}{3.31(10^{-6})} = 93.8(10^6)\text{Pa} = 93.8 \text{ MPa}$$

and the alternating torsional stress is

$$\tau_{xya} = K_{fs}\frac{TD}{2J_{net}} = 1.72\frac{120(42)(10^{-3})}{2(155)(10^{-9})} = 28.0(10^6)\text{Pa} = 28.0 \text{ MPa}$$

The midrange von Mises component σ'_m is zero. The alternating component σ'_a is given by:

$$\sigma'_a = \left(\sigma^2_{xa} + 3\tau^2_{xya}\right)^{1/2} = [93.8^2 + 3(28^2)]^{1/2} = 105.6 \text{ MPa}$$

Since $S_e = S_a$, the fatigue factor of safety n_f is

$$n_f = \frac{S_a}{\sigma'_a} = \frac{165}{105.6} = 1.56$$

The first-cycle yield factor of safety is

$$n_y = \frac{S_y}{\sigma'_a} = \frac{370}{105.6} = 3.50$$

This means that there is no localized yielding; so, the threat is from fatigue. See Fig. (3–11).
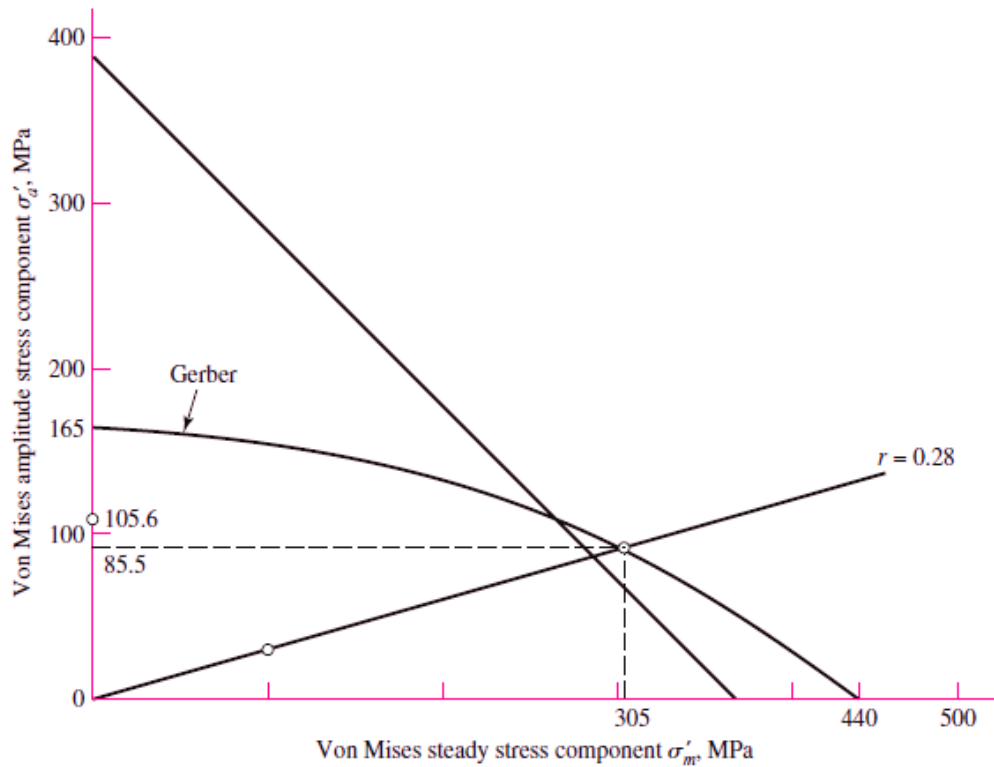
Figure (3–11)
Designer's fatigue diagram

(b) This part asks us to find the factors of safety when the alternating component is due to pulsating torsion, and a steady component is due to both torsion and bending. We have

$$T_a = (160 - 20)/2 = 70 \text{ N·m and } T_m = (160 + 20)/2 = 90 \text{ N·m}$$

The corresponding amplitude and steady-stress components are

$$\tau_{xya} = K_{fs}\frac{T_a D}{2J_{net}} = 1.72\frac{70(42)(10^{-3})}{2(155)(10^{-9})} = 16.3(10^6)\text{Pa} = 16.3 \text{ MPa}$$

$$\tau_{xym} = K_{fs}\frac{T_m D}{2J_{net}} = 1.72\frac{90(42)(10^{-3})}{2(155)(10^{-9})} = 21.0(10^6)\text{Pa} = 21.0 \text{ MPa}$$

The steady bending stress component σ_{xm} is

$$\sigma_{xm} = K_f\frac{M_m}{Z_{net}} = 2.07\frac{150}{3.31(10^{-6})} = 93.8(10^6)\text{Pa} = 93.8 \text{ MPa}$$

The von Mises components σ'_a and σ'_m are

$$\sigma'_a = [3(16.3)^2]^{1/2} = 28.2 \text{ MPa}$$

$$\sigma'_m = [(93.82)^2 + 3(21)^2]^{1/2} = 100.6 \text{ MPa}$$

From Table (3–6), the fatigue factor of safety is

$$n_f = \frac{1}{2}\left(\frac{440}{100.6}\right)^2\frac{28.2}{165}\left\{-1 + \sqrt{1 + \left[\frac{2(100.6)165}{440(28.2)}\right]^2}\right\} = 3.03$$

From the same table, with $r = \sigma'_a / \sigma'_m = 28.2/100.6 = 0.28$, the strengths can be shown to be $S_a = 85.5$ MPa and $S_m = 305$ MPa. See the plot in Fig. (3–11).

    The first-cycle yield factor of safety n_y is

$$n_y = \frac{S_y}{\sigma'_a + \sigma'_m} = \frac{370}{28.2 + 100.6} = 2.87$$

There is no notch yielding. The likelihood of failure may first come from first-cycle yielding at the notch. See the plot in Fig. (3–11).

Homework

(1) A 0.25-in drill rod was heat-treated and ground. Estimate the endurance strength if the rod is used in rotating bending, if $S_{ut} = 242.6$ kpsi. (*Ans./ S_e = 85.7 kpsi*)

(2) Estimate S_e' for the following materials:
(a) AISI 1020 CD steel.   (*Ans./ 34 kpsi*)
(b) AISI 1080 HR steel.   (*Ans./ 56 kpsi*)
(c) 2024 T3 aluminum. (*Ans./ no endurance limit*)
(d) AISI 4340 steel heat-treated to
a tensile strength of 250 kpsi. (*Ans./ 100 kpsi*)

(3) Estimate the endurance strength of a 32-mm-diameter rod of AISI 1035 steel having a machined finish and heat-treated to a tensile strength of 710 MPa. (*Ans./ S_e = 241 kpsi*)

(4) Two steels are being considered for manufacture of as-forged connecting rods. One is AISI 4340 Cr-Mo-Ni steel capable of being heat-treated to a tensile strength of 260 kpsi. The other is a plain carbon steel AISI 1040 with an attainable S_{ut} of 113 kpsi. If each rod is to have a size giving an equivalent diameter d_e of 0.75-in, is there any advantage to use the alloy steel for fatigue application?
(*Ans./ S_e = 14.3 and 18.6 kpsi. Not only is AISI 1040 steel a contender, it has a superior endurance strength. Can you see why?*)

(5) A rectangular bar is cut from an AISI 1018 cold-drawn steel flat. The bar is 60 mm wide by 10 mm thick and has a 12-mm hole drilled through the center as depicted in Fig. (1-8). The bar is concentrically loaded in push-pull fatigue by axial forces F_a, uniformly distributed across the width. Using a design factor of 1.8, estimate the largest force F_a that can be applied ignoring column action. (*Ans./ Largest force amplitude is 20.1 kN*)

(6) A bar of steel has the minimum properties $S_e = 276$ MPa, $S_y = 413$ MPa, and $S_{ut} = 551$ MPa. The bar is subjected to a steady torsional stress of 103 MPa and an alternating bending stress of 172 MPa. Find the factor of safety guarding against a static failure, and the factor of safety guarding against a fatigue failure. For the fatigue analysis use: (*a*) Modified Goodman criterion. (*b*) Gerber criterion. (*c*) ASME-elliptic criterion. (*Ans./ n_y = 1.67, n_f = 1.06, 1.31, 1.32*)

(7) Repeat question (6) but with a steady torsional stress of 138 MPa and an alternating bending stress of 69 MPa. (Ans./ n_y = 1.66, n_f = 1.46, 1.73, 1.59)

(8) Repeat question (6) but with a steady torsional stress of 103 MPa, an alternating torsional stress of 69 MPa, and an alternating bending stress of 83 MPa.   (Ans./ n_y = 1.34, n_f= 1.18, 1.47, 1.47)

(9) Repeat question (6) but with an alternating torsional stress of 207 MPa. (Ans./ n_y = 1.15, n_f = 0.77, 0.77, 0.77)

(10) Repeat question (6) but with an alternating torsional stress of 103 MPa and a steady bending stress of 103 MPa.(Ans./ n_y = 2, n_f = 1.2, 1.44, 1.44)

(11) The cold-drawn AISI 1018 steel bar shown in the figure is subjected to an axial load fluctuating between 800 and 3000 lbf. Estimate the factors of safety n_y and n_f using (a) a Gerber fatigue failure criterion, and (b) an ASME-elliptic fatigue failure criterion.

(Ans./ n_f = 2.17, 2.28)
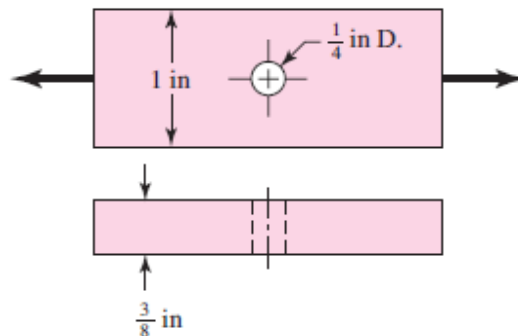
(12) Repeat question (11), with the load fluctuating between −800 and 3000 lbf. Assume no buckling. (Ans./ n_f = 1.6, 1.62)

(13) Repeat question (11), with the load fluctuating between 800 and −3000 lbf. Assume no buckling. (Ans./ n_f = 1.67, 1.67)

(14) The figure shows a formed round-wire cantilever   spring (S_{ut} = 188.1 kpsi) subjected to a varying force. It is apparent from the
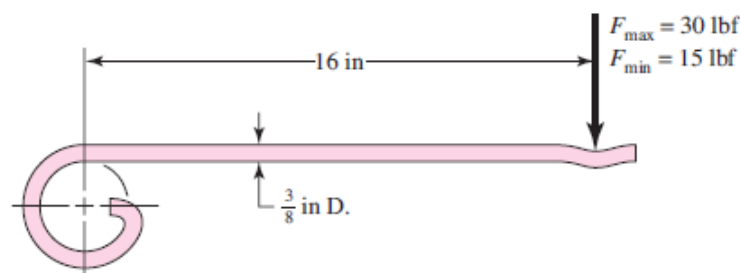
mounting details that there is no stress concentration. A visual inspection of the springs indicates that the surface finish corresponds closely to a hot-rolled finish. Estimate the factors of safety n_y and n_f using (*a*) Modified Goodman criterion, and (*b*) Gerber criterion.

(*Ans./ n_f = 0.955, 1.2*)

(15) The figure shows the free-body diagram of a connecting-link portion having stress concentration at three sections. The dimensions are $r = 0.25$ in, $d = 0.75$ in, $h = 0.5$ in, $w_1 = 3.75$ in, and $w_2 = 2.5$ in.
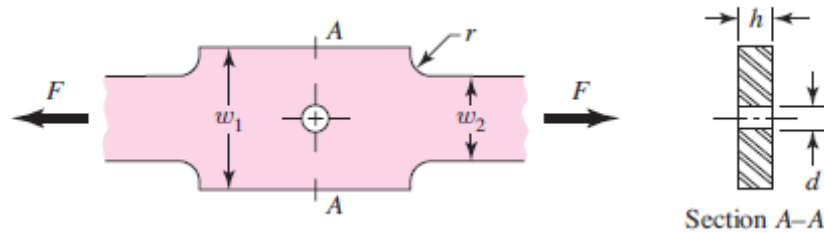
The forces *F* fluctuate between a tension of 4 kip and a compression of 16 kip. Neglect column action and find the least factor of safety if the material is cold-drawn AISI 1018 steel.

(*Ans./ Fillet: n_y = 4.22, n_f = 1.61; Hole: n_y = 5.06, n_f = 1.61; then: n = 1.61*)

(16) In the figure shown, shaft *A*, made of AISI 1010 hot-rolled steel, is welded to a fixed support and is subjected to loading by equal and opposite forces *F* via shaft *B*. A fatigue stress concentration K_{fs} of 1.6 is induced by the 3-mm fillet. The length of shaft *A* from the fixed support to the connection at shaft *B* is 1 m. The load *F* cycles from 0.5 to 2 kN.
(a) For shaft A, find the factor of safety for infinite life using the modified Goodman fatigue failure criterion.
(b) Repeat part (*a*) using the Gerber fatigue failure criterion.

(*Ans./ n_f = 1.36, 1.7*)
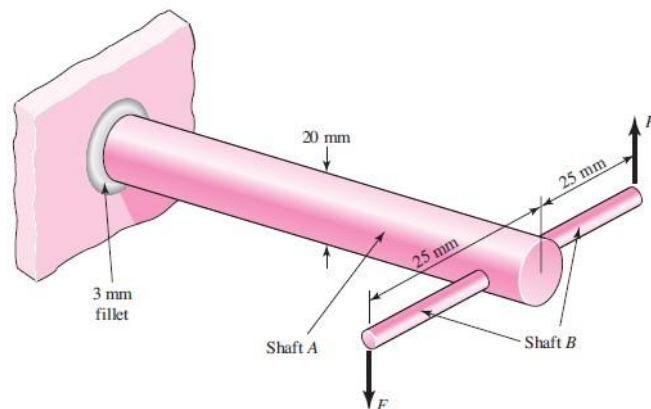
4. Shafts and Shaft Components

A *shaft* is a rotating member, usually of circular cross section, used to transmit power or motion. It provides the axis of rotation, or oscillation, of elements such as gears, pulleys, flywheels, cranks, sprockets, and the like and controls the geometry of their motion. An *axle* is a nonrotating member that carries no torque and is used to support rotating wheels, pulleys, and the like. A non-rotating axle can readily be designed and analyzed as a static beam, and will not subject to fatigue loading.

4.1 Shaft Materials

Necessary strength to resist loading stresses affects the choice of materials and their treatments. Many shafts are made from low carbon, cold-drawn or hot-rolled steel, such as ANSI 1020-1050 steels. Cold drawn steel is usually used for diameters under about 3 inches. The nominal diameter of the bar can be left unmachined in areas that do not require fitting of components. Hot rolled steel should be machined all over. For large shafts requiring much material removal, the residual stresses may tend to cause warping. If concentricity is important, it may be necessary to rough machine, then heat treat to remove residual stresses and increase the strength, then finish machine to the final dimensions.

4.2 Shaft Layout

The general layout of a shaft to accommodate shaft elements, e.g. gears, bearings, and pulleys, must be specified early in the design process in order to perform a free body force analysis and to obtain shear-moment diagrams. The geometry of a shaft is generally that of a stepped cylinder. The use of shaft shoulders is an excellent means of axially locating the shaft elements and to carry any thrust loads. Figure (4–1) shows an example of a stepped shaft supporting the gear of a worm-gear speed reducer. Each shoulder in the shaft serves a specific purpose, which you should attempt to determine by observation.

The geometric configuration of a shaft to be designed is often simply a revision of existing models in which a limited number of

changes must be made. If there is no existing design to use as a starter, then the determination of the shaft layout may have many solutions. This problem is illustrated by the two examples of Fig. (4–2). In Fig. (4–2a) a geared countershaft is to be supported by two bearings. In Fig. (4–2c) a fanshaft is to be configured. The solutions shown in Fig. (4–2b) and (7–2d) are not necessarily the best ones, but they do illustrate how the shaft-mounted devices are fixed and located in the axial direction, and how provision is made for torque transfer from one element to another.
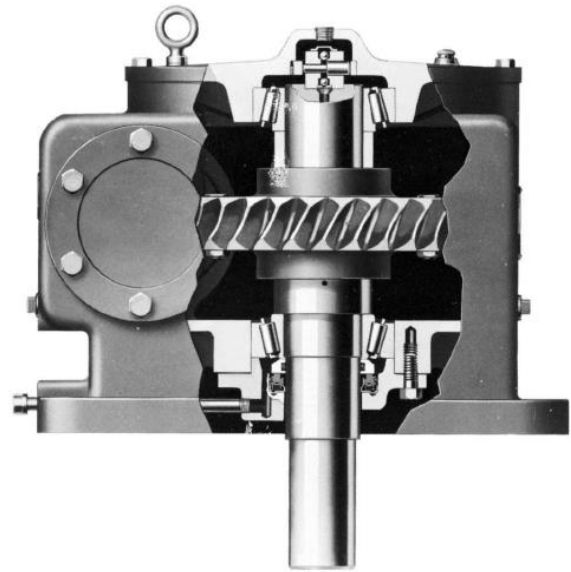
Figure (4–1)
A vertical worm-gear speed reducer.
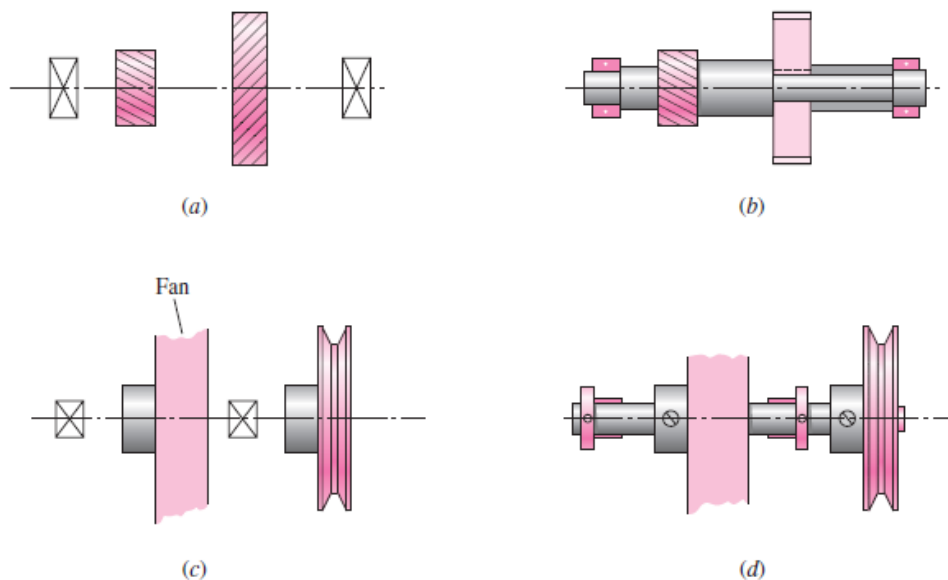
Figure (4–2)
(a) Choose a shaft configuration to support and locate the two gears and two bearings. (b) Solution uses an integral pinion, three shaft shoulders, key and keyway, and sleeve. The housing locates the bearings on their outer rings and receives the thrust loads. (c) Choose fanshaft configuration. (d) Solution uses sleeve bearings, a straight-through shaft, locating collars, and setscrews for collars, fan pulley, and fan itself. The fan housing supports the sleeve bearings.

There are no absolute rules for specifying the general layout, but the following guidelines may be helpful.

➢ *Axial Layout of Components*

The axial positioning of components is often dictated by the layout of the housing and other meshing components. In general, it is best to support load-carrying components between bearings, such as in Fig. (4–2a), rather than cantilevered outboard of the bearings, such as in Fig. (4–2c). Pulleys and sprockets often need to be mounted outboard for ease of installation of the belt or chain. The length of the cantilever should be kept short to minimize the deflection.

Only two bearings should be used in most cases. For extremely long shafts carrying several load-bearing components, it may be necessary to provide more than two bearing supports. In this case, particular care must be given to the alignment of the bearings.

In cases where axial loads are very small, it may be feasible to do without the shoulders entirely, and rely on press fits, pins, or collars with setscrews to maintain an axial location. See Fig. (4–2b) and (4–2d) for examples of some of these means of axial location.

➢ *Supporting Axial Loads*

In cases where axial loads are not trivial, it is necessary to provide a means to transfer the axial loads into the shaft, then through a bearing to the ground. This will be particularly necessary with helical or bevel gears, or tapered roller bearings, as each of these produces axial force components. Often, the same means of providing axial location, e.g., shoulders, retaining rings, and pins, will be used to also transmit the axial load into the shaft.

It is generally best to have only one bearing carry the axial load, to allow greater tolerances on shaft length dimensions, and to prevent binding if the shaft expands due to temperature changes. This is particularly important for long shafts. Figures (4–3 & 4–4) show examples of shafts with only one bearing carrying the axial load against a shoulder, while the other bearing is simply press-fit onto the shaft with no shoulder.
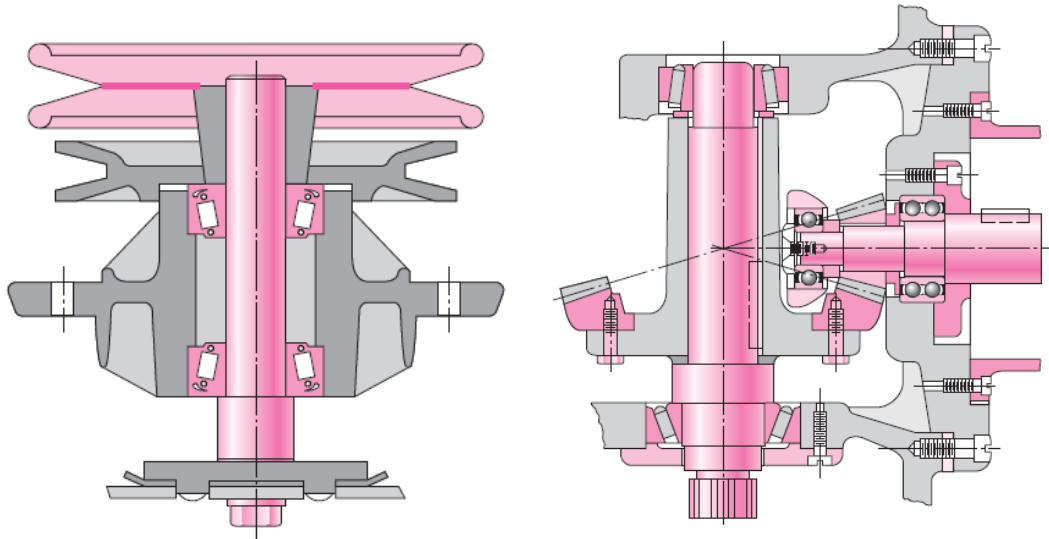
Figure (4–3)
Tapered roller bearings used in a
mowing machine spindle. This design
represents good practice for the situation
in which one or more torque-transfer
elements must be mounted outboard.
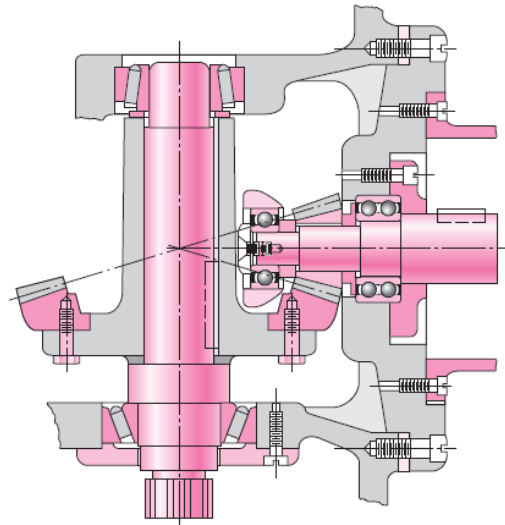
Figure (4–4)
A bevel-gear drive
in which
both pinion and
gear are
straddle-mounted.

➢ *Providing for Torque Transmission*

Most shafts serve to transmit torque from an input gear or pulley,
through the shaft, to an output gear or pulley. Of course, the shaft
itself must be sized to support the torsional stress and torsional
deflection. It is also necessary to provide a means of transmitting the
torque between the shaft and the gears. Common torque-transfer
elements are:

• Keys
• Splines
• Setscrews
• Pins
• Press or shrink fits
• Tapered fits

In addition to transmitting the torque, many of these devices are
designed to fail if the torque exceeds acceptable operating limits,
protecting more expensive components.

One of the most effective and economical means of transmitting moderate to high levels of torque is through a *key* that fits in a groove in the shaft and gear.

Splines are essentially stubby gear teeth formed on the outside of the shaft and on the inside of the hub of the load-transmitting component. Splines are generally much more expensive to manufacture than keys, and are usually not necessary for simple torque transmission. They are typically used to transfer high torques. For cases of low torque transmission, various means of transmitting torque are available. These include *pins*, *setscrews* in hubs, *tapered fits*, and *press fits*.

Press and shrink fits for securing hubs to shafts are used both for torque transfer and for preserving axial location. The resulting stress-concentration factor is usually quite small.

Tapered fits between the shaft and the shaft-mounted device, such as a wheel, are often used on the overhanging end of a shaft. Screw threads at the shaft end then permit the use of a nut to lock the wheel tightly to the shaft. This approach is useful because it can be disassembled, but it does not provide good axial location of the wheel on the shaft.

At the early stages of the shaft layout, the important thing is to select an appropriate means of transmitting torque, and to determine how it affects the overall shaft layout. It is necessary to know where the shaft discontinuities, such as keyways, holes, and splines, will be in order to determine critical locations for analysis.

➢ *Assembly and Disassembly*

Consideration should be given to the method of assembling the components onto the shaft, and the shaft assembly into the frame. This generally requires the largest diameter in the center of the shaft, with progressively smaller diameters towards the ends to allow components to be slid on from the ends. If a shoulder is needed on both sides of a component, one of them must be created by such means as a retaining ring or by a sleeve between two components. The gearbox itself will need means to physically position the shaft into its bearings, and the bearings into the frame. This is typically accomplished by providing access through the housing to the bearing at one end of the shaft. See Fig. (4–5) for examples.
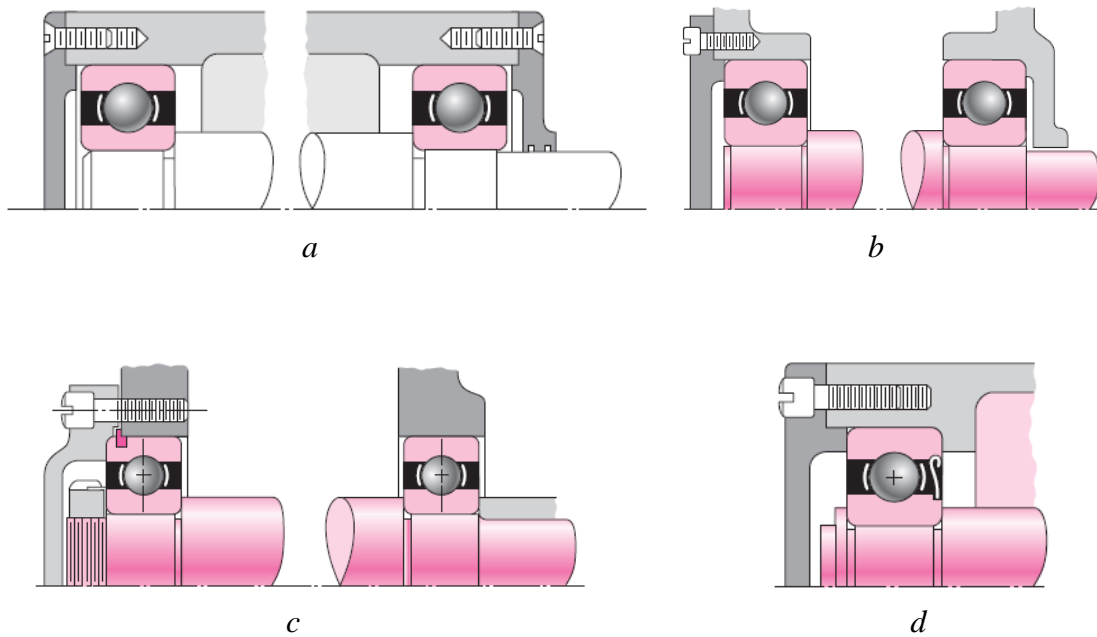
Figure (4–5)

(***a***) Arrangement showing bearing inner rings press-fitted to shaft while outer rings float in the housing. The axial clearance should be sufficient only to allow for machinery vibrations. Note the labyrinth seal on the right. (***b***) Similar to the arrangement of (*a*) except that the outer bearing rings are preloaded. (***c***) In this arrangement the inner ring of the left-hand bearing is locked to the shaft between a nut and a shaft shoulder. The locknut and washer are AFBMA standard. The snap ring in the outer race is used to positively locate the shaft assembly in the axial direction. Note the floating right-hand bearing and the grinding runout grooves in the shaft. (***d***) This arrangement is similar to (*c*) in that the left-hand bearing positions the entire shaft assembly. In this case the inner ring is secured to the shaft using a snap ring. Note the use of a shield to prevent dirt generated from within the machine from entering the bearing.

When components are to be press-fit to the shaft, the shaft should be designed so that it is not necessary to press the component down a long length of shaft. This may require an extra change in diameter, but it will reduce manufacturing and assembly cost by only requiring the close tolerance for a short length. Consideration should also be given to the necessity of disassembling the components from the shaft. This requires consideration of issues such as accessibility of retaining rings, space for pullers to access bearings, openings in the housing to allow pressing the shaft or bearings out, etc.

4.3 Shaft Design for Stress

Bending, torsion, and axial stresses may be present in both midrange and alternating components. For analysis, it is simple enough to combine the different types of stresses into alternating and midrange von Mises stresses, as shown in the fatigue part. It is sometimes convenient to customize the equations specifically for shaft applications. Axial loads are usually comparatively very small at critical locations where bending and torsion dominate, so they will be left out of the following equations.

Neglecting axial loads, the resulting equations for several of the commonly used failure curves are summarized below. The names given to each set of equations identifies the significant failure theory, followed by a fatigue failure locus name. For example, DE-Gerber indicates the stresses are combined using the distortion energy (DE) theory, and the Gerber criteria is used for the fatigue failure.

DE-Goodman

$$\frac{1}{n} = \frac{16}{\pi d^3}\left\{\frac{1}{S_e}\left[4(K_f M_a)^2 + 3(K_{fs} T_a)^2\right]^{1/2} + \frac{1}{S_{ut}}\left[4(K_f M_m)^2 + 3(K_{fs} T_m)^2\right]^{1/2}\right\}$$

$$d = \left(\frac{16n}{\pi}\left\{\frac{1}{S_e}\left[4(K_f M_a)^2 + 3(K_{fs} T_a)^2\right]^{1/2} + \frac{1}{S_{ut}}\left[4(K_f M_m)^2 + 3(K_{fs} T_m)^2\right]^{1/2}\right\}\right)^{1/3}$$

DE-Gerber

$$\frac{1}{n} = \frac{8A}{\pi d^3 S_e}\left\{1 + \left[1 + \left(\frac{2B S_e}{A S_{ut}}\right)^2\right]^{1/2}\right\}$$

$$d = \left(\frac{8nA}{\pi S_e}\left\{1 + \left[1 + \left(\frac{2B S_e}{A S_{ut}}\right)^2\right]^{1/2}\right\}\right)^{1/3}$$

where

$$A = \sqrt{4(K_f M_a)^2 + 3(K_{fs} T_a)^2}$$

$$B = \sqrt{4(K_f M_m)^2 + 3(K_{fs} T_m)^2}$$

DE-ASME Elliptic

$$\frac{1}{n} = \frac{16}{\pi d^3} \left[4\left(\frac{K_f M_a}{S_e}\right)^2 + 3\left(\frac{K_{fs} T_a}{S_e}\right)^2 + 4\left(\frac{K_f M_m}{S_y}\right)^2 + 3\left(\frac{K_{fs} T_m}{S_y}\right)^2 \right]^{1/2}$$

$$d = \left\{ \frac{16n}{\pi} \left[4\left(\frac{K_f M_a}{S_e}\right)^2 + 3\left(\frac{K_{fs} T_a}{S_e}\right)^2 + 4\left(\frac{K_f M_m}{S_y}\right)^2 + 3\left(\frac{K_{fs} T_m}{S_y}\right)^2 \right]^{1/2} \right\}^{1/3}$$

DE-Soderberg

$$\frac{1}{n} = \frac{16}{\pi d^3} \left\{ \frac{1}{S_e} \left[4(K_f M_a)^2 + 3(K_{fs} T_a)^2\right]^{1/2} + \frac{1}{S_{yt}} \left[4(K_f M_m)^2 + 3(K_{fs} T_m)^2\right]^{1/2} \right\}$$

$$d = \left(\frac{16n}{\pi} \left\{ \frac{1}{S_e} \left[4(K_f M_a)^2 + 3(K_{fs} T_a)^2\right]^{1/2} + \frac{1}{S_{yt}} \left[4(K_f M_m)^2 + 3(K_{fs} T_m)^2\right]^{1/2} \right\} \right)^{1/3}$$

To check for yielding,

$$\sigma'_{max} = \left[(\sigma_m + \sigma_a)^2 + 3(\tau_m + \tau_a)^2\right]^{1/2}$$

$$= \left[\left(\frac{32 K_f (M_m + M_a)}{\pi d^3}\right)^2 + 3\left(\frac{16 K_{fs}(T_m + T_a)}{\pi d^3}\right)^2 \right]^{1/2}$$

$$n_y = \frac{S_y}{\sigma'_{max}}$$

For a quick, conservative check, an estimate for σ'_{max} can be obtained by simply adding σ'_a and σ'_m. $(\sigma'_a + \sigma'_m)$ will always be greater than or equal to σ'_{max}, and will therefore be conservative.

EXAMPLE 4–1

At a machined shaft shoulder the small diameter d is 1.100 in, the large diameter D is 1.65 in, and the fillet radius is 0.11 in. The bending moment is 1260 lbf·in and the steady torsion moment is 1100 lbf·in. The heat-treated steel shaft has an ultimate strength of S_{ut} = 105 kpsi and a yield strength of S_y = 82 kpsi. The reliability goal is 0.99.

(a) Determine the fatigue factor of safety of the design using each of the fatigue failure criteria described in this section.
(b) Determine the yielding factor of safety.

Solution

(*a*) $D/d = 1.65/1.100 = 1.50$, $r/d = 0.11/1.100 = 0.10$, then,

$K_t = 1.68$, $K_{ts} = 1.42$, $q = 0.85$ & $q_{shear} = 0.92$ (HW).

$K_f = 1 + 0.85(1.68 - 1) = 1.58$ $K_{f\,s} = 1 + 0.92(1.42 - 1) = 1.39$

$k_a = 0.787$, $k_b = 0.870$, $k_c = k_d = k_f = 1$, $k_e = 0.814$ (HW)
then,
$$S_e = 0.787(0.870)0.814(0.5)(105) = 29.3 \text{ kpsi}$$

$$M_a = 1260 \text{ lbf·in}, \ T_m = 1100 \text{ lbf·in}, \ M_m = T_a = 0$$

Then

$$
\begin{array}{ll}
n = 1.62 & \text{DE-Goodman} \\
n = 1.87 & \text{DE-Gerber} \\
n = 1.88 & \text{DE-ASME Elliptic} \\
n = 1.56 & \text{DE-Soderberg}
\end{array}
$$

(b) For the yielding factor of safety, determine an   equivalent von Mises maximum stress

$$\sigma'_{max} = 18.300 \text{ kpsi, then, } n_y = 4.48$$

For comparison, a quick and very conservative check on yielding can be obtained by replacing σ'_{max} with $\sigma'_a + \sigma'_m$. This just saves the extra time of calculating σ'_{max} if σ'_a and σ'_m have already been determined. For this example,

$$n_y = S_y/(\sigma'_a + \sigma'_m) = 82.000/(\underline{15.235 + 10.134}) = 3.23 \text{ (\underline{HW})}$$

which is quite *conservative* compared with $n_y = 4.48$.

4.4 Miscellaneous Shaft Components

➢ *Setscrews*

Unlike bolts and cap screws, which depend on tension to develop a clamping force, the setscrew depends on compression to develop the clamping force. The resistance to axial motion of the collar or hub relative to the shaft is called *holding power*. This holding power, which is really a force resistance, is due to frictional resistance of the contacting portions of the collar and shaft as well as any slight penetration of the setscrew into the shaft.

Figure (4–6) shows the point types available with socket setscrews. These are also manufactured with screwdriver slots and with square heads.
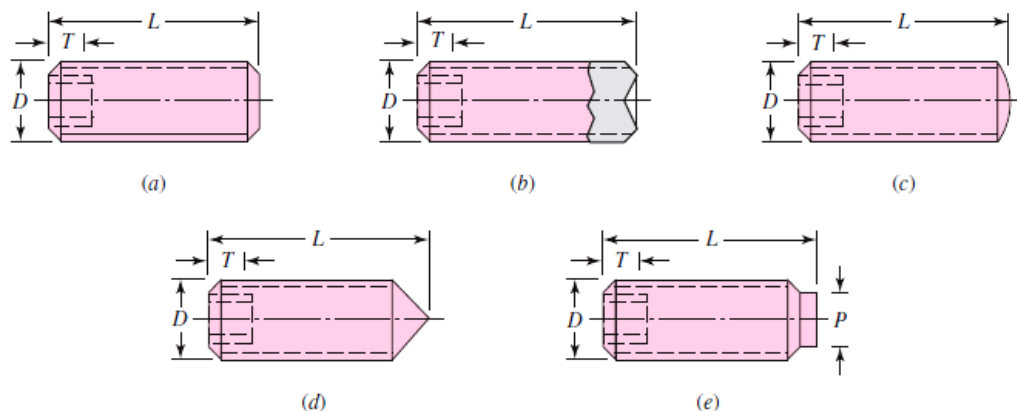
Figure (4–6)
Socket setscrews: (*a*) flat point; (*b*) cup point; (*c*) oval point; (*d*) cone point; (*e*) half-dog point.

Typical factors of safety are 1.5 to 2.0 for static loads and 4 to 8 for various dynamic loads. Setscrews should have a length of about half of the shaft diameter.

➢ *Keys and Pins*

Keys and pins are used on shafts to secure rotating elements, such as gears, pulleys, or other wheels. Keys are used to enable the transmission of torque from the shaft to the shaft-supported element. Pins are used for axial positioning and for the transfer of torque or thrust or both.

Figure (4–7) shows a variety of keys and pins. Pins are useful when the principal loading is shear and when both torsion and thrust are present. Taper pins are sized according to the diameter at the large end. The diameter at the small end is

$d = D − 0.0208L$
where

d = diameter at small end, in., D = diameter at large end, in., and L = length, in.
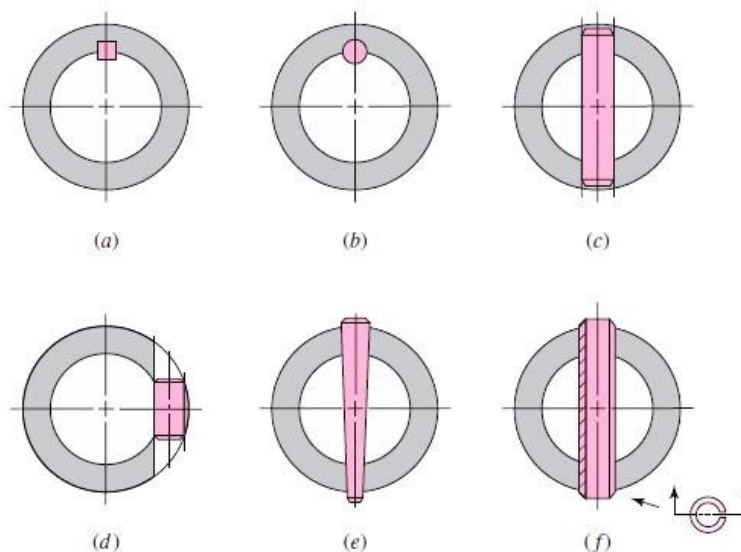
Figure (4–7)
(a) Square key; (b) round key; (c and d) round pins; (e) taper pin; (f) split tubular spring pin. The pins in parts (e) and (f) are shown longer than necessary, to illustrate the chamfer on the ends, but their lengths should be kept smaller than the hub diameters to prevent injuries due to projections on rotating parts.

For less important applications, a dowel pin or a drive pin can be used. A large variety of these are listed in manufacturers' catalogs. The square key, shown in Fig. (4–7a), is also available in rectangular sizes. The shaft diameter determines standard sizes for width, height, and key depth. The designer chooses an appropriate key length to carry the torsional load. Failure of the key can be by direct shear, or by bearing stress. The maximum length of a key is limited by the hub length of the attached element, and should generally not exceed about 1.5 times the shaft diameter to avoid excessive twisting with the angular deflection of the shaft. Multiple keys may be used as necessary to carry greater loads, typically oriented at 90° from one another. Excessive safety factors should be avoided in key design, since it is desirable in an overload situation for the key to fail, rather than more costly components.

Stock   key material is typically made from   low carbon cold-rolled steel, and is manufactured such that its dimensions never exceed the nominal dimension. This allows standard cutter sizes to be used for the keyseats. A setscrew is sometimes used along with a key to hold the hub axially, and to minimize rotational backlash when the shaft rotates in both directions.

The gib-head key, in Fig. (4–8a), is tapered so that, when firmly driven, it acts to prevent relative axial motion. This also gives the advantage that the hub position can be adjusted for the best axial location. The head makes removal possible without access to the other end, but the projection may be hazardous.
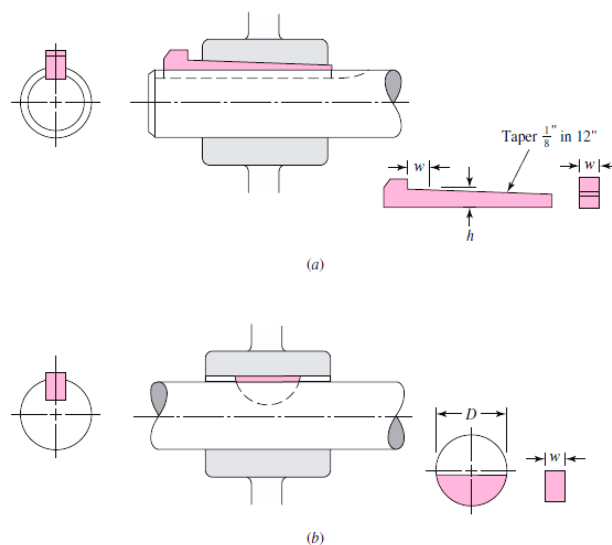
Figure (4–8)

(a) Gib-head key; (b) Woodruff key.

The Woodruff key, shown in Fig. (4–8*b*), is of general usefulness, especially when a wheel is to be positioned against a shaft shoulder, since the keyslot need not be machined into the shoulder stress-concentration region. The use of the Woodruff key also yields better concentricity after assembly of the wheel and shaft. This is especially important at high speeds, as, for example, with a turbine wheel and shaft. Woodruff keys are particularly useful in smaller shafts where their deeper penetration helps prevent key rolling.

➤ *Retaining Rings*

A retaining ring is frequently used instead of a shaft shoulder or a sleeve to axially position a component on a shaft or in a housing bore. As shown in Fig. (4–9), a groove is cut in the shaft or bore to receive the spring retainer. For sizes, dimensions, and axial load ratings, the manufacturers' catalogs should be consulted.
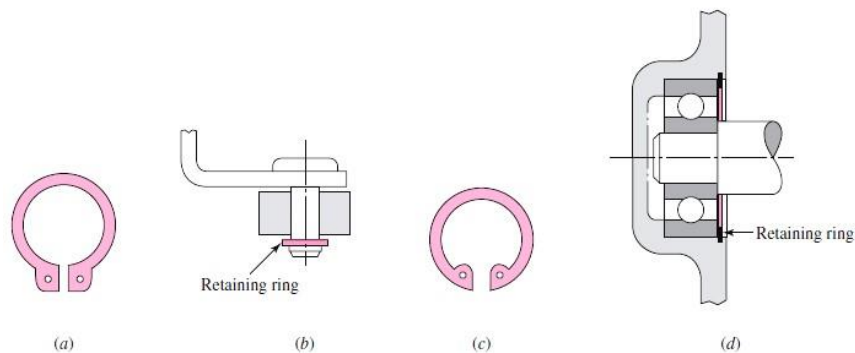
Figure (4–9)
Typical uses for retaining rings. (*a*) External ring and (*b*) its application; (*c*) internal ring and (*d*) its application.

For the rings to seat nicely in the bottom of the groove, and support axial loads against the sides of the groove, the radius in the bottom of the groove must be reasonably sharp, typically about one-tenth of the groove width. This causes comparatively high values for stress concentration factors, around 5 for bending and axial, and 3 for torsion. Care should be taken in using retaining rings, particularly in locations with high bending stresses.

5. Screws, Fasteners, and the Design of Nonpermanent Joints

The helical-thread screw was undoubtably an extremely important mechanical invention. It is the basis of power screws, which change angular motion to linear motion to transmit power or to develop large forces (presses, jacks, etc.), and threaded fasteners, an important element in nonpermanent joints.

5.1 Thread Standards and Definitions

The terminology of screw threads, illustrated in Fig. (5–1), is explained as follows:

The *pitch* is the distance between adjacent thread forms measured parallel to the thread axis. The pitch in U.S. units is the reciprocal of the number of thread forms per inch *N*.

The *major diameter* (*d*) is the largest diameter of a screw thread.

The *minor* (or root) *diameter* (d_r) is the smallest diameter of a screw thread.

The pitch diameter (d_p) is a theoretical diameter between the major and minor diameters.

The *lead* (*l*), not shown, is the distance the nut moves parallel to the screw axis when the nut is given one turn. For a single thread, as in Fig. (5–1), the lead is the same as the pitch.

A *multiple-threaded* product is one having two or more threads cut beside each other (imagine two or more strings wound side by side around a pencil). Standardized products such as screws, bolts, and nuts all have single threads; a *double-threaded* screw has a lead equal to twice the pitch, a *triple-threaded* screw has a lead equal to 3 times the pitch, and so on.

All threads are made according to the *right-hand rule* unless otherwise noted.

The *American National (Unified)* thread standard has been approved in Great Britain for use on all standard threaded products. The thread angle is 60° and the crests of the thread may be either flat or rounded.

Figure (5–2) shows the thread geometry of the metric M and MJ profiles. The M profile replaces the inch class and is the basic ISO 68 profile with 60° symmetric threads. The MJ profile has a rounded fillet at the root of the external thread and a larger minor

diameter of both the internal and external threads. This profile is especially useful where high fatigue strength is required.
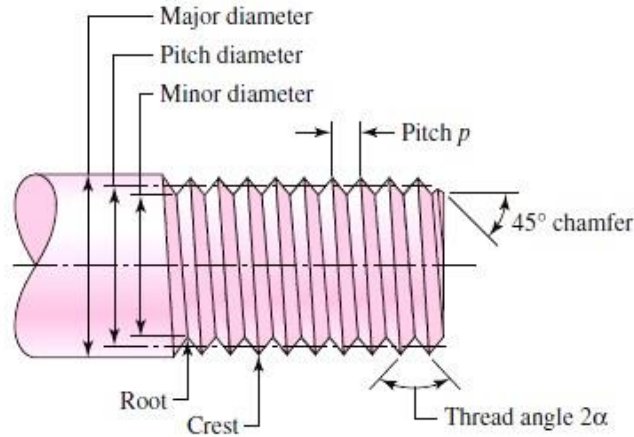
Figure (5–1)
Terminology of screw threads. Sharp vee threads shown for clarity; the crests and roots are actually flattened or rounded during the forming operation
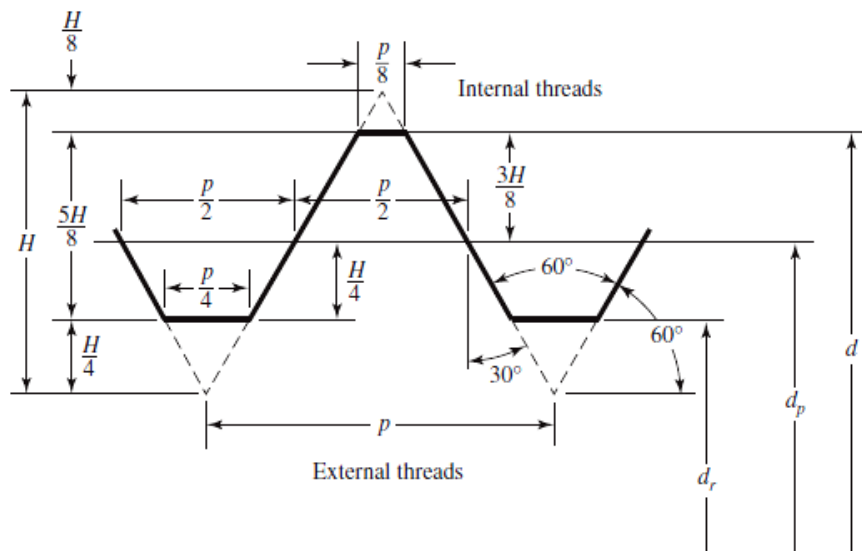

Figure (5–2)
Basic profile for metric M and MJ threads; d = major diameter
d_r = minor diameter, d_p = pitch diameter, p = pitch, $H = \sqrt{3}/2\ p$

Two major Unified thread series are in common use: UN and UNR. The difference between these is simply that a root radius must be used in the UNR series. Because of reduced thread stress-concentration factors, UNR series threads have improved fatigue strengths. Unified threads are specified by stating the nominal major diameter, the number of threads per inch, and the thread series, for example, 5/8 in-18 UNRF or 0.625 in-18 UNRF.

Metric threads are specified by writing the diameter and pitch in millimeters, in that order. Thus, M12 × 1.75 is a thread having a nominal major diameter of 12 mm and a pitch of 1.75 mm. Note that the letter M, which precedes the diameter, is the clue to the metric designation.

Square and Acme threads, shown in Fig. (5–3a and b), respectively, are used on screws when power is to be transmitted.
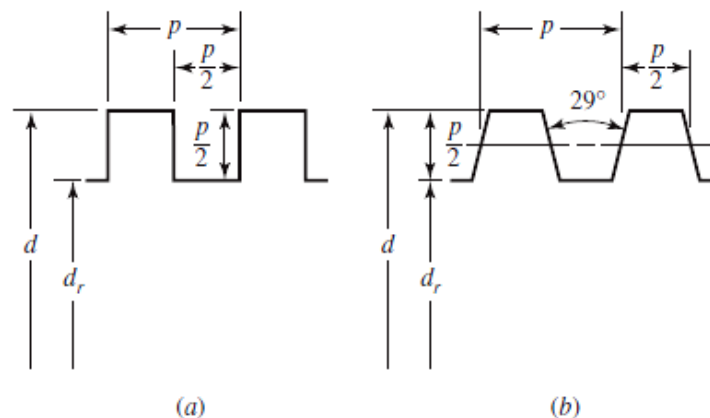
Figure (5–3)

(a) Square thread; (b) Acme thread.

Modifications are frequently made to both Acme and square threads. For instance, the square thread is sometimes modified by cutting the space between the teeth so as to have an included thread angle of 10 to 15°. This is not difficult, since these threads are usually cut with a single-point tool anyhow; the modification retains most of the high efficiency inherent in square threads and makes the cutting simpler. Acme threads are sometimes modified to a stub form by making the teeth shorter. This results in a larger minor diameter and a somewhat stronger screw.

5.2 The Mechanics of Power Screws

A power screw is a device used in machinery to change angular motion into linear motion, and, usually, to transmit power. Familiar applications include the lead screws of lathes, and the screws for vises, presses, and jacks.

An application of power screws to a power-driven jack is shown in Fig. (5–4).

In Fig. (5–5) a square-threaded power screw with single thread having a mean diameter d_m, a pitch p, a lead angle λ, and a helix angle ψ is loaded by the axial compressive force F. We wish to find an expression for the torque required to raise this load, and another expression for the torque required to lower the load.

First, imagine that a single thread of the screw is unrolled or developed (Fig. 5–6) for exactly a single turn. Then one edge of the thread will form the hypotenuse of a right triangle whose base is the circumference of the mean-thread-diameter circle and whose height is the lead. The angle λ, in

Figure (5–4)
The Joyce worm-gear screw jack.

Figs. (5–5) and (5–6), is the lead angle of the thread. We represent the summation of all the unit axial forces acting upon the normal thread area by F. To raise the load, a force P_R acts to the right (Fig. 5–6a), and to lower the load, P_L acts to the left (Fig. 5–6b). The friction force is the product of the coefficient of friction f with the normal force N, and acts to oppose the motion. The system is in equilibrium under the action of these forces, and hence, for raising the load, we have

$$\sum F_H = P_R - N \sin \lambda - f N \cos \lambda = 0$$
$$\sum F_V = F + f N \sin \lambda - N \cos \lambda = 0$$

a

In a similar manner, for lowering the load, we have

Figure (5–6)
Figure (5–5)
Portion of a power screw

Force diagrams: (*a*) lifting the
load; (*b*) lowering the load

$$\sum FH = -PL - N \sin \lambda + f N \cos \lambda = 0$$
$$\sum FV = F - f N \sin \lambda - N \cos \lambda = 0$$

b

Since we are not interested in the normal force *N*, we eliminate it
from each of these sets of equations and solve the result for *P*. For
raising the load, this gives

$$P_R = F(\sin \lambda + f \cos \lambda) / (\cos \lambda - f \sin \lambda)$$

c

and for lowering the load,

$$P_L = F(f \cos \lambda - \sin \lambda) / (\cos \lambda + f \sin \lambda)$$

d

Next, divide the numerator and the denominator of these equations
by cos λ and use the relation tan $\lambda = l/\pi d_m$ (Fig. 5–6). We then have,
respectively,

$$P_R = F [(l/\pi dm) + f] / [1 - (f l/\pi d_m)]$$

e

$$P_L = F [f - (l/\pi d_m)] / [1 + (f l/\pi d_m)]$$

f

Finally, noting that the torque is the product of the force *P* and the
mean radius $d_m/2$, for raising the load we can write:

$$T_R = \frac{F d_m}{2} \left(\frac{l + \pi f d_m}{\pi d_m - fl} \right)$$

5-1

where T_R is the torque required for two purposes: to overcome thread
friction and to raise the load.

The torque required to lower the load,

$$T_L = \frac{F d_m}{2} \left(\frac{\pi f d_m - l}{\pi d_m + fl} \right) \qquad\qquad \text{5-2}$$

This is the torque required to overcome a part of the friction in lowering the load. It may turn out, in specific instances where the lead is large or the friction is low, that the load will lower itself by causing the screw to spin without any external effort. In such cases, the torque T_L from Eq. (5–2) will be negative or zero. When a positive torque is obtained from this equation, the screw is said to be *self-locking*. Thus the condition for self-locking is

$$\pi f d_m > l$$

Dividing both sides of this inequality by πd_m. Recognizing that $l/\pi d_m = \tan \lambda$, we get

$$f > \tan \lambda \qquad\qquad \text{5-3}$$

This relation states that self-locking is obtained whenever the coefficient of thread friction is equal to or greater than the tangent of the thread lead angle. An expression for efficiency is also useful in the evaluation of power screws. If we let $f = 0$ in Eq.   (5–1), we obtain

$$T_o = Fl / 2\pi$$

which, since thread friction has been eliminated, is the torque required only to raise the load. The efficiency is therefore

$$e = \frac{T_0}{T_R} = \frac{Fl}{2\pi T_R}$$

The preceding equations have been developed for square threads where the normal thread loads are parallel to the axis of the screw. In the case of Acme or other threads, the normal thread load is inclined to the axis because of the thread angle 2α and the lead angle λ. Since lead angles are small, this inclination can be neglected and only the effect of the thread angle (Fig. 5–7a) considered. The effect of the angle α is to increase the frictional force by the wedging action of the threads. Therefore the frictional terms in Eq. (5–1) must be

divided by cos α. For raising the load, or for tightening a screw or bolt, this yields

$$T_R = \frac{F d_m}{2} \left(\frac{l + \pi f d_m \sec \alpha}{\pi d_m - f l \sec \alpha} \right) \qquad \text{5-4}$$

In using Eq. (5–5), remember that it is an approximation because the effect of the lead angle has been neglected.
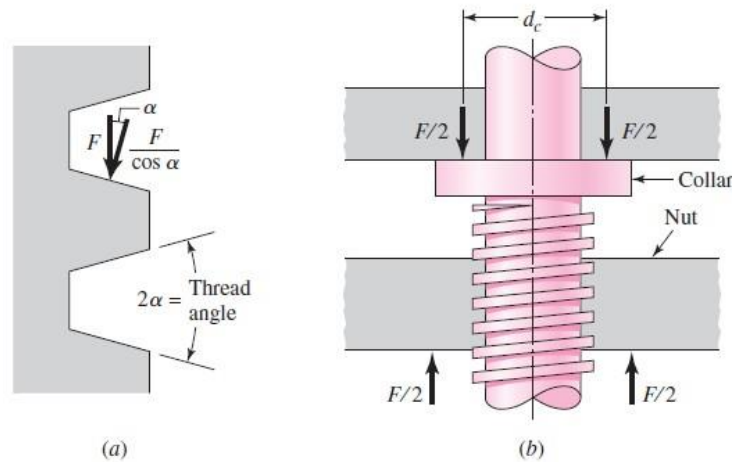

Figure (5–7)
(a) Normal thread force is increased because of angle α;
(b) thrust collar has frictional diameter d_c

For power screws, the Acme thread is not as efficient as the square thread, because of the additional friction due to the wedging action, but it is often preferred because it is easier to machine and permits the use of a split nut, which can be adjusted to take up for wear.

Usually a third component of torque must be applied in power-screw applications. When the screw is loaded axially, a thrust or collar bearing must be employed between the rotating and stationary members in order to carry the axial component. Figure (5–7b) shows a typical thrust collar in which the load is assumed to be concentrated at the mean collar diameter d_c. If f_c is the coefficient of collar friction, the torque required is

$$T_c = \frac{F f_c d_c}{2} \qquad \text{5-5}$$

For large collars, the torque should probably be computed in a manner similar to that employed for disk clutches.

Nominal body stresses in power screws can be related to thread parameters as follows. The maximum nominal shear stress τ in torsion of the screw body can be expressed as

$$\tau = \frac{16T}{\pi d_r^3} \qquad \text{5-6}$$

The axial stress σ in the body of the screw due to load F is

$$\sigma = \frac{F}{A} = \frac{4F}{\pi d_r^2} \qquad \text{5-7}$$

Nominal thread stresses in power screws can be related to thread parameters as follows. The bearing stress in Fig. (5–8), σ_B, is

$$\sigma_B = -\frac{F}{\pi d_m n_t p/2} = -\frac{2F}{\pi d_m n_t p} \qquad \text{5-8}$$

where n_t is the number of engaged threads.
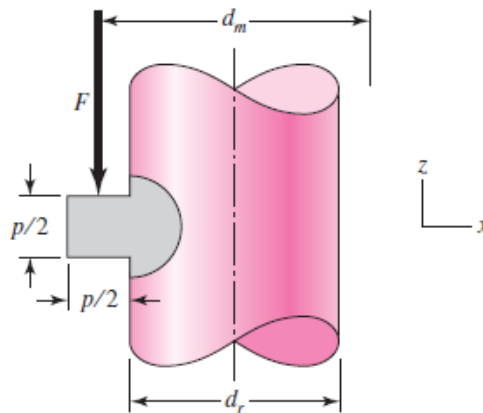
Figure (5–8)
Geometry of square thread useful in finding bending and
transverse shear stresses at the thread root

The bending stress at the root of the thread σ_b is found from:

$$\frac{I}{c} = \frac{(\pi d_r n_t)\,(p/2)^2}{6} = \frac{\pi}{24} d_r n_t p^2 \qquad M = \frac{Fp}{4}$$

$$\sigma_b = \frac{M}{I/c} = \frac{Fp}{4}\frac{24}{\pi d_r n_t p^2} = \frac{6F}{\pi d_r n_t p} \qquad\qquad 5\text{-}9$$

The transverse shear stress τ at the center of the root of the thread due to load F is

$$\tau = \frac{3V}{2A} = \frac{3}{2}\frac{F}{\pi d_r n_t p/2} = \frac{3F}{\pi d_r n_t p} \qquad\qquad 5\text{-}10$$

and at the top of the root it is zero. The von Mises stress σ' at the top of the root "plane" is found by first identifying the orthogonal normal stresses and the shear stresses. From the coordinate system of Fig. (5–8), we note

$$\sigma_x = \frac{6F}{\pi d_r n_t p} \qquad\qquad \tau_{xy} = 0$$

$$\sigma_y = 0 \qquad\qquad \tau_{yz} = \frac{16T}{\pi d_r^3}$$

$$\sigma_z = -\frac{4F}{\pi d_r^2} \qquad\qquad \tau_{zx} = 0$$

The screw-thread form is complicated from an analysis viewpoint. The tensile-stress area A_t , comes from experiment [see tables (5–1) & 5–2)] . A power screw lifting a load is in compression and its thread pitch is *shortened* by elastic deformation. Its engaging nut is in tension and its thread pitch is *lengthened*. The engaged threads cannot share the load equally. Some experiments show that the first engaged thread carries 0.38 of the load, the second 0.25, the third 0.18, and the seventh is free of load. In estimating thread stresses by the equations above, substituting $0.38F$ for F and setting n_t to 1 will give the largest level of stresses in the thread-nut combination.

EXAMPLE 5–1

A square-thread power screw has a major diameter of 32 mm and a pitch of 4 mm with double threads, and it is to be used in an application similar to that in Fig. (5–4). The given data   include $f = f_c = 0.08$, $d_c = 40$ mm, and $F = 6.4$ kN per screw.
(a) Find the thread depth, thread width, pitch diameter, minor diameter, and lead.
(b) Find the torque required to raise and lower the load.
(c) Find the efficiency during lifting the load.
(d) Find the body stresses, torsional and compressive.
(e) Find the bearing stress.
(f) Find the thread stresses bending at the root, shear at the root, and von Mises stress and maximum shear stress at the same location.

Solution

(a) From Fig. (5–3a) the thread depth and width are the same and equal to half the pitch, or 2 mm. Also

$d_m = d - p/2 = 32 - 4/2 = 30$ mm

$d_r = d - p = 32 - 4 = 28$ mm

$l = np = 2(4) = 8$ mm

(b) Using Eqs. (5–1) and (5–6), the torque required to turn the screw against the load is

$$T_R = \frac{F d_m}{2} \left(\frac{l + \pi f d_m}{\pi d_m - fl} \right) + \frac{F f_c d_c}{2}$$

$$= \frac{6.4(30)}{2} \left[\frac{8 + \pi(0.08)(30)}{\pi(30) - 0.08(8)} \right] + \frac{6.4(0.08)40}{2}$$

$$= 15.94 + 10.24 = 26.18 \text{ N} \cdot \text{m}$$

Using Eqs. (5–2) and (5–6), we find the load-lowering torque is

$$T_L = \frac{F d_m}{2} \left(\frac{\pi f d_m - l}{\pi d_m + fl} \right) + \frac{F f_c d_c}{2}$$

$$= \frac{6.4(30)}{2} \left[\frac{\pi(0.08)30 - 8}{\pi(30) + 0.08(8)} \right] + \frac{6.4(0.08)(40)}{2}$$

$$= -0.466 + 10.24 = 9.77 \text{ N} \cdot \text{m}$$

The minus sign in the first term indicates that the screw alone is not self-locking and would rotate under the action of the load except for the fact that the collar friction is present and must be overcome, too. Thus the torque required to rotate the screw "with" the load is less than is necessary to overcome collar friction alone.

(c) The overall efficiency in raising the load is

$$e = \frac{Fl}{2\pi T_R} = \frac{6.4(8)}{2\pi(26.18)} = 0.311$$

(d) The body shear stress τ due to torsional moment T_R at the outside of the screw body is

$$\tau = \frac{16 T_R}{\pi d_r^3} = \frac{16(26.18)(10^3)}{\pi(28^3)} = 6.07 \text{ MPa}$$

The axial nominal normal stress σ is

$$\sigma = -\frac{4F}{\pi d_r^2} = -\frac{4(6.4)10^3}{\pi(28^2)} = -10.39 \text{ MPa}$$

(e) The bearing stress σ_B is, with one   thread carrying 0.38F:

$$\sigma_B = -\frac{2(0.38F)}{\pi d_m(1)p} = -\frac{2(0.38)(6.4)10^3}{\pi(30)(1)(4)} = -12.9 \text{ MPa}$$

(f) The thread-root bending stress σb with one thread carrying 0.38F is:

$$\sigma_b = \frac{6(0.38F)}{\pi d_r(1)p} = \frac{6(0.38)(6.4)10^3}{\pi(28)(1)4} = 41.5 \text{ MPa}$$

The transverse shear at the extreme of the root cross section due to bending is zero. However, there is a circumferential shear stress at the extreme of the root cross section of the thread as shown in part (*d*) of 6.07 MPa. The three-dimensional stresses, after Fig. (5–8), noting the *y* coordinate is into the page, are

$$\sigma_x = 41.5 \text{ MPa} \qquad \tau_{xy} = 0$$
$$\sigma_y = 0 \qquad \tau_{yz} = 6.07 \text{ MPa}$$
$$\sigma_z = -10.39 \text{ MPa} \qquad \tau_{zx} = 0$$

$$\sigma' = (1/\sqrt{2})\{(41.5-0)^2+[0-(-10.39)]^2+(-10.39-41.5)^2+6(6.07)^2\}^{1/2}$$

$$= 48.7 \text{ MPa}$$

Alternatively, you can determine the principal stresses and then the von Mises stress noting that there are no shear stresses on the *x* face. This means that σ_x is a principal stress. The remaining principal stresses are:

$$\frac{-10.39}{2} \pm \sqrt{\left(\frac{-10.39}{2}\right)^2 + 6.07^2} = 2.79, -13.18 \text{ MPa}$$

$$\sigma' = \left\{\frac{[41.5-2.79]^2 + [2.79-(-13.18)]^2 + [-13.18-41.5]^2}{2}\right\}^{1/2}$$

$$= 48.7 \text{ MPa}$$

5.3 Threaded Fasteners

Figure (5–9) is a drawing of a standard hexagon-head bolt. Points of stress concentration are at the fillet, at the start of the threads (runout), and at the thread-root fillet in the plane of the nut when it is present. The diameter of the washer face is the same as the width across the flats of the hexagon.

The thread length of inch-series bolts, where *d* is the nominal diameter, is

$$LT = \begin{cases} 2d + \frac{1}{4} \text{ in} & L \le 6 \text{ in} \\ 2d + \frac{1}{2} \text{ in} & L > 6 \text{ in} \end{cases} \qquad 5\text{-}11$$

and for metric bolts is

$$LT = \begin{cases} 2d + 6 & L \le 125 \quad d \le 48 \\ 2d + 12 & 125 < L \le 200 \\ 2d + 25 & L > 200 \end{cases} \qquad 5\text{-}12$$

where the dimensions are in millimeters. The ideal bolt length is one in which only one or two threads project from the nut after it is tightened. Bolt holes may have burrs or sharp edges after drilling. These could bite into the fillet and increase stress concentration. Therefore, washers must always be used under the bolt head to prevent this. They should be of hardened steel and loaded onto the bolt so that the rounded edge of the stamped hole faces the washer face of the bolt. Sometimes it is necessary to use washers under the nut too.
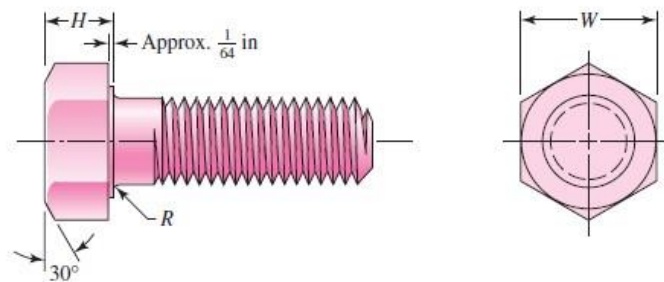
Figure (5–9)
Hexagon-head bolt; note the washer face, the fillet under the head, the start of threads, and the chamfer on both ends. Bolt lengths are always measured from below the head.

The purpose of a bolt is to clamp two or more parts together. The clamping load stretches or elongates the bolt; the load is obtained by twisting the nut until the bolt has elongated almost to the elastic limit. If the nut does not loosen, this bolt tension remains as the preload or clamping force. When tightening, the mechanic should, if possible, hold the bolt head stationary and twist the nut; in this way the bolt shank will not feel the thread-friction torque.

The head of a hexagon-head cap screw is slightly thinner than that of a hexagon- head bolt. Hexagon-head cap screws are used in the same applications as bolts and also in applications in which one of the clamped members is threaded. Three other common cap-screw head styles are shown in Fig. (5–10).
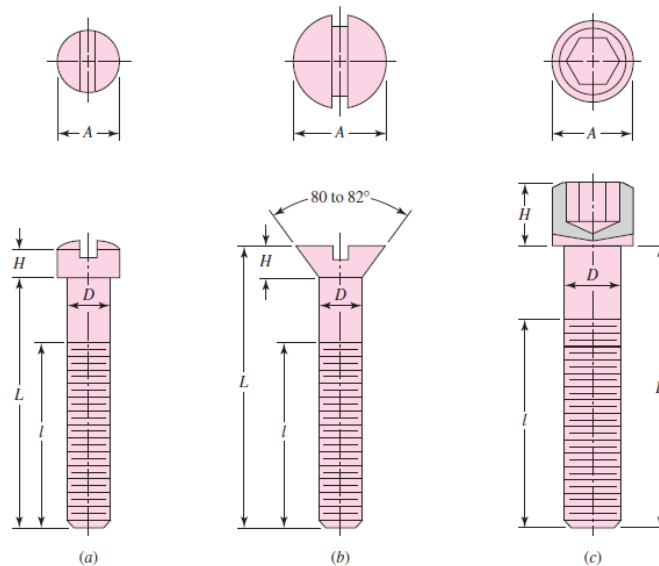
Figure (5–10)

Typical cap-screw heads: (*a*) fillister head; (*b*) flat head; (*c*) hexagonal socket head. Cap screws are also manufactured with hexagonal heads similar to the one shown in Fig. (5–9), as well as a variety of other head styles. This illustration uses one of the conventional methods of representing threads

A variety of machine-screw head styles are shown in Fig. (5–11). Inch-series machine screws are generally available in sizes from No. 0 to about 3/8 in. Several styles of hexagonal nuts are illustrated in Fig. (5–12). The material of the nut must be selected carefully to match that of the bolt. During tightening, the first thread of the nut tends to take the entire load; but yielding occurs, with some

strengthening due to the cold work that takes place, and the load is eventually divided over about three nut threads. For this reason you should never reuse nuts; in fact, it can be dangerous to do so.

(a) Round head 　　　(b) Flat head

(c) Fillister head 　　　(d) Oval head

(e) Truss head 　　　(f) Binding head

(g) Hex head (trimmed) 　　　(h) Hex head (upset)
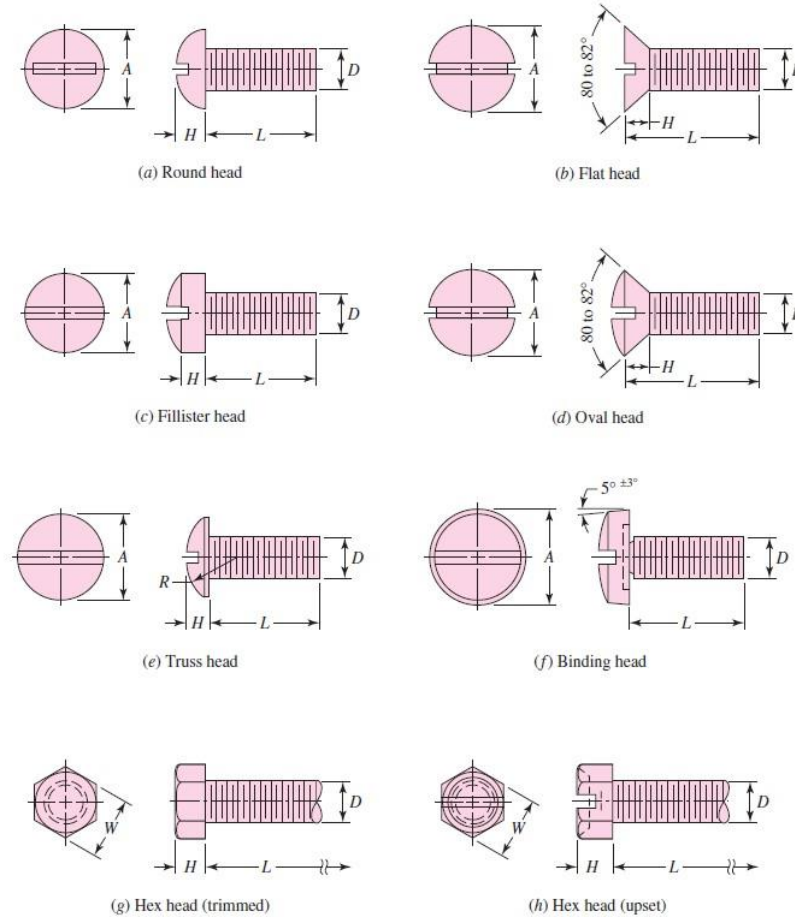
Figure (5–11)
Types of heads used on machine screws

(a)　(b)　(c)　(d)　(e)
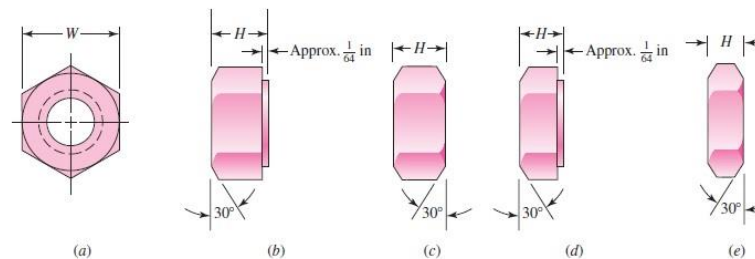
Figure (5–12)
Hexagonal nuts: (*a*) end view, general; (*b*) washer-faced regular nut;
(*c*) regular nut chamfered on both sides; (*d*) jam nut with washer
face; (*e*) jam nut chamfered on both sides.

5.4 Joints–Fastener, Member Stiffness and Bolt Strength

When a connection is desired that can be disassembled without destructive methods and that is strong enough to resist external tensile loads, moment loads, and shear loads, or a combination of these, then the simple bolted joint using hardened-steel w**ashers is a good** solution. Such a joint can also be dangerous unless it is properly designed and assembled by a *trained* mechanic.

A section through a tension-loaded bolted joint is illustrated in Fig. (5–13). **Notice the clearance space provided by the bolt holes. Notice, too, how the bolt threads extend into the body of the connection.**
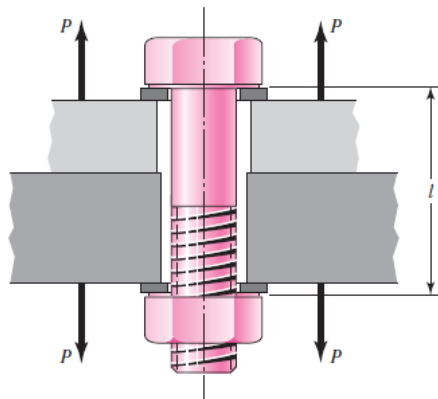
Figure (5–13)

A bolted connection loaded in tension by the forces *P*. Note the use of two washers. Note how the threads extend into the body of the connection. This is usual and is desired. *l* is the grip of the connection
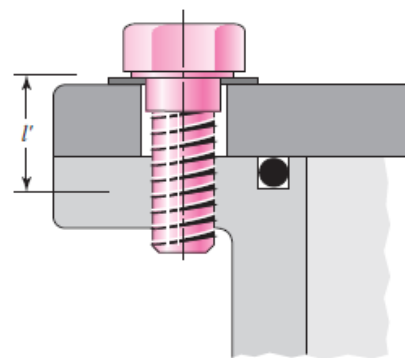
Figure (5–14)

Section of cylindrical pressure vessel. Hexaaggoonn--hhead cap screws are used to fasten the cylinder head to the body. Note the use of an O-ring seal. l ′ is the effective grip of the connection

As noted previously, the purpose of the bolt is to clamp the two, or more, parts together. Twisting the nut stretches the bolt to produce the clamping force. This clamping force is called the *pretension* or *bolt preload*. It exists in the connection after the nut has been properly tightened no matter whether the external tensile load *P* is exerted or not.

Of course, since the members are being clamped together, the clamping force that produces tension in the bolt induces compression in the members.

Figure (5–14) shows another tension-loaded connection. This joint uses cap screws threaded into one of the members. An alternative approach to this problem (of not using a nut) would be to use studs. A stud is a rod threaded on both ends. The stud is screwed into the lower member first; then the top member is positioned and fastened down with hardened washers and nuts. The studs are regarded as permanent, and so the joint can be disassembled merely by removing the nut and washer. Thus the threaded part of the lower member is not damaged by reusing the threads.

Y. Ito has used ultrasonic techniques to determine the pressure distribution at the member interface. The results show that the pressure stays high out to about 1.5 bolt radii. The pressure, however, falls off farther away from the bolt. Thus Ito suggests the use of Rotscher's pressure-cone method for stiffness calculations with a variable cone angle. Figure (5–15) illustrates the general cone geometry using a half-apex angle (α). C. C. Osgood reports a range of $25^\circ \leq \alpha \leq 33^\circ$ for most combinations.
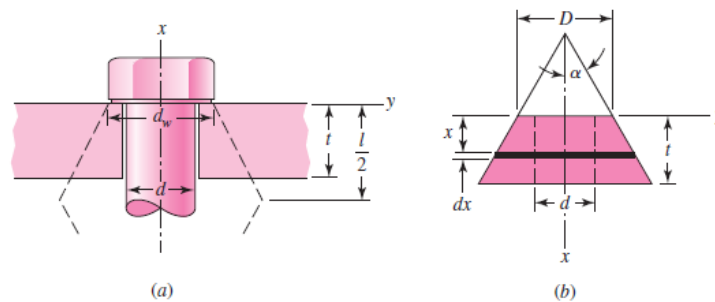
Figure (5–15)
Compression of a member with the equivalent elastic properties represented by a frustum of a hollow cone. Here, *l* represents the grip length.

In the specification standards for bolts, the strength is specified by stating ASTM minimum quantities, the *minimum proof strength (S_p),* or *minimum proof load,* and the *minimum tensile strength.*

The *proof load* is the maximum load (force) that a bolt can withstand without acquiring a permanent set. The *proof strength* is the quotient of the proof load and the tensile-stress area. The proof strength thus corresponds roughly to the proportional limit and corresponds to 0.0001 in permanent set in the fastener (first measurable deviation from elastic behavior). The value of the mean proof strength, the mean tensile strength, and the corresponding

standard deviations are not part of the specification codes, so it is the designer's responsibility to obtain these values, perhaps by laboratory testing, before designing to a reliability specification. Bolts in fatigue axial loading fail at the fillet under the head, at the thread runout, and at the first thread engaged in the nut.

5.5 Bolted and Riveted Joints Loaded in Shear

Riveted and bolted joints loaded in shear are treated exactly alike in design and analysis. Figure (5−16a) shows a riveted connection loaded in shear. Figure (5−16b) shows a failure by bending of the rivet or of the riveted members. The bending moment is approximately $M = Ft/2$, where F is the shearing force and t is the grip of the rivet, that is, the total thickness of the connected parts. The bending stress in the members or in the rivet is, neglecting stress concentration,

$$\sigma = \frac{M}{I/c}$$ 5-13

where I/c is the section modulus for the weakest member or for the rivet or rivets, depending upon which stress is to be found. The calculation of the bending stress in this manner is an assumption, because we do not know exactly how the load is distributed to the rivet or the relative deformations of the rivet and the members. Although this equation can be used to determine the bending stress, it is seldom used in design; instead its effect is compensated for by an increase in the factor of safety.

In Fig. (5−16c) failure of the rivet by pure shear is shown; the stress in the rivet is

$$\tau = \frac{F}{A}$$ 5-14

where A is the cross-sectional area of all the rivets in the group. It may be noted that it is standard practice in structural design to use the nominal diameter of the rivet rather than the diameter of the hole, even though a hot-driven rivet expands and nearly fills up the hole.
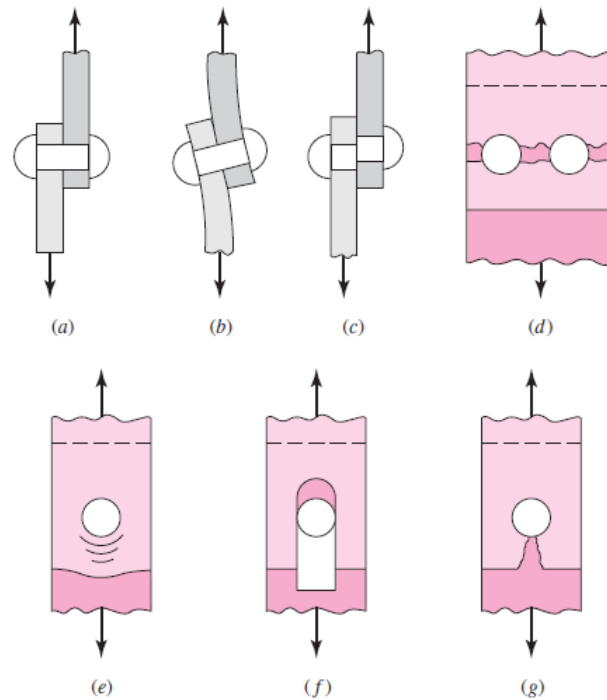
Figure (5–16)
Modes of failure in shear loading of a bolted or riveted connection: (*a*) shear loading; (*b*) bending of rivet; (*c*) shear of rivet; (*d*) tensile failure of members; (*e*) bearing of rivet on members or bearing of members on rivet; (*f*) shear tear-out; (*g*) tensile tear-out.

Rupture of one of the connected members or plates by pure tension is illustrated in Fig. (5–16*d*). The tensile stress is

$$\sigma = \frac{F}{A} \qquad\qquad \text{5-15}$$

where *A* is the net area of the plate, that is, the area reduced by an amount equal to the area of all the rivet holes. For brittle materials and static loads and for either ductile or brittle materials loaded in fatigue, the stress-concentration effects must be included. It is true that the use of a bolt with an initial preload and, sometimes, a rivet will place the area around the hole in compression and thus tend to nullify the effects of stress concentration, but unless definite steps are taken to ensure that the preload does not relax, it is on the conservative side to design as if the full stress-concentration effect

were present. The stress-concentration effects are not considered in structural design, because the loads are static and the materials ductile.

In calculating the area for Eq. (5–16), the designer should, of course, use the combination of rivet or bolt holes that gives the smallest area.

Figure (5–16*e*) illustrates a failure by crushing of the rivet or plate. Calculation of this stress, which is usually called a *bearing stress,* is complicated by the distribution of the load on the cylindrical surface of the rivet. The exact values of the forces acting upon the rivet are unknown, and so it is customary to assume that the components of these forces are uniformly distributed over the projected contact area of the rivet. This gives for the stress

$$\sigma = -\frac{F}{A} \qquad\qquad 5\text{-}16$$

where the projected area for a single rivet is $A = td$. Here, t is the thickness of the thinnest plate and d is the rivet or bolt diameter.

Edge shearing, or tearing, of the margin is shown in Fig. (5–16*f* and *g*), respectively. In structural practice this failure is avoided by spacing the rivets at least 1.5 diameters away from the edge. Bolted connections usually are spaced an even greater distance than this for satisfactory appearance, and hence this type of failure may usually be neglected.

In a rivet joint, the rivets all share the load in shear, bearing in the rivet, bearing in the member, and shear in the rivet. Other failures are participated in by only some of the joint. In a bolted joint, shear is taken by clamping friction, and bearing does not exist. When bolt preload is lost, one bolt begins to carry the shear and bearing until yielding slowly brings other fasteners in to share the shear and bearing. Finally, all participate, and this is the basis of most bolted-joint analysis if loss of bolt preload is complete. The usual analysis involves

• Bearing in the bolt (all bolts participate)
• Bearing in members (all holes participate)
• Shear of bolt (all bolts participate eventually)
• Distinguishing between thread and shank shear
• Edge shearing and tearing of member (edge bolts participate)
• Tensile yielding of member across bolt holes
• Checking member capacity

EXAMPLE 5–2

Two 1- by 4-in 1018 cold-rolled steel bars are butt-spliced with two 0.5- by 4-in 1018 cold-rolled splice plates using four 0.75 in-16 UNF grade 5 bolts as depicted in the figure. For a design factor of n_d = 1.5 estimate the static load F that can be carried if the bolts lose preload.

(a)

(b)
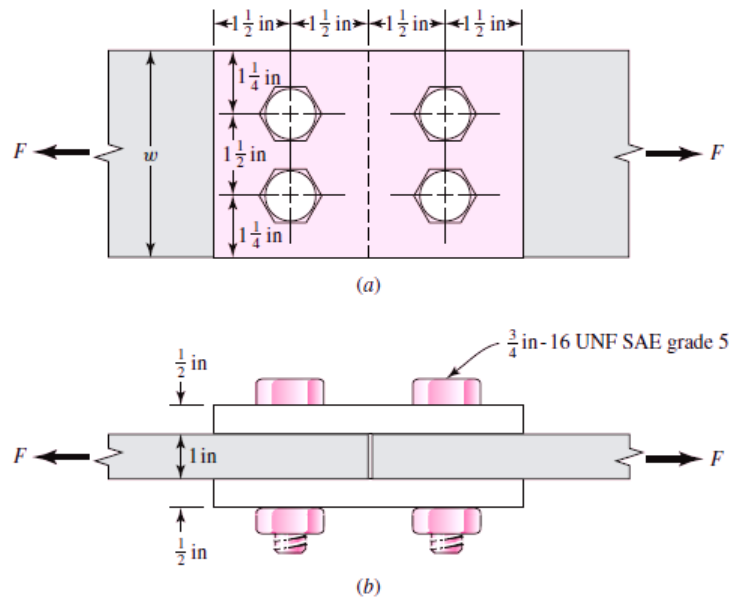
Solution

From Table (3–4), minimum strengths of S_y = 54 kpsi and S_{ut} = 64 kpsi are found for the members, and from Table (5–5) minimum strengths of S_p = 85 kpsi and S_{ut} = 120 kpsi for the bolts are found.

    $F/2$ is transmitted by each of the splice plates, but since the areas of the splice plates are half those of the center bars, the stresses associated with the plates are the same. So for stresses associated with the plates, the force and areas used will be those of the center plates.

Bearing in bolts, all bolts loaded:

$$\sigma = \frac{F}{2td} = \frac{S_p}{n_d} \qquad F = \frac{2tdS_p}{n_d} = \frac{2(1)\left(\frac{3}{4}\right)85}{1.5} = 85 \text{ kip}$$

Bearing in members, all bolts active:

$$\sigma = \frac{F}{2td} = \frac{(S_y)_{mem}}{n_d} \qquad F = \frac{2td(S_y)_{mem}}{n_d} = \frac{2(1)\left(\frac{3}{4}\right)54}{1.5} = 54 \text{ kip}$$

Shear of bolt, all bolts active: If the bolt threads do not extend into the shear planes for four shanks:

$$F = 0.577 \, \pi \, d^2 \, (S_p/n_d) = 0.577 \, \pi \, (0.75)^2 \, (85/1.5) = 57.8 \text{ kip}$$

If the bolt threads extend into a shear plane:

$$F = 4 \, A_r \, (0.577) \, (S_p/n_d) = 4 \, (0.351) \, (0.577) \, (85/1.5) = 45.9 \text{ kip}$$

Edge shearing of member at two margin bolts: From the figure,

$$\tau = \frac{F}{4at} = \frac{0.577(S_y)_{mem}}{n_d}$$

$$F = \frac{4at0.577(S_y)_{mem}}{n_d} = \frac{4(1.125)(1)0.577(54)}{1.5} = 93.5 \text{ kip}$$

Tensile yielding of members across bolt holes:

$$\sigma = \frac{F}{\left[4 - 2\left(\frac{3}{4}\right)\right]t} = \frac{(S_y)_{mem}}{n_d}$$

$$F = \frac{\left[4 - 2\left(\frac{3}{4}\right)\right]t(S_y)_{mem}}{n_d} = \frac{\left[4 - 2\left(\frac{3}{4}\right)\right](1)54}{1.5} = 90 \text{ kip}$$
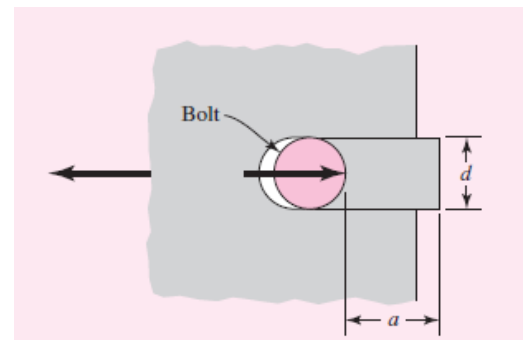
Member yield:

$$F = w \, t \, [(S_y)_{mem} / n_d] = 4 \, (1) \, (54/1.5) = 144 \text{ kip}$$

On the basis of bolt shear, the limiting value of the force is 45.9 kip, assuming the threads extend into a shear plane. However, it would be poor design to allow the threads to extend into a shear plane. So, assuming a *good* design based on bolt shear, the limiting value of the force is 57.8 kip. For the members, the bearing stress limits the load to 54 kip.

➢ *Shear Joints with Eccentric Loading*

Integral to the analysis of a shear joint is locating the center of relative motion between the two members. In Fig. (5–17) let A_1 to A_5 be the respective cross-sectional areas of a group of five pins, or hot-driven rivets, or tight-fitting shoulder bolts. Under this assumption the rotational pivot point lies at the centroid of the cross-sectional area pattern of the pins, rivets, or bolts. Using statics, we learn that the centroid G is located by the coordinates $\bar{x}$ and $\bar{y}$, where x_i and y_i are the distances to the ith area center:
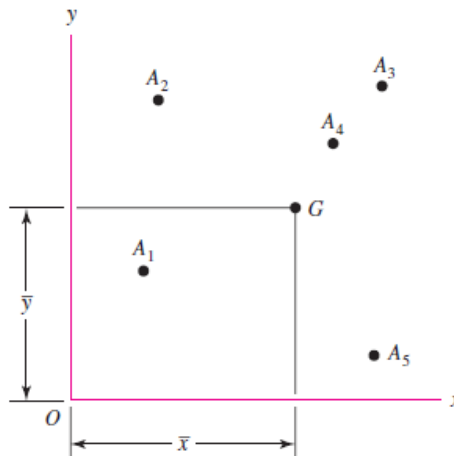
Figure (5–17)
Centroid of pins, rivets, or bolts

$$\bar{x} = \frac{A_1 x_1 + A_2 x_2 + A_3 x_3 + A_4 x_4 + A_5 x_5}{A_1 + A_2 + A_3 + A_4 + A_5} = \frac{\sum_1^n A_i x_i}{\sum_1^n A_i}$$

5-17

$$\bar{y} = \frac{A_1 y_1 + A_2 y_2 + A_3 y_3 + A_4 y_4 + A_5 y_5}{A_1 + A_2 + A_3 + A_4 + A_5} = \frac{\sum_1^n A_i y_i}{\sum_1^n A_i}$$

In many instances the centroid can be located by symmetry.

An example of eccentric loading of fasteners is shown in Fig. (5–18). This is a portion of a machine frame containing a beam subjected to the action of a bending load. In this case, the beam is fastened to vertical members at the ends with specially prepared load-sharing bolts. You will recognize the schematic representation in Fig. (5–18b) as a statically indeterminate beam with both ends fixed and with moment and shear reactions at each end.
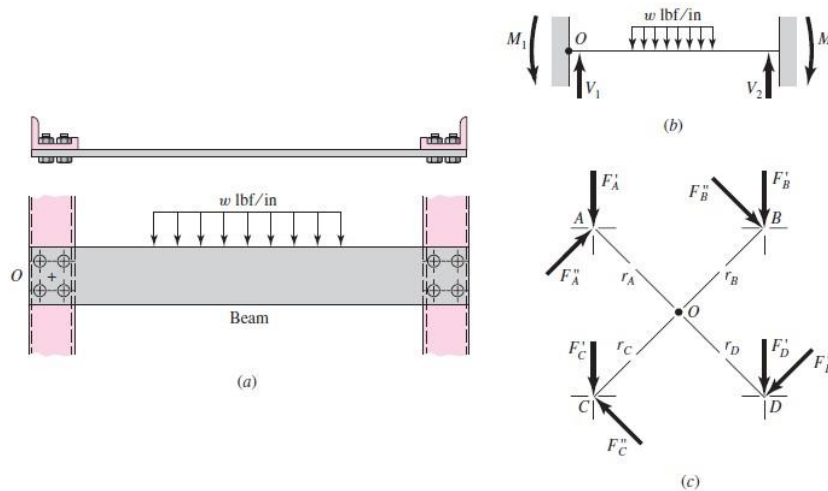
Figure (5–18)
(a) Beam bolted at both ends with distributed load; (b) free-body diagram of beam; (c) enlarged view of bolt group centered at O showing primary and secondary resultant shear forces

For convenience, the centers of the bolts at the left end of the beam are drawn to a larger scale in Fig. (5–18c). Point O represents the centroid of the group, and it is assumed in this example that all the bolts are of the same diameter. Note that the forces shown in Fig. (5–18c) are the *resultant* forces acting on the pins with a net force and moment equal and opposite to the *reaction* loads V_1 and M_1

acting at O. The total load taken by each bolt will be calculated in three steps. In the first step the shear V_1 is divided equally among the bolts so that each bolt takes $F' = V_1/n$, where n refers to the number of bolts in the group and the force F' is called the *direct load,* or *primary shear*. It is noted that an equal distribution of the direct load to the bolts assumes an absolutely rigid member. The arrangement of the bolts or the shape and size of the members sometimes justifies the use of another assumption as to the division of the load. The direct loads F' are shown as vectors on the loading diagram (Fig. 5–18*c*).

The *moment load,* or *secondary shear,* is the additional load on each bolt due to the moment M_1. If r_A, r_B, r_C , etc., are the radial distances from the centroid to the center of each bolt, the moment and moment loads are related as follows:

$$M_1 = F''_A r_A + F''_B r_B + F''_C r_C + \cdots \qquad \text{a}$$

where the F'' are the moment loads. The force taken by each bolt depends upon its radial distance from the centroid; that is, the bolt farthest from the centroid takes the greatest load, while the nearest bolt takes the smallest. We can therefore write

$$\frac{F''_A}{r_A} = \frac{F''_B}{r_B} = \frac{F''_C}{r_C} \qquad \text{b}$$

where again, the diameters of the bolts are assumed equal. If not, then one replaces F'' in Eq. (*b*) with the shear stresses $\tau'' = 4F''/\pi d^2$ for each bolt. Solving Eqs. (*a*) and (*b*) simultaneously, we obtain:

$$F''_n = \frac{M_1 r_n}{r_A^2 + r_B^2 + r_C^2 + \cdots} \qquad \text{5-18}$$

$$5$$

where the subscript n refers to the particular bolt whose load is to be found. These moment loads are also shown as vectors on the loading diagram.

In the third step the direct and moment loads are added vectorially to obtain the resultant load on each bolt. Since all the bolts or rivets are usually the same size, only that bolt having the maximum load need be considered. When the maximum load is found, the strength may be determined by using the various methods already described.

EXAMPLE 5–3

Shown in figure is a 15- by 200-mm rectangular steel bar cantilevered to a 250-mm steel channel using four tightly fitted bolts located at *A, B, C,* and *D*. For a load of *F* = 16 kN, find

(a) The resultant load on each bolt
(b) The maximum shear stress in each bolt
(c) The maximum bearing stress
(d) The critical bending stress in the bar

Dimensions in millimeters
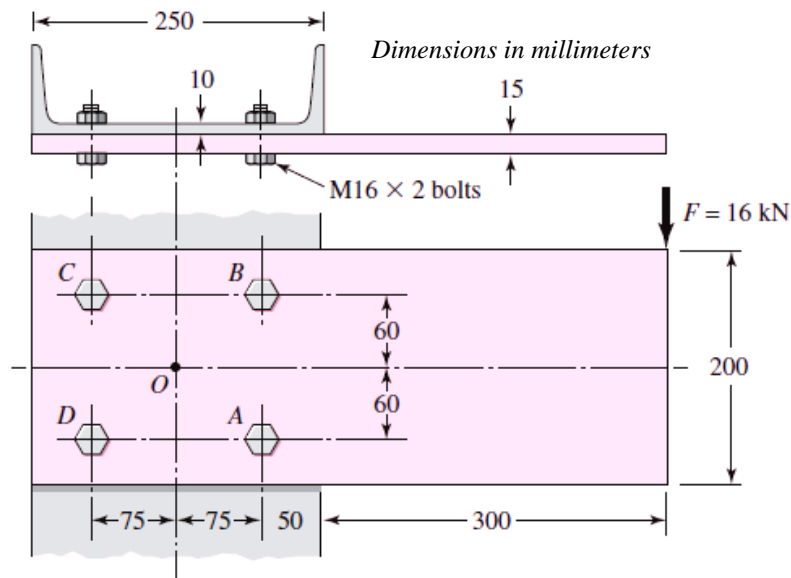
Solution

(a) Point *O*, the centroid of the bolt group, is found by symmetry. If a free-body diagram of the beam were constructed, the shear reaction *V* would pass through *O* and the moment reactions *M* would be about *O*. These reactions are

$$V = 16 \text{ kN} \qquad\qquad M = 16(425) = 6800 \text{ N·m}$$

In the following figure, the bolt group has been drawn to a larger scale and the reactions are shown.
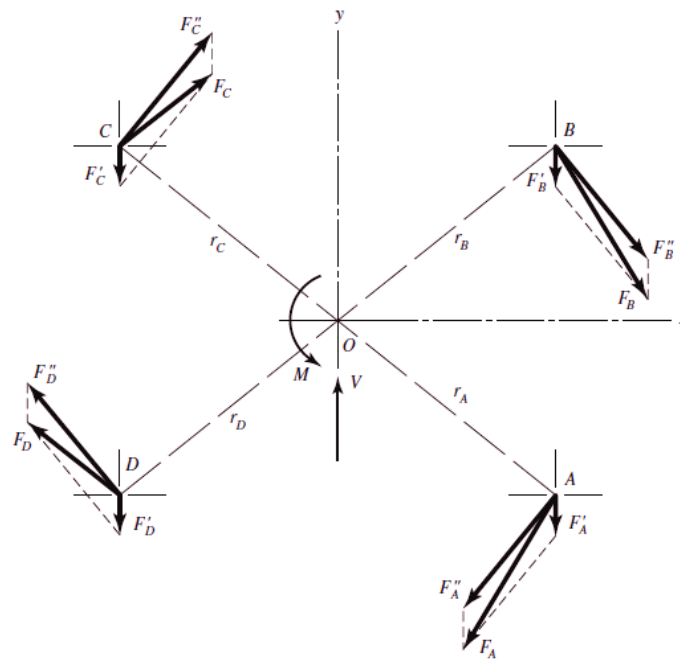
The distance from the centroid to the center of each bolt is

$$r = [(60)^2 + (75)^2]^{1/2} = 96 \text{ mm}$$

The primary shear load per bolt is

$$F' = \frac{V}{n} = \frac{16}{4} = 4 \text{ kN}$$

Since the secondary shear forces are equal, Eq. (5–19) becomes

$$F'' = \frac{Mr}{4r^2} = \frac{M}{4r} = \frac{6800}{4(96.0)} = 17.7 \text{ kN}$$

The primary and secondary shear forces are plotted to scale and the resultants obtained by using the parallelogram rule. The magnitudes are found by measurement (or analysis) to be

$$F_A = F_B = 21.0 \text{ kN}$$

(HW)

$$F_C = F_D = 14.8 \text{kN}$$

(b) Bolts *A* and *B* are critical because they carry the largest shear load. Does this shear act on the threaded portion of the bolt, or on

the unthreaded portion? The bolt length will be 25 mm plus the height of the nut plus about 2 mm for a washer. From net-tables, the nut height is 14.8 mm. Including two threads beyond the nut, this adds up to a length of 43.8 mm, and so a bolt 46 mm long will be needed. From Eq. (5–12) we compute the thread length as $L_T = 38$ mm. Thus the unthreaded portion of the bolt is $46 - 38 = 8$ mm long. This is less than the 15 mm for the plate in Fig. 8–28, and so the bolt will tend to shear across its minor diameter. Therefore, from table (5–1), the shear-stress area is $A_s = 144$ mm^2, and so the shear stress is

$$\tau = \frac{F}{A_s} = -\frac{21.0(10)^3}{144} = 146 \text{ MPa}$$

(c) The channel is thinner than the bar, and so the largest bearing stress is due to the pressing of the bolt against the channel web. The bearing area is $A_b = td = 10(16) = 160$ mm^2. Thus the bearing stress   is

$$\sigma = -\frac{F}{A_b} = -\frac{21.0(10)^3}{160} = -131 \text{ MPa}$$

(d) The critical bending stress in the bar is assumed to occur in a section parallel to the y axis and through bolts A and B. At this section the bending moment is

$$M = 16(300 + 50) = 5600 \text{ N·m}$$

The second moment of area through this section is obtained by the use of the transfer formula, as follows:

$$I = I_{\text{bar}} - 2(I_{\text{holes}} + \bar{d}^2 A)$$

$$= \frac{15(200)^3}{12} - 2\left[\frac{15(16)^3}{12} + (60)^2(15)(16)\right] = 8.26(10)^6 \text{ mm}^4$$

Then:

$$\sigma = \frac{Mc}{I} = \frac{5600(100)}{8.26(10)^6}(10)^3 = 67.8 \text{ MPa}$$

Table (5–1)
Diameters and Areas of Coarse-Pitch and Fine-Pitch Metric Threads

Nominal Major Diameter d mm	Coarse-Pitch Series			Fine-Pitch Series		
	Pitch p mm	Tensile-Stress Area A_t mm²	Minor-Diameter Area A_r mm²	Pitch p mm	Tensile-Stress Area A_t mm²	Minor-Diameter Area A_r mm²
1.6	0.35	1.27	1.07			
2	0.40	2.07	1.79			
2.5	0.45	3.39	2.98			
3	0.5	5.03	4.47			
3.5	0.6	6.78	6.00			
4	0.7	8.78	7.75			
5	0.8	14.2	12.7			
6	1	20.1	17.9			
8	1.25	36.6	32.8	1	39.2	36.0
10	1.5	58.0	52.3	1.25	61.2	56.3
12	1.75	84.3	76.3	1.25	92.1	86.0
14	2	115	104	1.5	125	116
16	2	157	144	1.5	167	157
20	2.5	245	225	1.5	272	259
24	3	353	324	2	384	365
30	3.5	561	519	2	621	596
36	4	817	759	2	915	884
42	4.5	1120	1050	2	1260	1230
48	5	1470	1380	2	1670	1630
56	5.5	2030	1910	2	2300	2250
64	6	2680	2520	2	3030	2980
72	6	3460	3280	2	3860	3800
80	6	4340	4140	1.5	4850	4800
90	6	5590	5360	2	6100	6020
100	6	6990	6740	2	7560	7470
110				2	9180	9080

The equations and data used to develop this table have been obtained from ANSI B1.1-1974 and B18.3.1-1978. The minor diameter was found from the equation $d_r = d - 1.226869\,p$, and the pitch diameter from $d_p = d - 0.649519\,p$. The mean of the pitch diameter and the minor diameter was used to compute the tensile-stress area.

Table (5–2)
Diameters and Area of Unified Screw Threads UNC and UNF

Size Designation	Nominal Major Diameter in	Coarse Series—UNC			Fine Series—UNF		
		Threads per Inch N	Tensile-Stress Area A_t in²	Minor-Diameter Area A_r in²	Threads per Inch N	Tensile-Stress Area A_t in²	Minor-Diameter Area A_r in²
0	0.0600				80	0.001 80	0.001 51
1	0.0730	64	0.002 63	0.002 18	72	0.002 78	0.002 37
2	0.0860	56	0.003 70	0.003 10	64	0.003 94	0.003 39
3	0.0990	48	0.004 87	0.004 06	56	0.005 23	0.004 51
4	0.1120	40	0.006 04	0.004 96	48	0.006 61	0.005 66
5	0.1250	40	0.007 96	0.006 72	44	0.008 80	0.007 16
6	0.1380	32	0.009 09	0.007 45	40	0.010 15	0.008 74
8	0.1640	32	0.014 0	0.011 96	36	0.014 74	0.012 85
10	0.1900	24	0.017 5	0.014 50	32	0.020 0	0.017 5
12	0.2160	24	0.024 2	0.020 6	28	0.025 8	0.022 6
$\frac{1}{4}$	0.2500	20	0.031 8	0.026 9	28	0.036 4	0.032 6
$\frac{5}{16}$	0.3125	18	0.052 4	0.045 4	24	0.058 0	0.052 4
$\frac{3}{8}$	0.3750	16	0.077 5	0.067 8	24	0.087 8	0.080 9
$\frac{7}{16}$	0.4375	14	0.106 3	0.093 3	20	0.118 7	0.109 0
$\frac{1}{2}$	0.5000	13	0.141 9	0.125 7	20	0.159 9	0.148 6
$\frac{9}{16}$	0.5625	12	0.182	0.162	18	0.203	0.189
$\frac{5}{8}$	0.6250	11	0.226	0.202	18	0.256	0.240
$\frac{3}{4}$	0.7500	10	0.334	0.302	16	0.373	0.351
$\frac{7}{8}$	0.8750	9	0.462	0.419	14	0.509	0.480
1	1.0000	8	0.606	0.551	12	0.663	0.625
$1\frac{1}{4}$	1.2500	7	0.969	0.890	12	1.073	1.024
$1\frac{1}{2}$	1.5000	6	1.405	1.294	12	1.581	1.521

This table was compiled from ANSI B1.1-1974. The minor diameter was found from the equation $d_r = d - 1.299038\ p$, and the pitch diameter from $d_p = d - 0.649519\ p$. The mean of the pitch diameter and the minor diameter was used to compute the tensile-stress area.

Table (5–3)
Preferred Pitches for Acme Threads

d, in	$\frac{1}{4}$	$\frac{5}{16}$	$\frac{3}{8}$	$\frac{1}{2}$	$\frac{5}{8}$	$\frac{3}{4}$	$\frac{7}{8}$	1	$1\frac{1}{4}$	$1\frac{1}{2}$	$1\frac{3}{4}$	2	$2\frac{1}{2}$	3
p, in	$\frac{1}{16}$	$\frac{1}{14}$	$\frac{1}{12}$	$\frac{1}{10}$	$\frac{1}{8}$	$\frac{1}{6}$	$\frac{1}{6}$	$\frac{1}{5}$	$\frac{1}{5}$	$\frac{1}{4}$	$\frac{1}{4}$	$\frac{1}{4}$	$\frac{1}{3}$	$\frac{1}{2}$

Table (5–4)
SAE Specifications for Steel Bolts

SAE Grade No.	Size Range Inclusive, in	Minimum Proof Strength,* kpsi	Minimum Tensile Strength,* kpsi	Minimum Yield Strength,* kpsi	Material	Head Marking
1	$\frac{1}{4}-1\frac{1}{2}$	33	60	36	Low or medium carbon	
2	$\frac{1}{4}-\frac{3}{4}$	55	74	57	Low or medium carbon	
	$\frac{7}{8}-1\frac{1}{2}$	33	60	36		
4	$\frac{1}{4}-1\frac{1}{2}$	65	115	100	Medium carbon, cold-drawn	
5	$\frac{1}{4}-1$	85	120	92	Medium carbon, Q&T	
	$1\frac{1}{8}-1\frac{1}{2}$	74	105	81		
5.2	$\frac{1}{4}-1$	85	120	92	Low-carbon martensite, Q&T	
7	$\frac{1}{4}-1\frac{1}{2}$	105	133	115	Medium-carbon alloy, Q&T	
8	$\frac{1}{4}-1\frac{1}{2}$	120	150	130	Medium-carbon alloy, Q&T	
8.2	$\frac{1}{4}-1$	120	150	130	Low-carbon martensite, Q&T	

*Minimum strengths are strengths exceeded by 99 percent of fasteners.

Table (5–5)
ASTM Specifications for Steel Bolts

ASTM Desig-nation No.	Size Range, Inclusive, in	Minimum Proof Strength,* kpsi	Minimum Tensile Strength,* kpsi	Minimum Yield Strength,* kpsi	Material	Head Marking
A307	$\frac{1}{4}-1\frac{1}{2}$	33	60	36	Low carbon	
A325, type 1	$\frac{1}{2}-1$	85	120	92	Medium carbon, Q&T	A325
	$1\frac{1}{8}-1\frac{1}{2}$	74	105	81		
A325, type 2	$\frac{1}{2}-1$	85	120	92	Low-carbon, martensite,	A325
	$1\frac{1}{8}-1\frac{1}{2}$	74	105	81	Q&T	
A325, type 3	$\frac{1}{2}-1$	85	120	92	Weathering steel,	A325
	$1\frac{1}{8}-1\frac{1}{2}$	74	105	81	Q&T	
A354, grade BC	$\frac{1}{4}-2\frac{1}{2}$	105	125	109	Alloy steel, Q&T	BC
	$2\frac{3}{4}-4$	95	115	99		
A354, grade BD	$\frac{1}{4}-4$	120	150	130	Alloy steel, Q&T	
A449	$\frac{1}{4}-1$	85	120	92	Medium-carbon, Q&T	
	$1\frac{1}{8}-1\frac{1}{2}$	74	105	81		
	$1\frac{3}{4}-3$	55	90	58		
A490, type 1	$\frac{1}{2}-1\frac{1}{2}$	120	150	130	Alloy steel, Q&T	A490
A490, type 3	$\frac{1}{2}-1\frac{1}{2}$	120	150	130	Weathering steel, Q&T	A490

*Minimum   strengths are strengths exceeded by 99 percent of fasteners.

Table (5–6)

Metric Mechanical-Property Classes for Steel Bolts, Screws, and Studs*

Property Class	Size Range, Inclusive	Minimum Proof Strength,* MPa	Minimum Tensile Strength,* MPa	Minimum Yield Strength,* MPa	Material	Head Marking
4.6	M5–M36	225	400	240	Low or medium carbon	4.6
4.8	M1.6–M16	310	420	340	Low or medium carbon	4.8
5.8	M5–M24	380	520	420	Low or medium carbon	5.8
8.8	M16–M36	600	830	660	Medium carbon, Q&T	8.8
9.8	M1.6–M16	650	900	720	Medium carbon, Q&T	9.8
10.9	M5–M36	830	1040	940	Low-carbon martensite, Q&T	10.9
12.9	M1.6–M36	970	1220	1100	Alloy, Q&T	12.9

*The thread length for bolts and cap screws is

$$l_T = \begin{cases} 2d + 6 \text{ mm}, & l \leq 125, d \leq 48 \text{ mm} \\ 2d + 12 \text{ mm}, & 125 < l \leq 200 \text{ mm} \\ 2d + 25 \text{ mm}, & l > 200 \text{ mm} \end{cases}$$

where L is the bolt length. The thread length for structural bolts is slightly shorter than given above.

✱Minimum   strengths are strength exceeded by 99 percent of fasteners.

Homework

(1) A power screw is 25 mm in diameter and has a thread pitch of 5 mm. (*a*) Find the thread depth, the thread width, the mean and root diameters, and the lead, provided square threads are used. (*b*) Repeat part (*a*) for Acme threads.

(2) Show that for zero collar friction the efficiency of a square-thread screw is given by the equation

$$e = \tan \lambda \frac{1 - f \tan \lambda}{\tan \lambda + f}$$

(3) A single-threaded power screw is 25 mm in diameter with a pitch of 5 mm. A vertical load on the screw reaches a maximum of 6 kN. The coefficients of friction are 0.05 for the collar and 0.08 for the threads. The frictional diameter of the collar is 40 mm. Find   the overall efficiency and the torque to "raise" and "lower" the load.

(*Ans./* 0.294, 16.23 N.m, 6.622 N.m)

(4) A screw clamp similar to the one shown in the figure has a handle with diameter 3/16 in made of cold-drawn AISI 1006 steel. The overall length is 3 in. The screw is 7/16 in-14 UNC and is $5\frac{3}{4}$ in long, overall. Distance *A* is 2 in. The clamp will accommodate parts up to $4\frac{3}{16}$ in high.

(a) What screw torque will cause the handle to bend permanently?
(b) What clamping force will the answer to part (*a*) cause   if the collar friction is neglected and if the thread friction is 0.075?

*The force F is perpendicular to the paper*
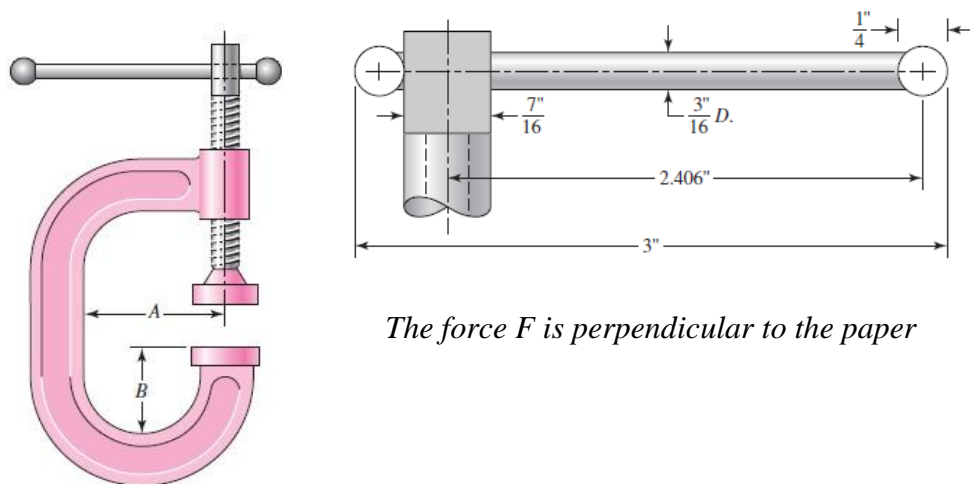
(5) Find the power required to drive a 40-mm power screw having double square threads with a pitch of 6 mm. The nut is to move at a velocity of 48 mm/s and move a load of $F = 10$ kN. The frictional coefficients are 0.1 for the threads and 0.15 for the collar. The frictional diameter of the collar is 60 mm. *(Ans./ 2.086 kW)*

(6) A single square-thread power screw has an input power of 3 kW at a speed of 1 rev/s. The screw has a diameter of 36 mm and a pitch of 6 mm. The frictional coefficients are 0.14 for the threads and 0.09 for the collar, with a collar friction radius of 45 mm. Find the axial resisting load F and the combined efficiency of the screw and collar.
*(Ans./ 65 kN, 0.13)*

(7) The figure shows a bolted lap joint that uses SAE grade 8 bolts. The members are made of cold-drawn AISI 1040 steel. Find the safe tensile shear load F that can be applied to this connection if the following factors of safety are specified: shear of bolts 3, bearing on bolts 2, bearing on members 2.5, and tension of members 3. *(Ans./ 5.18 kip)*
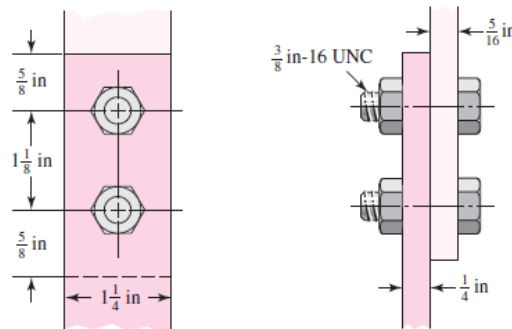

(8) The bolted connection shown in the figure uses SAE grade 5 bolts. The members are hot-rolled AISI 1018 steel. A tensile shear load $F = 4000$ lbf is applied to the connection. Find the factor of safety for all possible modes of failure. *(Ans./ 2.93, 4.32, 1.5, 3.25)*
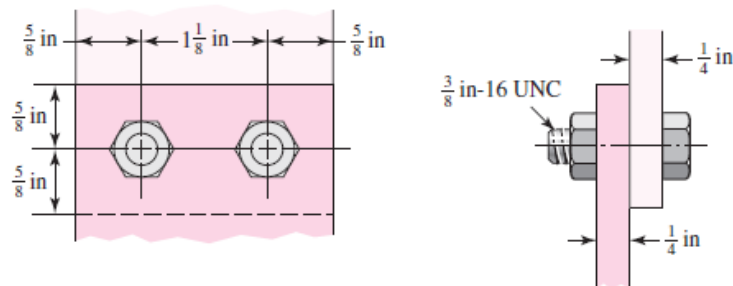
(9) A bolted lap joint using SAE grade 5 bolts and members made of cold-drawn SAE 1040 steel is shown in the figure. Find the tensile shear load F that can be applied to this connection if the following factors of safety are specified: shear of bolts 1.8, bearing on bolts 2.2, bearing on members 2.4, and tension of members 2.6. *(Ans./ 35.46)*
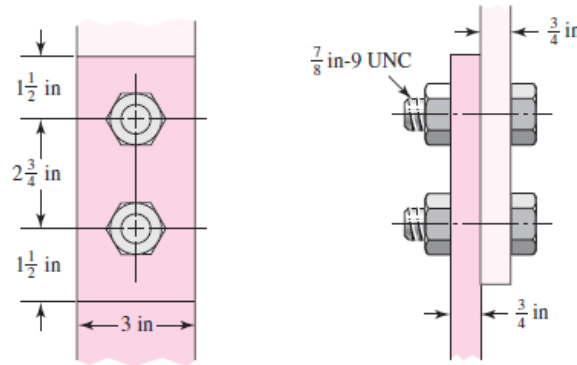
(10) The bolted connection shown in the figure is subjected to a tensile shear load of 20 kip. The bolts are SAE grade 5 and the material is cold-drawn AISI 1015 steel. Find the factor of safety of the connection for all possible modes of failure. *(Ans./ 3.52, 6.47, 3.31, 7.71)*
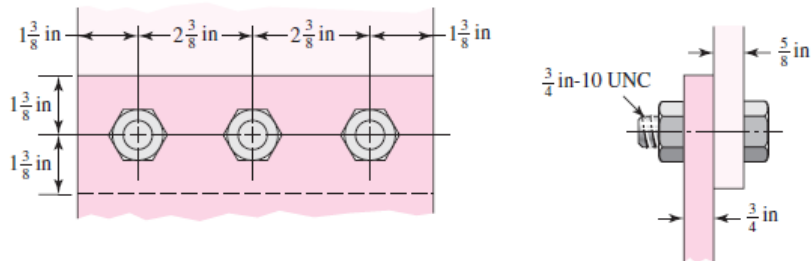
(11) The figure shows a connection that employs three SAE grade 5 bolts. The tensile shear load on the joint is 5400 lbf. The members are cold-drawn bars of AISI 1020 steel. Find the factor of safety for each possible mode of failure. *(Ans./ 3.26, 5.99, 3.71, 5.36)*
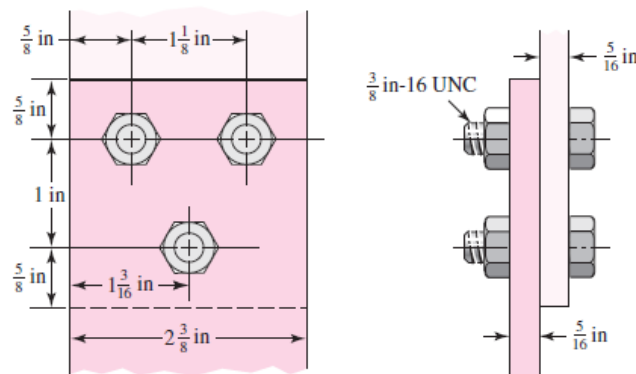
(12) A beam is made up by bolting together two cold-drawn bars of AISI 1018 steel as a lap joint, as shown in the figure. The bolts used are ISO 5.8. Ignoring any twisting, determine the factor of safety of the connection. *(Ans./ n = the minimum of (2.72, 5.29, 3.15) = 2.72)*
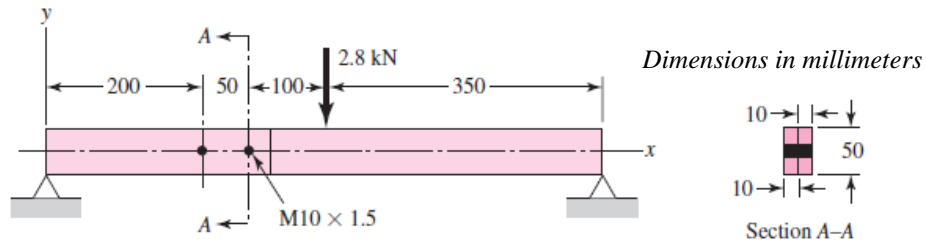
(13) A vertical channel 152×76 ($t = 6.4$ mm) has a cantilever beam bolted to it as shown. The channel is hot-rolled AISI 1006 steel. The bar is of hot-rolled AISI 1015 steel. The shoulder bolts are M12 × 1.75 ISO 5.8. For a design factor of 2.8, find the safe force *F* that can be applied to the cantilever. *(Ans./ F = 1.99 kN based on bearing on channel)*

Dimensions in millimeters
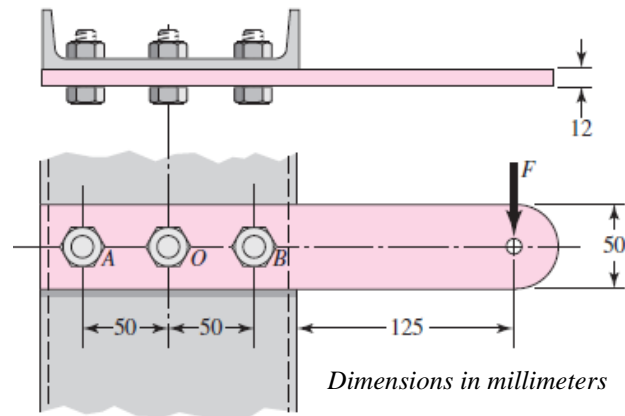
(14) Find the total shear load on each of the three bolts for the connection shown in the figure and compute the significant bolt shear stress and bearing stress. Find the second moment of area of the 8-mm plate on a section through the three bolt holes, and find the maximum bending stress in the plate. *(Ans./ 1.48(10)⁶ mm4, 110 MPa)*

Dimensions in millimeters

126

(15) A 3/8 - × 2-in AISI 1018 cold-drawn steel bar is cantilevered to support a static load of 300 lbf as illustrated. The bar is secured to the support using two 1/2 in-13 UNC SAE 5 bolts. Find the factor of safety for the following modes of failure: shear of bolt, bearing on bolt, bearing on member, and strength of member. (*Ans./* 5.79, 9.58, 5.63, 2.95)

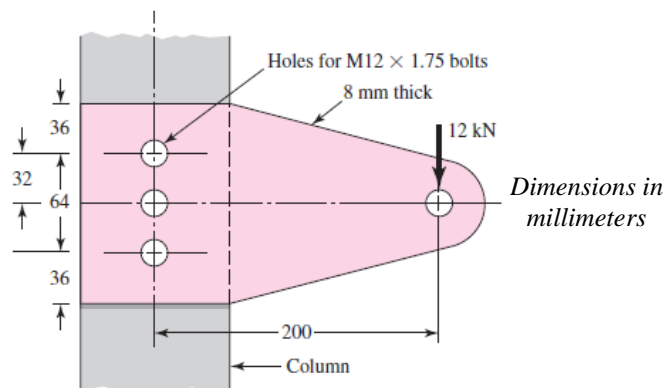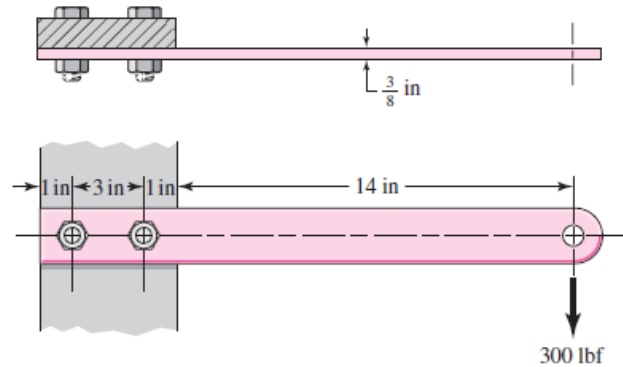(16) A cantilever is to be attached to the flat side of a channel used as a column. The cantilever is to carry a load as shown in the figure. To a designer the choice of a bolt array is usually an a priori decision. Such decisions are made from a background of knowledge of the effectiveness of various patterns.
(a) If two fasteners are used, should the array be arranged vertically, horizontally, or diagonally? How would you decide?
(b) If three fasteners are used, should a linear or triangular array be used? For a triangular array, what should be the orientation of the triangle? How would you decide?
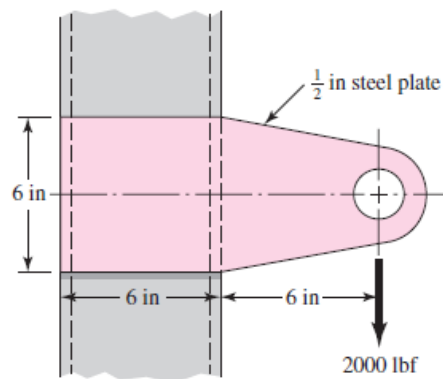
(17) Using your experience with Problem (*15*), specify a bolt pattern for this Problem and size the bolts.

6. Welding, Bonding, and the Design of Permanent Joints

Form can more readily pursue function with the help of joining processes such as welding, brazing, soldering, cementing, and gluing–processes that are used extensively in manufacturing today. Whenever parts have to be assembled or fabricated, there is usually good cause for considering one of these processes in preliminary design work. Particularly when sections to be joined are thin, one of these methods may lead to significant savings. The elimination of individual fasteners, with their holes and assembly costs, is an important factor. Also, some of the methods allow rapid machine assembly, furthering their attractiveness.

6.1 Welding Symbols

A weldment is fabricated by welding together a collection of metal shapes, cut to particular configurations. During welding, the several parts are held securely together, often by clamping or jigging. The welds must be precisely specified on working drawings, and this is done by using the welding symbol, shown in Fig. (6–1), as standardized by the American Welding Society (AWS). The arrow of this symbol points to the joint to be welded. The body of the symbol contains as many of the following elements as are deemed necessary:

• Reference line
• Arrow
• Basic weld symbols as in Fig. (6–2)
• Dimensions and other data
• Supplementary symbols
• Finish symbols
• Tail
• Specification or process

The *arrow side* of a joint is the line, side, area, or near member to which the arrow points. The side opposite the arrow side is the *other side*.
Figures (6–3 to 6–6) illustrate the types of welds used most frequently by designers. For general machine elements most welds are fillet welds, though butt welds are used a great deal in designing

pressure vessels. Of course, the parts to be joined must be arranged so that there is sufficient clearance for the welding operation. If unusual joints are required because of insufficient clearance or because of the section shape, the design may be a poor one and the designer should begin again and endeavor to synthesize another solution.
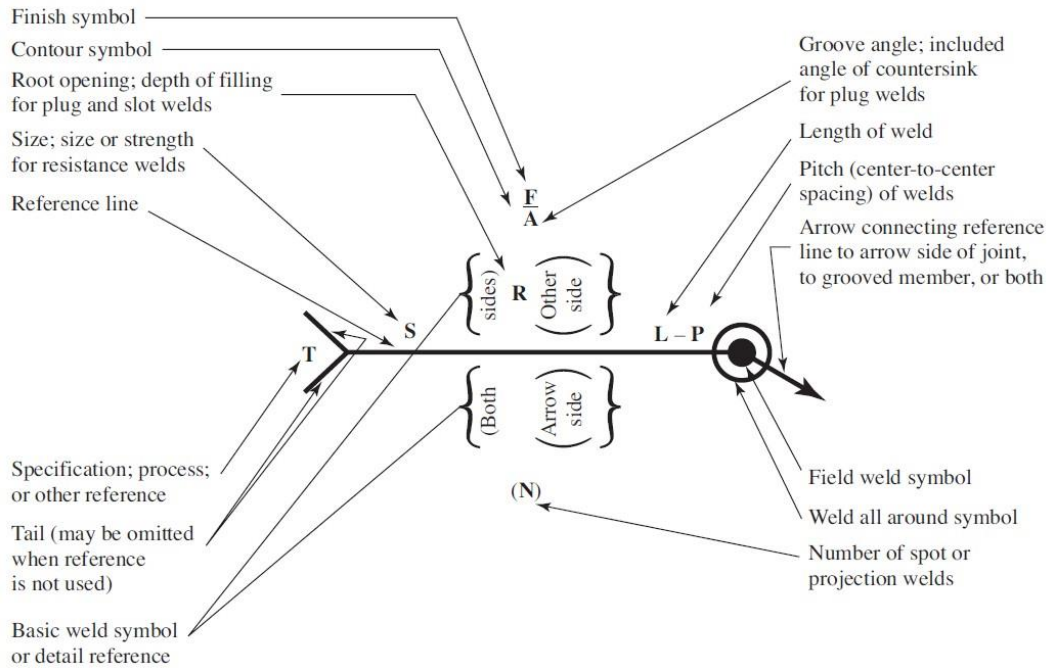
Figure (6–1)
The AWS standard welding symbol showing the location
of the symbol elements

Figure (6–2)
Arc- and gas-weld symbols
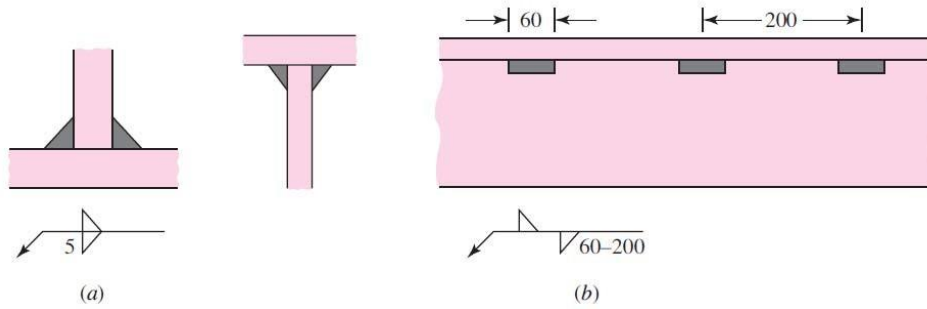
Figure (6–3)

Fillet welds. (*a*) The number indicates the leg size; the arrow should point only to one weld when both sides are the same. (*b*) The symbol indicates that the welds are intermittent and staggered 60 mm along on 200-mm centers

Figure (6–4)

The circle on the weld symbol indicates that the welding is to go all around
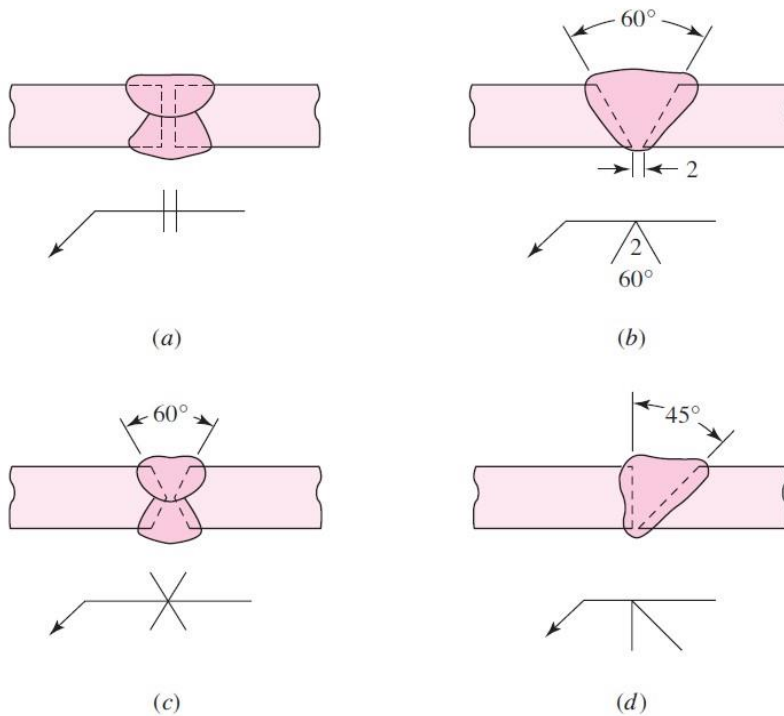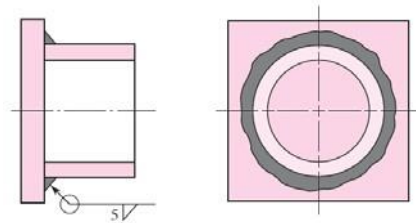
Figure (6–5)

Butt or groove welds: (*a*) square butt-welded on both sides; (*b*) single V with 60° bevel and root opening of 2 mm; (*c*) double V; (*d*) single bevel

(a)　　　　　　　　　　　　　　　　　　(b)

(c)　　　　　　　　　　　　　　　　　　(d)
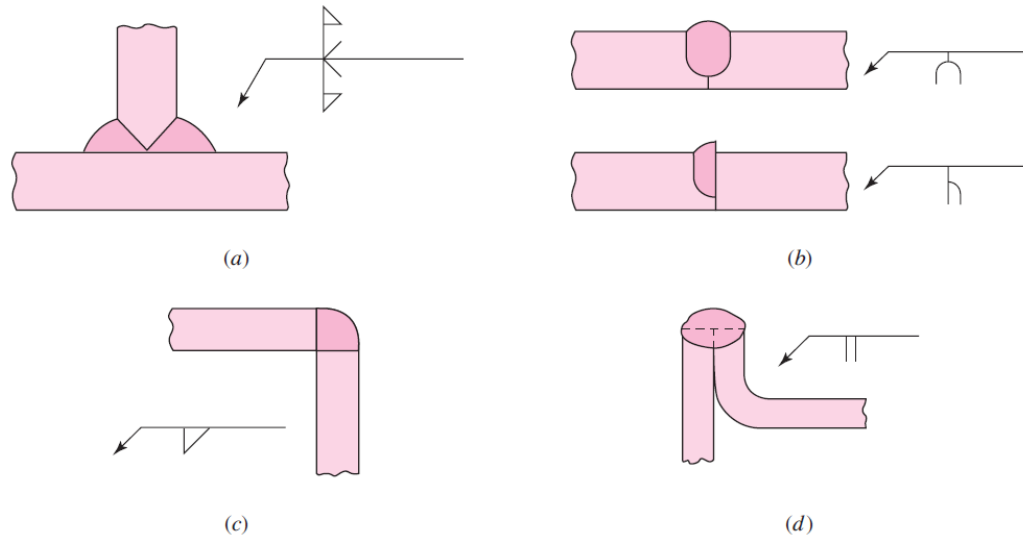
Figure (6–6)

Special groove welds: (*a*) T joint for thick plates; (*b*) U and J welds for thick plates; (*c*) corner weld (may also have a bead weld on inside for greater strength but should not be used for heavy loads); (*d*) edge weld for sheet metal and light loads

Since heat is used in the welding operation, there are metallurgical changes in the parent metal in the vicinity of the weld. Also, residual stresses may be introduced because of clamping or holding or, sometimes, because of the order of welding. Usually these residual stresses are not severe enough to cause concern; in some cases a light heat treatment after welding has been found helpful in relieving them. When the parts to be welded are thick, a preheating will also be of benefit. If the reliability of the component is to be quite high, a testing program should be established to learn what changes or additions to the operations are necessary to ensure the best quality.

6.2 Butt and Fillet Welds

Figure (6–7*a*) shows a single V-groove weld loaded by the tensile force *F*. For either tension or compression loading, the average normal stress is

$$\sigma = \frac{F}{hl} \qquad\qquad\qquad 6\text{-}1$$

where *h* is the weld throat and *l* is the length of the weld, as shown in the figure. Note that the value of *h* does not include the

reinforcement. The reinforcement can be desirable, but it varies somewhat and does produce stress concentration at point *A* in the figure. If fatigue loads exist, it is good practice to grind or machine off the reinforcement.
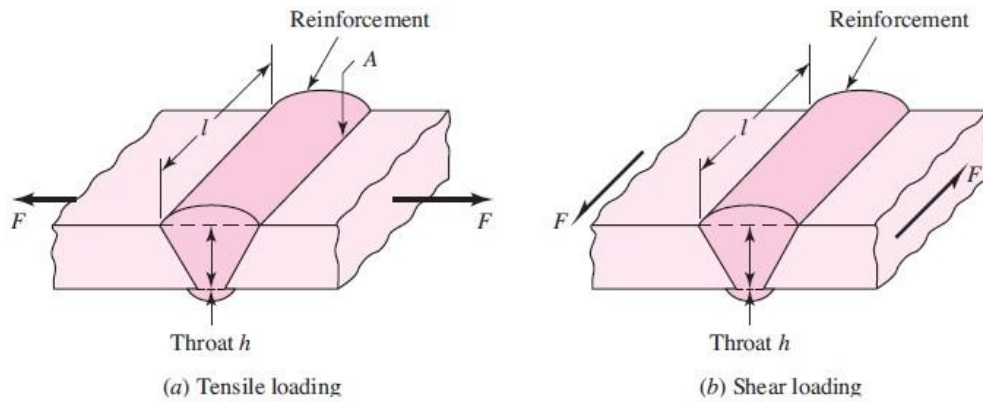

(a) Tensile loading   (b) Shear loading

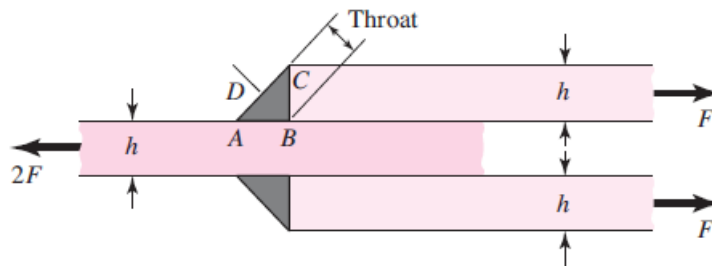**Figure (6–7)**
A typical butt joint

Figure (6–8)
A transverse fillet weld
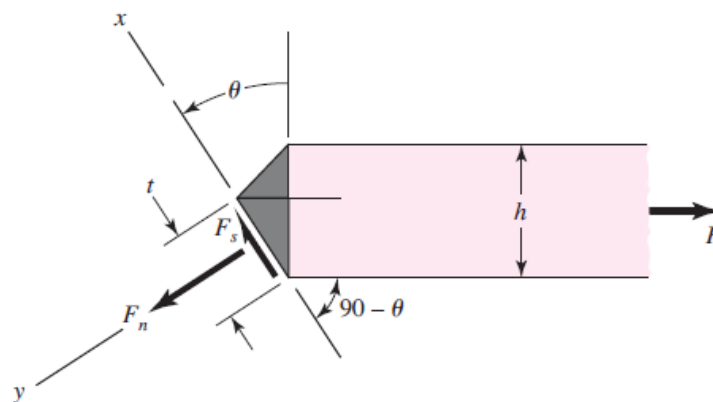
Figure (6–9)
Free body from Fig. (6–8)

The average stress in a butt weld due to shear loading (Fig. 6–7b) is

$$\tau = \frac{F}{hl} \qquad \text{6-2}$$

Figure (6–8) illustrates a typical transverse fillet weld. In Fig. (6–9), a portion of the welded joint has been isolated from Fig. (6–8) as a free body. At angle θ the forces on each weldment consist of a normal force F_n and a shear force F_s. Summing forces in the x and y directions gives

$$F_s = F \sin \theta \qquad \qquad \text{a}$$

$$F_n = F \cos \theta \qquad \qquad \text{b}$$

Using the law of sines for the triangle in Fig. (6–9) yields

$$\frac{t}{\sin 45°} = \frac{h}{\sin(90° - \theta + 45°)} = \frac{h}{\sin(135° - \theta)} = \frac{\sqrt{2}h}{\cos \theta + \sin \theta}$$

Solving for the throat length t gives

$$t = \frac{h}{\cos \theta + \sin \theta} \qquad \qquad \text{c}$$

The nominal stresses at the angle θ in the weldment, τ and σ, are

$$\tau = \frac{F_s}{A} = \frac{F \sin \theta (\cos \theta + \sin \theta)}{hl} = \frac{F}{hl}(\sin \theta \cos \theta + \sin^2 \theta) \qquad \text{d}$$

$$\sigma = \frac{F_n}{A} = \frac{F \cos \theta (\cos \theta + \sin \theta)}{hl} = \frac{F}{hl}(\cos^2 \theta + \sin \theta \cos \theta) \qquad \text{e}$$

The von Mises stress σ' at angle θ is

$$\sigma' = (\sigma^2 + 3\tau^2)^{1/2} = \frac{F}{hl}[(\cos^2 \theta + \sin \theta \cos \theta)^2 + 3(\sin^2 \theta + \sin \theta \cos \theta)^2]^{1/2} \qquad \text{f}$$

The largest von Mises stress occurs at $\theta = 62.5°$ with a value of $\sigma' = 2.16F/(hl)$. The corresponding values of τ and σ are $\tau = 1.196F/(hl)$ and $\sigma = 0.623F/(hl)$. The maximum shear stress can be found by differentiating Eq. (d) with respect to θ and equating to zero. The stationary point occurs at $\theta = 67.5°$ with a corresponding $\tau_{\max} = 1.207F/(hl)$ and $\sigma = 0.5F/(hl)$.

There are some experimental and analytical results that are helpful in evaluating Eqs. (*d*) through (*f*) and consequences. A model of the transverse fillet weld of Fig. (6–8) is easily constructed for photoelastic purposes and has the advantage of a balanced loading condition. Norris constructed such a model and reported the stress distribution along the sides *AB* and *BC* of the weld. An approximate graph of the results he obtained is shown as Fig. (6–10*a*). Note that stress concentration exists at *A* and *B* on the horizontal leg and at *B* on the vertical leg. C. H. Norris states that he could not determine the stresses at *A* and *B* with any certainty.
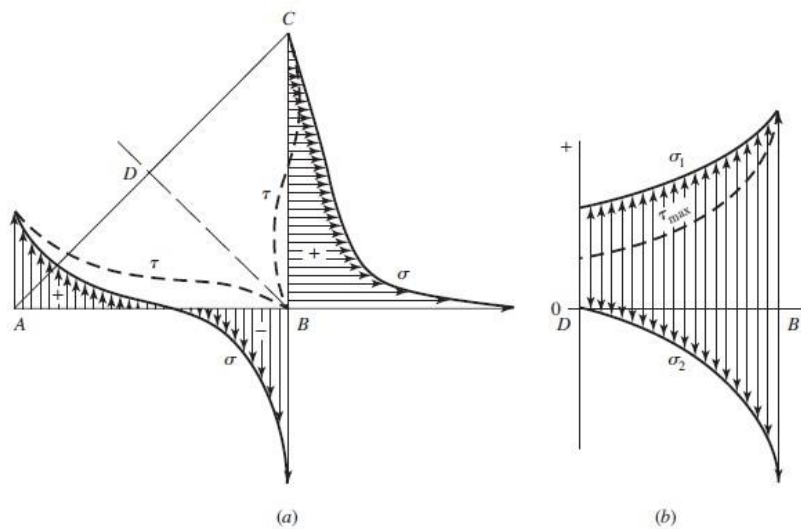

Figure (6–10)

Stress distribution in fillet welds: (*a*) stress distribution on the legs as reported by Norris; (*b*) distribution of principal stresses and maximum
Shear stress as reported by Salakian
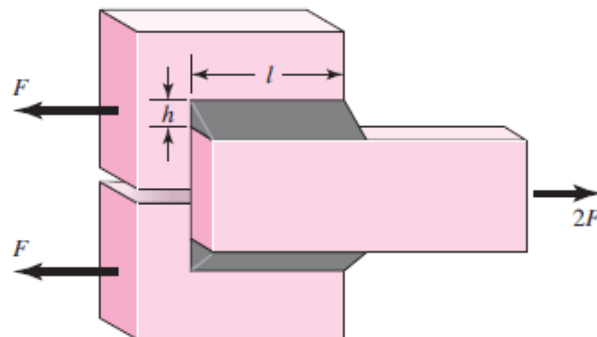
Figure (6–11)
Parallel fillet welds

A. G. Salakian and G. E. Claussen presents data for the stress distribution across the throat of a fillet weld (Fig. 6–10*b*). This graph is of particular interest because we have just learned that it is the throat stresses that are used in design. Again, the figure shows stress concentration at point *B*. Note that Fig. (6–10*a*) applies either to the weld metal or to the parent metal, and that Fig. (6–10*b*) applies only to the weld metal. The most important concept here is that we have *no analytical approach that predicts the existing stresses*. The geometry of the fillet is crude by machinery standards, and even if it were ideal, the macrogeometry is too abrupt and complex for our methods. There are also subtle bending stresses due to eccentricities. Still, in the absence of robust analysis, weldments must be specified and the resulting joints must be safe. The approach has been to use a simple *and conservative* model, verified by testing as conservative. For this model, the basis for weld analysis or design employs

$$\tau = \frac{F}{0.707hl} = \frac{1.414F}{hl} \qquad \qquad 6\text{-}3$$

which assumes the entire force *F* is accounted for by a shear stress in the minimum throat area. Note that this inflates the maximum estimated shear stress by a factor of $1.414/1.207 = 1.17$. Further, consider the parallel fillet welds shown in Fig. (6–11) where, as in Fig. (6–8), each weld transmits a force *F*. However, in the case of Fig. (6–11), the maximum shear stress *is* at the minimum throat area and corresponds to Eq. (6–3).

6.3 Stresses in Welded Joints in Torsion

Figure (6–12) illustrates a cantilever of length *l* welded to a column by two fillet welds. The reaction at the support of a cantilever always consists of a shear force *V* and a moment *M*. The shear force produces a *primary shear* in the welds of magnitude

$$\tau' = \frac{V}{A} \qquad \qquad 6\text{-}4$$

where *A* is the throat area of all the welds.

The moment at the support produces *secondary shear* or *torsion* of the welds, and this stress is given by the equation

$$\tau'' = \frac{Mr}{J} \qquad\qquad 6\text{-}5$$

where r is the distance from the centroid of the weld group to the point in the weld of interest and J is the second polar moment of area of the weld group about the centroid of the group. When the sizes of the welds are known, these equations can be solved and the results combined to obtain the maximum shear stress. Note that r is usually the farthest distance from the centroid of the weld group.
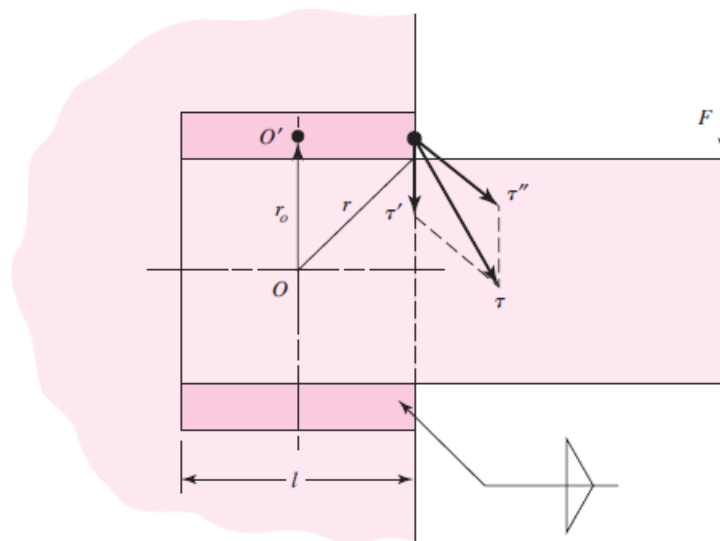
Figure (6–12)
This is a *moment connection;* such a connection
Produces *torsion* in the welds

Figure (6–13) shows two welds in a group. The rectangles represent the throat areas of the welds. Weld 1 has a throat width $b_1 = 0.707h_1$, and weld 2 has a throat width $d_2 = 0.707h_2$. Note that h_1 and h_2 are the respective weld sizes. The throat area of both welds together is

$$A = A_1 + A_2 = b_1d_1 + b_2d_2 \qquad\qquad a$$

This is the area that is to be used in Eq. (6–4).

The x axis in Fig. (6–13) passes through the centroid G_1 of weld 1. The second moment of area about this axis is

$$I_x = \frac{b_1d_1^3}{12}$$

Similarly, the second moment of area about an axis through G_1 parallel to the y axis is

$$I_y = \frac{d_1 b_1^3}{12}$$

Thus the second polar moment of area of weld 1 about its own centroid is

$$J_{G1} = I_x + I_y = \frac{b_1 d_1^3}{12} + \frac{d_1 b_1^3}{12} \qquad\qquad \text{b}$$

In a similar manner, the second polar moment of area of weld 2 about its centroid is

$$J_{G2} = \frac{b_2 d_2^3}{12} + \frac{d_2 b_2^3}{12} \qquad\qquad \text{c}$$
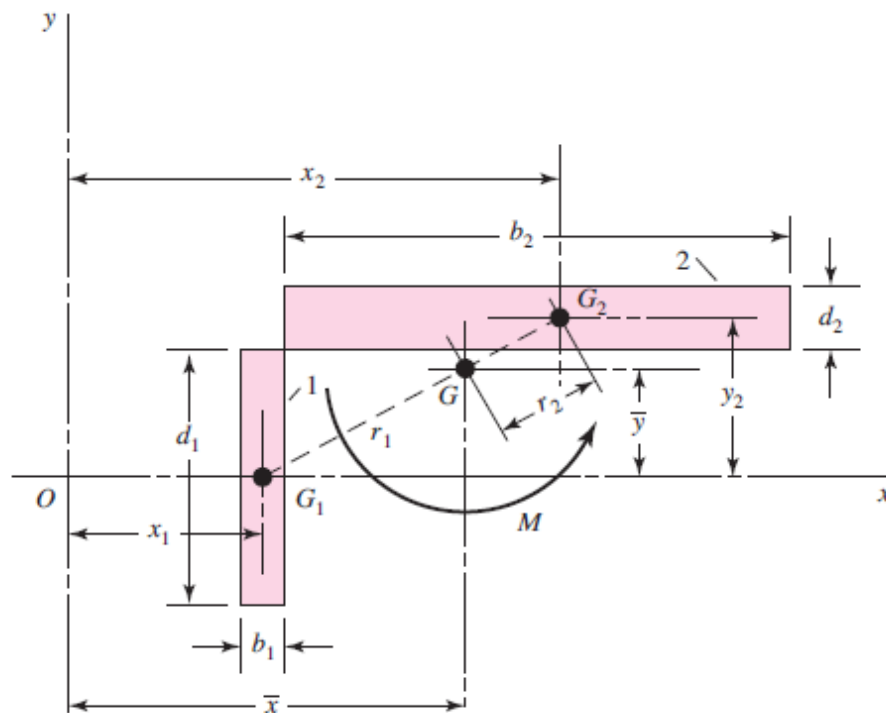
Figure (6–13)

The centroid G of the weld group is located at

$$\bar{x} = \frac{A_1 x_1 + A_2 x_2}{A} \qquad \bar{y} = \frac{A_1 y_1 + A_2 y_2}{A}$$

Using Fig. (6–13) again, we see that the distances r_1 and r_2 from G_1 and G_2 to G, respectively, are

$$r_1 = [(\bar{x} - x_1)^2 + \bar{y}^2]^{1/2} \qquad r_2 = [(y_2 - \bar{y})^2 + (x_2 - \bar{x})^2]^{1/2}$$

Now, using the parallel-axis theorem, we find the second polar moment of area of the weld group to be

$$J = \left(J_{G1} + A_1 r_1^2\right) + \left(J_{G2} + A_2 r_2^2\right) \hspace{3cm} d$$

This is the quantity to be used in Eq. (6–5). The distance r must be measured from G and the moment M computed about G.

The reverse procedure is that in which the allowable shear stress is given and we wish to find the weld size. The usual procedure is to estimate a probable weld size and then to use iteration.

Observe in Eqs. (*b*) and (*c*) the quantities b_1^3 and d_2^3,

respectively, which are the cubes of the weld widths. These quantities are small and can be neglected. This leaves the terms $b_1 d_1^3/12$ and $d_2 b_2^3/12$, which make J_{G1} and J_{G2} linear in the weld width. Setting the weld widths b_1 and d_2 to unity leads to the idea of treating each fillet weld as a line. The resulting second moment of area is then a *unit second polar moment of area*. The advantage of treating the weld size as a line is that the value of J_u is the same regardless of the weld size. Since the throat width of a fillet weld is 0.707h, the relationship between J and the unit value is

$$J = 0.707 \, h \, J_u \qquad\qquad 6\text{-}6$$

in which J_u is found by conventional methods for an area having unit width. The transfer formula for J_u must be employed when the welds occur in groups, as in Fig. (6–12). Table (6–1) lists the throat areas and the unit second polar moments of area for the most common fillet welds encountered. The example that follows is typical of the calculations normally made.

EXAMPLE 6–1

A 50-kN load is transferred from a welded fitting into a 200-mm steel channel as illustrated in Fig. (6–14). Estimate the maximum stress in the weld.
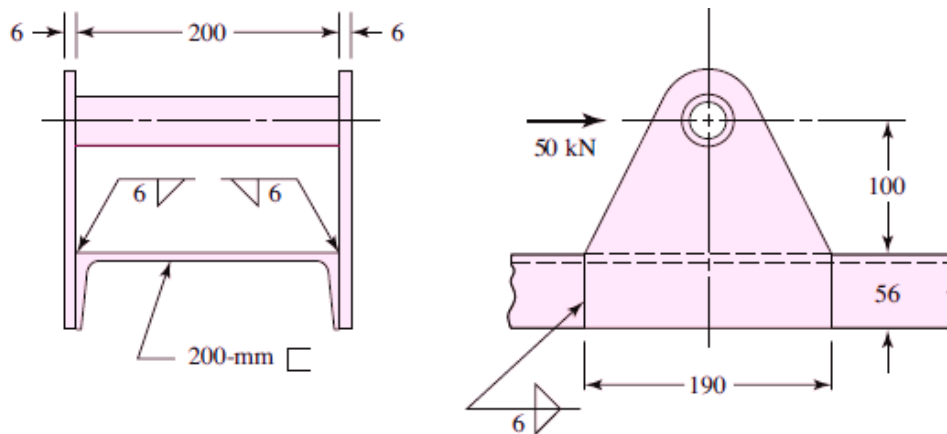
Figure (6–14)
Dimensions in millimeters

Solution

(1) Label the ends and corners of each weld by letter. Sometimes it is desirable to label each weld of a set by number. See Fig. (6–15).
(2) Estimate the primary shear stress τ'. As shown in Fig. (6–14), each plate is welded to the channel by means of three 6-mm fillet welds. Figure (6–15) shows that we have divided the load in half and are considering only a single plate. From case 4 of Table (6–1) we find the throat area as

$$A = 0.707(6)[2(56) + 190] = 1280 \text{ mm}^2$$

Then the primary shear stress is

$$\tau' = \frac{V}{A} = \frac{25(10)^3}{1280} = 19.5 \text{ MPa}$$

(3) Draw the τ' stress, to scale, at each lettered corner or end. See Fig. (9–16).
(4) Locate the centroid of the weld pattern. Using case 4 of Table (6–1), we find

$$\bar{x} = \frac{(56)^2}{2(56) + 190} = 10.4 \text{ mm}$$

This is shown as point O on Figs. (6–15) and (6–16).
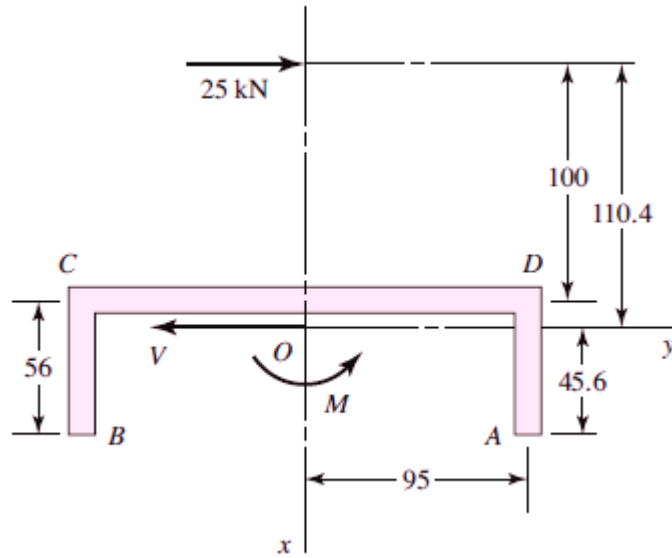
Figure (6–15)

Diagram showing the weld geometry; all dimensions in millimeters. Note that *V* and *M* represent loads applied by the welds *to the plate*
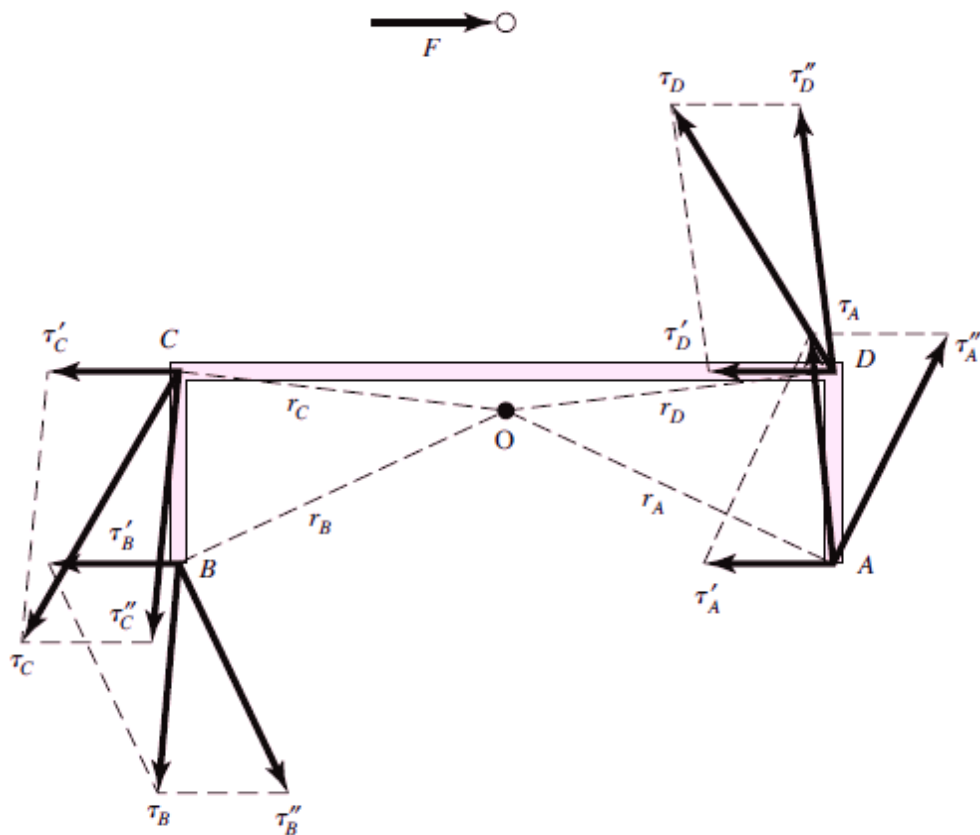
Figure (6–16)

Free-body diagram of one of the side plates

(5) Find the distances r_i (see Fig. 6–16):

$$r_A = r_B = [(190/2)^2 + (56 - 10.4)^2]^{1/2} = 105 \text{ mm}$$

$$r_C = r_D = [(190/2)^2 + (10.4)^2]^{1/2} = 95.6 \text{ mm}$$

(6) Find J. Using case 4 of Table (6–1) again, we get

$$J = 0.707(6) \left[\frac{8(56)^3 + 6(56)(190)^2 + (190)^3}{12} - \frac{(56)^4}{2(56) + 190} \right]$$

$$= 7.07(10)^6 \text{ mm}^4$$

(7) Find M:

$$M = Fl = 25(100 + 10.4) = 2760 \text{ N·m}$$

(8) Estimate the secondary shear stresses τ'' at each lettered end or corner:

$$\tau''_A = \tau''_B = \frac{Mr}{J} = \frac{2760(10)^3(105)}{7.07(10)^6} = 41.0 \text{ MPa}$$

$$\tau''_C = \tau''_D = \frac{2760(10)^3(95.6)}{7.07(10)^6} = 37.3 \text{ MPa}$$

(9) Draw the τ'' stress, to scale, at each corner and end. See Fig. (6–16). Note that this is a free-body diagram of one of the side plates, and therefore the τ' and τ'' stresses represent what the channel is doing to the plate (through the welds) to hold the plate in equilibrium.

(10) At each letter, combine the two stress components as vectors. This gives

$$\tau_A = \tau_B = 37 \text{ MPa}$$

$$\tau_C = \tau_D = 44 \text{ MPa}$$
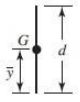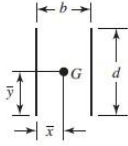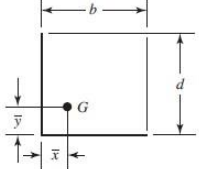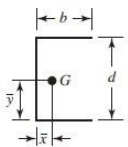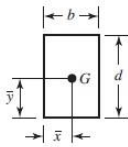
(11) Identify the most highly stressed point:

$$\tau_{\max} = \tau_C = \tau_D = 44 \text{ MPa}$$

Table (6–1)

Torsional Properties of Fillet Welds

G is centroid of weld group; h is weld size; plane of torque couple is in the plane of the paper; all welds are of unit width

Weld	Throat Area	Location of G	Unit Second Polar Moment of Area
	$A = 0.70\,hd$	$\bar{x} = 0$ $\bar{y} = d/2$	$J_u = d^3/12$
	$A = 1.41\,hd$	$\bar{x} = b/2$ $\bar{y} = d/2$	$J_u = \dfrac{d(3b^2 + d^2)}{6}$
	$A = 0.707h(2b + d)$	$\bar{x} = \dfrac{b^2}{2(b+d)}$ $\bar{y} = \dfrac{d^2}{2(b+d)}$	$J_u = \dfrac{(b+d)^4 - 6b^2d^2}{12(b+d)}$
	$A = 0.707h(2b + d)$	$\bar{x} = \dfrac{b^2}{2b+d}$ $\bar{y} = d/2$	$J_u = \dfrac{8b^3 + 6bd^2 + d^3}{12} - \dfrac{b^4}{2b+d}$
	$A = 1.414h(b + d)$	$\bar{x} = b/2$ $\bar{y} = d/2$	$J_u = \dfrac{(b+d)^3}{6}$
	$A = 1.414\,\pi hr$		$J_u = 2\pi r^3$

6.4 Stresses in Welded Joints in Bending

Figure (6–17a) shows a cantilever welded to a support by fillet welds at top and bottom. A free-body diagram of the beam would show a shear-force reaction V and a moment reaction M. The shear force produces a primary shear in the welds of magnitude

$$\tau' = \frac{V}{A}$$

a

where A is the total throat area.

The moment M induces a throat shear stress component of 0.707τ in the welds. Treating the two welds of Fig. (6–17b) as lines we find the unit second moment of area to be

$$I_u = \frac{bd^2}{2} \qquad\qquad b$$

The second moment of area I, based on weld throat area, is

$$I = 0.707hI_u = 0.707h(bd^2/2) \qquad\qquad c$$

The nominal throat shear stress is now found to be

$$\tau = \frac{Mc}{I} = \frac{Md/2}{0.707hbd^2/2} = \frac{1.414M}{bdh} \qquad\qquad d$$
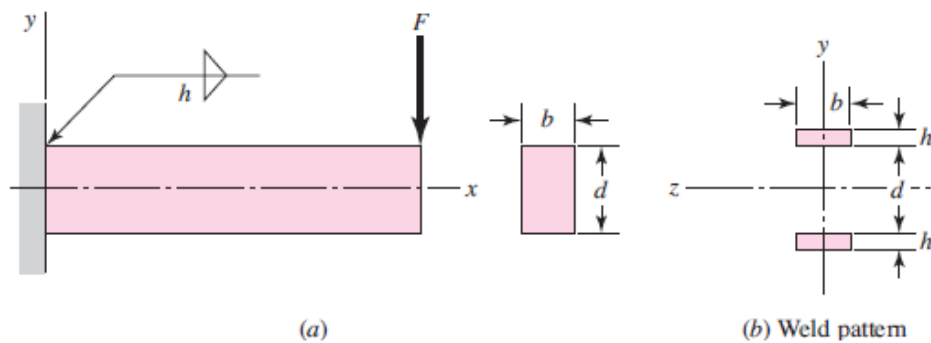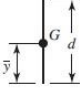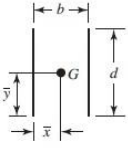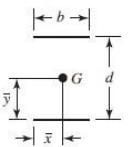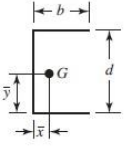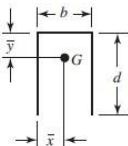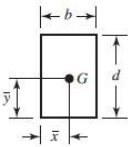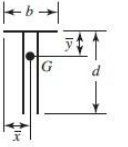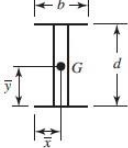
Figure (6–17)
　　　　A rectangular cross-section cantilever welded to a support
　　　　at the top and bottom edges

The second moment of area in Eq. (d) is based on the distance d between the two welds. If this moment is found by treating the two welds as having rectangular footprints, the distance between the weld throat centroids is approximately $(d + h)$. This would produce a slightly larger second moment of area, and result in a smaller level of stress. This method of treating welds as a line does not interfere with the conservatism of the model. It also makes Table (6–2) possible with all the conveniences that ensue.

Table (6–2)

Bending Properties of Fillet Welds

I_u, unit second moment of area, is taken about a horizontal axis through G, the centroid of the weld group, h is weld size; the plane of the bending couple is normal to the plane of the paper and parallel to the y-axis; all welds are of the same size

Weld	Throat Area	Location of G	Unit Second Moment of Area
	$A = 0.707hd$	$\bar{x} = 0$ $\bar{y} = d/2$	$I_u = \dfrac{d^3}{12}$
	$A = 1.414hd$	$\bar{x} = b/2$ $\bar{y} = d/2$	$I_u = \dfrac{d^3}{6}$
	$A = 1.414hd$	$\bar{x} = b/2$ $\bar{y} = d/2$	$I_u = \dfrac{bd^2}{2}$
	$A = 0.707h(2b + d)$	$\bar{x} = \dfrac{b^2}{2b+d}$ $\bar{y} = d/2$	$I_u = \dfrac{d^2}{12}(6b + d)$
	$A = 0.707h(b + 2d)$	$\bar{x} = b/2$ $\bar{y} = \dfrac{d^2}{b+2d}$	$I_u = \dfrac{2d^3}{3} - 2d^2\bar{y} + (b + 2d)\bar{y}^2$
	$A = 1.414h(b + d)$	$\bar{x} = b/2$ $\bar{y} = d/2$	$I_u = \dfrac{d^2}{6}(3b + d)$
	$A = 0.707h(b + 2d)$	$\bar{x} = b/2$ $\bar{y} = \dfrac{d^2}{b+2d}$	$I_u = \dfrac{2d^3}{3} - 2d^2\bar{y} + (b + 2d)\bar{y}^2$
	$A = 1.414h(b + d)$	$\bar{x} = b/2$ $\bar{y} = d/2$	$I_u = \dfrac{d^2}{6}(3b + d)$
	$A = 1.414\pi hr$		$I_u = \pi r^3$

6.5 The Strength of Welded Joints

The properties of electrodes vary considerably, but Table (6–3) lists the minimum properties for some electrode classes.

It is preferable, in designing welded components, to select a steel that will result in a fast, economical weld even though this may require a sacrifice of other qualities such as machinability. Under the proper conditions, all steels can be welded, but best results will be obtained if steels having a UNS specification between G10140 and G10230 are chosen. All these steels have a tensile strength in the hot-rolled condition in the range of 60 to 70 kpsi.

Table (6–3)

Minimum Weld-Metal Properties

AWS Electrode Number	Tensile Strength kpsi (MPa)	Yield Strength kpsi (MPa)	Percent Elongation
E60xx	62 (427)	50 (345)	17–25
E70xx	70 (482)	57 (393)	22
E80xx	80 (551)	67 (462)	19
E90xx	90 (620)	77 (531)	14–17
E100xx	100 (689)	87 (600)	13–16
E120xx	120 (827)	107 (737)	14

The designer can choose factors of safety or permissible working stresses with more confidence if he or she is aware of the values of those used by others. One of the best standards to use is the American Institute of Steel Construction (AISC) code for building construction. Table (6–4) lists the formulas specified by the code for calculating these permissible stresses for various loading conditions. The factors of safety implied by this code are easily calculated. For tension, $n = 1/0.6 = 1.67$. For shear, $n = 0.577/0.4 = 1.44$, using the distortion-energy theory as the criterion of failure.

It is important to observe that the electrode material is often the strongest material present. If a bar of AISI 1010 steel is welded to one of 1018 steel, the weld metal is actually a mixture of the electrode material and the 1010 and 1018 steels. Furthermore, a welded cold-drawn bar has its cold-drawn properties replaced with the hot-rolled properties in the vicinity of the weld. Finally, remembering that the weld metal is usually the strongest, do check the stresses in the parent metals.

Table (6–4)
Stresses Permitted by the AISC Code for Weld Metal

Type of Loading	Type of Weld	Permissible Stress	n
Tension	Butt	$0.60S_y$	1.67
Bearing	Butt	$0.90S_y$	1.11
Bending	Butt	$0.60\text{–}0.66S_y$	1.52–1.67
Simple compression	Butt	$0.60S_y$	1.67
Shear	Butt or fillet	$0.30S_{ut}^*$	

* Shear stress on base metal should not exceed $0.4S_y$ of base metal.

The fatigue stress-concentration factors listed in Table (6–5) are suggested for use. These factors should be used for the parent metal as well as for the weld metal.

Table (6–5)
Fatigue Stress-Concentration Factors, K_{fs}

Type of Weld	K_{fs}
Reinforced butt weld	1.2
Toe of transverse fillet weld	1.5
End of parallel fillet weld	2.7
T-butt joint with sharp corners	2.0

6.6 Static Loading

Some examples of statically loaded joints are useful in comparing and contrasting the conventional method of analysis and the welding code methodology.

EXAMPLE 6–2

A 1/2-in by 2-in rectangular-cross-section 1015 bar carries a static load of 16.5 kip. It is welded to a gusset plate with a 3/8-in fillet weld 2 in long on both sides with an E70XX electrode (the allowable force per unit length is 5.57 kip/in of weldment) as depicted in Fig. (6–18). Use the welding code method.
(a) Is the weld metal strength satisfactory?
(b) Is the attachment strength satisfactory?

Solution

(*a*)

$F = 5.57l = 5.57(4) = 22.28$ kip

Since $22.28 > 16.5$ kip, weld metal strength is satisfactory.

(*b*) Check shear in attachment adjacent to the welds. From Table (6–4) and Table (3–4), from which $S_y = 27.5$ kpsi, the allowable attachment shear stress is

$$\tau_{all} = 0.4S_y = 0.4(27.5) = 11 \text{ kpsi}$$

The shear stress τ on the base metal adjacent to the weld is

$$\tau = \frac{F}{2hl} = \frac{16.5}{2(0.375)2} = 11 \text{ kpsi}$$

Since $\tau_{all} \geq \tau$, the attachment is satisfactory near the weld beads. The tensile stress in the shank of the attachment σ is

$$\sigma = \frac{F}{tl} = \frac{16.5}{(1/2)2} = 16.5 \text{ kpsi}$$

The allowable tensile stress σ_{all}, from Table (6–4), is $0.6S_y$ and, with welding code safety level preserved,

$$\sigma_{all} = 0.6S_y = 0.6(27.5) = 16.5 \text{ kpsi}$$

Since $\sigma_{all} \geq \sigma$, the shank tensile stress is satisfactory.
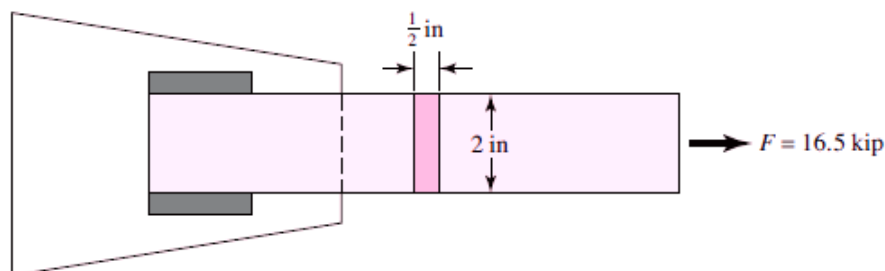
Figure (6–18)

EXAMPLE 6–3

A specially rolled A36 structural steel section for the attachment has a cross section as shown in Fig. (6–19) and has yield and ultimate tensile strengths of 36 and 58 kpsi, respectively. It is statically loaded through the attachment centroid by a load of $F = 24$ kip. Unsymmetrical weld tracks can compensate for eccentricity such that there is no moment to be resisted by the welds. Specify the weld track lengths l_1 and l_2 for a 5/16-in fillet weld using an E70XX electrode. This is part of a design problem in which the design variables include weld lengths and the fillet leg size.

Solution

The *y* coordinate of the section centroid of the attachment is

$$\bar{y} = \frac{\sum y_i A_i}{\sum A_i} = \frac{1(0.75)2 + 3(0.375)2}{0.75(2) + 0.375(2)} = 1.67 \text{ in}$$

Summing moments about point *B* to zero gives

$$\sum M_B = 0 = -F_1 b + F \bar{y} = -F_1(4) + 24(1.67)$$

from which
$F_1 = 10$ kip

It follows that
$F_2 = 24 - 10 = 14$ kip

The weld throat areas have to be in the ratio $14/10 = 1.4$, that is, $l_2 = 1.4 l_1$. The weld length design variables are coupled by this relation, so l_1 is the weld length design variable. The other design variable is the fillet weld leg size h, which has been decided by the problem statement. From Table (6–4), the allowable shear stress on the throat τ_{all} is
$\tau_{all} = 0.3(70) = 21$ kpsi

The shear stress τ on the 45° throat is

$$\tau = \frac{F}{(0.707)h(l_1 + l_2)} = \frac{F}{(0.707)h(l_1 + 1.4 l_1)}$$

$$= \frac{F}{(0.707)h(2.4 l_1)} = \tau_{all} = 21 \text{ kpsi}$$

from which the weld length l_1 is

$$l_1 = \frac{24}{21(0.707)0.3125(2.4)} = 2.16 \text{ in}$$

and

$$l_2 = 1.4l_1 = 1.4(2.16) = 3.02 \text{ in}$$
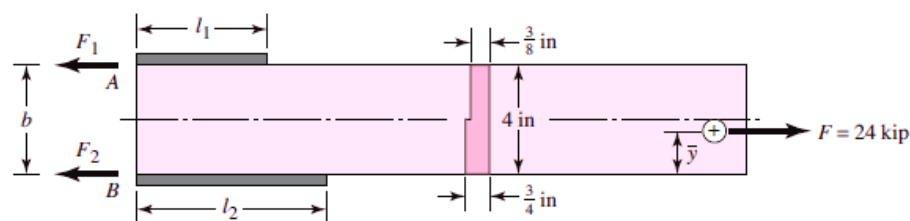
Figure (6–19)

These are the weld-bead lengths required by weld metal strength. The attachment shear stress allowable in the base metal, from Table (6–4), is

$$\tau_{all} = 0.4 \, S_y = 0.4 \, (36) = 14.4 \text{ kpsi}$$

The shear stress τ in the base metal adjacent to the weld is

$$\tau = \frac{F}{h(l_1 + l_2)} = \frac{F}{h(l_1 + 1.4l_1)} = \frac{F}{h(2.4l_1)} = \tau_{all} = 14.4 \text{ kpsi}$$

from which

$$l_1 = \frac{F}{14.4h(2.4)} = \frac{24}{14.4(0.3125)2.4} = 2.22 \text{ in}$$

$$l_2 = 1.4l_1 = 1.4(2.22) = 3.11 \text{ in}$$

$l_2 = 1.4 \, l_1 = 1.4 \, (2.22) = 3.11$ in

These are the weld-bead lengths required by base metal (attachment) strength. The base metal controls the weld lengths. For the allowable tensile stress σ_{all} in the shank of the attachment, the AISC allowable for tension members is $0.6Sy$; therefore,

$$\sigma_{all} = 0.6 \, S_y = 0.6 \, (36) = 21.6 \text{ kpsi}$$

The nominal tensile stress σ is *uniform* across the attachment cross section because of the load application at the centroid. The stress σ is

$$\sigma = \frac{F}{A} = \frac{24}{0.75(2) + 2(0.375)} = 10.7 \text{ kpsi}$$

Since $\sigma_{all} \geq \sigma$, the shank section is satisfactory. With l_1 set to a nominal 2.25 in, l_2 should be $1.4(2.25) = 3.15$ in.

Decision
Set $l_1 = 2.25$ in, $l_2 = 3.25$ in. The small magnitude of the departure from $l_2/l_1 = 1.4$ is not serious. The joint is essentially moment-free.

EXAMPLE 6–4

Perform an adequacy assessment of the statically loaded welded cantilever carrying 500 lbf depicted in Fig. (6–20). The cantilever is made of AISI 1018 HR steel and welded with a 3/8-in fillet weld as shown in the figure. An E6010 electrode was used, and the design factor was 3.0.
(a) Use the conventional method for the weld metal.
(b) Use the conventional method for the attachment (cantilever) metal.

Solution

(a) From Table (6–3), $S_y = 50$ kpsi, $S_{ut} = 62$ kpsi. From Table (6–2), second pattern, $b = 0.375$ in, $d = 2$ in, so

$A = 1.414hd = 1.414\,(0.375)\,(2) = 1.06\ \text{in}^2$

$I_u = d^3/6 = 2^3/6 = 1.33\ \text{in}^3$

$I = 0.707hI_u = 0.707\,(0.375)\,(1.33) = 0.353\ \text{in}^4$

$$\tau' = \frac{F}{A} = \frac{500(10^{-3})}{1.06} = 0.472\ \text{kpsi}$$

Primary shear:

Secondary shear: $\tau'' = \dfrac{Mr}{I} = \dfrac{500(10^{-3})(6)(1)}{0.353} = 8.50 \text{ kpsi}$

The shear magnitude τ is the Pythagorean combination:

$$\tau = (\tau'^2 + \tau''^2)^{1/2} = (0.472^2 + 8.50^2)^{1/2} = 8.51 \text{ kpsi}$$

The factor of safety based on a minimum strength and the distortion- energy criterion is:

$$n = \dfrac{S_{sy}}{\tau} = \dfrac{0.577(50)}{8.51} = 3.39$$

Since $n > n_d$, that   is, $3.39 > 3.0$, the weld metal has satisfactory strength.

(b) From Table (3–4), minimum strengths are $S_{ut} = 58 \text{ kpsi}$ and $S_y = 32 \text{ kpsi}$. Then

$$\sigma = \dfrac{M}{I/c} = \dfrac{M}{bd^2/6} = \dfrac{500(10^{-3})6}{0.375(2^2)/6} = 12 \text{ kpsi}$$

$$n = \dfrac{S_y}{\sigma} = \dfrac{32}{12} = 2.67$$

Since $n < n_d$, that is, $2.67 < 3.0$, the joint is unsatisfactory as to the attachment strength.
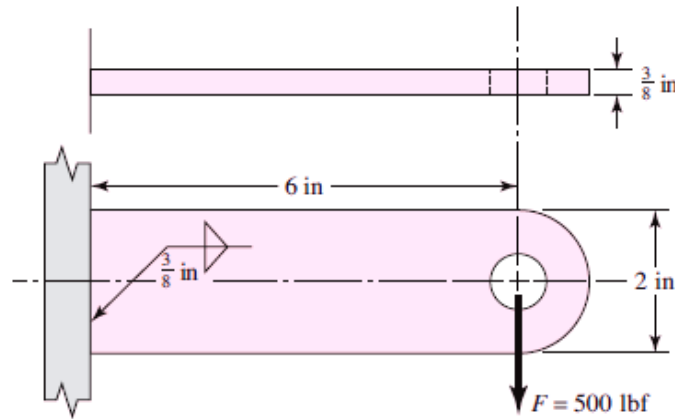
Figure (6–20)

6.7 Fatigue Loading

In fatigue, the Gerber criterion is best; however, you will find that the Goodman criterion is in common use. Recall, that the fatigue stress concentration factors are given in Table (6–5).
        Some examples of fatigue loading of welded joints follow.

EXAMPLE 6–5

The 1018 steel strap of Fig. (6–21) has a 1000-lbf, completely reversed load applied. Determine the factor of safety of the weldment for infinite life.

Solution

From Table (3–4) for the 1018 attachment metal the strengths are $S_{ut} = 58$ kpsi and $S_y = 32$ kpsi. For the E6010 electrode, $S_{ut} = 62$ kpsi and $S_y = 50$ kpsi. The fatigue stress-concentration factor, from Table (6–5), is $K_{fs} = 2.7$. From Table (3–1), p. 49,

$$k_a = 39.9(58)^{-0.995} = 0.702$$

The shear area is:

$$A = 2(0.707)(0.375)(2) = 1.061 \text{ in}^2$$

For a uniform shear stress on the throat, $k_b = 1$.

From Eq. (3–8), p. 51, for torsion (shear), $k_c = 0.59$

$$k_d = k_e = k_f = 1$$
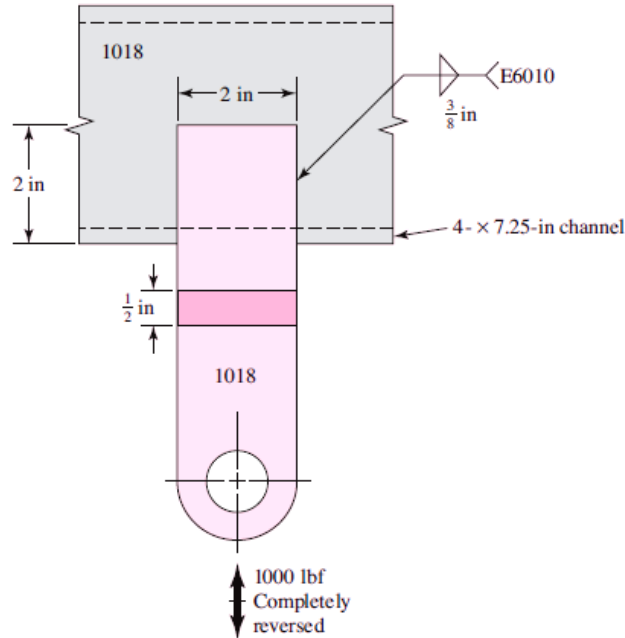
Figure (6–21)

From Eqs. (3–1), p. 48, and (3–2), p. 49,

$$S_{se} = 0.702(1)(0.59)(1)(1)(1)(0.5)(58) = 12 \text{ kpsi}$$

$K_{fs} = 2.7$ $F_a = 1000 \text{ lbf}$ $F_m = 0$

Only primary shear is present:

$$\tau_a' = \frac{K_{fs} F_a}{A} = \frac{2.7(1000)}{1.061} = 2545 \text{ psi} \qquad \tau_m' = 0 \text{ psi}$$

In the absence of a midrange component, the fatigue factor of safety n_f is given by

$$n_f = \frac{S_{se}}{\tau_a'} = \frac{12\,000}{2545} = 4.72$$

EXAMPLE 6–6

The 1018 steel strap of Fig. (6–22) has a repeatedly applied load of 2000 lbf ($F_a = F_m = 1000$ lbf). Determine the fatigue factor of safety fatigue strength of the weldment.

Solution

From Table (3–1), p. 49,

$$k_a = 39.9(58)^{-0.995} = 0.702$$

$$A = 2(0.707)(0.375)(2) = 1.061 \text{ in}^2$$

For uniform shear stress on the throat $k_b = 1$

From Eq. (3–8), p. 51, $k_c = 0.59$

From Eqs. (3–1), p. 48, and (3–2), p. 49,

$$S_{se} = 0.702(1)(0.59)(1)(1)(1)(0.5)(58) = 12 \text{ kpsi}$$

From Table (6–5), $K_{fs} = 2$

Only primary shear is present:

$$\tau'_a = \tau'_m = \frac{K_{fs}F_a}{A} = \frac{2(1000)}{1.061} = 1885 \text{ psi}$$

$S_{su} = 0.67S_{ut}$, This, together with the Gerber fatigue failure criterion for shear stresses from Table (3–6), p. 66, gives

$$n_f = \frac{1}{2}\left(\frac{0.67S_{ut}}{\tau_m}\right)^2 \frac{\tau_a}{S_{se}}\left[-1+\sqrt{1+\left(\frac{2\tau_m S_{se}}{0.67S_{ut}\tau_a}\right)^2}\right]$$

$$n_f = \frac{1}{2}\left[\frac{0.67(58)}{1.885}\right]^2 \frac{1.885}{12.0}\left\{-1+\sqrt{1+\left[\frac{2(1.885)12.0}{0.67(58)1.885}\right]^2}\right\} = 5.85$$

Figure (6–22)

6.8 Resistance Welding

The heating and consequent welding that occur when an electric current is passed through several parts that are pressed together is called *resistance welding*. *Spot welding* and *seam welding* are forms of resistance welding most often used. The advantages of resistance welding over other forms are the speed, the accurate regulation of time and heat, the uniformity of the weld, and the mechanical properties that result. In addition the process is easy to automate, and filler metal and fluxes are not needed.

The spot- and seam-welding processes are illustrated schematically in Fig. (6–23). Seam welding is actually a series of overlapping spot welds, since the current is applied in pulses as the work moves between the rotating electrodes.

Failure of a resistance weld occurs either by shearing of the weld or by tearing of the metal around the weld. Because of the possibility of tearing, it is good practice to avoid loading a resistance-welded joint in tension. Thus, for the most part, design so that the spot or seam is loaded in pure shear. The shear stress is then

simply the load divided by the area of the spot. Because the thinner sheet of the pair being welded may tear, the strength of spot welds is often specified by stating the load per spot based on the thickness of the thinnest sheet. Such strengths are best obtained by experiment.

Somewhat larger factors of safety should be used when parts are fastened by spot welding rather than by bolts or rivets, to account for the metallurgical changes in the materials due to the welding.

(a)   (b)
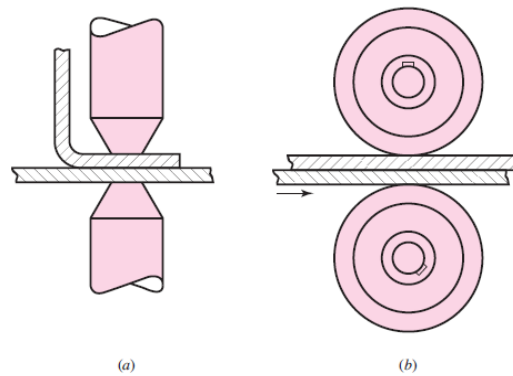
Figure (6–23)

6.9 Adhesive Bonding

The use of polymeric adhesives to join components for structural, semistructural, and nonstructural applications has expanded greatly in recent years as a result of the unique advantages adhesives may offer for certain assembly processes and the development of new adhesives with improved robustness and environmental acceptability. The increasing complexity of modern assembled structures and the diverse types of materials used have led to many joining applications that would not be possible with more conventional joining techniques. Adhesives are also being used either in conjunction with or to replace mechanical fasteners and welds. Reduced weight, sealing capabilities, and reduced part count and assembly time, as well as improved fatigue and corrosion resistance, all combine to provide the designer with opportunities for

customized assembly. Figure (6–24) illustrates the numerous places where adhesives are used on a modern automobile. Indeed, the fabrication of many modern vehicles, devices, and structures is dependent on adhesives.
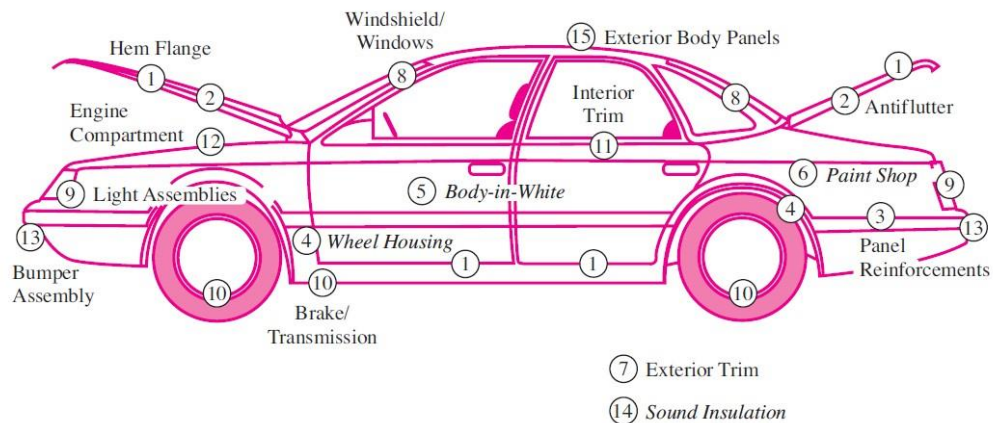
Figure (6–23)

Diagram of an automobile body showing at least 15 locations at which adhesives and sealants could be used or are being used. Particular note should be made of the windshield (8), which is considered a load-bearing structure in modern automobiles and is adhesively bonded. Also attention should be paid to hem flange bonding (1), in which adhesives are used to bond and seal. Adhesives are used to bond friction surfaces in brakes and clutches (10). Antiflutter adhesive bonding (2) helps control deformation of hood and trunk lids under wind shear. Thread-sealing adhesives are used in engine applications (12).

In well-designed joints and with proper processing procedures, use of adhesives can result in significant reductions in weight. Eliminating mechanical fasteners eliminates the weight of the fasteners, and also may permit the use of thinner-gauge materials because stress concentrations associated with the holes are eliminated. The capability of polymeric adhesives to dissipate energy can significantly reduce noise, vibration, and harshness, crucial in modern automobile performance. Adhesives can be used to assemble heat-sensitive materials or components that might be damaged by drilling holes for mechanical fasteners. They can be used to join dissimilar materials or thin-gauge stock that cannot be joined through other means.

Types of Adhesive

There are numerous adhesive types for various applications. They may be classified in a variety of ways depending on their chemistry (e.g., epoxies, polyurethanes, polyimides), their form (e.g., paste, liquid, film, pellets, tape), their type (e.g., hot melt, reactive hot melt, thermosetting, pressure sensitive, contact), or their load-carrying capability (structural, semistructural, or nonstructural).

Structural adhesives are relatively strong adhesives that are normally used well below their glass transition temperature; common examples include epoxies and certain acrylics. Such adhesives can carry significant stresses, and they lend themselves to structural applications. For many engineering applications, semistructural applications (where failure would be less critical) and nonstructural applications (of headliners, etc., for aesthetic purposes) are also of significant interest to the design engineer, providing cost effective means required for assembly of finished products. These include *contact adhesives,* where a solution or emulsion containing an elastomeric adhesive is coated onto both adherends, the solvent is allowed to evaporate, and then the two adherends are brought into contact. Examples include rubber cement and adhesives used to bond laminates to countertops. *Pressure-sensitive adhesives* are very low modulus elastomers that deform easily under small pressures, permitting them to wet surfaces. When the substrate and adhesive are brought into intimate contact, van der Waals forces are sufficient to maintain the contact and provide relatively durable bonds. Pressure-sensitive adhesives are normally purchased as tapes or labels for nonstructural applications, although there are also double-sided foam tapes that can be used in semistructural applications. As the name implies, *hot melts* become liquid when heated, wetting the surfaces and then cooling into a solid polymer. These materials are increasingly applied in a wide array of engineering applications by more sophisticated versions of the glue guns in popular use. *Anaerobic adhesives* cure within narrow spaces deprived of oxygen; such materials have been widely used in mechanical engineering applications to lock bolts or bearings in place. Cure in other adhesives may be induced by exposure to ultraviolet light or electron beams, or it may be catalyzed by certain materials that are ubiquitous on many surfaces, such as water.

Homework

(1) The figure shows a horizontal steel bar 3/8 in thick loaded in steady tension and welded to a vertical support. Find the load *F* that will cause a shear stress of 20 kpsi in the throats of the welds.
(*Ans.*/17.7 kip)
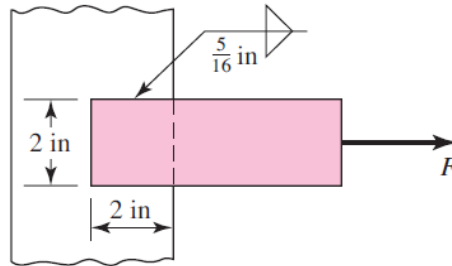
(2) For the weldment of question (*1*) the electrode specified is E7010. For the electrode metal, what is the allowable load on the weldment? (*Ans.*/ 18.56 kip)

(3) The members being joined in question (*1*) are cold-rolled 1018 for the bar and hot-rolled 1018 for the vertical support. What load on the weldment is allowable because member metal is incorporated into the welds? (*Ans.*/ 11.3 kip)

(4) A 5/16 -in steel bar is welded to a vertical support as shown in the figure. What is the shear stress in the throat of the welds if the force *F* is 32 kip? (*Ans.*/ 18.1 kip)
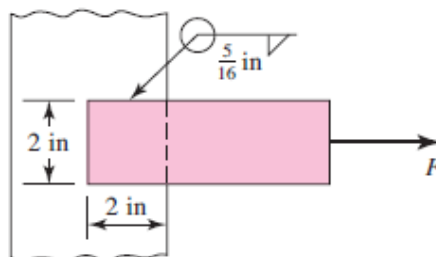
(5) A 3/4 -in-thick steel bar, to be used as a beam, is welded to a vertical support by two fillet welds as illustrated.
(a) Find the safe bending force *F* if the permissible shear stress in the welds is 20 kpsi. (*Ans.*/ 2.17 kip)

(b) In part (*a*) you found a simple expression for *F* in terms of the allowable shear stress. Find the allowable load if the electrode is E7010, the bar is hot-rolled 1020, and the support is hot-rolled 1015.

(*Ans./* 1.19 kip)
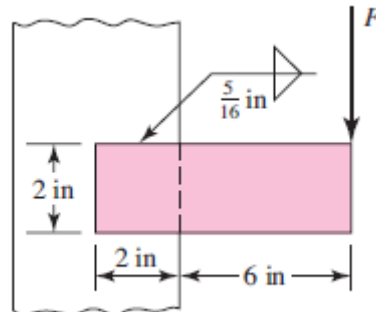
(6) The weldment shown in the figure is subjected to an alternating force *F*. The hot-rolled steel bar is 10 mm thick and is of AISI 1010 steel. The vertical support is likewise of 1010 steel. The electrode is 6010. Estimate the fatigue load *F* the bar will carry   if three 6-mm fillet welds are used. (*Ans./* 22.1 kN)

Dimensions in millimeters
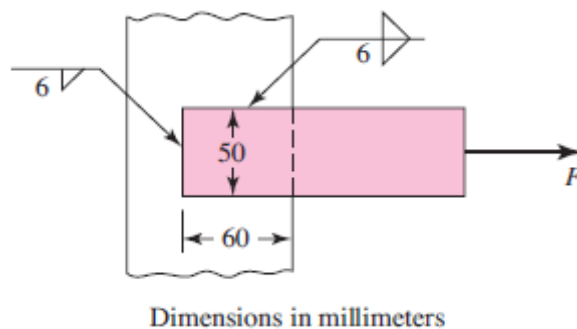
(7) The permissible shear stress for the weldment illustrated is 140 MPa. Estimate the load, *F*, that will cause this stress in the weldment throat. (*Ans./* 49.2 kN)
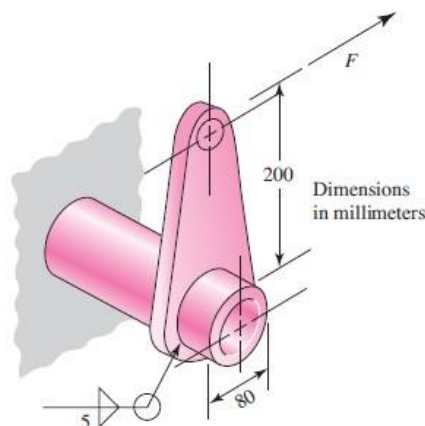
(8) A torque $T = 20(10^3)$ lbf·in is applied to the weldment shown. Estimate the maximum shear stress in the weld throat.   *(Ans./ 18 kpsi)*
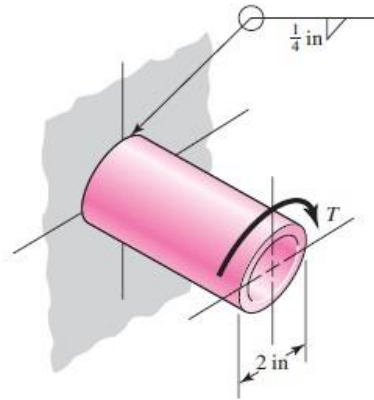
(9) Find the maximum shear stress in the throat of the weld metal in the figure. *(Ans./ 5.44 kpsi)*
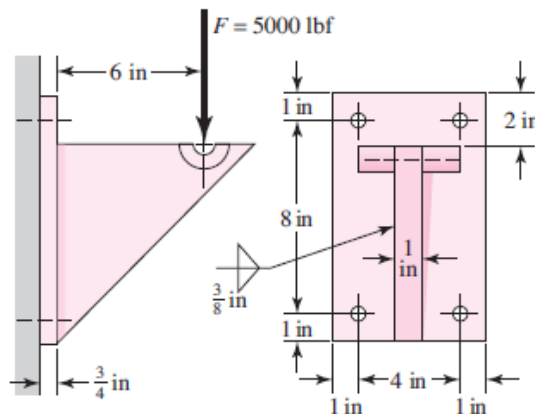
(10) The figure shows a welded steel bracket loaded by a static force F. Estimate the factor of safety if the allowable shear stress in the weld throat is 120 MPa. *(Ans./3.57)*

Dimensions in millimeters

163
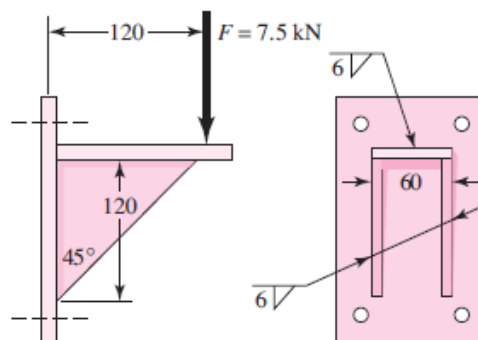
7. Mechanical Springs Mechanical Springs

A spring is defined as an elastic body, whose function is to distort when loaded and to recover its original shape when the load is removed. In general, springs may be classified as wire springs, flat springs, or special-shaped springs, and there are variations within these divisions. Wire springs include helical springs of round or square wire, made to resist and deflect under tensile, compressive, or torsional loads. Flat springs include cantilever and elliptical types, wound motor- or clock-type power springs, and flat spring washers, usually called Belleville springs.

7.1 Stresses in Helical Springs

Figure (7–1*a*) shows a round-wire helical compression spring loaded by the axial force **F**. We designate **D** as the *mean coil diameter* and **d** as the *wire diameter*. Now imagine that the spring is cut at some point (Fig. 7–1*b*), then, at the *inside* fiber of the spring,

$$\tau_{max} = \frac{Tr}{J} + \frac{F}{A} \qquad 7\text{-}1$$

at the inside fiber of the spring. Substitution of $\tau_{max} = \tau$, T = F D/2, r = d/2, J = πd^4 /32, and A = πd^2 /4 gives

Figure (7–1)

164
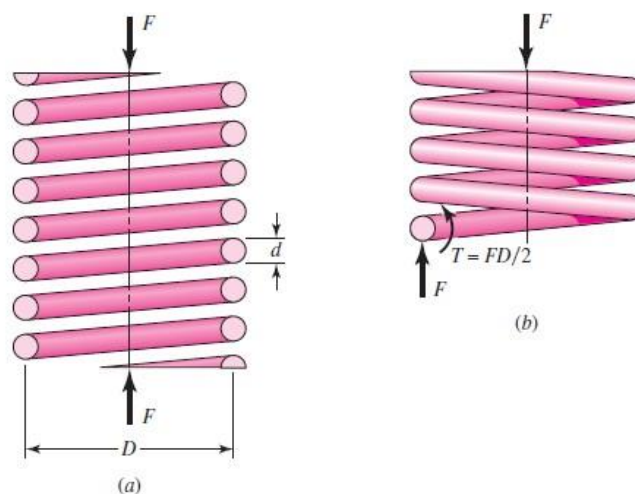
(a) Axially loaded helical spring; *(b)* free-body diagram showing that the wire is subjected to a direct shear and a torsional shear.

$$\tau = \frac{8FD}{\pi d^3} + \frac{4F}{\pi d^2}$$

Now we define the *spring index*

$$C = \frac{D}{d} \qquad\qquad 7\text{-}2$$

which is a measure of coil curvature. With this relation, Eq. (7–1) can be rearranged to give

$$\tau = K_s \frac{8FD}{\pi d^3} \qquad\qquad 7\text{-}3$$

where K_s is a *shear-stress correction factor* and is defined by the equation

$$K_s = \frac{2C + 1}{2C} \qquad\qquad 7\text{-}4$$

For most springs, C ranges from about 6 to 12. Equation (7–3) is quite general and applies for both static and dynamic loads.

The use of square or rectangular wire is not recommended for springs unless space limitations make it necessary. Springs of special wire shapes are not made in large quantities, unlike those of round wire; they have not had the benefit of refining development and hence may not be as strong as springs made from round wire. When space is severely limited, the use of nested round-wire springs should always be considered. They may have an economical advantage over the special-section springs, as well as a strength advantage.

7.2 The Curvature Effect

Equation (7–1) is based on the wire being straight. However, the curvature of the wire increases the stress on the inside of the spring but decreases it only slightly on the outside. This curvature stress is primarily important in fatigue because the loads are lower and there is no opportunity for localized yielding. For static loading, these stresses can normally be neglected because of strain-strengthening with the first application of load.

Unfortunately, it is necessary to find the curvature factor in a roundabout way. The reason for this is that the published equations also include the effect of the direct shear stress. Suppose K_s in Eq. (7–3) is replaced by another K factor, which corrects for both curvature and direct shear. Then this factor is given by either of the equations

$$K_W = \frac{4C - 1}{4C - 4} + \frac{0.615}{C} \qquad \text{7-5}$$

$$K_B = \frac{4C + 2}{4C - 3} \qquad \text{7-6}$$

The first of these is called the *Wahl factor,* and the second, the *Bergsträsser factor.* Since the results of these two equations differ by less than 1 percent, Eq. (7–6) is preferred. The curvature correction factor can now be obtained by canceling out the effect of the direct shear. Thus, using Eq. (7–6) with Eq. (7–4), the curvature correction factor is found to be

$$K_c = \frac{K_B}{K_s} = \frac{2C(4C + 2)}{(4C - 3)(2C + 1)}$$

Now, K_S , K_B or K_W , and K_C are simply stress correction factors applied multiplicatively to *Tr/J* at the critical location to estimate a particular stress. There is *no* stress concentration factor. We will use $\tau = K_B(8FD)/(\pi d^3)$ to predict the largest shear stress.

7.3 Deflection of Helical Springs

The deflection-force relations are quite easily obtained by using Castigliano's theorem. The total strain energy for a helical spring is composed of a torsional component and a shear component. The strain energy is

$$U = \frac{T^2 l}{2GJ} + \frac{F^2 l}{2AG}$$

Substituting T = F.D/2, l = π DN, J = πd^4 /32, and A = πd^2 /4 results in

$$U = \frac{4F^2 D^3 N}{d^4 G} + \frac{2F^2 DN}{d^2 G}$$

where N = N_a = number of active coils. Then using Castigliano's theorem, to find total deflection y gives:

$$y = \frac{\partial U}{\partial F} = \frac{8FD^3 N}{d^4 G} + \frac{4FDN}{d^2 G}$$

Since C = D/d, the previous Equation can be rearranged to yield

$$y = \frac{8FD^3N}{d^4G}\left(1 + \frac{1}{2C^2}\right) \doteq \frac{8FD^3N}{d^4G}$$

The spring rate, also called the scale of the spring, is k = F/y, and so

$$k \doteq \frac{d^4G}{8D^3N}$$

7.4 Compression Springs

The four types of ends generally used for compression springs are illustrated in Fig. (7–2). A spring with *plain ends* has a noninterrupted helicoid; the ends are the same as if a long spring had been cut into sections. A spring with plain ends that are *squared* or *closed* is obtained by deforming the ends to a zero-degree helix angle. Springs should always be both squared and ground for important applications, because a better transfer of the load is obtained.

(a) Plain end, right hand

(c) Squared and ground end, left hand

(b) Squared or closed end, right hand

(d) Plain end, ground, left hand
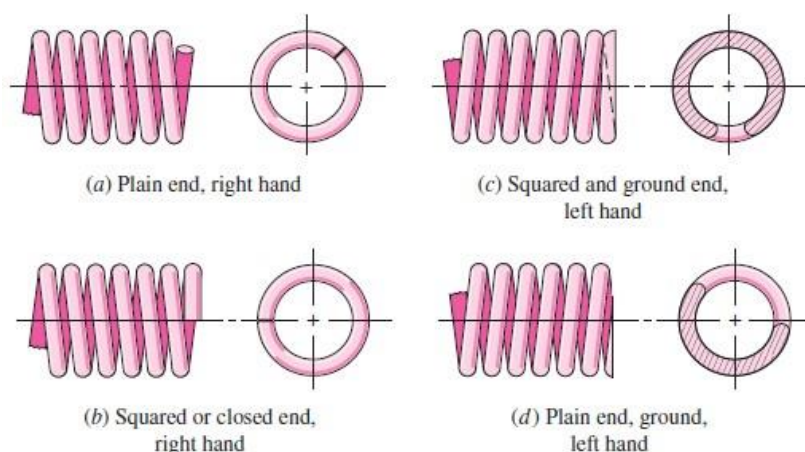
Figure (7–2)
Types of ends for compression springs: (*a*) both ends plain;
(*b*) both ends squared; (*c*) both ends squared and ground;
(*d*) both ends plain and ground.

Table (7–1) shows how the type of end used affects the number of coils and the spring length. Note that the digits 0, 1, 2, and 3 appearing in Table (7–1) are often used without question. *Some of these need closer scrutiny as they may not be integers.*This depends on how a springmaker forms the ends. Forys pointed out that squared and ground ends give a solid length L_s of

$$L_s = (N_t - a)\, d$$

where *a* varies, with an average of 0.75, so the entry dN_t in Table (7–1) may be overstated. The way to check these variations is to take springs from a particular springmaker, close them solid, and measure the solid height. Another way is to look at the spring and count the wire diameters in the solid stack.

Set removal or *presetting* is a process used in the manufacture of compression springs to induce useful residual stresses. It is done by making the spring longer than needed and then compressing it to

its solid height. This operation *sets* the spring to the required final free length and, since the torsional yield strength has been exceeded, induces residual stresses opposite in direction to those induced in service. Springs to be preset should be designed so that 10 to 30 percent of the initial free length is removed during the operation. If the stress at the solid height is greater than 1.3 times the torsional yield strength, distortion may occur. If this stress is much less than 1.1 times, it is difficult to control the resulting free length.

Set removal increases the strength of the spring and so is especially useful when the spring is used for energy-storage purposes. However, set removal should not be used when springs are subject to fatigue.

Table (7–1)
Formulas for the Dimensional Characteristics of Compression-Springs.
(N_a = Number of Active Coils)

Term	Type of Spring Ends			
	Plain	Plain and Ground	Squared or Closed	Squared and Ground
End coils, N_e	0	1	2	2
Total coils, N_t	N_a	$N_a + 1$	$N_a + 2$	$N_a + 2$
Free length, L_0	$pN_a + d$	$p(N_a + 1)$	$pN_a + 3d$	$pN_a + 2d$
Solid length, L_s	$d(N_t + 1)$	dN_t	$d(N_t + 1)$	dN_t
Pitch, p	$(L_0 - d)/N_a$	$L_0/(N_a + 1)$	$(L_0 - 3d)/N_a$	$(L_0 - 2d)/N_a$

7.5 Spring Materials

Springs are manufactured either by hot- or cold-working processes, depending upon the size of the material, the spring index, and the properties desired. In general, prehardened wire should not be used if $D/d < 4$ or if $d > 1/4$ in. Winding of the spring induces residual stresses through bending, but these are normal to the direction of the torsional working stresses in a coil spring. Quite frequently in spring manufacture, they are relieved, after winding, by a mild thermal treatment.

A great variety of spring materials are available to the designer, including plain carbon steels, alloy steels, and corrosion-resisting steels, as well as nonferrous materials such as phosphor bronze, spring brass, beryllium copper, and various nickel alloys.

Spring materials may be compared by an examination of their tensile strengths; these vary so much with wire size that they cannot be specified until the wire size is known. The material and its processing also, of course, have an effect on tensile strength. It turns out that the graph of tensile strength versus wire diameter is almost a straight line for some materials when plotted on log-log paper. Writing the equation of this line as

$$S_{ut} = \frac{A}{d^m}$$

furnishes a good means of estimating minimum tensile strengths when the intercept A and the slope m of the line are known. Values of these constants have been worked out from recent data and are given for strengths in units of kpsi and MPa in Table (7–3). In Eq. (7–10) when d is measured in millimeters, then A is in MPa · mm^m and when d is measured in inches, then A is in kpsi · in^m.

A very rough estimate of the torsional yield strength can be obtained by assuming that the tensile yield strength is between 60 and 90 percent of the tensile strength. Then the distortion-energy theory can be employed to obtain the torsional yield strength ($S_{ys} = 0.577S_y$). This approach results in the range

$$0.35S_{ut} \le S_{sy} \le 0.52S_{ut} \qquad for\ steels \qquad 7\text{-}11$$

For wires listed in Table (7–4), the maximum allowable shear stress in a spring can be seen in column 3. Music wire and hard-drawn steel spring wire have a low end of range $S_{sy} = 0.45S_{ut}$. Valve spring wire, Cr-Va, Cr-Si, and other (not shown) hardened and tempered carbon and low-alloy steel wires as a group have $S_{sy} \ge 0.50S_{ut}$. Many nonferrous materials (not shown) as a group have $S_{sy} \ge 0.35S_{ut}$. In view of this, *Joerres* uses the maximum allowable torsional stress for static application shown in Table (7–5). For specific materials for which you have torsional yield information use this table as a guide. *Joerres* provides set-removal information in Table (7–5), that $S_{sy} \ge 0.65S_{ut}$ increases strength through cold work, but at the cost of an additional operation by the springmaker. Sometimes the additional operation can be done by the manufacturer during assembly. Some correlations with carbon steel springs show that the tensile yield strength of spring wire in torsion can be estimated from $0.75S_{ut}$. The corresponding estimate of the yield strength in shear based on distortion energy theory is

$S_{sy} = 0.577(0.75)S_{ut} = 0.433S_{ut} = 0.45S_{ut}$. *Samónov* discusses the problem of allowable stress and shows that

$$S_{sy} = \tau_{all} = 0.56S_{ut} \qquad\qquad 7\text{-}12$$

for high-tensile spring steels, which is close to the value given by Joerres for hardened alloy steels. He points out that this value of allowable stress is specified by Draft Standard 2089 of the German Federal Republic when Eq. (7–3) is used without stress-correction factor.

Table (7–2)
High-Carbon and Alloy Spring Steels

Name of Material	Similar Specifications	Description
Music wire, 0.80–0.95*C*	UNS G10850 AISI 1085 ASTM A228-51	This is the best, toughest, and most widely used of all spring materials for small springs. It has the highest tensile strength and can withstand higher stresses under repeated loading than any other spring material. Available in diameters 0.12 to 3 mm (0.005 to 0.125 in). Do not use above 120°C (250°F) or at subzero temperatures.
Oil-tempered wire, 0.60–0.70*C*	UNS G10650 AISI 1065 ASTM 229-41	This general-purpose spring steel is used for many types of coil springs where the cost of music wire is prohibitive and in sizes larger than available in music wire. Not for shock or impact loading. Available in diameters 3 to 12 mm (0.125 to 0.5000 in), but larger and smaller sizes may be obtained. Not for use above 180°C (350°F) or at subzero temperatures.
Hard-drawn wire, 0.60–0.70*C*	UNS G10660 AISI 1066 ASTM A227-47	This is the cheapest general-purpose spring steel and should be used only where life, accuracy, and deflection are not too important. Available in diameters 0.8 to 12 mm (0.031 to 0.500 in). Not for use above 120°C (250°F) or at subzero temperatures.
Chrome-vanadium	UNS G61500 AISI 6150 ASTM 231-41	This is the most popular alloy spring steel for conditions involving higher stresses than can be used with the high-carbon steels and for use where fatigue resistance and long endurance are needed. Also good for shock and impact loads. Widely used for aircraft-engine valve springs and for temperatures to 220°C (425°F). Available in annealed or pretempered sizes 0.8 to 12 mm (0.031 to 0.500 in) in diameter.
Chrome-silicon	UNS G92540 AISI 9254	This alloy is an excellent material for highly stressed springs that require long life and are subjected to shock loading. Rockwell hardnesses of C50 to C53 are quite common, and the material may be used up to 250°C (475°F). Available from 0.8 to 12 mm (0.031 to 0.500 in) in diameter.

Table (7–3)
Constants A and m of $S_{ut} = A/d^m$ for Estimating Minimum Tensile Strength of Common Spring Wires

*Surface is smooth, free of defects, and has a bright, lustrous finish. †Has a slight heat-treating scale which must be removed before plating. ‡Surface is smooth and bright with no visible marks. §Aircraft-quality tempered wire, can also be obtained annealed. "Tempered to Rockwell C49, but may be obtained untempered. #Type 302 stainless steel. * *Temper CA510.

Material	ASTM No.	Exponent m	Diameter, in	A, Kpsi.in^m	Diameter, mm	A, MPa.mm^m	Relative Cost of Wire
Music wire*	A228	0.145	0.004–0.256	201	0.10–6.5	2211	2.6
OQ&T wire†	A229	0.187	0.020–0.500	147	0.5–12.7	1855	1.3
Hard-drawn wire‡	A227	0.190	0.028–0.500	140	0.7–12.7	1783	1.0
Chrome-vanadium wire§	A232	0.168	0.032–0.437	169	0.8–11.1	2005	3.1
Chrome-silicon wire‖	A401	0.108	0.063–0.375	202	1.6–9.5	1974	4.0
302 Stainless wire#	A313	0.146	0.013–0.10	169	0.3–2.5	1867	7.6–11
		0.263	0.10–0.20	128	2.5–5	2065	
		0.478	0.20–0.40	90	5–10	2911	
Phosphor-bronze wire**	B159	0	0.004–0.022	145	0.1–0.6	1000	8.0
		0.028	0.022–0.075	121	0.6–2	913	
		0.064	0.075–0.30	110	2–7.5	932	

Table (7–4)
Mechanical Properties of Some Spring Wires

Material	Elastic Limit, Percent of S_{ut} Tension	Torsion	Diameter d, in	E Mpsi	GPa	G Mpsi	GPa
Music wire A228	65–75	45–60	<0.032	29.5	203.4	12.0	82.7
			0.033–0.063	29.0	200	11.85	81.7
			0.064–0.125	28.5	196.5	11.75	81.0
			>0.125	28.0	193	11.6	80.0
HD spring A227	60–70	45–55	<0.032	28.8	198.6	11.7	80.7
			0.033–0.063	28.7	197.9	11.6	80.0
			0.064–0.125	28.6	197.2	11.5	79.3
			>0.125	28.5	196.5	11.4	78.6
Oil tempered A239	85–90	45–50		28.5	196.5	11.2	77.2
Valve spring A230	85–90	50–60		29.5	203.4	11.2	77.2
Chrome-vanadium A231	88–93	65–75		29.5	203.4	11.2	77.2
A232	88–93			29.5	203.4	11.2	77.2
Chrome-silicon A401	85–93	65–75		29.5	203.4	11.2	77.2
Stainless steel							
A313*	65–75	45–55		28	193	10	69.0
17-7PH	75–80	55–60		29.5	208.4	11	75.8
414	65–70	42–55		29	200	11.2	77.2
420	65–75	45–55		29	200	11.2	77.2
431	72–76	50–55		30	206	11.5	79.3
Phosphor-bronze B159	75–80	45–50		15	103.4	6	41.4
Beryllium-copper B197	70	50		17	117.2	6.5	44.8
	75	50–55		19	131	7.3	50.3
Inconel alloy X-750	65–70	40–45		31	213.7	11.2	77.2

*Also includes 302, 304, and 316.

Table (7–5)
Maximum Allowable Torsional Stresses for Helical Compression Springs in Static Applications

Material	Maximum Percent of Tensile Strength	
	Before Set Removed (includes K_W or K_B)	After Set Removed (includes K_S)
Music wire and cold-drawn carbon steel	45	60–70
Hardened and tempered carbon and low-alloy steel	50	65–75
Austenitic stainless steels	35	55–65
Nonferrous alloys	35	55–65

EXAMPLE 7–1

A helical compression spring is made of no.16 music wire of diameter ($d = 0.037$ in). The outside diameter of the spring is 7/16 in. The ends are squared and there are 12.5 total turns.
(a) Estimate the torsional yield strength of the wire.
(b) Estimate the static load corresponding to the yield strength.
(c) Estimate the scale of the spring.
(d) Estimate the deflection that would be caused by the load in part (b).
(e) Estimate the solid length of the spring.

Solution

(a) From Table (7–3), we find $A = 201$ kpsi·in^m and $m = 0.145$. Therefore, from Eq. (7–10)

$$S_{ut} = \frac{A}{d^m} = \frac{201}{0.037^{0.145}} = 324 \text{ kpsi}$$

Then, from Table (7–5),

$$S_{sy} = 0.45S_{ut} = 0.45(324) = 146 \text{ kpsi}$$

(b) The mean spring coil diameter is $D = 7/16 - 0.037 = 0.4$ in, and so the spring index is $C = 0.4/0.037 = 10.8$. Then, from Eq. (7–6),

$$K_B = \frac{4C + 2}{4C - 3} = \frac{4(10.8) + 2}{4(10.8) - 3} = 1.124$$

Now rearrange Eq. (7–3) replacing K_S and τ with K_B and S_{ys}, respectively, and solve for F:

$$F = \frac{\pi d^3 S_{sy}}{8 K_B D} = \frac{\pi (0.037^3) 146(10^3)}{8(1.124) 0.400} = 6.46 \text{ lbf}$$

(c) From Table (7–1), $N_a = 12.5 - 2 = 10.5$ turns. In Table (7–4), $G = 11.85$ Mpsi, and the scale of the spring is found to be, from Eq. (7–9),

$$k = \frac{d^4 G}{8 D^3 N_a} = \frac{0.037^4 (11.85) 10^6}{8(0.400^3) 10.5} = 4.13 \text{ lbf/in}$$

(d)

$$y = \frac{F}{k} = \frac{6.46}{4.13} = 1.56 \text{ in}$$

(*e*) From Table (7–1),

$$L_S = (N_t + 1) \, d = (12.5 + 1) \, 0.037 = 0.5 \text{ in}$$

7.6 Helical Compression Spring Design for Static Service

The preferred range of spring index is $4 \leq C \leq 12$, with the lower indexes being more difficult to form (because of the danger of surface cracking) and springs with higher indexes tending to tangle often enough to require individual packing. This can be the first item of the design assessment. The recommended range of active turns is $3 \leq N_a \leq 15$. To maintain linearity when a spring is about to close, it is necessary to avoid the gradual touching of coils (due to non-perfect pitch). A helical coil spring force-deflection characteristic is ideally linear. Practically, it is nearly so, but not at each end of the force-deflection curve. The spring force is not reproducible for very small deflections, and near closure, nonlinear behavior begins as the

number of active turns diminishes as coils begin to touch. The designer confines the spring's operating point to the central 75 percent of the curve between no load, $F = 0$, and closure, $F = F_S$. Thus, the maximum operating force should be limited to $F_{max} \leq 7/8 \, F_S$.

$$F_s = (1 + \xi)F_{max}$$

it follows that
$$F_s = (1 + \xi)F_{max} = (1 + \xi)\left(\frac{7}{8}\right)F_s$$

From the outer equality $\xi = 1/7 = 0.143 = 0.15$. Thus, it is recommended that $\xi \geq 0.15$. In addition to the relationships and material properties for springs, we now have some recommended design   conditions to follow,

$$4 \leq C \leq 12 \qquad \qquad \xi \geq 0.15 \qquad \text{namely:}$$
$$3 \leq N_a \leq 15 \qquad \qquad n_s \geq 1.2$$

where ns is the factor of safety at closure (solid height). When considering designing a spring for high volume production, the figure of merit can be the cost of the wire from which the spring is wound. The fom would be proportional to the relative material cost, weight density, and volume:

$$\text{fom} = -(\text{relative material cost})\frac{\gamma \pi^2 d^2 N_t D}{4}$$

STATIC SPRING DESIGN

Choose d

Over-a-rod	Free	In-a-hole
As-wound or set	As-wound Set removed	As-wound or set

$D = d_{rod} + d + \text{allow}$ $S_{sy} = \text{const}(A)/d^{m\dagger}$ $S_{sy} = 0.65 A/d^{m}$ $D = d_{hole} - d - \text{allow}$

$$C = \frac{2\alpha - \beta}{4\beta} + \sqrt{\left(\frac{2\alpha - \beta}{4\beta}\right)^2 - \frac{3\alpha}{4\beta}} \qquad D = \frac{S_{sy}\pi d^3}{8n_s(1 + \xi)F_{max}}$$

$$\alpha = \frac{S_{sy}}{n_s} \qquad \beta = \frac{8(1 + \xi)F_{max}}{\pi d^2}$$

$$D = Cd$$

$$C = D/d$$

$$K_B = (4C + 2)/(4C - 3)$$

$$\tau_s = K_B 8(1 + \xi)F_{max}D/(\pi d^3)$$

$$n_s = S_{sy}/\tau_s$$

$$OD = D + d$$

$$ID = D - d$$

$$N_a = Gd^4 y_{max}/(8D^3 F_{max})$$

N_t: Table 10–1

L_s: Table 10–1

L_O: Table 10–1

$$(L_O)_{cr} = 2.63D/\alpha$$

$$\text{fom} = -(\text{rel. cost})\gamma\pi^2 d^2 N_t D/4$$
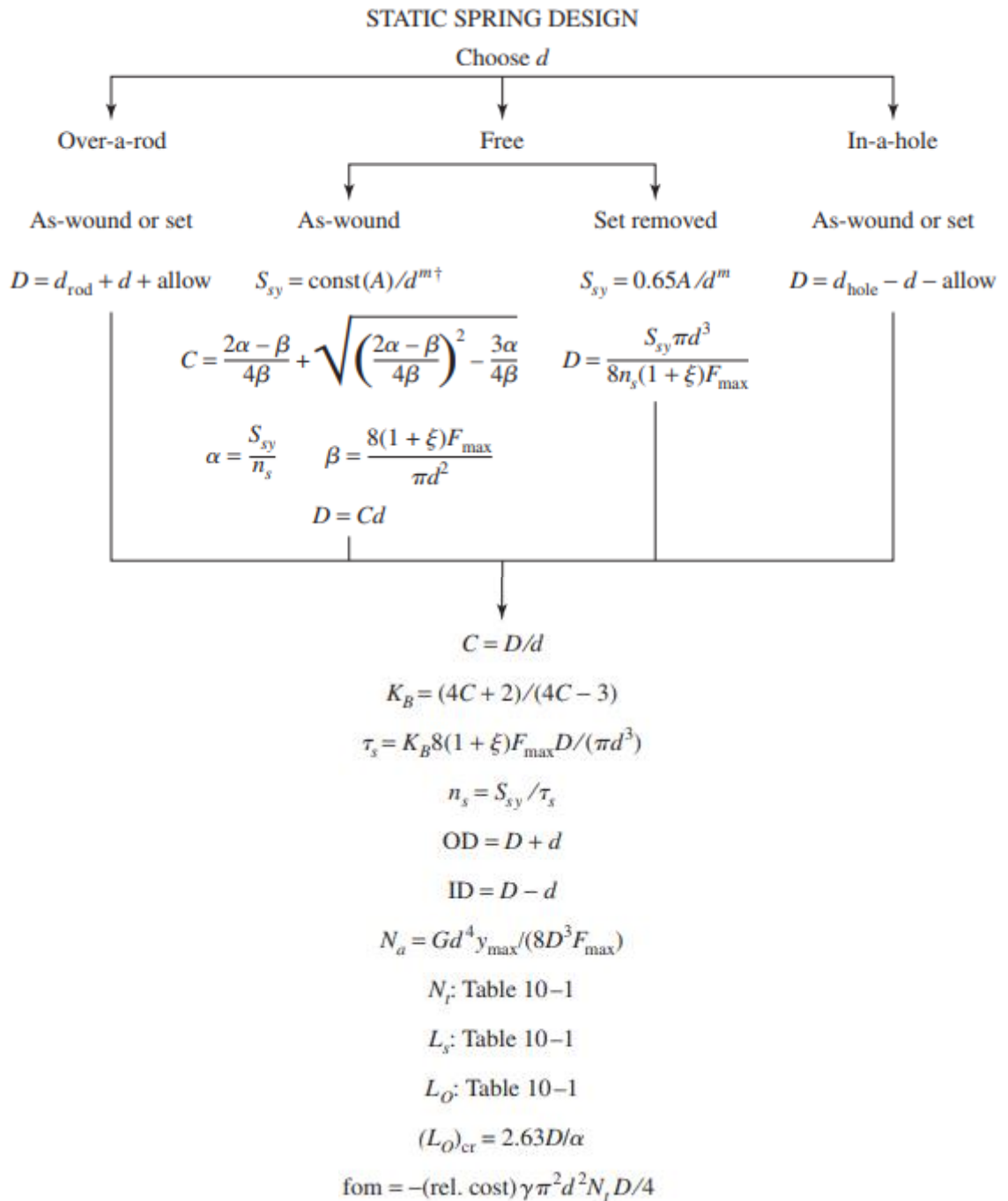
Design Strategy:

Make the a priori decisions, with hard-drawn steel wire the first choice (relative material cost is 1.0). Choose a wire size d. With all decisions made, generate a column of parameters: d, D, C, OD or ID, Na, Ls, L₀, (L₀)cr, ns , and fom. By incrementing wire sizes available, we can scan the table of parameters and apply the design recommendations by inspection. After wire sizes are eliminated, choose the spring design with the highest figure of merit. This will give the optimal design despite the presence of a discrete design variable d and aggregation of equality and inequality constraints. The column vector of information can be generated by using the

flowchart displayed in Fig. 10–3. It is general enough to accommodate to the situations of as-wound and set-removed springs, operating over a rod, or in a hole free of rod or hole. In as-wound springs the controlling equation must be solved for the spring index as follows. $\tau = S_{sy}/ns$, C = D/d, KB from Eq. (10–6), and Eq. (10–17),

$$\frac{S_{sy}}{n_s} = K_B \frac{8 F_s D}{\pi d^3} = \frac{4C + 2}{4C - 3} \left[\frac{8(1 + \xi) F_{max} C}{\pi d^2} \right]$$

Let:

$$\alpha = \frac{S_{sy}}{n_s}$$

$$\beta = \frac{8 (1 + \xi) F_{max}}{\pi d^2}$$

Substituting previous Equations and simplifying yields a quadratic equation in C. The larger of the two solutions will yield the spring index

$$C = \frac{2\alpha - \beta}{4\beta} + \sqrt{\left(\frac{2\alpha - \beta}{4\beta} \right)^2 - \frac{3\alpha}{4\beta}}$$

Example: A music wire helical compression spring is needed to support a 20-lbf load after being compressed 2 in. Because of assembly considerations the solid height cannot exceed 1 in and the free length cannot be more than 4 in. Design the spring.

Solution: The a priori decisions are • Music wire, A228; from Table 10–4, A = 201 000 psi-in^m ; m = 0.145; from Table 10–5, E = 28.5 Mpsi, G = 11.75 Mpsi (expecting d > 0.064 in)
• Ends squared and ground
• Function: F_{max} = 20 lbf, y_{max} = 2 in
• Safety: use design factor at solid height of $(n_s)_d$ = 1.2
 • Robust linearity: ξ = 0.15
• Use as-wound spring (cheaper), S_{sy} = 0.45S_{ut} from Table 10–6
• Decision variable: d = 0.080 in, music wire gage #30, Table A–28. From Fig. 10–3 and Table 10–6,

$$S_{sy} = 0.45 \frac{201\ 000}{0.080^{0.145}} = 130\ 455\ \text{psi}$$

$$\alpha = \frac{S_{sy}}{1.2} = \frac{130\ 455}{1.2} = 108\ 713\,\text{psi}$$

$$OD = 0.843 + 0.080 = 0.923\ \text{in}$$

$$N_a = \frac{0.080^4(11.75)10^6(2)}{8(0.843)^3 20} = 10.05\ \text{turns}$$

$$N_t = 10.05 + 2 = 12.05\ \text{total turns}$$

$$\frac{3(108\ 713)}{4(9151.4)} = 10.53$$

$$L_s = 0.080(12.05) = 0.964\ \text{in}$$

$$L_0 = 0.964 + (1 + 0.15)2 = 3.264\ \text{in}$$

$$(L)_{cr} = 2.63(0.843/0.5) = 4.43\ \text{in}$$

$$\text{fom} = -2.6\pi^2(0.080)^2 12.05(0.843)/4 = -0.417$$

$$\tau_s = 1.128\frac{8(1+0.15)20(0.8424)}{\pi(0.080)^3} = 108\ 700\ \text{psi}$$

$$n_s = \frac{130\ 445}{108\ 700} = 1.2$$

e

: Indexing is used in machine operations when a circular part being manufactured must be divided into a certain number of segments. Figure 10–4 shows a portion of an indexing fixture used to successively position a part for the operation. When the knob is momentarily pulled up, part 6, which holds the workpiece, is rotated about a vertical axis to the next position and locked in place by releasing the index pin. In this example we wish to design the spring to exert a force of about 3 lbf and to fit in the space defined in the figure caption.

Solution: Since the fixture is not a high-production item, a stock spring will be selected. These are available in music wire. In one catalog there are 76 stock springs available having an outside diameter of 0.480 in and designed to work in a 1 2 -in hole. These are made in seven different wire sizes, ranging from 0.038 up to 0.063 in, and in free lengths from 1 2 to 2 1 2 in, depending upon the wire size.

Since the pull knob must be raised 3 4 in for indexing and the space for the spring is 1 3 8 in long when the pin is down, the solid length cannot be more than 5 8 in. Let us begin by selecting a spring having an outside diameter of 0.480 in, a wire size of 0.051 in, a free length

of 1 3 4 in, 111 2 total turns, and plain ends. Then m = 0.145 and A = 201 kpsi · in^m for music wire. Then

$$S_{sy} = 0.45\frac{A}{d^m} = 0.45\frac{201}{0.051^{0.145}} = 139.3 \text{ kpsi}$$

With plain ends, from Table 10–1, the number of active turns is

$$N_a = N_t = 11.5 \text{ turns}$$

The mean coil diameter is $D = OD - d = 0.480 - 0.051 = 0.429$ in. From Eq. (10–9) the spring rate is, for $G = 11.85(10^6)$ psi from Table 10–5,

$$k = \frac{d^4 G}{8D^3 N_a} = \frac{0.051^4(11.85)10^6}{8(0.429)^3 11.5} = 11.0 \text{ lbf/in}$$

From Table 10–1, the solid height L_s is

$$L_s = d(N_t + 1) = 0.051(11.5 + 1) = 0.638 \text{ in}$$

The spring force when the pin is down, F_{min}, is

$$F_{min} = k y_{min} = 11.0(1.75 - 1.375) = 4.13 \text{ lbf}$$

When the spring is compressed solid, the spring force F_s is

$$F_s = k y_s = k(L_0 - L_s) = 11.0(1.75 - 0.638) = 12.2 \text{ lbf}$$

Since the spring index is $C = D/d = 0.429/0.051 = 8.41$,

$$K_B = \frac{4C + 2}{4C - 3} = \frac{4(8.41) + 2}{4(8.41) - 3} = 1.163$$

and for the as-wound spring, the shear stress when compressed solid is

$$\tau_s = K_B \frac{8F_s D}{\pi d^3} = 1.163\frac{8(12.2)0.429}{\pi(0.051)^3} = 116\,850 \text{ psi}$$

The factor of safety when the spring is compressed solid is

ate and Ls we must $$n_s = \frac{S_{sy}}{\tau_s} = \frac{139.3}{116.9} = 1.19$$ is larger than 5 8 in, investigate   other

springs with a smaller wire size. After several investigations another spring has possibilities. It is as-wound music wire, d = 0.045 in, 20 gauge (see Table A–25) OD = 0.480 in, N$_t$ = 11.5 turns, L$_0$ = 1.75 in. S$_{sy}$ is still 139.3 kpsi, and

$$D = OD - d = 0.480 - 0.045 = 0.435 \text{ in}$$

$$N_a = N_t = 11.5 \text{ turns}$$

$$k = \frac{0.045^4(11.85)10^6}{8(0.435)^3 11.5} = 6.42 \text{ lbf/in}$$

$$L_s = d(N_t + 1) = 0.045(11.5 + 1) = 0.563 \text{ in}$$

$$F_{\min} = ky_{\min} = 6.42(1.75 - 1.375) = 2.41 \text{ lbf}$$

$$F_s = 6.42(1.75 - 0.563) = 7.62 \text{ lbf}$$

$$C = \frac{D}{d} = \frac{0.435}{0.045} = 9.67$$

$$K_B = \frac{4(9.67) + 2}{4(9.67) - 3} = 1.140$$

$$\tau_s = 1.140 \frac{8(7.62)0.435}{\pi(0.045)^3} = 105\,600 \text{ psi}$$

$$n_s = \frac{S_{sy}}{\tau_s} = \frac{139.3}{105.6} = 1.32$$

Now ns > 1.2, buckling is not possible as the coils are guarded by the hole surface, and the solid length is less than 5 8 in, so this spring is selected. By using a stock spring, we take advantage of economy of scale.

Fatigue Loading of Helical Compression Springs
Springs are almost always subject to fatigue loading. In many instances the number of cycles of required life may be small, say, several thousand for a padlock spring or a toggle-switch spring. But the valve spring of an automotive engine must sustain millions of cycles of operation without failure; so it must be designed for infinite life. To improve the fatigue strength of dynamically loaded

springs, shot peening can be used. It can increase the torsional fatigue strength by 20 percent or more. Shot size is about 1 64 in, so spring coil wire diameter and pitch must allow for complete coverage of the spring surface. The best data on the torsional endurance limits of spring steels are those reported by Zimmerli.10 He discovered the surprising fact that size, material, and tensile strength have no effect on the endurance limits (infinite life only) of spring steels in sizes under 3 8 in (10 mm). We have already observed that endurance limits tend to level out at high tensile strengths (Fig. 6–17), p. 275, but the reason for this is not clear. Zimmerli suggests that it may be because the original surfaces are alike or because plastic flow during testing makes them the same. Unpeened springs were tested from a minimum torsional stress of 20 kpsi to a maximum of 90 kpsi and peened springs in the range 20 kpsi to 135 kpsi. The corresponding endurance strength components for infinite life were found to be
Unpeened:

$$S_{sa} = 35 \text{ kpsi (241 MPa)} \qquad S_{sm} = 55 \text{ kpsi (379 MPa)}$$

Peened:

$$S_{sa} = 57.5 \text{ kpsi (398 MPa)} \qquad S_{sm} = 77.5 \text{ kpsi (534 MPa)}$$

For example, given an unpeened spring with $S_{su} = 211.5$ kpsi, the Gerber ordinate intercept for shear,

$$S_{se} = \frac{S_{sa}}{1 - \left(\dfrac{S_{sm}}{S_{su}}\right)^2} = \frac{35}{1 - \left(\dfrac{55}{211.5}\right)^2} = 37.5 \text{ kpsi}$$

In constructing certain failure criteria on the designers' torsional fatigue diagram, the torsional modulus of rupture S_{su} is needed. We shall use this equation:

$$S_{su} = 0.67 S_{ut}$$

In the case of shafts and many other machine members, fatigue loading in the form of completely reversed stresses is quite ordinary. Helical springs, on the other hand, are never used as both compression and extension springs. In fact, they are usually assembled with a preload so that the working load is additional. The worst condition, then, would occur when there is no preload, that is, when $\tau_{min} = 0$. Now, we define:

$$F_a = \frac{F_{max} - F_{min}}{2} \qquad\qquad F_m = \frac{F_{max} + F_{min}}{2}$$

When applied to the axial spring force F. Then the shear stress amplitude is:

$$\tau_a = K_B \frac{8 F_a D}{\pi d^3}$$

where K_B is the Bergsträsser factor, obtained from Eq. (10–6), and corrects for both direct shear and the curvature effect. the Wahl factor K_W can be used instead, if desired. The midrange shear stress is given by the equation

$$\tau_m = K_B \frac{8 F_m D}{\pi d^3}$$

Example: An as-wound helical compression spring, made of music wire, has a wire size of 0.092 in, an outside coil diameter of 9 16 in, a free length of 4 3 8 in, 21 active coils, and both ends squared and ground. The spring is unpeened. This spring is to be assembled with a preload of 5 lbf and will operate with a maximum load of 35 lbf during use. (a) Estimate the factor of safety guarding against fatigue failure using a torsional Gerber fatigue failure criterion with Zimmerli data. (b) Repeat part (a) using the Sines torsional fatigue criterion (steady stress component has no effect), with Zimmerli data. (c) Repeat using a torsional Goodman failure criterion with Zimmerli data. (d) Estimate the critical frequency of the spring.
Solution The mean coil diameter is D = 0.5625 − 0.092 = 0.4705 in. The spring index is C = D/d = 0.4705/0.092 = 5.11. Then

$$K_B = \frac{4C + 2}{4C - 3} = \frac{4(5.11) + 2}{4(5.11) - 3} = 1.287$$

$$F_a = \frac{35 - 5}{2} = 15 \text{ lbf} \qquad F_m = \frac{35 + 5}{2} = 20 \text{ lbf}$$

The alternating shear-stress component is found:

$$\tau_a = K_B \frac{8 F_a D}{\pi d^3} = (1.287) \frac{8(15)0.4705}{\pi (0.092)^3} (10^{-3}) = 29.7 \text{ kpsi}$$

the midrange shear-stress component

$$\tau_m = K_B \frac{8 F_m D}{\pi d^3} = 1.287 \frac{8(20)0.4705}{\pi (0.092)^3} (10^{-3}) = 39.6 \text{ kpsi}$$

From Table 10–4 we find $A = 201 \text{ kpsi} \cdot \text{in}^m$ and $m = 0.145$. The ultimate tensile strength is estimated as:

$$S_{ut} = \frac{A}{d^m} = \frac{201}{0.092^{0.145}} = 284.1 \text{ kpsi}$$

Also the shearing ultimate strength is estimated from:

$$S_{su} = 0.67 S_{ut} = 0.67(284.1) = 190.3 \text{ kpsi}$$

The load-line slope $r = \tau_a/\tau_m = 29.7/39.6 = 0.75$.
(a) The Gerber ordinate intercept for the Zimmerli data

$$S_{se} = \frac{S_{sa}}{1 - (S_{sm}/S_{su})^2} = \frac{35}{1 - (55/190.3)^2} = 38.2 \text{ kpsi}$$

The amplitude component of strength S_{sa}

$$S_{sa} = \frac{r^2 S_{su}^2}{2 S_{se}} \left[-1 + \sqrt{1 + \left(\frac{2 S_{se}}{r S_{su}} \right)^2} \right]$$

$$= \frac{0.75^2 190.3^2}{2(38.2)} \left\{ -1 + \sqrt{1 + \left[\frac{2(38.2)}{0.75(190.3)} \right]^2} \right\} = 35.8 \text{ kpsi}$$

(b) The Sines failure criterion ignores S_{sm} so that, for the Zimmerli data with $S_{sa} = 35$ kpsi,

$$n_f = \frac{S_{sa}}{\tau_a} = \frac{35}{29.7} = 1.18$$

(c) The ordinate intercept S for the Goodman failure criterion with the Zimmerli data

$$S_{sa} = \frac{r S_{se} S_{su}}{r S_{su} + S_{se}} = \frac{0.75(49.2)190.3}{0.75(190.3) + 49.2} = 36.6 \text{ kpsi}$$

$$S_{se} = \frac{}{1 - (S_{sm}/S_{su})} = \frac{}{1 - (55/190.3)} = \text{ kpsi}$$

litude component of the strength S_{sa} for the Goodman criterion:

The fatigue factor of safety is given by:

$$n_f = \frac{S_{sa}}{\tau_a} = \frac{36.6}{29.7} = 1.23$$

(c) Using Eq. (10–9) and Table 10–5, we estimate the spring rate as:

$$k = \frac{d^4 G}{8 D^3 N_a} = \frac{0.092^4 [11.75(10^6)]}{8(0.4705)^3 21} = 48.1 \text{ lbf/in}$$

we estimate the spring weight as:

$$W = \frac{\pi^2 (0.092^2) 0.4705 (21) 0.284}{4} = 0.0586 \text{ lbf}$$

Example : A music wire helical compression spring with infinite life is needed to resist a dynamic load that varies from 5 to 20 lbf at 5 Hz while the end deflection varies from 1 2 to 2 in. Because of assembly considerations, the solid height cannot exceed 1 in and the free length cannot be more than 4 in. The spring maker has the following wire sizes in stock: 0.069, 0.071, 0.080, 0.085, 0.090, 0.095, 0.105, and 0.112 in.

Solution: The a priori decisions are: • Material and condition: for music wire, A = 201 kpsi · in^m , m = 0.145, G = 11.75(10^6) psi; relative cost is 2.6 • Surface treatment: unpeened • End treatment: squared and ground • Robust linearity: ξ = 0.15 • Set: use in as-wound condition • Fatigue-safe: n_f = 1.5 using the Sines-Zimmerli fatigue-failure criterion • Function: F_{min} = 5 lbf, F_{max} = 20 lbf, ymin = 0.5 in, y_{max} = 2 in, spring operates free (no rod or hole) • Decision variable: wire size d The figure of merit will be the volume of wire to wind the spring, Eq. (10–22). The design strategy will be to set wire size d, build a table, inspect the table, and choose the satisfactory spring with the highest figure of merit.

Set $d = 0.112$ in. Then

$$F_a = \frac{20 - 5}{2} = 7.5 \text{ lbf} \qquad F_m = \frac{20 + 5}{2} = 12.5 \text{ lbf}$$

$$k = \frac{F_{max}}{y_{max}} = \frac{20}{2} = 10 \text{ lbf/in}$$

$$S_{ut} = \frac{201}{0.112^{0.145}} = 276.1 \text{ kpsi}$$

$$S_{su} = 0.67(276.1) = 185.0 \text{ kpsi}$$

$$S_{sy} = 0.45(276.1) = 124.2 \text{ kpsi}$$

criterion, $S_{se} = S_{sa} = 35$ kpsi. Equation (10–23) can be used to determine C with S_{se}, n_f, and Fa in place of S_{sy}, n_s, and $(1 + \xi)F_{max}$, respectively. Thus,

$$\alpha = \frac{S_{se}}{n_f} = \frac{35\ 000}{1.5} = 23\ 333 \text{ psi}$$

$$\beta = \frac{8F_a}{\pi d^2} = \frac{8(7.5)}{\pi(0.112^2)} = 1522.5 \text{ psi}$$

$$C = \frac{2(23\ 333) - 1522.5}{4(1522.5)} + \sqrt{\left[\frac{2(23\ 333) - 1522.5}{4(1522.5)}\right]^2 - \frac{3(23\ 333)}{4(1522.5)}} = 14.005$$

$$D = Cd = 14.005(0.112) = 1.569 \text{ in}$$

$$F_s = (1 + \xi)F_{max} = (1 + 0.15)20 = 23 \text{ lbf}$$

$$N_a = \frac{d^4 G}{8 D^3 k} = \frac{0.112^4 (11.75)(10^6)}{8(1.569)^3 10} = 5.98 \text{ turns}$$

$$N_t = N_a + 2 = 5.98 + 2 = 7.98 \text{ turns}$$

$$L_s = d N_t = 0.112(7.98) = 0.894 \text{ in}$$

$$L_0 = L_s + \frac{F_s}{k} = 0.894 + \frac{23}{10} = 3.194 \text{ in}$$

$$ID = 1.569 - 0.112 = 1.457 \text{ in}$$

$$OD = 1.569 + 0.112 = 1.681 \text{ in}$$

$$OD = 1.569 + 0.112 = 1.681 \text{ in}$$

$$y_s = L_0 - L_s = 3.194 - 0.894 = 2.30 \text{ in}$$

$$(L_0)_{cr} < \frac{2.63 D}{\alpha} = 2.63 \frac{(1.569)}{0.5} = 8.253 \text{ in}$$

$$K_B = \frac{4(14.005) + 2}{4(14.005) - 3} = 1.094$$

$$W = \frac{\pi^2 d^2 D N_a \gamma}{4} = \frac{\pi^2 0.112^2 (1.569) 5.98(0.284)}{4} = 0.0825 \text{ lbf}$$

$$\tau_a = K_B \frac{8F_a D}{\pi d^3} = 1.094 \frac{8(7.5)1.569}{\pi 0.112^3} = 23\ 334 \text{ psi}$$

$$\tau_m = \tau_a \frac{F_m}{F_a} = 23\ 334 \frac{12.5}{7.5} = 38\ 890 \text{ psi}$$

$$\tau_s = \tau_a \frac{F_s}{F_a} = 23\ 334 \frac{23}{7.5} = 71\ 560 \text{ psi}$$

$$n_f = \frac{S_{sa}}{\tau_a} = \frac{35\ 000}{23\ 334} = 1.5$$

$$n_s = \frac{S_{sy}}{\tau_s} = \frac{124\ 200}{71\ 560} = 1.74$$

$$\text{fom} = -(\text{relative material cost})\pi^2 d^2 N_t D/4$$

$$= -2.6\pi^2(0.112^2)(7.98)1.569/4 = -1.01$$

8. Rolling-Contact Bearings

The terms *rolling-contact bearing, antifriction bearing,* and *rolling bearing* are all used to describe that class of bearing in which the main load is transferred through elements in rolling contact rather than in sliding contact. In a rolling bearing the starting friction is about twice the running friction, but still it is negligible in comparison with the starting friction of a sleeve bearing. Load, speed, and the operating viscosity of the lubricant do affect the frictional characteristics of a rolling bearing. It is probably a mistake to describe a rolling bearing as "antifriction," but the term is used generally throughout the industry.

From the mechanical designer's standpoint, the study of antifriction bearings differs in several respects when compared with the study of other topics because the bearings they specify have already been designed. The specialist in antifriction-bearing design is confronted with the problem of designing a group of elements that compose a rolling bearing: these elements must be designed to fit into a space whose dimensions are specified; they must be designed to receive a load having certain characteristics; and finally, these elements must be designed to have a satisfactory life when operated under the specified conditions. Bearing specialists must therefore consider such matters as fatigue loading, friction, heat, corrosion resistance, kinematic problems, material properties, lubrication, machining tolerances, assembly, use, and cost. From a consideration of all these factors, bearing specialists arrive at a compromise that, in their judgment, is a good solution to the problem as stated.

Bearing Types

Bearings are manufactured to take pure radial loads, pure thrust loads, or a combination of the two kinds of loads. The nomenclature of a ball bearing is illustrated in Fig. (8–1), which also shows the four essential parts of a bearing. These are the outer ring, the inner ring, the balls or rolling elements, and the separator. In low-priced bearings, the separator is sometimes omitted, but it has the important function of separating the elements so that rubbing contact will not occur.

Some of the various types of standardized bearings that are manufactured are shown in Fig. (8–2). The single-row deep-groove

bearing will take radial load as well as some thrust load. The balls are inserted into the grooves by moving the inner ring to an eccentric position. The balls are separated after loading, and the separator is then inserted.
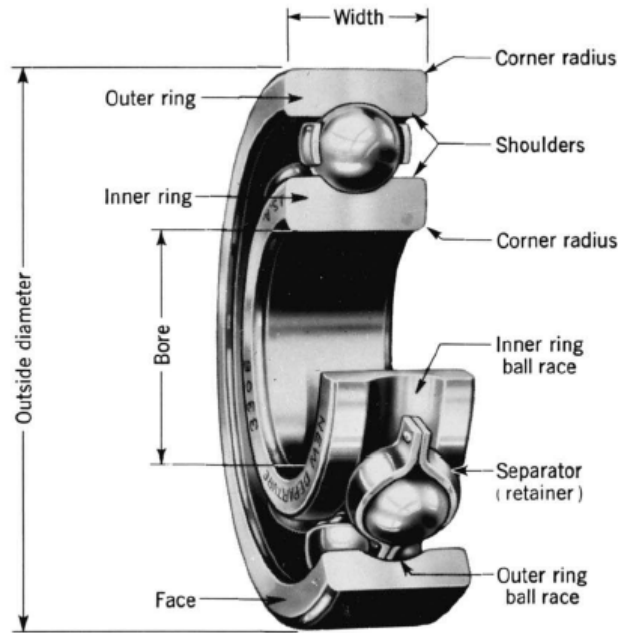

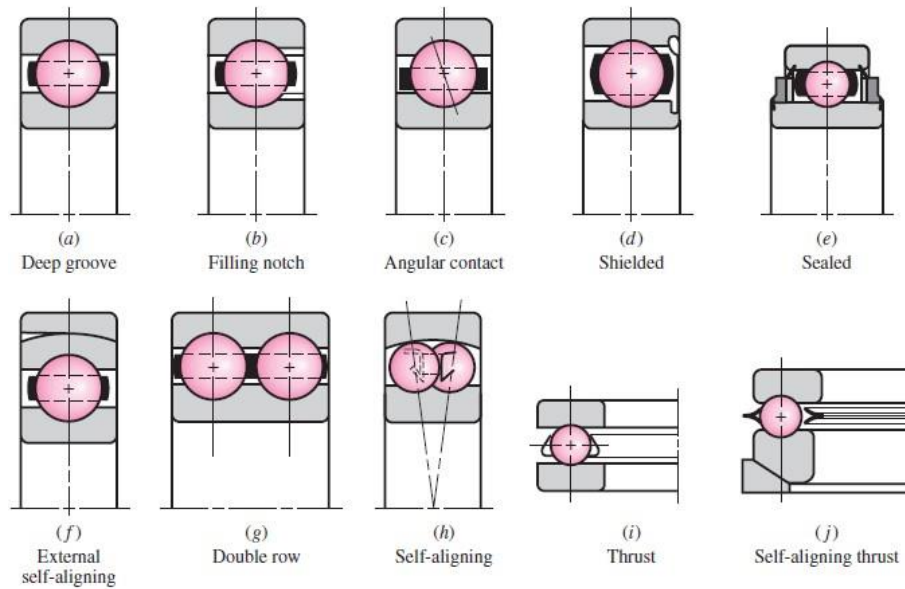**Figure (8–1)**
Nomenclature of a ball bearing

Figure (8–2)
Various types of ball bearings

The use of a filling notch (Fig. 8–2*b*) in the inner and outer rings enables a greater number of balls to be inserted, thus increasing the load capacity. The thrust capacity is decreased, however, because of the bumping of the balls against the edge of the notch when thrust loads are present. The angular-contact bearing (Fig.8–2*c*) provides a greater thrust capacity.

All these bearings may be obtained with shields on one or both sides. The shields are not a complete closure but do offer a measure of protection against dirt. A variety of bearings are manufactured with seals on one or both sides. When the seals are on both sides, the bearings are lubricated at the factory. Although a sealed bearing is supposed to be lubricated for life, a method of relubrication is sometimes provided.

Single-row bearings will withstand a small amount of shaft misalignment of deflection, but where this is severe, self-aligning bearings may be used. Double-row bearings are made in a variety of types and sizes to carry heavier radial and thrust loads. Sometimes two single-row bearings are used together for the same reason, although a double-row bearing will generally require fewer parts and occupy less space. The one way ball thrust bearings (Fig. 8–2*i*) are made in many types and sizes.

Some of the large variety of standard roller bearings available are illustrated in Fig. (8–3). Straight roller bearings (Fig. 8–3*a*) will carry a greater radial load than ball bearings of the same size because of the greater contact area. However, they have the disadvantage of requiring almost perfect geometry of the raceways and rollers. A slight misalignment will cause the rollers to skew and get out of line. For this reason, the retainer must be heavy. Straight roller bearings will not, of course, take thrust loads.

Helical rollers are made by winding rectangular material into rollers, after which they are hardened and ground. Because of the inherent flexibility, they will take considerable misalignment. If necessary, the shaft and housing can be used for raceways instead of separate inner and outer races. This is especially important if radial space is limited.

The spherical-roller thrust bearing (Fig. 8–3*b*) is useful where heavy loads and misalignment occur. The spherical elements have the advantage of increasing their contact area as the load is increased.

Needle bearings (Fig. 8–3*d*) are very useful where radial space is limited. They have a high load capacity when separators are

used, but may be obtained without separators. They are furnished both with and without races. Tapered roller bearings (Fig. 8–3*e*, *f*) combine the advantages of ball and straight roller bearings, since they can take either radial or thrust loads or any combination of the two, and in addition, they have the high load-carrying capacity of straight roller bearings. The tapered roller bearing is designed so that all elements in the roller surface and the raceways intersect at a common point on the bearing axis. The bearings described here represent only a small portion of the many available for selection. Many special-purpose bearings are manufactured, and bearings are also made for particular classes of machinery. Typical of these are:

• Instrument bearings, which are high-precision and are available in stainless steel and high-temperature materials
• Nonprecision bearings, usually made with no separator and sometimes having split or stamped sheet-metal races
• Ball bushings, which permit either rotation or sliding motion or both
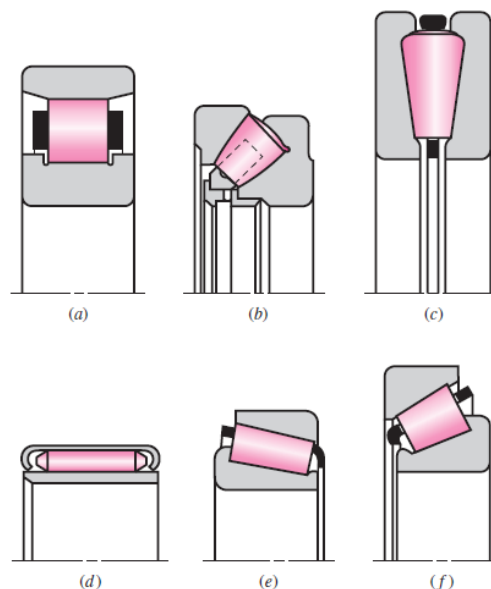• Bearings with flexible rollers

Figure (8–3)
Types of roller bearings: (*a*) straight roller; (*b*) spherical roller, thrust; (*c*) tapered roller, thrust; (*d*) needle; (*e*) tapered roller; (*f*) steep-angle tapered roller

9. Lubrication and Journal Bearings

The object of lubrication is to reduce friction, wear, and heating of machine parts that move relative to each other. A lubricant is any substance that, when inserted between the moving surfaces, accomplishes these purposes. In a sleeve bearing, a shaft, or *journal,* rotates or oscillates within a sleeve, or *bushing,* and the relative motion is sliding. In an antifriction bearing, the main relative motion is rolling. A follower may either roll or slide on the cam. Gear teeth mate with each other by a combination of rolling and sliding. Pistons slide within their cylinders. All these applications require lubrication to reduce friction, wear, and heating.

The field of application for journal bearings is immense. The crankshaft and connecting-rod bearings of an automotive engine must operate for thousands of miles at high temperatures and under varying load conditions. The journal bearings used in the steam turbines of power-generating stations are said to have reliabilities approaching 100 percent. At the other extreme there are thousands of applications in which the loads are light and the service relatively unimportant; a simple, easily installed bearing is required, using little or no lubrication. In such cases an antifriction bearing might be a poor answer because of the cost, the elaborate enclosures, the close tolerances, the radial space required, the high speeds, or the increased inertial effects. Instead, a nylon bearing requiring no lubrication, a powder-metallurgy bearing with the lubrication "built in," or a bronze bearing with ring oiling, wick feeding, or solid-lubricant film or grease lubrication might be a very satisfactory solution. Recent metallurgy developments in bearing materials, combined with increased knowledge of the lubrication process, now make it possible to design journal bearings with satisfactory lives and very good reliabilities.

Types of Lubrication

Five distinct forms of lubrication may be identified:
1. Hydrodynamic
2. Hydrostatic
3. Elastohydrodynamic
4. Boundary
5. Solid film

Hydrodynamic lubrication means that the load-carrying surfaces of the bearing are separated by a relatively thick film of lubricant, so as to prevent metal-to-metal contact, and that the stability thus obtained can be explained by the laws of fluid mechanics. Hydrodynamic lubrication does not depend upon the introduction of the lubricant under pressure, though that may occur; but it does require the existence of an adequate supply at all times. The film pressure is created by the moving surface itself pulling the lubricant into a wedge-shaped zone at a velocity sufficiently high to create the pressure necessary to separate the surfaces against the load on the bearing. Hydrodynamic lubrication is also called *full-film, or fluid, lubrication.*

  Hydrostatic lubrication is obtained by introducing the lubricant, which is sometimes air or water, into the load-bearing area at a pressure high enough to separate the surfaces with a relatively thick film of lubricant. So, unlike hydrodynamic lubrication, this kind of lubrication does not require motion of one surface relative to another. We shall not deal with hydrostatic lubrication in this book, but the subject should be considered in designing bearings where the velocities are small or zero and where the frictional resistance is to be an absolute minimum.

  Elastohydrodynamic lubrication is the phenomenon that occurs when a lubricant is introduced between surfaces that are in rolling contact, such as mating gears or rolling bearings. The mathematical explanation requires the Hertzian theory of contact stress and fluid mechanics.

  Insufficient surface area, a drop in the velocity of the moving surface, a lessening in the quantity of lubricant delivered to a bearing, an increase in the bearing load, or an increase in lubricant temperature resulting in a decrease in viscosity-any one of these-may prevent the buildup of a film thick enough for full-film lubrication. When this happens, the highest asperities may be separated by lubricant films only several molecular dimensions in thickness. This is called *boundary lubrication.* The change from hydrodynamic to boundary lubrication is not at all a sudden or abrupt one. It is probable that a mixed hydrodynamic- and boundary-type lubrication occurs first, and as the surfaces move closer together, the boundary-type lubrication becomes predominant. The viscosity of the lubricant is not of as much importance with boundary lubrication as is the chemical composition.

When bearings must be operated at extreme temperatures, a *solid-film lubricant* such as graphite or molybdenum disulfide must be used because the ordinary mineral oils are not satisfactory. Much research is currently being carried out in an effort, too, to find composite bearing materials with low wear rates as well as small frictional coefficients.

Bearing Types

A bearing may be as simple as a hole machined into a cast-iron machine member. It may still be simple yet require detailed design procedures, as, for example, the two piece grooved pressure-fed connecting-rod bearing in an automotive engine. Or it may be as elaborate as the large water-cooled, ring-oiled bearings with built-in reservoirs used on heavy machinery.

Thrust Bearings

The lubricant is brought into the radial grooves and pumped into the wedge-shaped space by the motion of the runner. Full-film, or hydrodynamic, lubrication is obtained if the speed of the runner is continuous and sufficiently high, if the lubricant has the correct viscosity, and if it is supplied in sufficient quantity.

Boundary-Lubricated Bearings

When two surfaces slide relative to each other with only a partial lubricant film between them, *boundary lubrication* is said to exist. Boundary- or thin-film lubrication occurs in hydrodynamically lubricated bearings when they are starting or stopping, when the load increases, when the supply of lubricant decreases, or whenever other operating changes happen to occur. There are, of course, a very large number of cases in design in which boundary-lubricated bearings must be used because of the type of application or the competitive situation.

10. Gears

This part addresses gear geometry, the kinematic relations, and the forces transmitted by the four principal types of gears: spur, helical, bevel, and worm gears. The forces transmitted between meshing gears supply torsional moments to shafts for motion and power transmission and create forces and moments that affect the shaft and its bearings.

10.1 Types of Gears

Spur gears, illustrated in Fig. (10–1), have teeth parallel to the axis of rotation and are used to transmit motion from one shaft to another, parallel, shaft. Of all types, the spur gear is the simplest and, for this reason, will be used to develop the primary kinematic relationships of the tooth form.

Helical gears, shown in Fig. (10–2), have teeth inclined to the axis of rotation. Helical gears can be used for the same applications as spur gears and, when so used, are not as noisy, because of the more gradual engagement of the teeth during meshing. The inclined tooth also develops thrust loads and bending couples, which are not present with spur gearing. Sometimes helical gears are used to transmit motion between nonparallel shafts.

Bevel gears, shown in Fig. (10–3), have teeth formed on conical surfaces and are used mostly for transmitting motion between intersecting shafts. The figure actually illustrates *straight-tooth bevel gears. Spiral bevel gears* are cut so the tooth is no longer straight, but forms a circular arc. *Hypoid gears* are quite similar to spiral bevel gears except that the shafts are offset and nonintersecting.
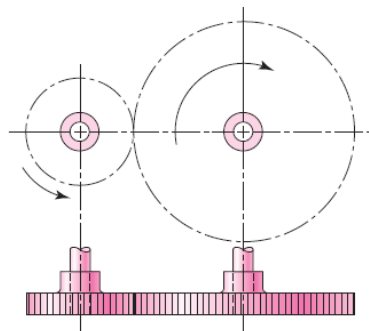

Figure (10–1)
Spur gears are used to transmit rotary
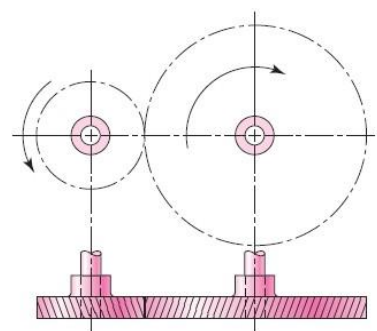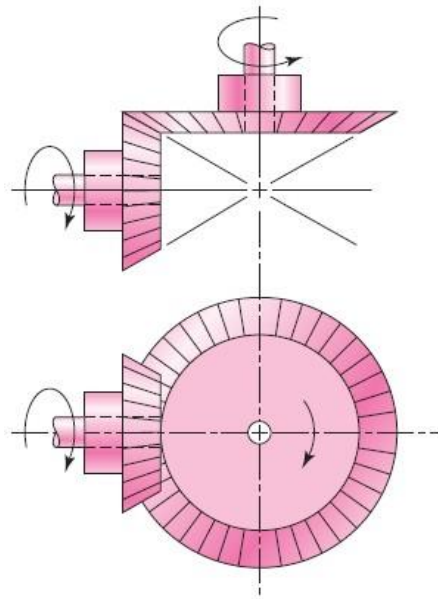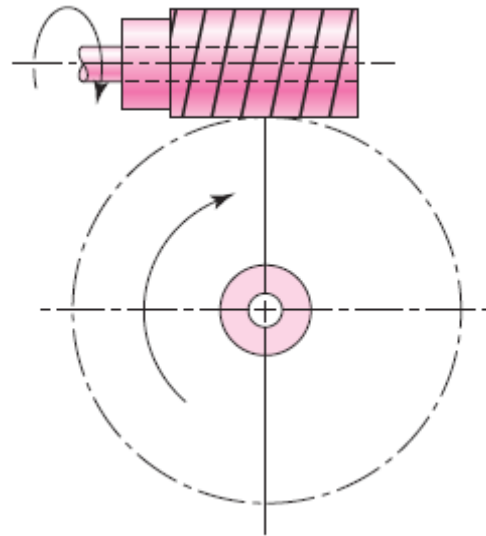motion between parallel shafts

Figure (10–2)
Helical gears are used to transmit motion
between parallel or nonparallel shafts

Figure (10–3)
Bevel gears are used to transmit rotary
motion between intersecting shafts
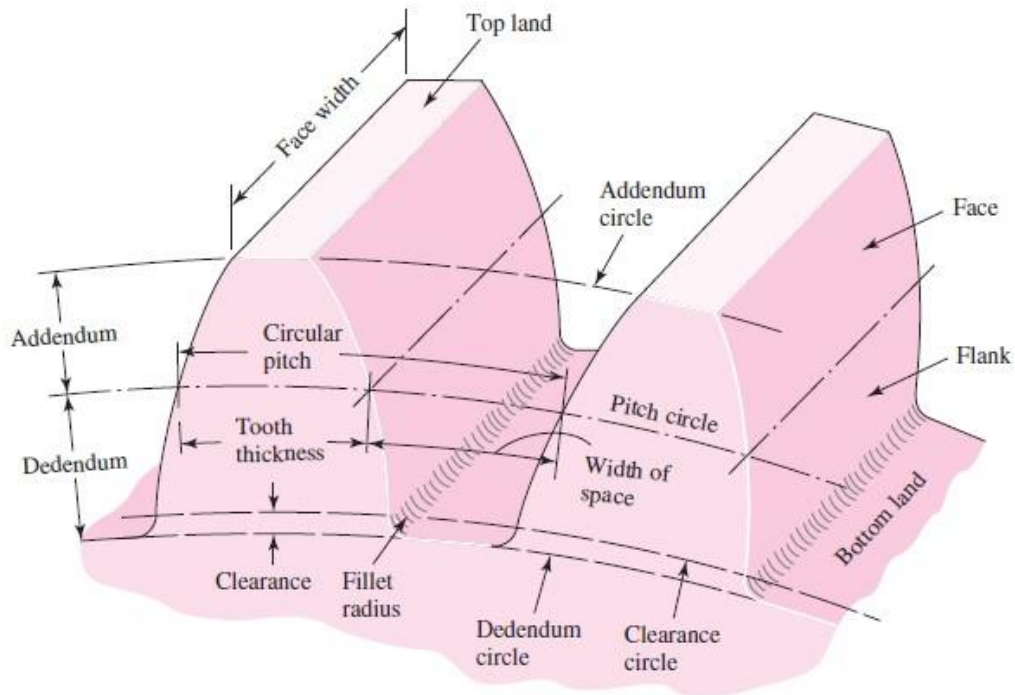

Figure (10–4)
Worm gearsets are used to transmit rotary
motion between nonparallel and
nonintersecting shafts

Worms and *worm gears,* shown in Fig. (10–4), represent the fourth basic gear type. As shown, the worm resembles a screw. The direction of rotation of the worm gear, also called the worm wheel, depends upon the direction of rotation of the worm and upon whether the worm teeth are cut right-hand or left-hand. Worm-gear sets are also made so that the teeth of one or both wrap partly around the other. Such sets are called *single-enveloping* and *double-enveloping* worm-gear sets. Worm-gear sets are mostly used when the speed ratios of the two shafts are quite high, say, 3 or more.

10.2 Nomenclature

The terminology of spur-gear teeth is illustrated in Fig. (10–5). The *pitch circle* is a theoretical circle upon which all calculations are usually based; its diameter is the *pitch diameter.* The pitch circles of a pair of mating gears are tangent to each other. A *pinion* is the smaller of two mating gears. The larger is often called the *gear.*

The *circular pitch p* is the distance, measured on the pitch circle, from a point on one tooth to a corresponding point on an adjacent tooth. Thus the circular pitch is equal to the sum of the *tooth thickness* and the *width of space.*

Figure (10–5)

Nomenclature of spur-gear teeth

The *module m* is the ratio of the pitch diameter to the number of teeth. The customary unit of length used is the millimeter. The module is the index of tooth size in SI.

The *diametral pitch P* is the ratio of the number of teeth on the gear to the pitch diameter. Thus, it is the reciprocal of the module. Since diametral pitch is used only with U.S. units, it is expressed as teeth per inch.

The *addendum a* is the radial distance between the *top land* and the pitch circle. The *dedendum b* is the radial distance from the *bottom land* to the pitch circle. The *whole depth ht* is the sum of the addendum and the dedendum.

The *clearance circle* is a circle that is tangent to the addendum circle of the mating gear. The *clearance c* is the amount by which the dedendum in a given gear exceeds the addendum of its mating gear. The *backlash* is the amount by which the width of a tooth space exceeds the thickness of the engaging tooth measured on the pitch circles.

The following relations are useful:

$$P = \frac{N}{d} \qquad\qquad\qquad — \qquad\qquad\qquad 10\text{-}1$$

$$m = \frac{d}{N} \qquad \text{10-2}$$

$$R = \frac{\pi d}{N} = \pi m \qquad \text{10-3}$$

$$p\,P = \pi \qquad \text{10-4}$$

where
P = diametral pitch, teeth per inch
N = number of teeth
d = pitch diameter, in
m = module, mm
d = pitch diameter, mm
p = circular pitch

10.3 Conjugate Action

When the tooth profiles are designed so as to produce a constant angular velocity ratio during meshing, these are said to have *conjugate action*. In theory, at least, it is possible arbitrarily to select any profile for one tooth and then to find a profile for the meshing tooth that will give conjugate action. One of these solutions is the *involute profile,* which, with few exceptions, is in universal use for gear teeth and is the only one with which we should be concerned.

10.4 Involute Properties

An involute curve may be generated as shown in Fig. (10–6a). A partial flange *B* is attached to the cylinder *A*, around which is wrapped a cord *def,* which is held tight. Point *b* on the cord represents the tracing point, and as the cord is wrapped and unwrapped about the cylinder, point *b* will trace out the involute curve *ac*. The radius of the curvature of the involute varies continuously, being zero at point *a* and a maximum at point *c*. At point *b* the radius is equal to the distance *be*, since point *b* is instantaneously rotating about point *e*. Thus the generating line *de* is normal to the involute at all points of intersection and, at the same time, is always tangent to the cylinder *A*. The circle on which the involute is generated is called the *base circle.*
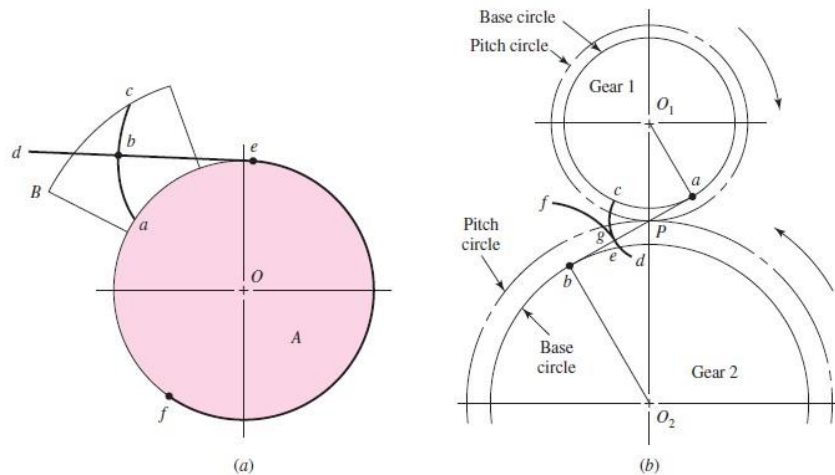
Figure (10–6)
(a) Generation of an involute; (b) involute action

Let us now examine the involute profile to see how it satisfies the requirement for the transmission of uniform motion. In Fig. (10–6b), two gear blanks with fixed centers at O_1 and O_2 are shown having base circles whose respective radii are O_1a and O_2b. We now imagine that a cord is wound clockwise around the base circle of gear 1, pulled tight between points a and b, and wound counterclockwise around the base circle of gear 2. If, now, the base circles are rotated in different directions so as to keep the cord tight, a point g on the cord will trace out the involutes cd on gear 1 and ef on gear 2. The involutes are thus generated simultaneously by the tracing point. The tracing point, therefore, represents the point of contact, while the portion of the cord ab is the generating line. The point of contact moves along the generating line; the generating line does not change position, because it is always tangent to the base circles; and since the generating line is always normal to the involutes at the point of contact, the requirement for uniform motion is satisfied.

10.5 Fundamentals

When two gears are in mesh, their pitch circles roll on one another without slipping. Designate the pitch radii as r_1 and r_2 and the angular velocities as ω_1 and ω_2, respectively. Then the pitch-line velocity is

$$V = |r_1\omega_1| = |r_2\omega_2|$$

Thus the relation between the radii on the angular velocities is

$$\left|\frac{\omega_1}{\omega_2}\right| = \frac{r_2}{r_1}$$ 10-5

Suppose now we wish to design a speed reducer such that the input speed is 1800 rev/min and the output speed is 1200 rev/min. This is a ratio of 3:2; the gear pitch diameters would be in the same ratio, for example, a 4-in pinion driving a 6-in gear. The various dimensions found in gearing are always based on the pitch circles.
      Suppose we specify that an 18-tooth pinion is to mesh with a 30-tooth gear and that the diametral pitch of the gearset is to be 2 teeth per inch. Then, from Eq. (10–1), the pitch diameters of the pinion and gear are, respectively,

$$d_1 = \frac{N_1}{P} = \frac{18}{2} = 9\text{in} \qquad d_2 = \frac{N_2}{P} = \frac{30}{2} = 15\text{in}$$

The first step in drawing teeth on a pair of mating gears is shown in Fig. (10–7). The center distance is the sum of the pitch radii, in this case 12-in. So locate the pinion and gear centers O_1 and O_2, 12-in apart. Then construct the pitch circles of radii r_1 and r_2. These are tangent at *P*, the *pitch point*. Next draw line *ab*, the common tangent, through the pitch point. We now designate gear 1 as the driver, and since it is rotating counterclockwise, we draw a line *cd* through point *P* at an angle ϕ to the common tangent *ab*. The line *cd* has three names, all of which are in general use. It is called the *pressure line,* the *generating line,* and the *line of action*. It represents the direction in which the resultant force acts between the gears. The angle ϕ is called the *pressure angle,* and it usually has values of 20° or 25°, though 14.5^o was once used.
      Next, on each gear draw a circle tangent to the pressure line. These circles are the *base circles*. Since they are tangent to the pressure line, the pressure angle determines their size. As shown in Fig. (10–8), the radius of the base circle is

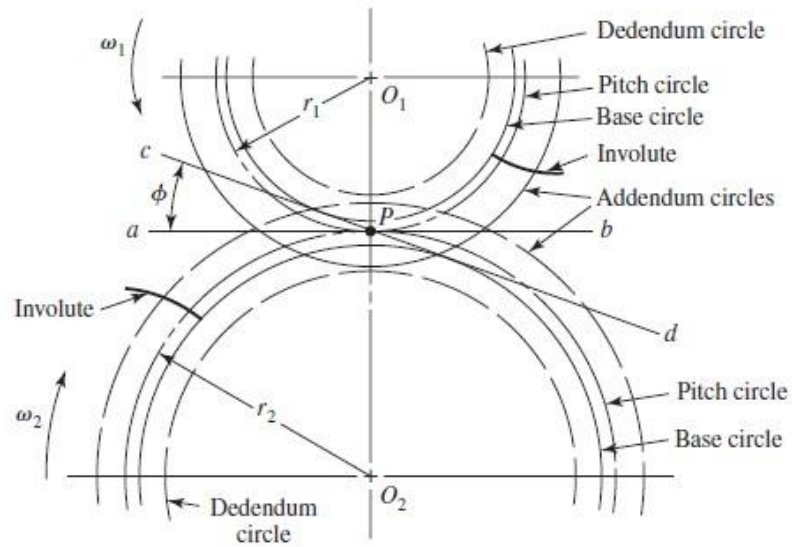$$r_b = r\cos\phi$$ 10-6

where *r* is the pitch radius.
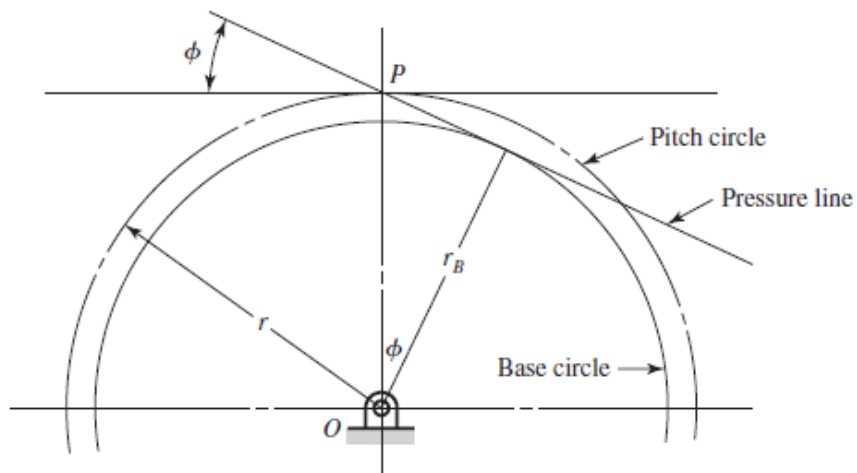
Figure (10–7)
Circles of a gear layout

Figure (10–8)
Base circle radius can be related to the pressure angle ϕ
and the pitch circle radius by $r_b = r \cos \phi$

Now generate an involute on each base circle as previously
described and as shown in Fig. (10–7). This involute is to be used
for one side of a gear tooth. It is not necessary to draw another curve
in the reverse direction for the other side of the tooth, because we are
going to use a template which can be turned over to obtain the other
side.

The addendum and dedendum distances for standard interchangeable teeth are, as we shall learn later, $1/P$ and $1.25/P$, respectively. Therefore, for the pair of gears we are constructing,

$$a = \frac{1}{P} = \frac{1}{2} = 0.5 \text{ in} \qquad b = \frac{1.25}{P} = \frac{1.25}{2} = 0.625 \text{ in}$$

Using these distances, draw the addendum and dedendum circles on the pinion and on the gear as shown in Fig. (10–7).

To draw a tooth, we must know the tooth thickness. From Eq. (10–4), the circular pitch is

$$p = \frac{\pi}{P} = \frac{\pi}{2} = 1.57 \text{in}$$

Therefore, the tooth thickness is

$$t = \frac{p}{2} = \frac{1.57}{2} = 0.785 \text{in}$$

measured on the pitch circle. Using this distance for the tooth thickness as well as the tooth space, draw as many teeth as desired, using the template, after the points have been marked on the pitch circle. In Fig. (10–9) only one tooth has been drawn on each gear. You may run into trouble in drawing these teeth if one of the base circles happens to be larger than the dedendum circle. The reason for this is that the involute begins at the base circle and is undefined below this circle. So, in drawing gear teeth, we usually draw a radial line for the profile below the base circle. The actual shape, however, will depend upon the kind of machine tool used to form the teeth in manufacture, that is, how the profile is generated.

The portion of the tooth between the clearance circle and the dedendum circle includes the fillet. In this instance the clearance is

$$c = b - a = 0.625 - 0.5 = 0.125 \text{ in}$$

The construction is finished when these fillets have been drawn.

Referring again to Fig. (10–9), the pinion with center at O_1 is the driver and turns counterclockwise. The pressure, or generating, line is the same as the cord used in Fig. (10–6a) to generate the involute, and contact occurs along this line. The initial contact will take place when the flank of the driver comes into contact with the tip of the driven tooth. This occurs at point a in Fig. (10–9), where the addendum circle of the driven gear crosses the pressure line. If

we now construct tooth profiles through point *a* and draw radial lines from the intersections of these profiles with the pitch circles to the gear centers, we obtain the *angle of approach* for each gear.
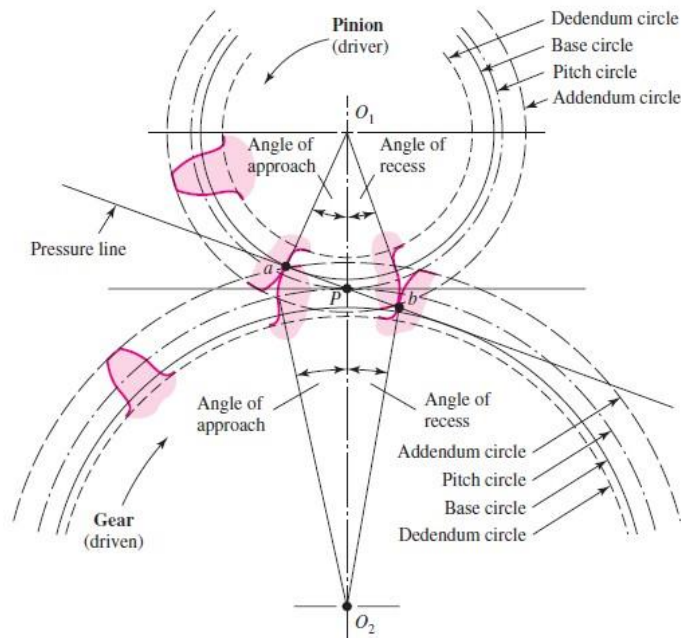

Figure (10–9)
Tooth action

As the teeth go into mesh, the point of contact will slide up the side of the driving tooth so that the tip of the driver will be in contact just before contact ends. The final point of contact will therefore be where the addendum circle of the driver crosses the pressure line. This is point *b* in Fig. (10–9). By drawing another set of tooth profiles through *b*, we obtain the *angle of recess* for each gear in a manner similar to that of finding the angles of approach. The sum of the angle of approach and the angle of recess for either gear is called the *angle of action.* The line *ab* is called *the line of action.*

We may imagine a *rack* as a spur gear having an infinitely large pitch diameter. Therefore, the rack has an infinite number of teeth and a base circle which is an infinite distance from the pitch point. The sides of involute teeth on a rack are straight lines making an angle to the line of centers equal to the pressure angle. Figure (10–10) shows an involute rack in mesh with a pinion. Corresponding sides on involute teeth are parallel curves; the *base pitch* is the constant and fundamental distance between them along a

common normal as shown in Fig. (10–10). The base pitch is related to the circular pitch by the equation

$$p_b = p_c \cos \phi \qquad\qquad 10\text{-}7$$
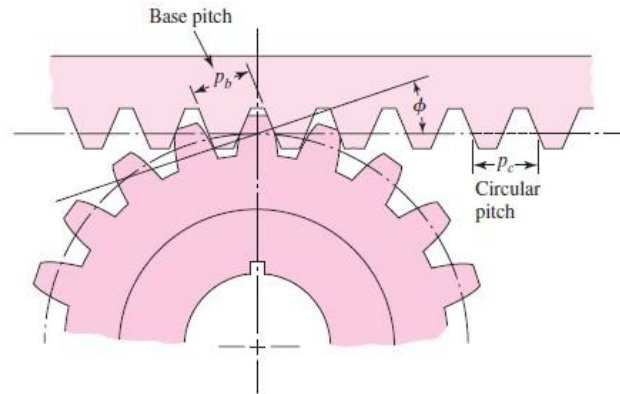
where p_b is the base pitch.

Figure (10–10)

Involute-toothed pinion and rack

Figure (10–11) shows a pinion in mesh with an *internal, or ring, gear.* Note that both of the gears now have their centers of rotation on the same side of the pitch point. Thus the positions of the addendum and dedendum circles with respect to the pitch circle are reversed; the addendum circle of the internal gear lies *inside* the pitch circle. Note, too, from Fig. (10–11), that the base circle of the internal gear lies inside the pitch circle near the addendum circle.

Another interesting observation concerns the fact that the operating diameters of the pitch circles of a pair of meshing gears need not be the same as the respective design pitch diameters of the gears, though this is the way they have been constructed in Fig. (10–9). If we increase the center distance, we create two new operating pitch circles having larger diameters because they must be tangent to each other at the pitch point. Thus the pitch circles of gears really do not come into existence until a pair of gears are brought into mesh.

Changing the center distance has no effect on the base circles, because these were used to generate the tooth profiles. Thus the base circle is basic to a gear. Increasing the center distance increases the

pressure angle and decreases the length of the line of action, but the teeth are still conjugate, the requirement for uniform motion transmission is still satisfied, and the angular-velocity ratio has not changed.
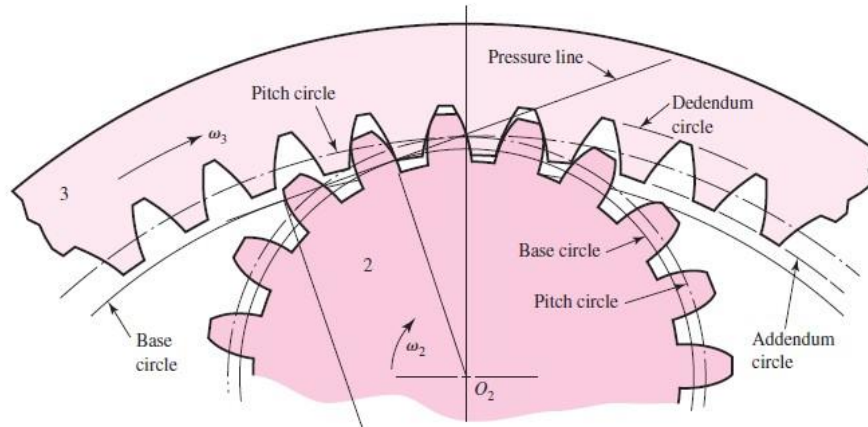

Figure (10–11)
Internal gear and pinion

EXAMPLE 10–1

A gearset consists of a 16-tooth pinion driving a 40-tooth gear. The diametral pitch is 2, and the addendum and dedendum are $1/P$ and $1.25/P$, respectively. The gears are cut using a pressure angle of 20°.
(a) Compute the circular pitch, the center distance, and the radii of the base circles.
(b) In mounting these gears, the center distance was incorrectly made 1/4 in larger. Compute the new values of the pressure angle and the pitch-circle diameters.

Solution

(a) $p = \pi/P = \pi/2 = 1.57$ in

The pitch diameters of the pinion and gear are, respectively,

$$d_P = 16/2 = 8 \text{ in} \qquad d_G = 40/2 = 20 \text{ in}$$

Therefore the center distance is

$$(d_P + d_G)/2 = (8 + 20)/2 = 14 \text{ in}$$

Since the teeth were cut on the 20° pressure angle, the base-circle radii are found to be, using $r_b = r \cos \phi,$

$$r_b \text{ (pinion)} = (8/2) \cos 20^{\circ} = 3.76 \text{ in}$$

$$r_b \text{ (gear)} = (20/2) \cos 20^{\circ} = 9.4 \text{ in}$$

(*b*) Designating d'_P and d'_G as the new pitch-circle diameters, the 1/4-in increase in the center distance requires that

$$(d'_P + d'_G)/2 = 14.25 \tag{1}$$

Also, the velocity ratio does not change, and hence

$$d'_P/d'_G = 16/40 \tag{2}$$

Solving Eqs. (1) and (2) simultaneously yields

$$d'_P = 8.143 \text{ in} \qquad d'_G = 20.357 \text{ in}$$

Since $r_b = r \cos \phi$, the new pressure angle is

$$\phi' = \cos^{-1} [r_b \text{ (pinion)}]/(d'_P /2) = \cos^{-1} [3.76/(8.143/2)] = 22.56^{\circ}$$

10.6 Contact Ratio

The zone of action of meshing gear teeth is shown in Fig. (10–12). We recall that tooth contact begins and ends at the intersections of the two addendum circles with the pressure line. In Fig. (10–12) initial contact occurs at *a* and final contact at *b*. Tooth profiles drawn through these points intersect the pitch circle at *A* and *B*, respectively. As shown, the distance *AP* is called the *arc of approach* q_a , and the distance *PB*, the *arc of recess* q_r . The sum of these is the *arc of action* q_t.

      Now, consider a situation in which the arc of action is exactly equal to the circular pitch, that is, $q_t = p$. This means that one tooth and its space will occupy the entire arc *AB*. In other words, when a tooth is just beginning contact at *a*, the previous tooth is simultaneously ending its contact at *b*. Therefore, during the tooth action from *a* to *b*, there will be exactly one pair of teeth in contact.
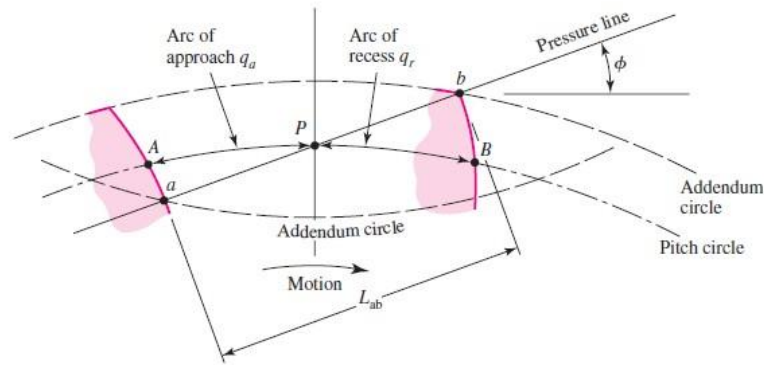
Figure (10–12)
Definition of contact ratio

Next, consider a situation in which the arc of action is greater than the circular pitch, but not very much greater, say, $q_t = 1.2p$. This means that when one pair of teeth is just entering contact at a, another pair, already in contact, will not yet have reached b.

Thus, for a short period of time, there will be two teeth in contact, one in the vicinity of A and another near B. As the meshing proceeds, the pair near B must cease contact, leaving only a single pair of contacting teeth, until the procedure repeats itself.

Because of the nature of this tooth action, either one or two pairs of teeth in contact, it is convenient to define the term *contact ratio* m_c as

$$m_c = q_t/p \qquad\qquad 10\text{-}8$$

a number that indicates the average number of pairs of teeth in contact. Note that this ratio is also equal to the length of the path of contact divided by the base pitch. Gears should not generally be designed having contact ratios less than about 1.2, because inaccuracies in mounting might reduce the contact ratio even more, increasing the possibility of impact between the teeth as well as an increase in the noise level.

An easier way to obtain the contact ratio is to measure the line of action ab instead of the arc distance AB. Since ab in Fig. (10–12) is tangent to the base circle when extended, the base pitch p_b must be used to calculate m_c instead of the circular pitch as in Eq. (10–8). If the length of the line of action is L_{ab}, the contact ratio is

$$m_c = L_{ab}/p \cos \phi \qquad\qquad 10\text{-}9$$

in which Eq. (10–7) was used for the base pitch.

10.7 Interference

The contact of portions of tooth profiles that are not conjugate is called *interference*. Consider Fig. (10–13). Illustrated are two 16-tooth gears that have been cut to the now obsolete 14.5° pressure angle. The driver, gear 2, turns clockwise. The initial and final points of contact are designated *A* and *B*, respectively, and are located on the pressure line. Now notice that the points of tangency of the pressure line with the base circles *C* and *D* are located *inside* of points *A* and *B*. Interference is present.
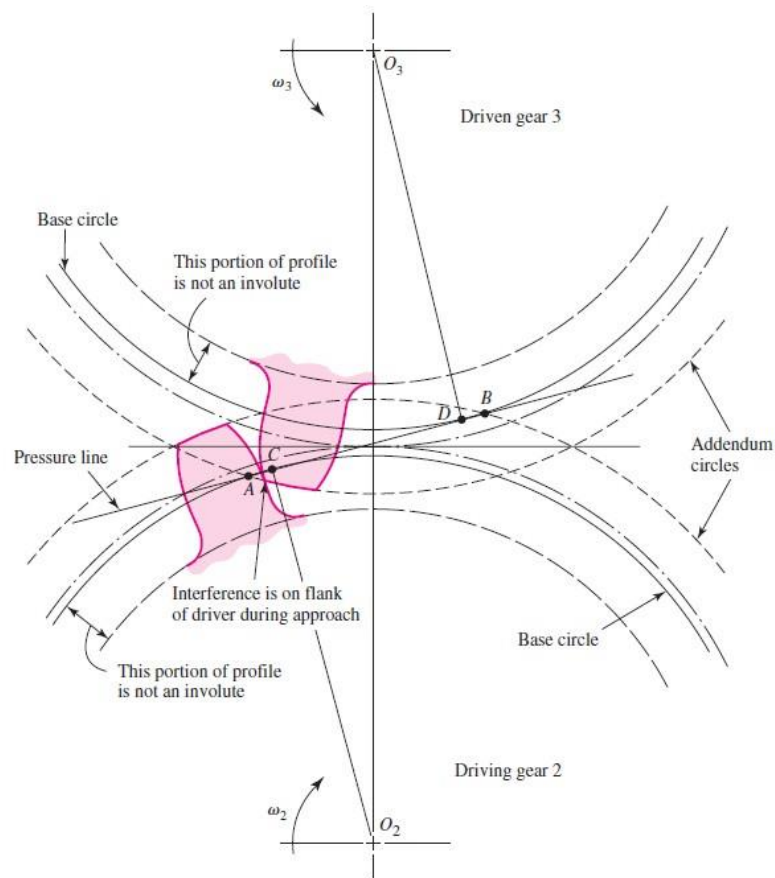

Figure (10–13)
                    Interference in the action of gear teeth

The interference is explained as follows. Contact begins when the tip of the driven tooth contacts the flank of the driving tooth. In this case the flank of the driving tooth first makes contact with the driven tooth at point *A*, and this occurs *before* the involute portion of

the driving tooth comes within range. In other words, contact is occurring below the base circle of gear 2 on the *noninvolute* portion of the flank. The actual effect is that the involute tip or face of the driven gear tends to dig out the noninvolute flank of the driver.

In this example the same effect occurs again as the teeth leave contact. Contact should end at point *D* or before. Since it does not end until point *B*, the effect is for the tip of the driving tooth to dig out, or interfere with, the flank of the driven tooth.

When gear teeth are produced by a generation process, interference is automatically eliminated because the cutting tool removes the interfering portion of the flank. This effect is called *undercutting;* if undercutting is at all pronounced, the undercut tooth is considerably weakened. Thus the effect of eliminating interference by a generation process is merely to substitute another problem for the original one.

The smallest number of teeth on a spur pinion and gear, one-to-one gear ratio, which can exist without interference is N_P . This number of teeth for spur gears is given by

$$N_P = \frac{2k}{3\sin^2 \phi}\left(1 + \sqrt{1 + 3\sin^2 \phi}\right) \qquad\qquad 10\text{-}10$$

where $k = 1$ for full-depth teeth, 0.8 for stub teeth and ϕ = pressure angle.

For a 20° pressure angle, with $k = 1$,

$$N_P = \frac{2(1)}{3\sin^2 20^\circ}\left(1 + \sqrt{1 + 3\sin^2 20^\circ}\right) = 12.3 = 13 \text{ teeth}$$

Thus 13 teeth on pinion and gear are interference-free. Realize that 12.3 teeth is possible in meshing arcs, but for fully rotating gears, 13 teeth represents the least number. For a 14.5° pressure angle, $N_P = 23$ teeth, so one can appreciate why few 14.5°-tooth systems are used, as the higher pressure angles can produce a smaller pinion with accompanying smaller center-to-center distances.

If the mating gear has more teeth than the pinion, that is, $m_G = N_G / N_P = m$ is more than one, then the smallest number of teeth on the pinion without interference is given by

$$N_P = \frac{2k}{(1 + 2m)\sin^2 \phi}\left(m + \sqrt{m^2 + (1 + 2m)\sin^2 \phi}\right) \qquad\qquad 10\text{-}11$$

For example, if $m = 4$, $\phi = 20\circ$,

$$N_P = \frac{2(1)}{[1 + 2(4)]\sin^2 20^\circ}\left(4 + \sqrt{4^2 + [1 + 2(4)]\sin^2 20^\circ}\right) = 15.4 = 16 \text{ teeth}$$

Thus a 16-tooth pinion will mesh with a 64-tooth gear without interference.

The largest gear with a specified pinion that is interference-free is

$$4k - 2N_P \sin \phi \qquad\qquad N_G = \frac{N_P^2 \sin^2 \phi - 4k^2}{\qquad} \qquad\qquad 10\text{-}12$$

For example, for a 13-tooth pinion with a pressure angle ϕ of 20°,

$$N_G = \frac{13^2 \sin^2 20^o - 4(1)^2}{4(1) - 2(13)\sin^2 20^o} = 16.45 = 16 \text{ teeth}$$

For a 13-tooth spur pinion, the maximum number of gear teeth possible without interference is 16.

The smallest spur pinion that will operate with a rack without interference is

$$N_P = \qquad\qquad\qquad \frac{2k}{\sin^2 \phi} \qquad\qquad 10\text{-}13$$

For a 20° pressure angle full-depth tooth the smallest number of pinion teeth to mesh with a rack is

$$N_P = \qquad\qquad\qquad \frac{2(1)}{\sin^2 20^o} = 17.1 = 18 \text{ teeth}$$

Since gear-shaping tools amount to contact with a rack, and the gear-hobbing process is similar, the minimum number of teeth to prevent interference to prevent undercutting by the hobbing process is equal to the value of N_P when N_G is infinite.

The importance of the problem of teeth that have been weakened by undercutting cannot be overemphasized. Of course, interference can be eliminated by using more teeth on the pinion. However, if the pinion is to transmit a given amount of power, more teeth can be used only by increasing the pitch diameter.

Interference can also be reduced by using a larger pressure angle. This results in a smaller base circle, so that more of the tooth profile becomes involute. The demand for smaller pinions with fewer teeth thus favors the use of a 25° pressure angle even though the frictional forces and bearing loads are increased and the contact ratio decreased.

10.8 The Forming of Gear Teeth

There are a large number of ways of forming the teeth of gears, such as *sand casting, shell molding, investment casting, permanent-mold casting, die casting,* and *centrifugal casting*. Teeth can also be formed by using the *powder-metallurgy process;* or, by using *extrusion,* a single bar of aluminum may be formed and then sliced into gears. Gears that carry large loads in comparison with their size are usually made of steel and are cut with either *form cutters* or *generating cutters.* In form cutting, the tooth space takes the exact form of the cutter. In generating, a tool having a shape different from the tooth profile is moved relative to the gear blank so as to obtain the proper tooth shape. One of the newest and most promising of the methods of forming teeth is called *cold forming,* or *cold rolling,* in which dies are rolled against steel blanks to form the teeth. The mechanical properties of the metal are greatly improved by the rolling process, and a high-quality generated profile is obtained at the same time.

Gear teeth may be machined by milling, shaping, or hobbing. They may be finished by shaving, burnishing, grinding, or lapping.

Gears made of thermoplastics such as nylon and polycarbonate are quite popular and are easily manufactured by *injection molding*. These gears are of low to moderate precision, low in cost for high production quantities, and capable of light loads, and can run without lubrication.

Finishing

Gears that run at high speeds and transmit large forces may be subjected to additional dynamic forces if there are errors in tooth profiles. Errors may be diminished somewhat by finishing the tooth profiles. The teeth may be finished, after cutting, by either shaving or burnishing. Several shaving machines are available that cut off a minute amount of metal, bringing the accuracy of the tooth profile within the limits of 250 μin.

Burnishing, like shaving, is used with gears that have been cut but not heat-treated. In burnishing, hardened gears with slightly oversize teeth are run in mesh with the gear until the surfaces become smooth.

Grinding and lapping are used for hardened gear teeth after heat treatment. The grinding operation employs the generating

principle and produces very accurate teeth. In lapping, the teeth of the gear and lap slide axially so that the whole surface of the teeth is abraded equally.

10.9 Straight Bevel Gears

When gears are used to transmit motion between intersecting shafts, some form of bevel gear is required. A bevel gearset is shown in Fig. (10–14). Although bevel gears are usually made for a shaft angle of 90°, they may be produced for almost any angle. The teeth may be cast, milled, or generated. Only the generated teeth may be classed as accurate.

       The terminology of bevel gears is illustrated in Fig. (10–14). The pitch of bevel gears is measured at the large end of the tooth, and both the circular pitch and the pitch diameter are calculated in the same manner as for spur gears. It should be noted that the clearance is uniform. The pitch angles are defined by the pitch cones meeting at the apex, as shown in the figure. They are related to the tooth numbers as follows:

$$\tan \gamma = \frac{N_P}{N_G} \qquad\qquad \tan \Gamma = \frac{N_G}{N_P} \qquad\qquad \text{10-14}$$

where the subscripts P and G refer to the pinion and gear, respectively, and where γ and Γ are, respectively, the pitch angles of the pinion and gear.
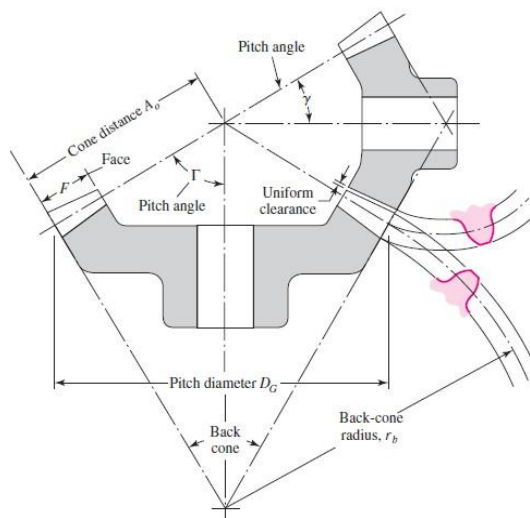

Figure (10–14)
Terminology of bevel gears

Figure (10–14) shows that the shape of the teeth, when projected on the back cone, is the same as in a spur gear having a radius equal to the back-cone distance r_b. This is called Tredgold's approximation. The number of teeth in this imaginary gear is

$$N' = \frac{2\pi r_b}{p} \qquad\qquad\qquad \text{10-15}$$

where N' is the *virtual number of teeth* and p is the circular pitch measured at the large end of the teeth. Standard straight-tooth bevel gears are cut by using a 20° pressure angle, unequal addenda and dedenda, and full-depth teeth. This increases the contact ratio, avoids undercut, and increases the strength of the pinion.

10.10 Parallel Helical Gears

Helical gears, used to transmit motion between parallel shafts, are shown in Fig. (10–2). The helix angle is the same on each gear, but one gear must have a right-hand helix and the other a left-hand helix. The shape of the tooth is an involute helicoid and is illustrated in Fig. (10–15). If a piece of paper cut in the shape of a parallelogram is wrapped around a cylinder, the angular edge of the paper becomes a helix. If we unwind this paper, each point on the angular edge generates an involute curve. This surface obtained when every point on the edge generates an involute is called an *involute helicoid.*
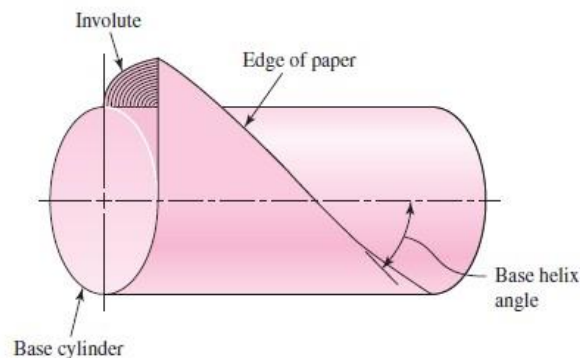

Figure (10–15)
An involute helicoid

The initial contact of spur-gear teeth is a line extending all the way across the face of the tooth. The initial contact of helical-gear teeth is a point that extends into a line as the teeth come into more

engagement. In spur gears the line of contact is parallel to the axis of rotation; in helical gears the line is diagonal across the face of the tooth. It is this gradual engagement of the teeth and the smooth transfer of load from one tooth to another that gives helical gears the ability to transmit heavy loads at high speeds. Because of the nature of contact between helical gears, the contact ratio is of only minor importance, and it is the contact area, which is proportional to the face width of the gear, that becomes significant.

Helical gears subject the shaft bearings to both radial and thrust loads. When the thrust loads become high or are objectionable for other reasons, it may be desirable to use double helical gears. A double helical gear (herringbone) is equivalent to two helical gears of opposite hand, mounted side by side on the same shaft. They develop opposite thrust reactions and thus cancel out the thrust load.

When two or more single helical gears are mounted on the same shaft, the hand of the gears should be selected so as to produce the minimum thrust load.
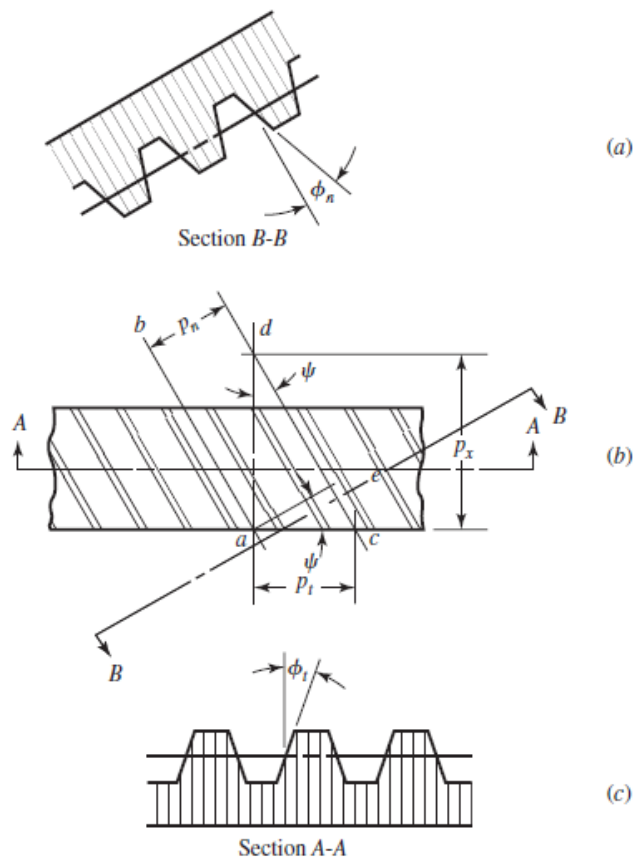

Figure (10–16)
Nomenclature of helical gears

Figure (10–16) represents a portion of the top view of a helical rack. Lines *ab* and *cd* are the centerlines of two adjacent helical teeth taken on the same pitch plane. The angle ψ is the *helix angle.* The distance *ac* is the *transverse circular pitch pt* in the plane of rotation (usually called the *circular pitch*). The distance *ae* is the *normal circular pitch p_n* and is related to the transverse circular pitch as follows:

$$p_n = p_t \cos \psi \qquad \text{10-16}$$

The distance *ad* is called the *axial pitch p_x* and is related by the expression

$$p_x = \frac{p_t}{\tan \psi} \qquad \text{10-17}$$

Since $p_n P_n = \pi$, the *normal diametral pitch* is

$$P_n = \frac{P_t}{\cos \psi} \qquad \text{10-18}$$

The pressure angle ϕ_n in the normal direction is different from the pressure angle ϕ_t in the direction of rotation, because of the angularity of the teeth. These angles are related by the equation

$$\cos \psi = \frac{\tan \phi_n}{\tan \phi_t} \qquad \qquad \text{10-19}$$

Figure (10–17) illustrates a cylinder cut by an oblique plane *ab* at an angle ψ to a right section. The oblique plane cuts out an arc having a radius of curvature of *R*. For the condition that $\psi = 0$, the radius of curvature is $R = D/2$. If we imagine the angle ψ to be slowly increased from zero to 90°, we see that *R* begins at a value of $D/2$ andincreases until, when $\psi = 90^o$, $R = \infty$. The radius *R* is the apparent pitch radius of a helical-gear tooth when viewed in the direction of the tooth elements. A gear of the same pitch and with the radius *R* will have a greater number of teeth, because of the increased radius. In helical-gear terminology this is called the *virtual number of teeth.* It can be shown by analytical geometry that the virtual number of teeth is related to the actual number by the equation

$$N' = \frac{N}{\cos^3 \psi} \qquad \text{10-20}$$

where *N'* is the virtual number of teeth and *N* is the actual number of teeth. It is necessary to know the virtual number of teeth in design for strength and also, sometimes, in cutting helical teeth. This

apparently larger radius of curvature means that few teeth may be used on helical gears, because there will be less undercutting.
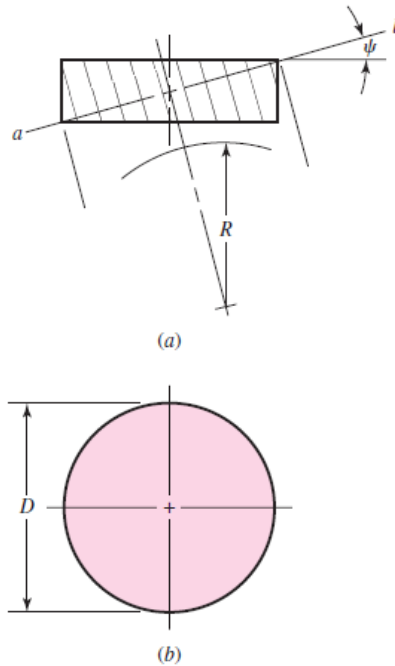

(a)

(b)

Figure (10–17)
A cylinder cut by an oblique plane

EXAMPLE 10–2

A stock helical gear has a normal pressure angle of $20°$, a helix angle of $25°$, and a transverse diametral pitch of 6 teeth/in, and has 18 teeth. Find:
(a) The pitch diameter
(b) The transverse, the normal, and the axial pitches
(c) The normal diametral pitch
(d) The transverse pressure angle

Solution

(a)
$$d = \frac{N}{P_t} = \frac{18}{6} = 3 \text{ in}$$

(b)
$$p_t = \frac{\pi}{P} = \frac{\pi}{6} = 0.5236 \text{ in}$$

$$p_n = p_t \cos \psi = 0.5236 \cos 25^\circ = 0.4745 \text{ in}$$

$p_x =$
$$\frac{p_t}{\tan \psi} = \frac{0.5236}{\tan 25^\circ} = 1.123 \text{ in}$$

(c)
$$P_n = \frac{P_t}{\cos \psi} = \frac{6}{\cos 25^\circ} = 6.62 \text{ teeth/in}$$

(d)
$$\phi_t = \tan^{-1}\left(\frac{\tan \phi_n}{\cos \psi}\right) = \tan^{-1}\left(\frac{\tan 20^\circ}{\cos 25^\circ}\right) = 21.88^\circ$$

Just like teeth on spur gears, helical-gear teeth can interfere. Equation (10–19) can be solved for the pressure angle ϕ_t in the tangential (rotation) direction to give

$$\phi_t = \tan^{-1}\left(\frac{\tan \phi_n}{\cos \psi}\right)$$

The smallest tooth number N_P of a helical-spur pinion that will run without interference with a gear with the same number of teeth is

$$N_P = \frac{2k \cos \psi}{3 \sin^2 \phi}\left(1 + \sqrt{1 + 3\sin^2 \phi_t}\right) \qquad \text{10-21}$$

For example, if the normal pressure angle ϕ_n is 20°, the helix angle ψ is 30°, then ϕ_t is

$$\phi_t = \tan^{-1}\left(\frac{\tan 20^\circ}{\cos 35^\circ}\right) = 22.8^\circ$$

$$N_P = \frac{2(1)\cos 30^\circ}{3\sin^2 22.8^\circ}\left(1 + \sqrt{1 + 3\sin^2 22.8^\circ}\right) = 8.48 = 9 \text{ teeth}$$

For a given gear ratio $m_G = N_G/N_P = m$, the smallest pinion tooth count is

$$N_P = \frac{2k \cos \psi}{(1 + 2m)\sin^2 \phi_t}\left(m + \sqrt{m^2 + (1 + 2m)\sin^2 \phi_t}\right) \qquad \text{10-22}$$

The largest gear with a specified pinion is given by

$$N_G = \frac{N_P^2 \sin^2 \phi_t - 4k^2\cos^2 \psi}{4k\cos \psi - 2N_P\sin \phi_t} \qquad \text{10-23}$$

For example, for a nine-tooth pinion with a pressure angle ϕ_n of 20°, a helix angle ψ of 30°, and recalling that the tangential pressure angle ϕ_t is 22.8^o,

$$N_G = \frac{9^2 \sin^2 22.8^o - 4(1)^2 \cos^2 30^o}{4(1)\cos 30^o - 2(9)\sin^2 22.8^o} = 12.02 = 12 \text{ teeth}$$

The smallest pinion that can be run with a rack is

$$N = \frac{2k \cos \psi}{\sin^2 \phi_t} \qquad\qquad\qquad \text{10-24}$$

For a normal pressure angle ϕ_n of 20° and a helix angle ψ of 30°, and $\phi_t = 22.80^o$,

$$N_P = \frac{2(1)\cos 30^o}{\sin^2 22.8^o} = 11.5 = 12 \text{ teeth}$$

For helical-gear, the number of teeth in mesh across the width of the gear will be greater than unity and a term called *face-contact ratio* is used to describe it. This increase of contact ratio, and the gradual sliding engagement of each tooth, results in quieter gears.

10.11 Worm Gears

The nomenclature of a worm gear is shown in Fig. (10–18). The worm and worm gear of a set have the same hand of helix as for crossed helical gears, but the helix angles are usually quite different. The helix angle on the worm is generally quite large, and that on the gear very small. Because of this, it is usual to specify the lead angle λ on the worm and helix angle ψ_G on the gear; the two angles are equal for a 90° shaft angle. The worm lead angle is the complement of the worm helix angle, as shown in Fig. (10–18).

In specifying the pitch of worm gearsets, it is customary to state the *axial pitch* p_x of the worm and the *transverse circular pitch* p_t, often simply called the circular pitch, of the mating gear. These are equal if the shaft angle is 90°. The pitch diameter of the gear is the diameter measured on a plane containing the worm axis, as shown in Fig. (10–18); it is the same as for spur gears and is

$$d_G = \frac{N_G p_t}{\pi} \qquad\qquad\qquad \text{10-25}$$

Since it is not related to the number of teeth, the worm may have any pitch diameter; this diameter should, however, be the same

as the pitch diameter of the hob used to cut the worm-gear teeth. Generally, the pitch diameter of the worm should be selected so as to fall into the range

$$\frac{C^{0.875}}{3} \le d_w \le \frac{C^{0.875}}{1.7} \qquad \text{10-26}$$

where *C* is the center distance. These proportions appear to result in optimum horsepower capacity of the gearset.

The *lead L* and the *lead angle* λ of the worm have the following relations:

$$L = p_x N_W \qquad \text{10-27}$$

$$\tan \lambda = \frac{L}{\pi d_w} \qquad \text{10-28}$$
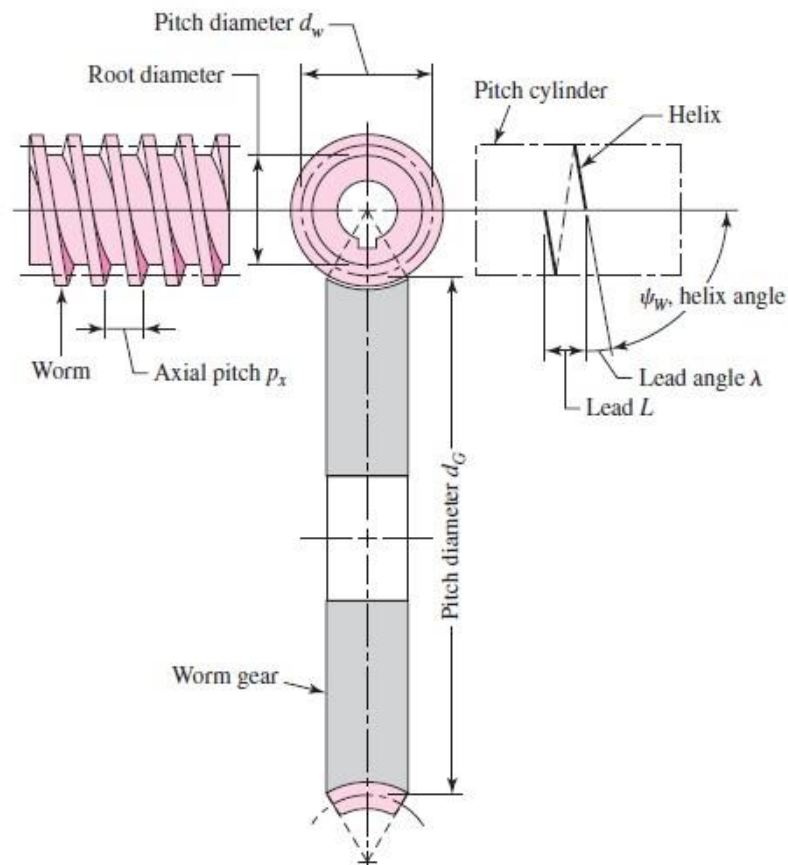
Figure (10–18)
Nomenclature of a single enveloping worm gearset

10.12 Tooth Systems

A *tooth system -standardized by the American Gear Manufacturers Association (AGMA)-* is a standard that specifies the relationships involving addendum, dedendum, working depth, tooth thickness, and pressure angle. The standards were originally planned to attain interchangeability of gears of all tooth numbers, but of the same pressure angle and pitch.

   Table (10–1) contains the standards most used for spur gears. A 14.5^o pressure angle was once used for these but is now obsolete; the resulting gears had to be comparatively larger to avoid interference problems.

   Table (10–2) is particularly useful in selecting the pitch or module of a gear. Cutters are generally available for the sizes shown in this table.

Table (10–1)
Standard and Commonly Used Tooth Systems for Spur Gears

Tooth System	Pressure Angle ϕ, deg	Addendum a	Dedendum b
Full depth	20	$1/P_d$ or $1m$	$1.25/P_d$ or $1.25m$ $1.35/P_d$ or $1.35m$
	$22\frac{1}{2}$	$1/P_d$ or $1m$	$1.25/P_d$ or $1.25m$ $1.35/P_d$ or $1.35m$
	25	$1/P_d$ or $1m$	$1.25/P_d$ or $1.25m$ $1.35/P_d$ or $1.35m$
Stub	20	$0.8/P_d$ or $0.8m$	$1/P_d$ or $1m$

Table (10–2)
Tooth Sizes in General Uses

Diametral Pitch	
Coarse	2, $2\frac{1}{4}$, $2\frac{1}{2}$, 3, 4, 6, 8, 10, 12, 16
Fine	20, 24, 32, 40, 48, 64, 80, 96, 120, 150, 200

Modules	
Preferred	1, 1.25, 1.5, 2, 2.5, 3, 4, 5, 6, 8, 10, 12, 16, 20, 25, 32, 40, 50
Next Choice	1.125, 1.375, 1.75, 2.25, 2.75, 3.5, 4.5, 5.5, 7, 9, 11, 14, 18, 22, 28, 36, 45

Table (10–3) lists the standard tooth proportions for straight bevel gears. These sizes apply to the large end of the teeth. The nomenclature is defined in Fig. (10–14).

Table (10–3)
Tooth Proportions for 20° Straight Bevel-Gear Teeth

Tooth System	Formula
Working depth	$h_k = 2.0/P$
Clearance	$c = (0.188/P) + 0.002$ in
Addendum of gear	$a_G = \dfrac{0.54}{P} + \dfrac{0.460}{P(m_{90})^2}$
Gear ratio	$m_G = N_G/N_P$
Equivalent 90° ratio	$m_{90} = m_G$ when $\Gamma = 90°$
	$m_{90} = \sqrt{m_G \dfrac{\cos \gamma}{\cos \Gamma}}$ when $\Gamma \neq 90°$
Face width	$F = 0.3A_0$ or $F = \dfrac{10}{P}$, whichever is smaller
Minimum number of teeth	Pinion 16 15 14 13
	Gear 16 17 20 30

Standard tooth proportions for helical gears are listed in Table (10–4). Tooth proportions are based on the normal pressure angle; these angles are standardized the same as for spur gears.

Though there will be exceptions, the face width of helical gears should be at least 2 times the axial pitch to obtain good helical-gear action.

Tooth forms for worm gearing have not been highly standardized, perhaps because there has been less need for it. The pressure angles used depend upon the lead angles and must be large enough to avoid undercutting of the worm-gear tooth on the side at which contact ends. A satisfactory tooth depth, which remains in about the right proportion to the lead angle, may be obtained by making the depth a proportion of the axial circular   pitch. Table (10–5) summarizes what may be regarded as good practice for pressure angle and tooth depth.

Table (10–4)

Standard Tooth Proportions for Helical Gears

*All dimensions are in inches, and angles are in degrees. ** B_n is the normal backlash

| Quantity*	Formula	Quantity*	Formula
Addendum	$\dfrac{1.00}{P_n}$	External gears:	
Dedendum	$\dfrac{1.25}{P_n}$	Standard center distance	$\dfrac{D+d}{2}$
Pinion pitch diameter	$\dfrac{N_P}{P_n \cos \psi}$	Gear outside diameter	$D+2a$
Gear pitch diameter	$\dfrac{N_G}{P_n \cos \psi}$	Pinion outside diameter	$d+2a$
Normal arc tooth thickness**	$\dfrac{\pi}{P_n} - \dfrac{B_n}{2}$	Gear root diameter	$D-2b$
Pinion base diameter	$d \cos \phi_t$	Pinion root diameter	$d-2b$
		Internal gears:	
Gear base diameter	$D \cos \phi_t$	Center distance	$\dfrac{D-d}{2}$
Base helix angle	$\tan^{-1}(\tan \psi \cos \phi_t)$	Inside diameter	$D-2a$
		Root diameter	$D+2b$

Table (10–5)

Recommended Pressure Angles and Tooth Depths for Worm Gearing

Lead Angle λ,deg	Pressure Angle ϕ_n, deg	Addendum a	Dedendum b_G
0–15	$14\frac{1}{2}$	$0.3683p_x$	$0.3683p_x$
15–30	20	$0.3683p_x$	$0.3683p_x$
30–35	25	$0.2865p_x$	$0.3314p_x$
35–40	25	$0.2546p_x$	$0.2947p_x$
40–45	30	$0.2228p_x$	$0.2578p_x$

The *face width F_G* of the worm gear should be made equal to the length of a tangent to the worm pitch circle between its points of intersection with the addendum circle, as shown in Fig. (10–19).

Figure (10–19)
A graphical depiction of the face width of the worm of a worm gearset
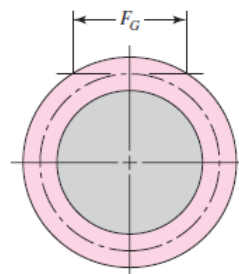
10.13 Gear Trains

Consider a pinion 2 driving a gear 3. The speed of the driven gear is

$$n_3 = \left| \frac{N_2}{N_3} n_2 \right| = \left| \frac{d_2}{d_3} n_2 \right| \qquad \text{10-29}$$

where

n = revolutions or rev/min
N = number of teeth
d = pitch diameter

Equation (10–29) applies to any gearset no matter whether the gears are spur, helical, bevel, or worm. The absolute-value signs are used to permit complete freedom in choosing positive and negative directions. In the case of spur and parallel helical gears, the directions ordinarily correspond to the right-hand rule and are positive for counterclockwise rotation.

Rotational directions are somewhat more difficult to deduce for worm and crossed helical gearsets. Figure (10–20) will be of help in these situations. The gear train shown in Fig. (10–21) is made up of five gears. The speed of gear 6 is

$$n_6 = -\frac{N_2}{N_3} \frac{N_3}{N_4} \frac{N_5}{N_6} n_2 \qquad (a)$$

Hence we notice that gear 3 is an idler, that its tooth numbers cancel in Eq. (*a*), and hence that it affects only the direction of rotation of gear 6. We notice, furthermore, that gears 2, 3, and 5 are drivers, while 3, 4, and 6 are driven members. We define the *train value e* as

$$e = \frac{\text{product of driving tooth numbers}}{\text{product of driven tooth numbers}} \qquad \text{10-30}$$

Note that pitch diameters can be used in Eq. (13–30) as well. When Eq. (10–30) is used for spur gears, *e* is positive if the last gear rotates in the same sense as the first, and negative if the last rotates in the opposite sense.

Now we can write

$$n_L = e\, n_F \qquad \text{10-31}$$

where n_L is the speed of the last gear in the train and n_F is the speed of the first.
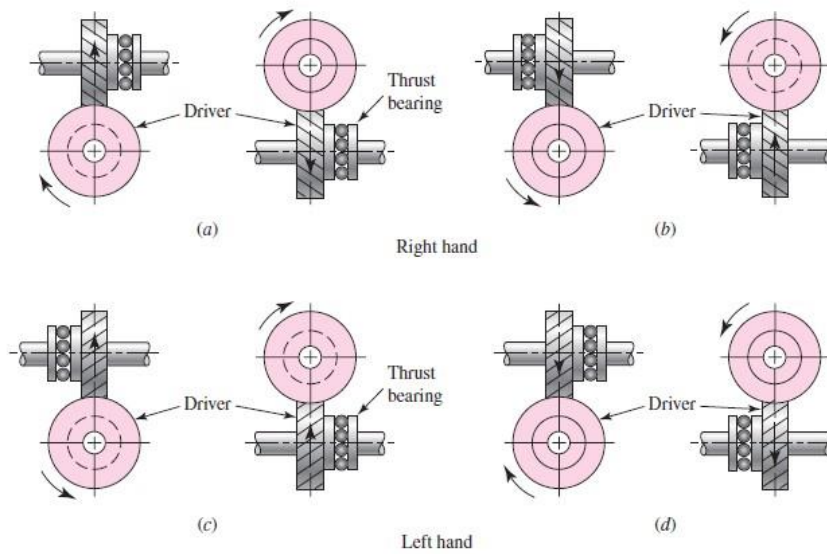
Figure (10–20)
   Thrust, rotation, and hand relations for crossed helical gears. Note that
   each pair of drawings refers to a single gearset. These relations
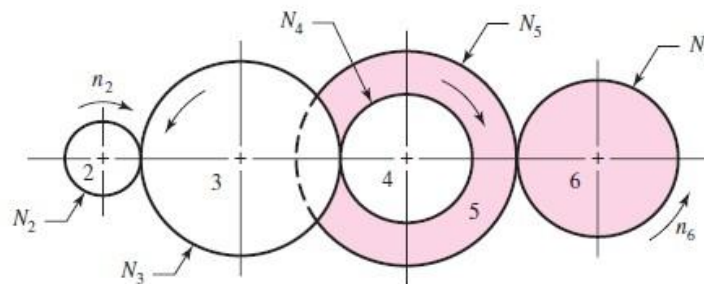   also apply to worm gearsets

Figure (10–21)
A gear train

As a rough guideline, a train value of up to 10 to 1 can be obtained
with one pair of gears. Greater ratios can be obtained in less space
and with fewer dynamic problems by compounding additional pairs
of gears. A two-stage compound gear train, such as shown in
Fig. (10–22), can obtain a train value of up to 100 to 1.
       The design of gear trains to accomplish a specific train value
is straightforward. Since numbers of teeth on gears must be integers,
it is better to determine them first, and then obtain pitch diameters
second. Determine the number of stages necessary to obtain the

overall ratio, then divide the overall ratio into portions to be accomplished in each stage. To minimize package size, keep the portions as evenly divided between the stages as possible. In cases where the overall train value need only be approximated, each stage can be identical. For example, in a two-stage compound gear train, assign the square root of the overall train value to each stage. If an exact train value is needed, attempt to factor the overall train value into integer components for each stage. Then assign the smallest gear(s) to the minimum number of teeth allowed for the specific ratio of each stage, in order to avoid interference. Finally, applying the ratio for each stage, determine the necessary number of teeth for the mating gears. Round to the nearest integer and check that the resulting overall ratio is within acceptable tolerance.
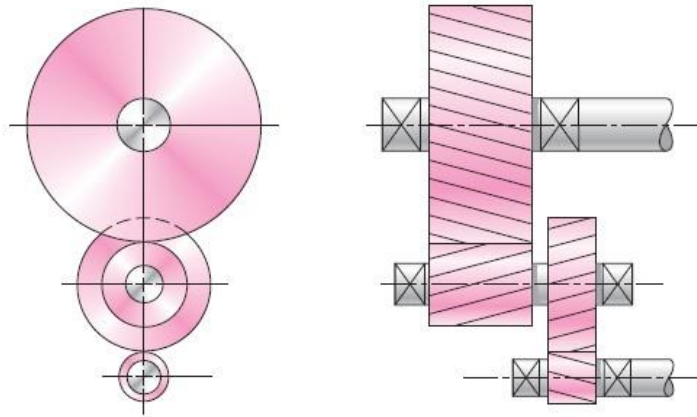

Figure (10–22)
A two stage compound gear train

EXAMPLE 10–3

A gearbox is needed to provide a 30:1 (±1 percent) increase in speed, while minimizing the overall gearbox size. Specify appropriate teeth numbers.

Solution

Since the ratio is greater than 10:1, but less than 100:1, a two-stage compound gear train, such as in Figure (10–22), is needed. The portion to be accomplished in each stage is $\sqrt{30} = 5.4772$. For this

ratio, assuming a typical 20° pressure angle, the minimum number of teeth to avoid interference is 16, according to Eq. (10–11). The number of teeth necessary for the mating gears is

$$16\sqrt{30} = 87.64 = 88 \text{ teeth}$$

From Eq. (10–30), the overall train value is

$$e = (88/16)(88/16) = 30.25$$

This is within the 1 percent tolerance. If a closer tolerance is desired, then increase the pinion size to the next integer and try again.

EXAMPLE 10–4

A gearbox is needed to provide an *exact* 30:1 increase in speed, while minimizing the overall gearbox size. Specify appropriate teeth numbers.

Solution

The previous example demonstrated the difficulty with finding integer numbers of teeth to provide an exact ratio. In order to obtain integers, factor the overall ratio into two integer stages.

$e = 30 = (6)(5)$

$$N_2/N_3 = 6 \quad \text{and} \quad N_4/N_5 = 5$$

With two equations and four unknown numbers of teeth, two free choices are available. Choose N_3 and N_5 to be as small as possible without interference. Assuming a 20° pressure angle, Eq. (10–11) gives the minimum as 16, Then

$N_2 = 6 \; N_3 = 6 \, (16) = 96$
$N_4 = 5 \; N_5 = 5 \, (16) = 80$

The overall train value is then exact.

$e = (96/16)(80/16) = (6)(5) = 30$

It is sometimes desirable for the input shaft and the output shaft of a two-stage compound geartrain to be in-line, as shown in Fig. (10–23). This configuration is called a *compound reverted geartrain*. This requires the distances between the shafts to be the same for both stages of the train, which adds to the complexity of the design task. The distance constraint is

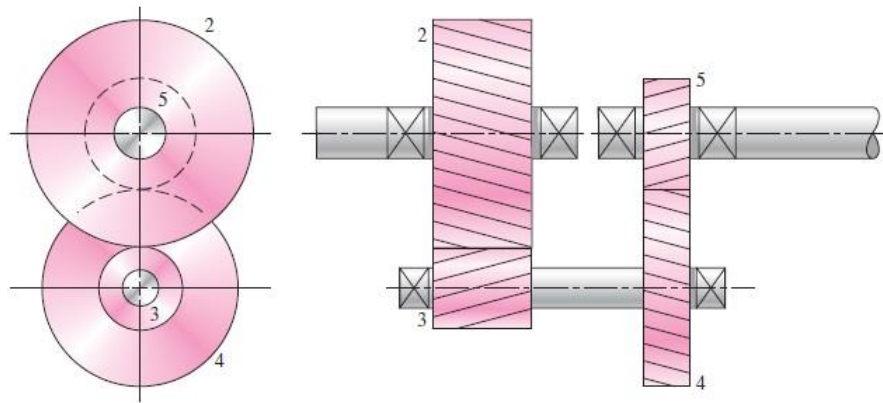$$d_2/2 + d_3/2 = d_4/2 + d_5/2$$

Figure (10–23)
A compound reverted gear train

The diametral pitch relates the diameters and the numbers of teeth, $P=N/d$. Replacing all the diameters gives

$$N_2/(2P) + N_3/(2P) = N_4/(2P) + N_5/(2P)$$

Assuming a constant diametral pitch in both stages, we have the geometry condition stated in terms of numbers of teeth:

$$N_2 + N_3 = N_4 + N_5$$

This condition must be exactly satisfied, in addition to the previous ratio equations, to provide for the in-line condition on the input and output shafts.

EXAMPLE 10–5

A gearbox is needed to provide an exact 30:1 increase in speed, while minimizing the overall gearbox size. The input and output shafts should be in-line. Specify appropriate teeth numbers.

Solution

The governing equations are

$$N_2/N_3 = 6 \qquad N_4/N_5 = 5 \qquad N_2 + N_3 = N_4 + N_5$$

With three equations and four unknown numbers of teeth, only one free choice is available. Of the two smaller gears, N_3 and N_5, the free choice should be used to minimize N_3 since a greater gear ratio is to be achieved in this stage. To avoid interference, the minimum for N_3 is 16.

Applying the governing equations yields

$$N_2 = 6N_3 = 6(16) = 96$$

$$N_2 + N_3 = 96 + 16 = 112 = N_4 + N_5$$

Substituting $N_4 = 5N_5$ gives

$$112 = 5N_5 + N_5 = 6N_5$$

$$N_5 = 112/6 = 18.67$$

If the train value need only be approximated, then this can be rounded to the nearest integer. But for an exact solution, it is necessary to choose the initial free choice for N_3 such that solution of the rest of the teeth numbers results exactly in integers. This can be done by trial and error, letting $N_3=17$, then 18, etc., until it works. Or, the problem can be normalized to quickly determine the minimum free choice. Beginning again, let the free choice be $N_3=1$. Applying the governing equations gives

$$N_2 = 6N_3 = 6(1) = 6$$

$$N_2 + N_3 = 6 + 1 = 7 = N_4 + N_5$$

Substituting $N_4 = 5N_5$, we find

$7 = 5N_5 + N_5 = 6N_5$

$N_5 = 7/6$

This fraction could be eliminated if it were multiplied by a multiple of 6. The free choice for the smallest gear N_3 should be selected as a multiple of 6 that is greater than the minimum allowed to avoid interference. This would indicate that $N_3 = 18$. Repeating the application of the governing equations for the final time yields

$N_2 = 6N_3 = 6(18) = 108$

$N_2 + N_3 = 108 + 18 = 126 = N_4 + N_5$

$126 = 5N_5 + N_5 = 6N_5$

$N_5 = 126/6 = 21$

$N_4 = 5N_5 = 5(21) = 105$

Thus,

$N_2 = 108 \qquad N_3 = 18 \qquad N_4 = 105 \qquad N_5 = 21$

Checking, we calculate $e = (108/18)(105/21) = (6)(5) = 30$. And checking the geometry constraint for the in-line requirement, we calculate

$N_2 + N_3 = N_4 + N_5$
$108 + 18 = 105 + 21$
$126 = 126$

Unusual effects can be obtained in a gear train by permitting some of the gear axes to rotate about others. Such trains are called *planetary,* or *epicyclic, gear trains.* Planetary trains always include a *sun gear,* a *planet carrier* or *arm,* and one or more *planet gears,* as shown in Fig. (10–24). Planetary gear trains are unusual mechanisms because they have two degrees of freedom; that is, for constrained motion, a planetary train must have two inputs. For example, in Fig. (10–24) these two inputs could be the motion of any two of the elements of the train. We might, say, specify that the sun gear rotates at

100 rev/min clockwise and that the ring gear rotates at 50 rev/min counterclockwise; these are the inputs. The output would be the motion of the arm. In most planetary trains one of the elements is attached to the frame and has no motion.
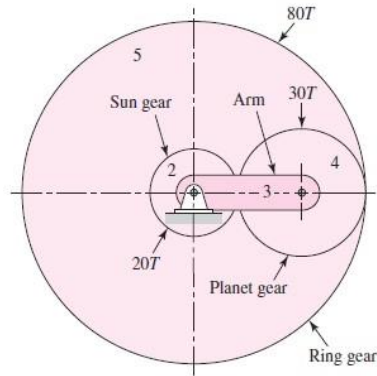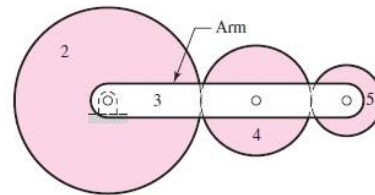

Figure (10–24)
A planetary gear train

Figure (10–25)
A gear train on the arm of a
planetary gear train

Figure (10–25) shows a planetary train composed of a sun gear 2, an arm or carrier 3, and planet gears 4 and 5. The angular velocity of gear 2 relative to the arm in rev/min is

$$n_{23} = n_2 - n_3 \qquad (b)$$

Also, the velocity of gear 5 relative to the arm is

$$n_{53} = n_5 - n_3 \qquad (c)$$

Dividing Eq. (*c*) by Eq. (*b*) gives

$$\frac{n_{53}}{n_{23}} = \frac{n_5 - n_3}{n_2 - n_3} \qquad (d)$$

Equation (*d*) expresses the ratio of gear 5 to that of gear 2, and both velocities are taken relative to the arm. Now this ratio is the same and is proportional to the tooth numbers, whether the arm is rotating or not. It is the train value. Therefore, we may write

$$e = \frac{n_5 - n_3}{n_2 - n_3} \qquad \underline{\qquad} \qquad (e)$$

This equation can be used to solve for the output motion of any planetary train. It is more conveniently written in the form

$$e = \frac{n_L - n_A}{n_F - n_A} \qquad \text{10-32}$$

where

n_F = rev/min of first gear in planetary train
n_L = rev/min of last gear in planetary train
n_A = rev/min of arm

EXAMPLE 10–6

In Fig. (10–24) the sun gear is the input, and it is driven clockwise at 100 rev/min. The ring gear is held stationary by being fastened to the frame. Find the rev/min and direction of rotation of the arm and gear 4.

Solution

Designate $n_F = n_2 = -100$ rev/min, and $n_L = n_5 = 0$. Unlocking gear 5 and holding the arm stationary, in our imagination, we find

$$e = -\left(\frac{20}{30}\right)\left(\frac{30}{80}\right) = -0.25$$

Substituting this value in Eq. (10–32) gives

$$-0.25 = \frac{0 - n_A}{(-100) - n_A} \qquad \text{or} \qquad n_A = -20 \text{ rev/min}$$

To obtain the speed of gear 4, we follow the procedure outlined by Eqs. (*b*), (*c*), and (*d*). Thus

$$n_{43} = n_4 - n_3 \qquad\qquad n_{23} = n_2 - n_3$$

and so

$$\frac{n_{43}}{n_{23}} = \frac{n_4 - n_3}{n_2 - n_3} \qquad\qquad (1)$$

But

$$\frac{n_{43}}{n_{23}} = -\frac{20}{30} = -\frac{2}{3} \qquad\qquad (2)$$

Substituting the known values in Eq. (1) gives

$$-\frac{2}{3} = \frac{n_4 - (-20)}{-100 - (-20)}$$

Solving gives

$$n_4 = 33.333 \text{ rev/min}$$

10.14 Force Analysis—Spur Gearing

Beginning with the numeral 1 for the frame of the machine, we shall designate the input gear as gear 2, and then number the gears successively 3, 4, etc., until we arrive at the last gear in the train. Next, there may be several shafts involved, and usually one or two gears are mounted on each shaft as well as other elements. We shall designate the shafts, using lowercase letters of the alphabet, *a*, *b*, *c*, etc.

With this notation we can now speak of the force exerted by gear 2 against gear 3 as F_{23}. The force of gear 2 against a shaft *a* is F_{2a}. We can also write F_{a2} to mean the force of a shaft *a* against gear 2. Unfortunately, it is also necessary to use superscripts to indicate directions. The coordinate directions will usually be indicated by the *x*, *y*, and *z* coordinates, and the radial and tangential directions by superscripts *r* and *t*. With this notation, F_{43}^t is the tangential component of the force of gear 4 acting against gear 3.

Figure (10–26*a*) shows a pinion mounted on shaft *a* rotating clockwise at n_2 rev/min and driving a gear on shaft *b* at n_3 rev/min. The reactions between the mating teeth occur along the pressure line. In Fig. (10–26*b*) the pinion has been separated from the gear and the shaft, and their effects have been replaced by forces. F_{a2} and T_{a2} are the force and torque, respectively, exerted by shaft *a* against pinion 2. F_{32} is the force exerted by gear 3 against the pinion. Using a similar approach, we obtain the free-body diagram of the gear shown in Fig. (10–26*c*).

In Fig. (10–27), the free-body diagram of the pinion has been redrawn and the forces have been resolved into tangential and radial components. We now define

$$W_t = F_{32}^t \tag{a}$$

as the *transmitted load*. This tangential load is really the useful component, because the radial component F_{43}^r serves no useful purpose. It does not transmit power. The applied torque and the transmitted load are seen to be related by the equation

$$T = \frac{d}{2} W_t \qquad (b)$$

where we have used $T = T_{a2}$ and $d = d_2$ to obtain a general relation.

The power H transmitted through a rotating gear can be obtained from the standard relationship of the product of torque T and angular velocity ω.

$$H = T\omega = (W_t \, d/2)\omega \qquad 10\text{-}33$$
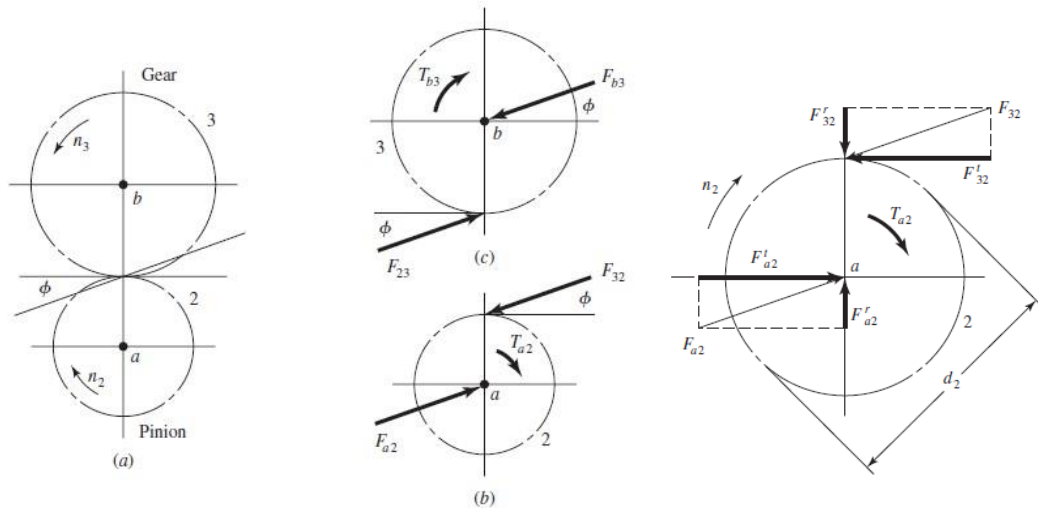
Figure (10–26)
Free-body diagrams of the forces and moments acting upon two gears of a simple gear train

Figure (10–27)
Resolution of gear forces

While any units can be used in this equation, the units of the resulting power will obviously be dependent on the units of the other parameters. It will often be desirable to work with the power in either horsepower or kilowatts, and appropriate conversion factors should be used.

Since meshed gears are reasonably efficient, with losses of less than 2 percent, the power is generally treated as constant through the mesh. Consequently, with a pair of meshed gears,

Eq. (10–33) will give the same power regardless of which gear is used for d and ω.

Gear data is often tabulated using *pitch-line velocity*, which is the linear velocity of a point on the gear at the radius of the pitch circle; thus $V = (d/2)\,\omega$. Converting this to customary units gives

$V = \pi dn/12$ 10-34

where
V = pitch-line velocity, ft/min
d = gear diameter, in
n = gear speed, rev/min

Many gear design problems will specify the power and speed, so it is convenient to solve Eq. (10–33) for W_t. With the pitch-line velocity and appropriate conversion factors incorporated, Eq. (10–33) can be rearranged and expressed in customary units as

$W_t = 33000\ H/V$ 10-35

where
W_t = transmitted load, lbf
H = power, hp
V = pitch-line velocity, ft/min

The corresponding equation in SI is

$W_t = 60000H/\pi dn$ 10-36

where
W_t = transmitted load, kN
H = power, kW
d = gear diameter, mm
n = speed, rev/min

EXAMPLE 10–7

Pinion 2 in Fig. (10–28*a*) runs at 1750 rev/min and transmits 2.5 kW to idler gear 3. The teeth are cut on the 20° full-depth system and have a module of $m = 2.5$ mm. Draw a free-body diagram of gear 3 and show all the forces that act upon it.

Solution

The pitch diameters of gears 2 and 3 are

$d_2 = N_2m = 20(2.5) = 50$ mm

$d_3 = N_3m = 50(2.5) = 125$ mm

From Eq. (10–36) we find the transmitted load to be

$W_t = 60000H/\pi d_2 n = 60000(2.5)/\pi(50)(1750) = 0.546$ kN

Thus, the tangential force of gear 2 on gear 3 is $F_{23}^t = 0.546$ kN, as shown in Fig. (10–28*b*). Therefore

$$F_{23}^r = F_{23}^t \tan 20^o = (0.546) \tan 20^o = 0.199 \text{ kN}$$

and so

$$F_{23} = \frac{F_{23}^t}{\cos 20^o} = \frac{0.546}{\cos 20^o} = 0.581 \text{ kN}$$

Since gear 3 is an idler, it transmits no power (torque) to its shaft, and so the tangential reaction of gear 4 on gear 3 is also equal to W_t. Therefore

$$F_{43}^t = 0.546 \text{ kN} \qquad F_{43}^r = 0.199 \text{ kN} \qquad F_{43} = 0.581 \text{ kN}$$

and the directions are shown in Fig. (10–28*b*). The shaft reactions in the *x* and *y* directions are

$$F_{b3}^x = -(F_{23}^t + F_{43}^r) = -(-0.546 + 0.199) = 0.347 \text{ kN}$$

$$F_{b3}^y = -(F_{23}^r + F_{43}^t) = -(0.199 - 0.546) = 0.347 \text{ kN}$$

The resultant shaft reaction is

$$F_{b3} = \sqrt{(0.347)^2 + (0.347)^2} = 0.491 \text{ kN}$$
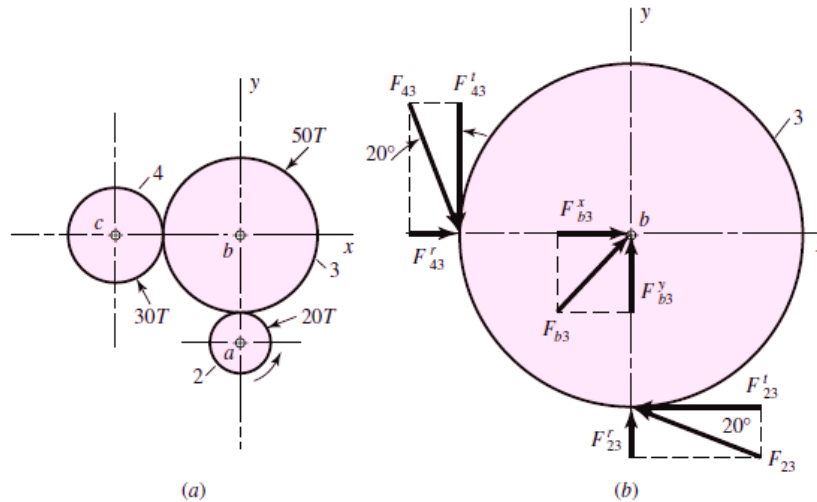
These are shown on the figure.

Figure (10–28)
A gear train containing an idler gear. (*a*) The gear train
(b) Free-body of the idler gear

10.15 Force Analysis—Bevel Gearing

In determining shaft and bearing loads for bevel-gear applications, the usual practice is to use the tangential or transmitted load that would occur if all the forces were concentrated at the midpoint of the tooth. While the actual resultant occurs somewhere between the midpoint and the large end of the tooth, there is only a small error in making this assumption. For the transmitted load, this gives

$$W_t = T/r_{av} \qquad\qquad 10\text{-}37$$

where T is the torque and r_{av} is the pitch radius at the midpoint of the tooth for the gear under consideration.

The forces acting at the center of the tooth are shown in Fig. (10–28). The resultant force W has three components: a tangential force W_t, a radial force W_r, and an axial force W_a. From the trigonometry of the figure,

$$\begin{aligned} W_r &= W_t \tan\phi \cos\gamma \\ W_a &= W_t \tan\phi \sin\gamma \end{aligned} \qquad 10\text{-}38$$

The three forces W_t, W_r, and W_a are at right angles to each other and can be used to determine the bearing loads by using the methods of statics.
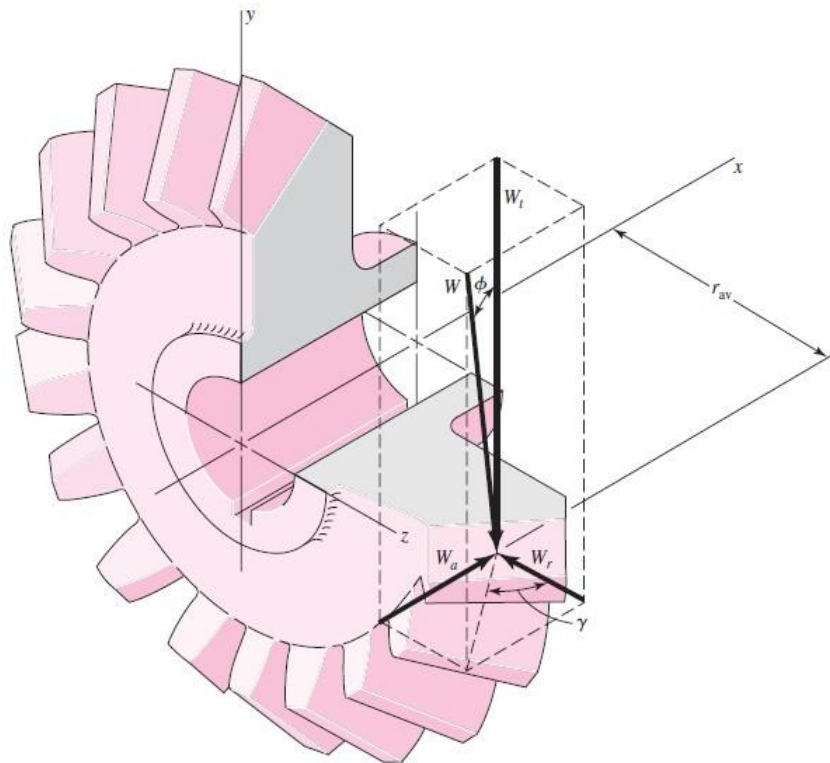
Figure (10–29)
Bevel-gear tooth forces

Homework

(1) A 17-tooth spur pinion has a diametral pitch of 8 teeth/in, runs at 1120 rev/min, and drives a gear at a speed of 544 rev/min. Find the number of teeth on the gear and the theoretical center-to-center distance. (*Ans./* 35 teeth, 3.25 in)

(2) A 15-tooth spur pinion has a module of 3 mm and runs at a speed of 1600 rev/min. The driven gear has 60 teeth. Find the speed of the driven gear, the circular pitch, and the theoretical center to-center distance. (*Ans./* 400 rev/min, $p = 3\pi$ mm, $C = 112.5$ mm)

(3) A spur gearset has a module of 4 mm and a velocity ratio of 2.80. The pinion has 20 teeth. Find the number of teeth on the driven gear, the pitch diameters, and the theoretical center-to-center distance.

(4) A 21-tooth spur pinion mates with a 28-tooth gear. The diametral pitch is 3 teeth/in and the pressure angle is 20°. Make a drawing of the gears showing one tooth on each gear. Find and tabulate the following results: the addendum, dedendum, clearance, circular pitch, tooth thickness, and base-circle diameters; the lengths of the arc of approach, recess, and action; and the base pitch and contact ratio. (*Ans./* $a = 0.3333$ in, $b = 0.4167$ in, $c = 0.0834$ in, $p = 1.047$ in, $t = 0.523$ in, $d_1 = 7$ in, $d_{1b} = 6.578$ in, $d_2 = 9.333$ in, $d_{2b} = 8.77$ in, $p_b = 0.984$ in, $m_c = 1.55$)

(5) A 20° straight-tooth bevel pinion having 14 teeth and a diametral pitch of 6 teeth/in drives a 32-tooth gear. The two shafts are at right angles and in the same plane. Find: the cone distance, the pitch angles, the pitch diameters, and the face width. (*Ans./* $d_P = 2.333$ in, $d_G = 5.333$ in, $\gamma = 23.63^o$, $\Gamma = 66.37^o$, $A_0 = 2.910$ in, $F = 0.873$ in)

(6) A parallel helical gearset uses a 17-tooth pinion driving a 34-tooth gear. The pinion has a right-hand helix angle of 30°, a normal pressure angle of 20°, and a normal diametral pitch of 5 teeth/in. Find: the normal, transverse, and axial circular pitches, the normal base circular pitch, the transverse diametral pitch and the transverse pressure angle, the addendum, dedendum, and pitch diameter of each gear.

(7) A parallel helical gearset consists of a 19-tooth pinion driving a 57-tooth gear. The pinion has a left-hand helix angle of 20°, a normal pressure angle of 14.5^o, and a normal diametral pitch of

10 teeth/in. Find: the normal, transverse, and axial circular pitches, the transverse diametral pitch and the transverse pressure angle, the addendum, dedendum, and pitch diameter of each gear.

(8) For a spur gearset with $\phi = 20^o$, while avoiding interference, find: the smallest pinion tooth count that will run with itself, the smallest pinion tooth count at a ratio $m_G = 2.5$, the largest gear tooth count possible with this pinion, and the smallest pinion that will run with a rack. (*Ans./* 15, 16, 18)

(9) Repeat question (*8*) for a helical gearset with $\phi_n = 20^o$ and $\psi = 30^o$.

(10) The decision has been made to use $\phi_n = 20^o$, $P_t = 6$ teeth/in, and $\psi = 30^o$ for a 2:1 reduction. Choose a suitable pinion and gear tooth count to avoid interference. (*Ans./* 10:20 and higher)

 (11) Repeat question (*10*) with a 6:1 reduction.

(12) By employing a pressure angle larger than standard, it is possible to use fewer pinion teeth, and hence obtain smaller gears without undercutting during machining. If the gears are spur gears, what is the smallest possible pressure angle ϕ_t that can be obtained without undercutting for a 9-tooth pinion to mesh with a rack?

(13) A parallel-shaft gearset consists of an 18-tooth helical pinion driving a 32-tooth gear. The pinion has a left-hand helix angle of 25°, a normal pressure angle of 20°, and a normal module of 3 mm. Find: the normal, transverse, and axial circular pitches, the transverse module and the transverse pressure angle, and the pitch diameters of the two gears.   (*Ans./* $p_n = 3\pi$ mm, $p_t = 10.40$ mm, $p_x = 22.30$ mm, $m_t = 3.310$ mm, $\phi_t = 21.88^o$, $d_p = 59.58$ mm, $d_G = 105.92$ mm)

(14) The double-reduction helical gearset shown in the figure is driven through shaft *a* at a speed of 900 rev/min. Gears 2 and 3 have a normal diametral pitch of 10 teeth/in, a 30° helix angle, and a normal pressure angle of 20°. The second pair of gears in the train, gears 4 and 5, have a normal diametral pitch of 6 teeth/in, a 25° helix angle, and a normal pressure angle of 20°. The tooth numbers are: $N_2 = 14$, $N_3 = 54$, $N_4 = 16$, $N_5 = 36$. Find: the speed and direction of shaft *c*, and the center distance between shafts.

Dimensions in inches
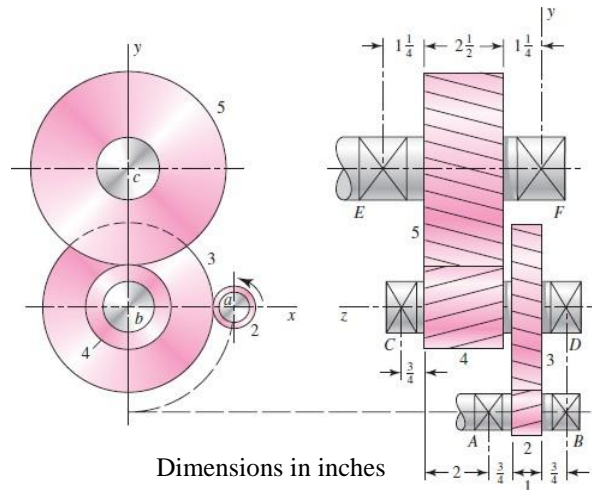
(15) Shaft *a* in the figure rotates at 600 rev/min in the direction shown. Find the speed and direction of rotation of shaft *d*. (*Ans./* $e = 4/51$, $n_d = 47.06$ rev/min cw)
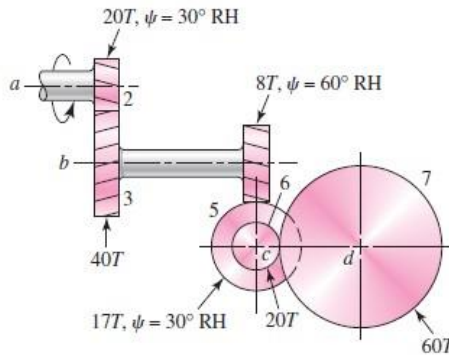

(16) The mechanism train shown consists of an assortment of gears and pulleys to drive gear 9. Pulley 2 rotates at 1200 rev/min in the direction shown. Determine the speed and direction of rotation of gear 9.
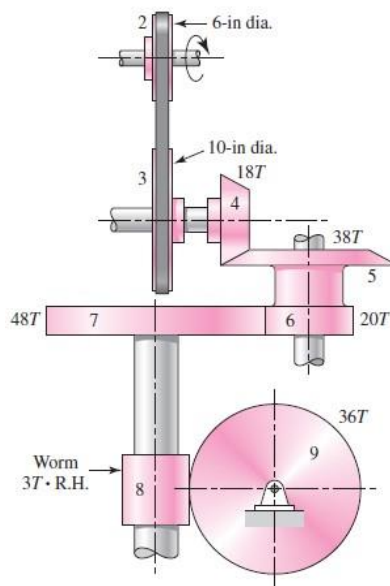
(17) The figure shows a gear train consisting of a pair of helical gears and a pair of miter gears. The helical gears have a $17.5°$ normal pressure angle and a helix angle as shown. Find: the speed of shaft c, the distance between shafts a and b, and the diameter of the miter gears.

Dimensions in inches
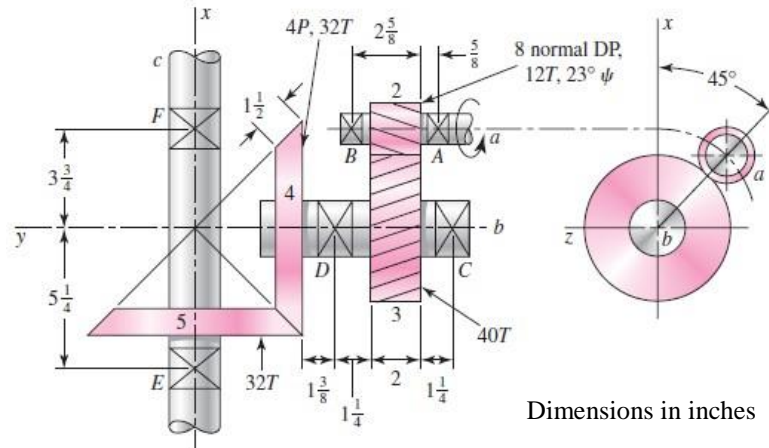
(18) The tooth numbers for the automotive differential shown in the figure are $N_2 = 17$, $N_3 = 54$, $N_4 = 11$, $N_5 = N6 = 16$. The drive shaft turns at 1200 rev/min. (*a*) What are the wheel speeds if the car is traveling in a straight line on a good road surface? (*b*) Suppose the right wheel is jacked up and the left wheel resting on a good road surface. What is the speed of the right wheel? (*c*) Suppose, with a rear-wheel drive vehicle, the auto is parked with the right wheel resting on a wet icy surface. Does the answer to part (*b*) give you any hint as to what would happen if you started the car and attempted to drive on?
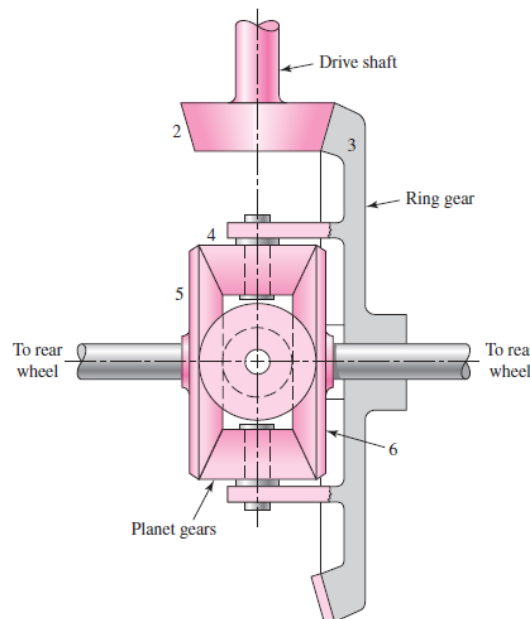
(19) The figure illustrates an all-wheel drive concept using three differentials, one for the front axle, another for the rear, and the third connected to the drive shaft. (*a*) Explain why this concept may allow greater acceleration. (*b*) Suppose either the center of the rear differential, or both, can be locked for certain road conditions. Would either or both of these actions provide greater traction? Why?
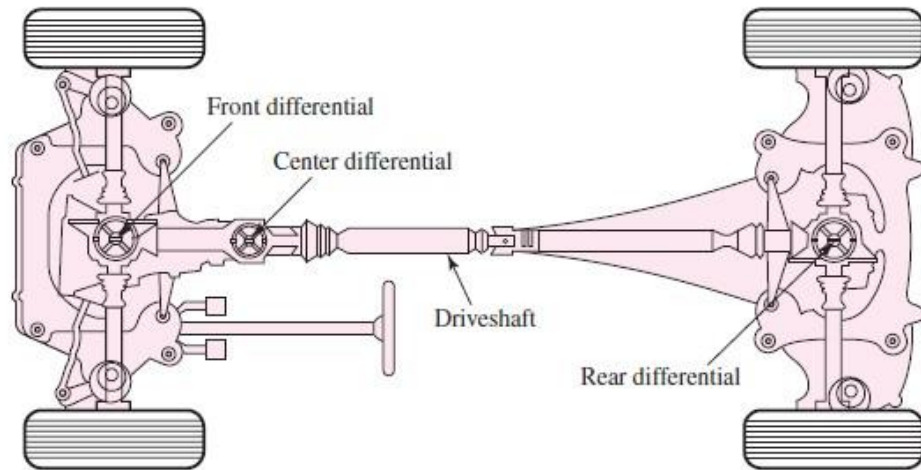

The Audi "Quattro concept," showing the three differentials that provide permanent all-wheel drive

(20) In the reverted planetary train illustrated, find the speed and direction of rotation of the arm if gear 2 is unable to rotate and gear 6 is driven at 12 rev/min in the clockwise direction.
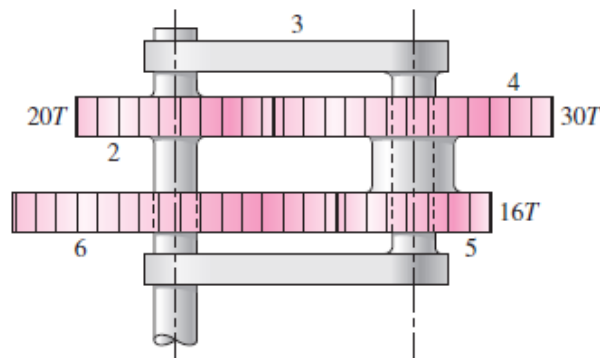
(21) In the gear train of question (*20*), let gear 2 be driven at 180 rev/min counterclockwise while gear 6 is held stationary. What is the speed and direction of rotation of the arm?

(22) Tooth numbers for the gear train shown in the figure are $N_2 = 12$, $N_3 = 16$, and $N_4 = 12$. How many teeth must internal gear 5 have? Suppose gear 5 is fixed. What is the speed of the arm if shaft a rotates counterclockwise at 320 rev/min? (*Ans./ n_A = 68.57 rev/min cw*)
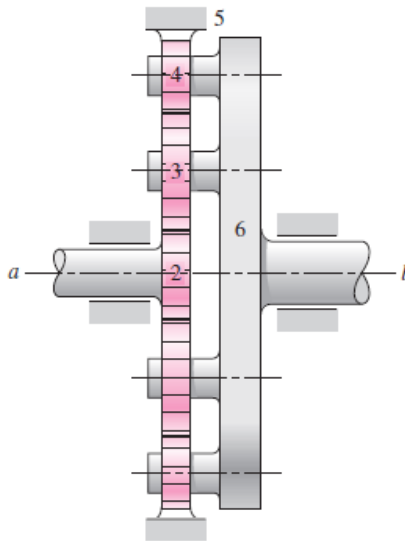
(23) The tooth numbers for the gear train illustrated are $N_2 = 24$, $N_3 = 18$, $N_4 = 30$, $N_6 = 36$, and $N_7 = 54$. Gear 7 is fixed. If shaft b is turned through 5 revolutions, how many turns will shaft a make?